MARINE PHYSICAL LABORATORY

SCRIPPS INSTITUTION OF OCEANOGRAPHY

San Diego, California 92152



# VERTICAL DIRECTIONALITY MEASUREMENTS OF AMBIENT NOISE IN THE NE PACIFIC

**B. J. Sotirin and W. S. Hodgkiss**



**MPL TECHNICAL MEMORANDUM 412**

MPL-U 46/89
August 1989

*Approved for public release; distribution unlimited.*

| | |
|---|---|
| 1a. REPORT SECURITY CLASSIFICATION<br>UNCLASSIFIED | 1b. RESTRICTIVE MARKINGS |
| 2a. SECURITY CLASSIFICATION AUTHORITY | 3. DISTRIBUTION / AVAILABILITY OF REPORT<br>Approved for public release; distribution unlimited. |
| 2b. DECLASSIFICATION / DOWNGRADING SCHEDULE | |
| 4. PERFORMING ORGANIZATION REPORT NUMBER(S)<br>MPL TECHNICAL MEMORANDUM 412 [MPL-U-46/89] | 5. MONITORING ORGANIZATION REPORT NUMBER(S) |
| 6a. NAME OF PERFORMING ORGANIZATION<br>Marine Physical Laboratory<br>6b. OFFICE SYMBOL (If applicable)<br>MPL | 7a. NAME OF MONITORING ORGANIZATION<br>Office of Naval Research<br>Department of the Navy |
| 6c. ADDRESS (City, State, and ZIP Code)<br>University of California, San Diego<br>Scripps Institution of Oceanography<br>San Diego, CA 92152 | 7b. ADDRESS (City, State, and ZIP Code)<br>800 North Quincy Street<br>Arlington, VA 22217-5000 |
| 8a. NAME OF FUNDING / SPONSORING ORGANIZATION<br>Office of Naval Research<br>8b. OFFICE SYMBOL (If applicable)<br>ONR | 9. PROCUREMENT INSTRUMENT IDENTIFICATION NUMBER<br>N00014-87-C-0127; N00014-87-K-0225 |
| 8c. ADDRESS (City, State, and ZIP Code)<br>Department of the Navy<br>800 North Quincy Street<br>Arlington, VA 22217-5000 | 10. SOURCE OF FUNDING NUMBERS<br>PROGRAM ELEMENT NO. / PROJECT NO. / TASK NO / WORK UNIT ACCESSION NO. |
| 11. TITLE (Include Security Classification)<br>VERTICAL DIRECTIONALITY MEASUREMENTS OF AMBIENT NOISE IN THE NE PACIFIC | |
| 12. PERSONAL AUTHOR(S)<br>B. J. Sotirin and W. S. Hodgkiss | |
| 13a. TYPE OF REPORT<br>tech memo<br>13b. TIME COVERED<br>FROM _____ TO _____<br>14. DATE OF REPORT (Year, Month, Day)<br>August 1989<br>15. PAGE COUNT | |
| 16. SUPPLEMENTARY NOTATION | |
| 17. COSATI CODES<br>FIELD / GROUP / SUB-GROUP | 18. SUBJECT TERMS (Continue on reverse if necessary and identify by block number)<br>vertical directionality, ambient noise, spatial distribution. |

19. ABSTRACT (Continue on reverse if necessary and identify by block number)

Vertical directionality measurements of the ambient noise field between 15 and 130 Hz are presented. These data were measured by a large aperture array deployed vertically from R/P *FLIP* at 35° N, 126° W in 4700 m of water. Spatial distribution is plotted as a function of frequency during specified times and as a function of time at specified frequencies during the onset of a local storm. Spectral levels of beams dominated by local noise sources display a threshold type behavior as wind speed increases. Spectral levels of beams dominated by distant shipping reveal the fine-scale structure of the ambient noise pedestal. Spatial distribution is also plotted as a function of depth at specified frequencies and wind speeds, although due to the temporal variability of the noise, no significant differences were seen with depth.

| | |
|---|---|
| 20. DISTRIBUTION / AVAILABILITY OF ABSTRACT<br>☐ UNCLASSIFIED/UNLIMITED ☒ SAME AS RPT ☐ DTIC USERS | 21. ABSTRACT SECURITY CLASSIFICATION<br>UNCLASSIFIED |
| 22a. NAME OF RESPONSIBLE INDIVIDUAL<br>W. S. Hodgkiss | 22b. TELEPHONE (Include Area Code)<br>(619) 534-1798<br>22c. OFFICE SYMBOL |

DD FORM 1473, 84 MAR 83 APR edition may be used until exhausted
All other editions are obsolete

SECURITY CLASSIFICATION OF THIS PAGE

☆ U.S. Government Printing Office: 1986—607-044

# Vertical Directionality Measurements of Ambient Noise in the NE Pacific

*B. J. Sotirin and W. S. Hodgkiss*

Marine Physical Laboratory
Scripps Institution of Oceanography
University of California, San Diego
La Jolla, CA 92093

Vertical directionality measurements of the ambient noise field between 15 and 150 Hz are presented. These data were measured by a large aperture array deployed vertically from R/P *FLIP* at 35° N, 126° W in 4700 m of water. Spatial distribution is plotted as a function of frequency during specified times and as a function of time at specified frequencies during the onset of a local storm. Spectral levels of beams dominated by local noise sources display a threshold type behavior as wind speed increases. Spectral levels of beams dominated by distant shipping reveal the fine-scale structure of the ambient noise pedestal. Spatial distribution is also plotted as a function of depth at specified frequencies and wind speeds, although due to the temporal variability of the noise, no significant differences were seen with depth.

# Vertical Directionality Measurements of Ambient Noise in the NE Pacific

*B. J. Sotirin and W. S. Hodgkiss*

Marine Physical Laboratory
Scripps Institution of Oceanography
University of California, San Diego
La Jolla, CA 92093

## I. Introduction

The spatial distribution at low frequencies and low local wind speeds may be described as a broad pedestal of energy arriving between ±20° of horizontal in the deep sound channel with levels up to 25 dB above the higher angle levels [Anderson, 1979; Burgess and Kewley, 1983]. This distribution varies with local wind speed, as the higher angle levels increase with increasing wind speed, undermining the clarity of the pedestal shape [Hodgkiss and Fisher, 1987; Sotirin and Hodgkiss, 1989b].

The origin of the sound arriving at the near horizontal angles warrants some discussion. Ray tracing diagrams show that surface reflecting rays which do not interact with the bottom arrive within a narrow band of angles around ±12° to ±15°. The noise content of these rays is enhanced by the sound generated by surface ships. Theoretically, this implies that the low frequency spatial distribution should have a double-humped pattern with the width of the notch between the humps decreasing with depth [Cavanagh and Renner, 1980]. Measurements, however, show a pedestal with broad frequency and spatial characteristics. Two mechanisms were suggested by Anderson [1979] to account for the additional noise at near horizontal angles, one based on the shallower sound speed minimum at high latitudes and the other on sloping bottom reflection referred to now as high latitude ducting and down slope conversion (or the slope enhancement effect) respectively. These mechanisms would convert noise traveling at near vertical angles to horizontal angles such that the noise would travel with low loss in the deep sound channel, filling in the predicted noise notch. Levels within the pedestal of low frequency ambient noise spatial distribution then, are primarily from distant sources.

Storm induced noise has been observed at frequencies above 150 Hz as the spectral levels increase with wind speed. At lower frequencies however, there has been no consensus regarding the extent of the wind dependencies. Efforts to conform to the logarithmic functions seen at high frequencies has led to a variety of predicted spectral levels [Urick, 1984]. Difficulties arise in estimating the "wind dependent portion" [Crouch and Burt, 1972] of an omnidirectional signal which may be affected by other sources. The obvious experimental answer is the use of the directional capabilities of an array. This has been the approach of several investigators [Burgess and Kewley, 1983; Hodgkiss and Fisher, 1987] however changes in location and time introduce spectral level variations, which complicate the wind induced noise estimation.

The advent of large aperture arrays with many elements provides the capability of measuring ambient noise characteristics with high resolution. In this report, use of a large aperture array enables us to present the fine-scale structure of the ambient noise field. Analysis and interpretation of this data is documented in [Sotirin and Hodgkiss, 1989b]. The array was deployed at three nominal depths covering the water column from 400 m to 3100 m at 7.5 m sampling increments from Research Platform *FLIP* which was moored in the NE Pacific. A detailed estimate of the variability in the spatial distribution of ambient noise as wind speed increases from 2 m/s to 12 m/s over a 21 hour period is provided by the 900 m array aperture which produces a narrow 1° beam at 100 Hz.

## II. Experiment and Data Processing Description

The low frequency (20-200 Hz) vertical directionality data was collected by a 900 m aperture array, with 120 individual elements equally spaced at 7.5 m, deployed from R/P *FLIP*. The experiment site was about 400 nm west of Monterey CA, at 35° N, 126° W in about 4700 m of water off the Monterey Fan. Area noise levels were relatively high [Urick, 1984], typically about 80 dB//$\mu$Pa/$\sqrt{\text{Hz}}$ at 50 Hz, with northern shipping lanes to the north, coastal shipping to the east, and during the experiment, storm tracks to the south. Data, which were recorded almost continuously over a 20 day period during September 1987, included local wind velocity and swell height, local shipping densities, water current velocities at 43 m and 90 m depths, array navigation data and the low frequency acoustic data.

The data processing procedure converted individual element time series to spatial spectra. The integrity of the data selected were verified by examining time series and spectra for representative elements. A 2 s time series of the 120 channels were scanned at the beginning, middle and end of each time series to note any channel variations. For each 2 minute segment analyzed, the time series for a representative element was plotted over the segment to identify any obvious contaminants. Calculating the spectra of one channel per array section provided a mid-process verification of the data. Further processing consisted of selecting specified frequency bins, compensating for an array sampling offset [Sotirin and Hodgkiss, 1989a] and beamforming across the array aperture. The data segment (65536 2-ms samples for each of the 120 channels) was transformed to the frequency domain using a 1024-point Fast Fourier Transform (FFT) and a Kaiser-Bessel ($\alpha$=2.5) window. Estimates (0.49 Hz/bin) were selected at 5 Hz increments from 15 to 130 Hz, avoiding narrow band contaminants at 60, 115 and 120 Hz by shifting frequency slightly to 61.0, 113.8 and 118.7 Hz. A frequency dependent phase correction was implemented to account for the sampling offset and the spatial conversion was accomplished using an FFT beamformer. The beamformer was implemented with M=512 points, a Kaiser-Bessel ($\alpha$=1.5) shading function w(n) and a spatial sampling frequency of 0.131579 samples/meter. This sampling deviates slightly from the array design element spacing of 7.5 m due to strain in the kevlar strength member under tension. The spatial samples were incoherently averaged, and converted from electrical angle $\phi$ to physical angle $\theta = \text{asin}(\phi/kd)$. The averaged magnitude square results were calibrated to dB re 1 $\mu$Pa/$\sqrt{\text{Hz}}$ Deg by normalizing by the number of points in the FFT, the power in the window function ($\frac{1}{N}\sum_{n=0}^{N} w^2(n)$) and the spatial sampling frequency, and by converting wavenumber to degrees with

the factor $dk_v/d\theta = \frac{\pi f}{180c}\cos(\frac{\pi}{180}\theta)$, where $k_v$ is the digital spatial frequency $\frac{1}{\lambda}\sin\theta$ analogous to the digital time frequency f. This normalization presents the data in terms of average narrowband intensity received by the array per vertical degree.

## III. Results

The ambient noise directionality data presented were selected from several areas of interest. The passage of a storm increased local wind speed from 2 to 12 m/s over a 21 hour period from Julian day (Jday) 257 at 2300 Greenwich Mean Time (GMT) until 1940 GMT the following day (Jday 258). Two minute samples were selected every 20 minutes during this event to provide a detailed investigation of the directional variability with increasing wind speed. A second time series is presented to show the variability in the spatial distribution on a shorter time scale (about 1 hour). During a second storm, the array was deployed at three nominal depths which provides an opportunity to examine the variation of wind effects with depth at three nominal wind speeds.

The long time series (21 hours) is presented first as omnidirectional levels as a function of frequency (1/2 Hz bands centered at 15, 20, 25, 30, 35, 40, 45, 50, 55, 60, 65, 70, 75, 80, 85, 90, 95, 100, 105, 110, 115, 120, 125 and 130 Hz) and time (sampled every 20 minutes). Selected array channel estimates were averaged and the mean was removed from each of the narrowband time series which were then passed through a 4-sample (time corrected) running mean filter to provide the estimates in Figure 1. The corresponding filtered wind speed estimates are also shown. This same data is presented in Figure 2 as spatial spectra versus frequency, at each 20-minute interval and corresponding local wind speed, and in Figure 3 as spatial spectra versus time, for equally spaced 20-minute samples, and for the same 24 frequencies. Although the spectra, calibrated to dB re 1 $\mu$Pa/ per $\sqrt{\text{Hz}}$ per vertical degree with positive angles looking up and negative angles looking down, are plotted as a function of time during the storm, the higher angle levels reflect the increasing wind speeds. To observe this variation with wind speed, selected angles (2, 8, 14, 20, $\pm$50, 60, 70 and $\pm$80°) were extracted, normalized and plotted individually in Figure 4 at 15, 35, 55, 75, and 95 Hz. The number to the right of each directional time series is the normalization factor. The lower time series represents the corresponding unfiltered wind speed estimates in meters per second.

The second set of time series consists of consecutive 2-minute estimates of the spatial distribution to show the short-time scale (about 1 hour) temporal variability at specific frequencies (15, 35, 55, 75, 95 and 115 Hz). Data acquired on Julian day 268 at 1000 GMT with the array deployed at a mid-depth of 2650 m and a local wind speed of 2-3 m/s is presented in Figure 5. Data acquired on Julian day 258 at 1430 GMT with the array deployed at a mid-depth of 850 m and a local wind speed of 10-11 m/s is presented in Figure 6.

The variation in spatial distribution as a function of depth is presented in Figures 7-9. Nine 2 minute data segments were processed with characteristics shown in Table 1. The mid-array depth for the three deployments was 850, 1750 and 2650 m. The recorded wind speeds corresponding to the data segments were within 0.5 m/s of 3.1, 7.2 and 11.3 m/s, for the low, medium and high designations respectively. The spatial distribution is plotted at each of 24 frequencies (15, 20, 25, 30, 35, 40, 45, 50, 55, 60, 65, 70, 75, 80, 85, 90, 95, 100, 105, 110, 115, 120, 125 and 130

Hz) as a function of array depth and wind speed. Figure 7 is plotted with the data corresponding to the shallow array depth in the foreground, followed by that for the mid array depth and deep array depth each offset by 5 mm. Figure 8 is plotted with the data corresponding to the low wind speed in the foreground, followed by that for the mid wind speed and high wind speed each offset by 5 mm. Figure 9 is the spatial distribution as a function of frequency at a specific array depth and wind speed.

## Acknowledgments

This work was supported by the Office of Naval Research under Contract nos. N00014-87-K-0225 and N00014-87-C-0127.

## References

Anderson, V. C., "Variation of the vertical directionality of noise with depth in the North Pacific," J. Acoust. Soc. Am., Vol. 66, no. 5, pp. 1446-1452, Nov. 1979.

Burgess, A. S. and D. J. Kewley, "Wind-generated surface noise source levels in deep water East of Australia," J. Acoust. Soc. Am., Vol. 73, no. 1, pp. 201-210, January 1983.

Cavanagh, R. C. and W. W. Renner, "Vertical directionality and depth dependence of averaged acoustic signals and noise," J. Acoust. Soc. Am., Vol. 68, no. 5, pp. 1467-1474, Nov. 1980.

Crouch, W. W. and P. J. Burt, "The logarithmic dependence of surface-generated ambient-sea-noise spectrum level on wind speed," J. Acoust. Soc. Am., Vol. 51, no. 3, part 2, pp. 1066-1072, 1972.

Hodgkiss, W. S. and F. H. Fisher, "Vertical directionality of ambient noise at 32° N as a function of longitude," Technical Memorandum 387, Marine Physical Laboratory, Scripps Institution of Oceanography, San Diego, CA, 1987.

Sotirin, B. J. and W. S. Hodgkiss, "On array performance: A methodology of system calibration and noise identification," MPL TM-410, Marine Physical Laboratory, Scripps Institution of Oceanography, La Jolla, CA, June 1989a.

Sotirin, B. J. and W. S. Hodgkiss, "Large aperture array measurements of the vertical ambient noise field," TM-411, Marine Physical Laboratory, Scripps Institution of Oceanography, La Jolla, CA, July 1989b.

Urick, R. J., *Ambient noise in the sea*, Washington, D.C.: Undersea Warfare Technology Office, Naval Sea Systems Command, Department of the Navy, 1984.

**Figure 1.**

**Omnidirectional narrowband 21 hour time series.**

Spectral levels vs. wind speed

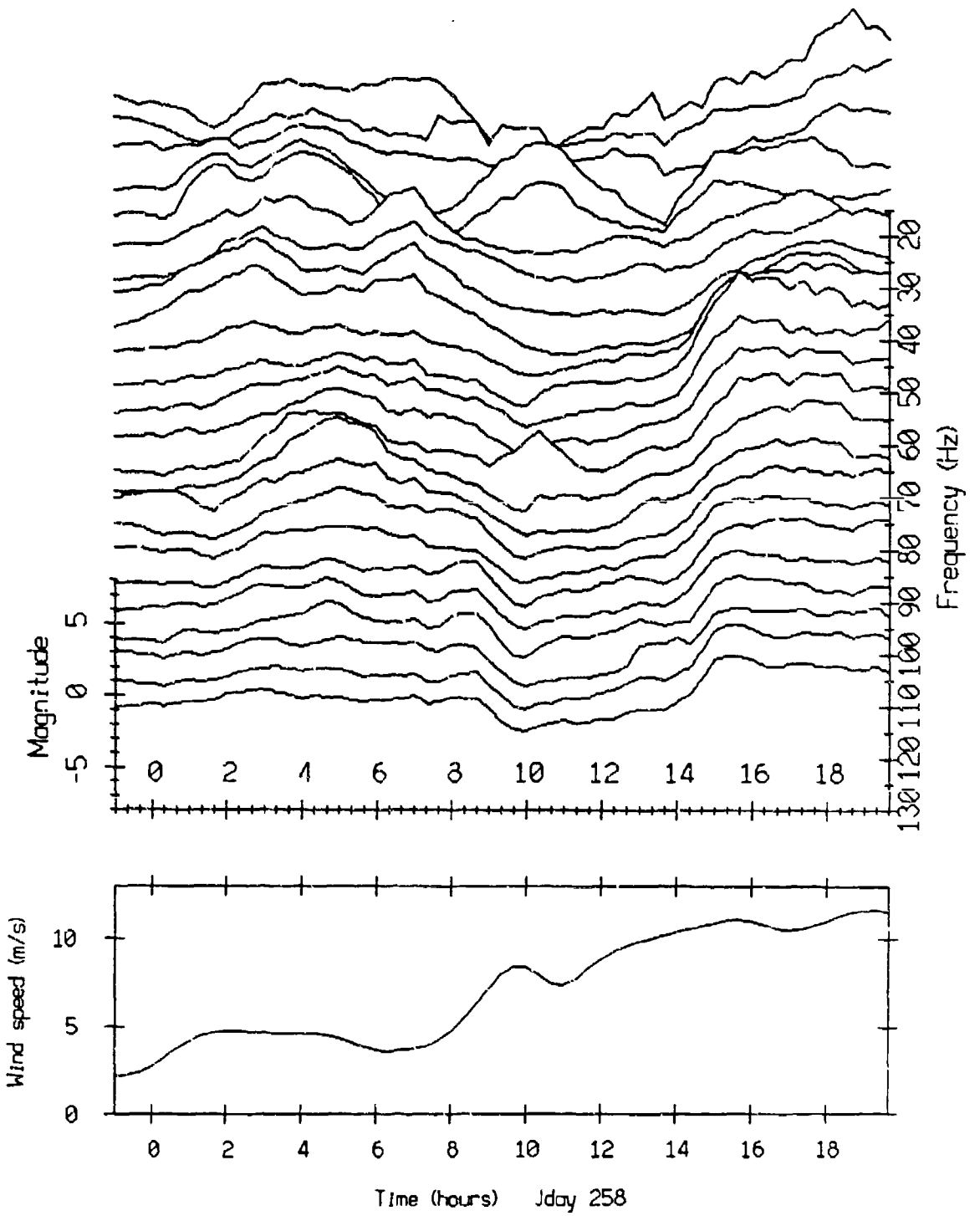

**Figure 2.**

**Spatial spectra versus frequency at specified times.**

Spatial Distribution During Storm at 2300 GMT

wind speed: 2.1 m/s

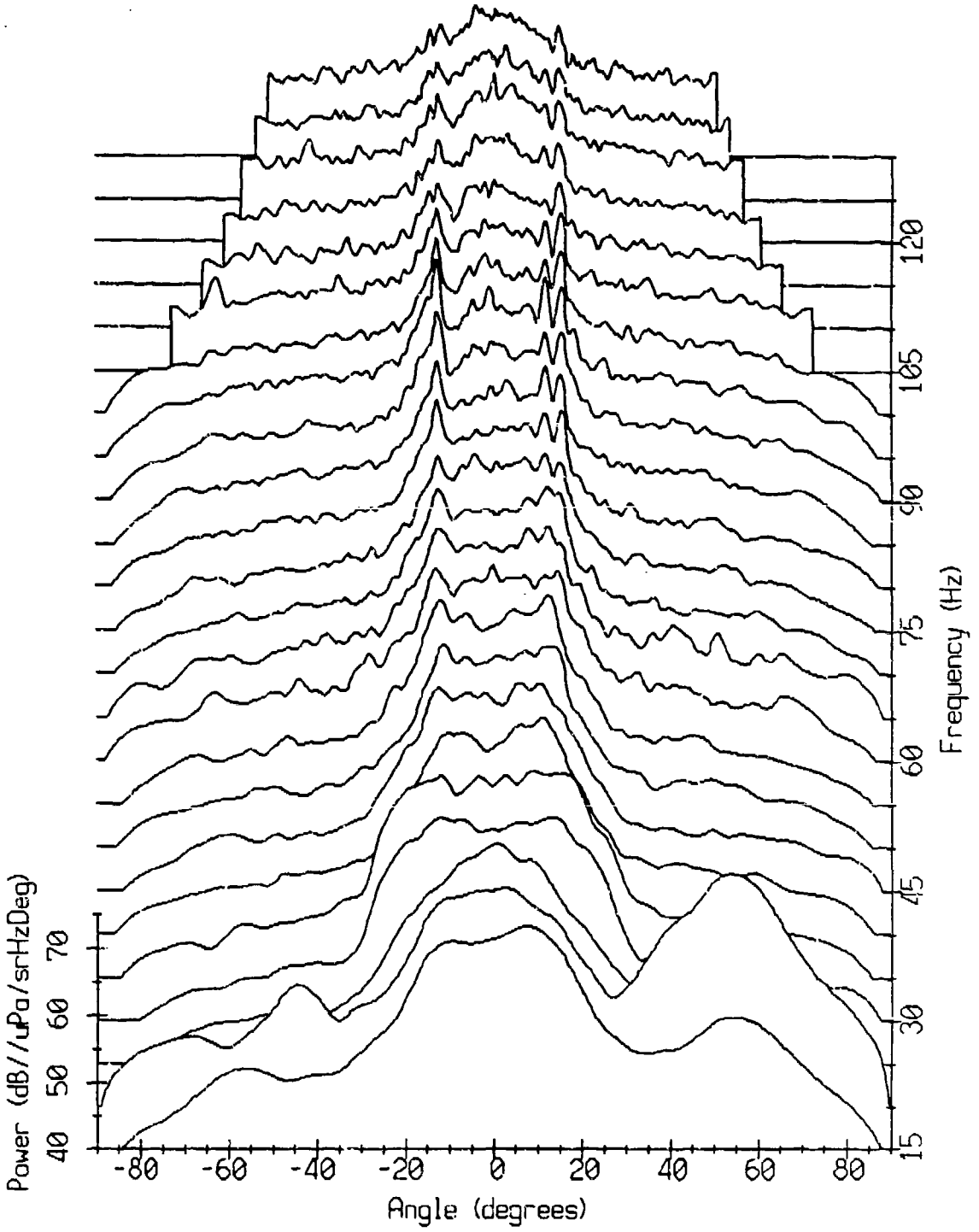

Spatial Distribution During Storm at 2320 GMT

wind speed: 2.1 m/s

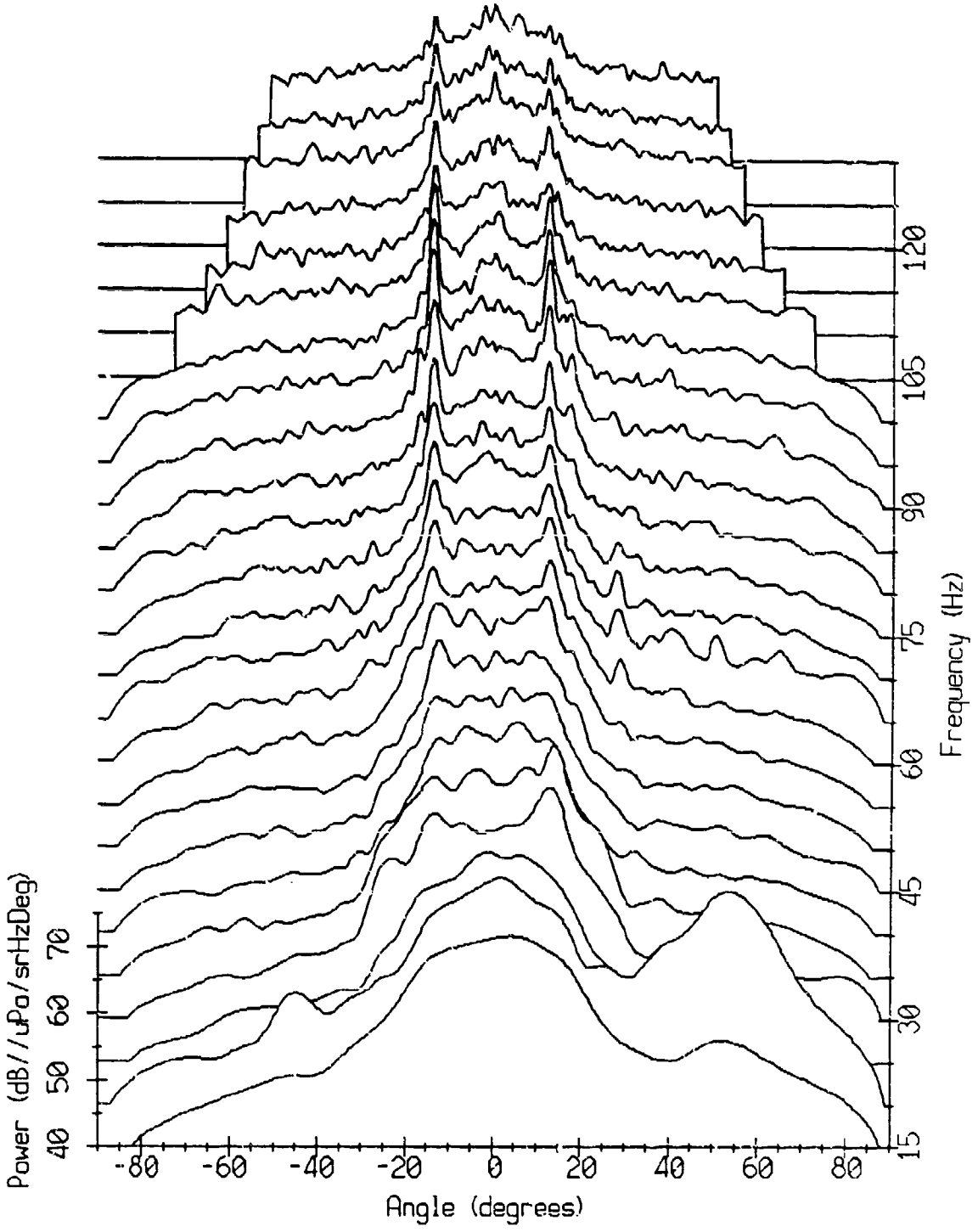

Spatial Distribution During Storm at 2340 GMT

wind speed: 2.1 m/s

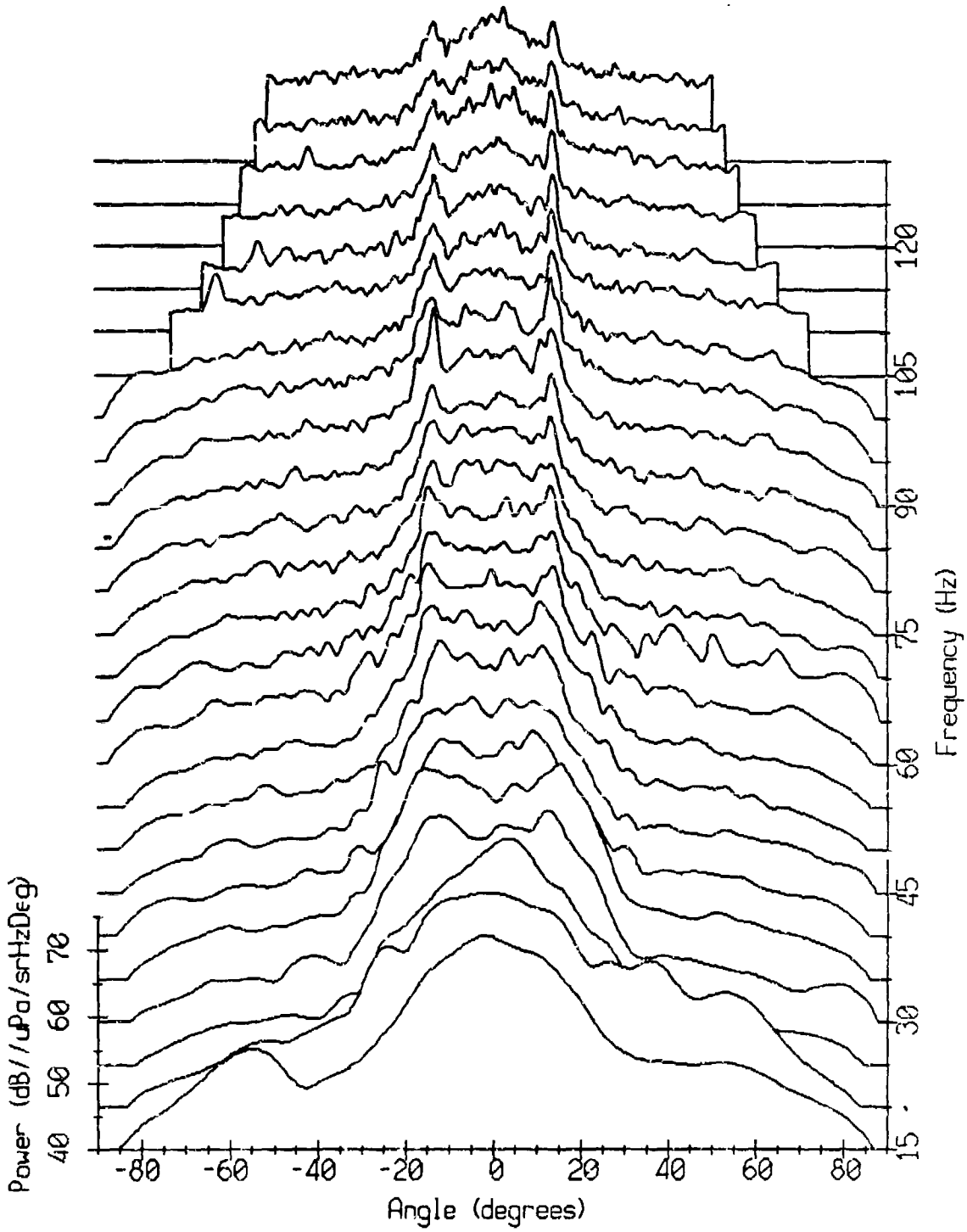

Spatial Distribution During Storm at 0000 GMT

wind speed: 2.3 m/s

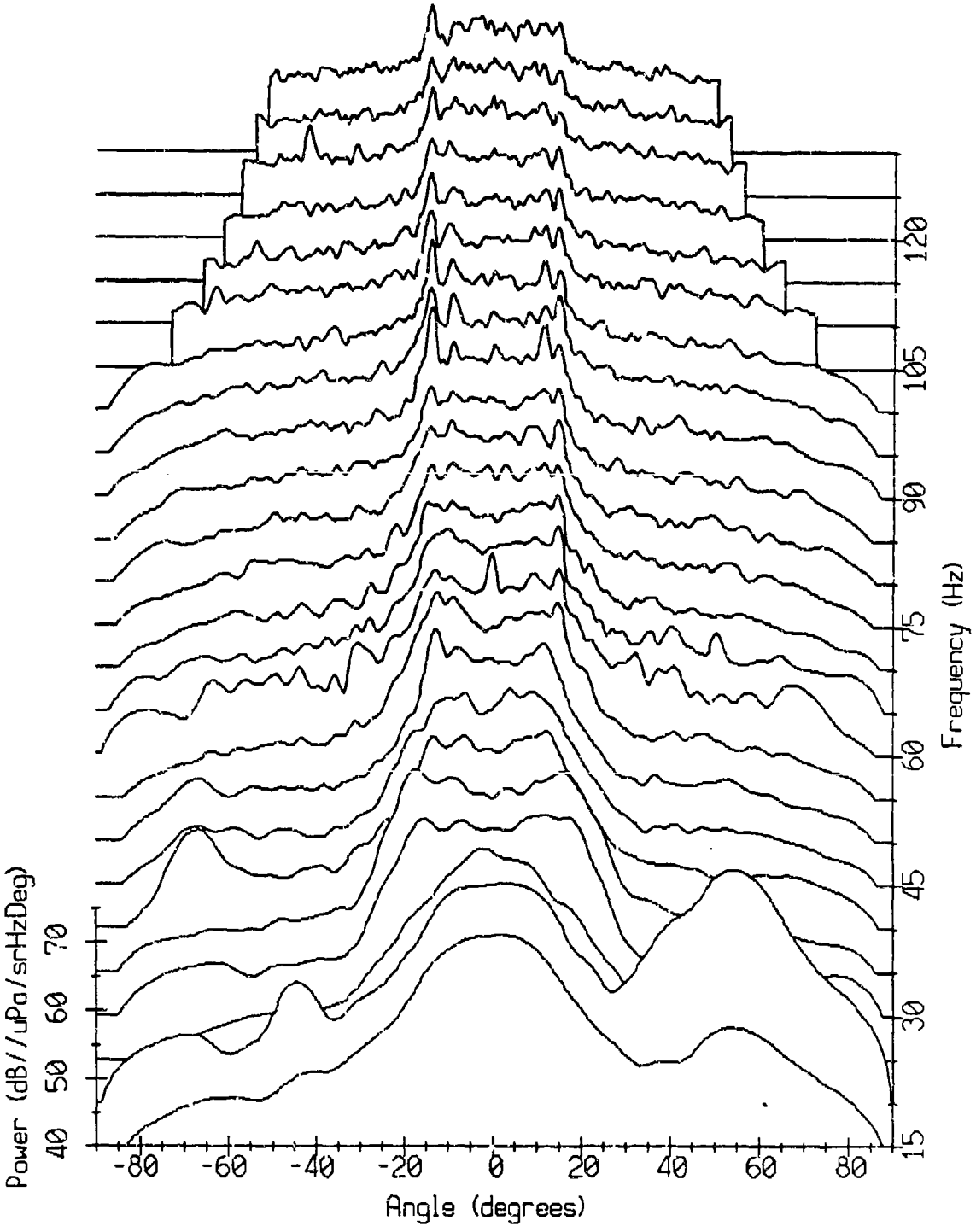

Spatial Distribution During Storm at 0020 GMT

wind speed: 2.9 m/s

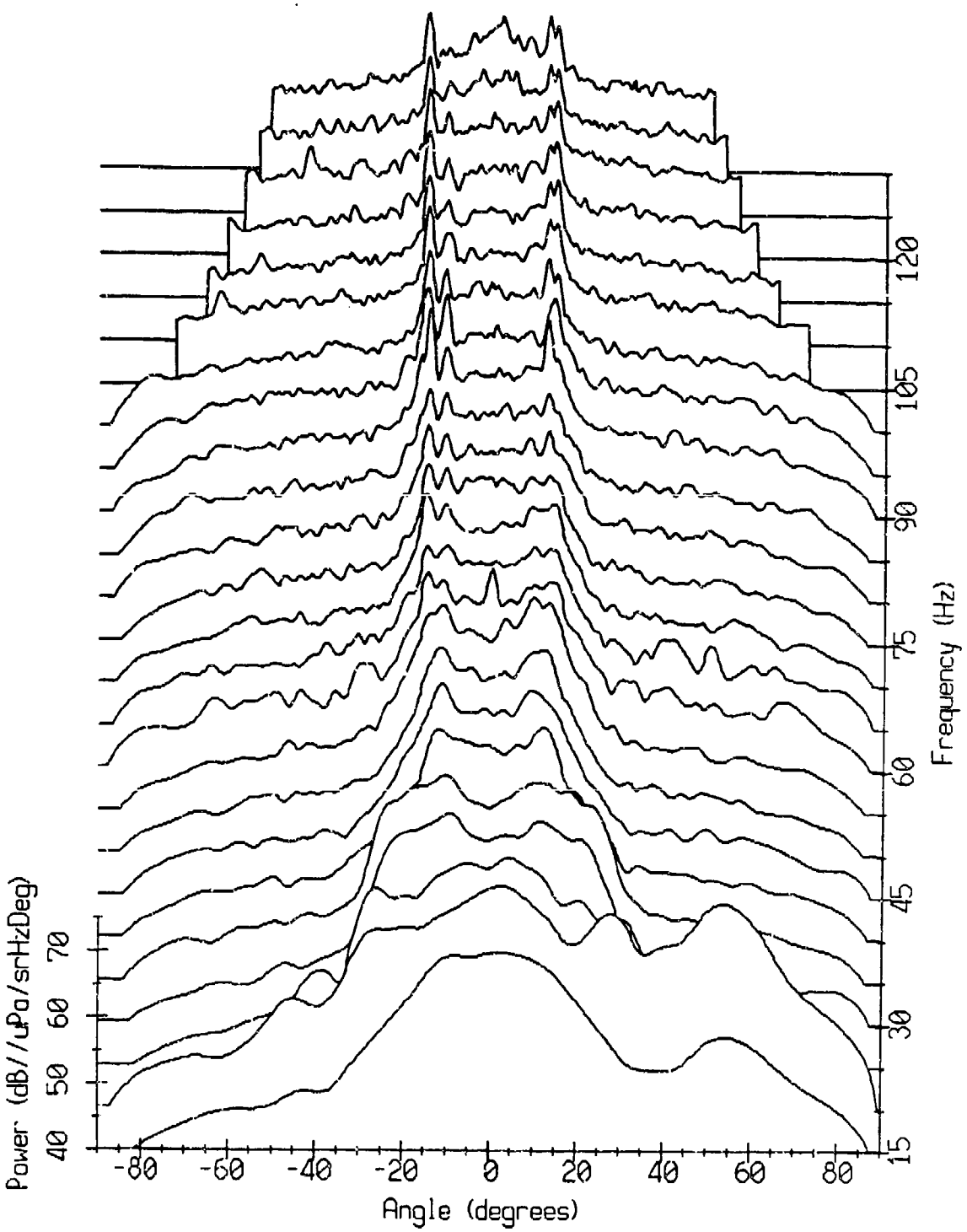

Spatial Distribution During Storm at 0040 GMT

wind speed: 3.5 m/s

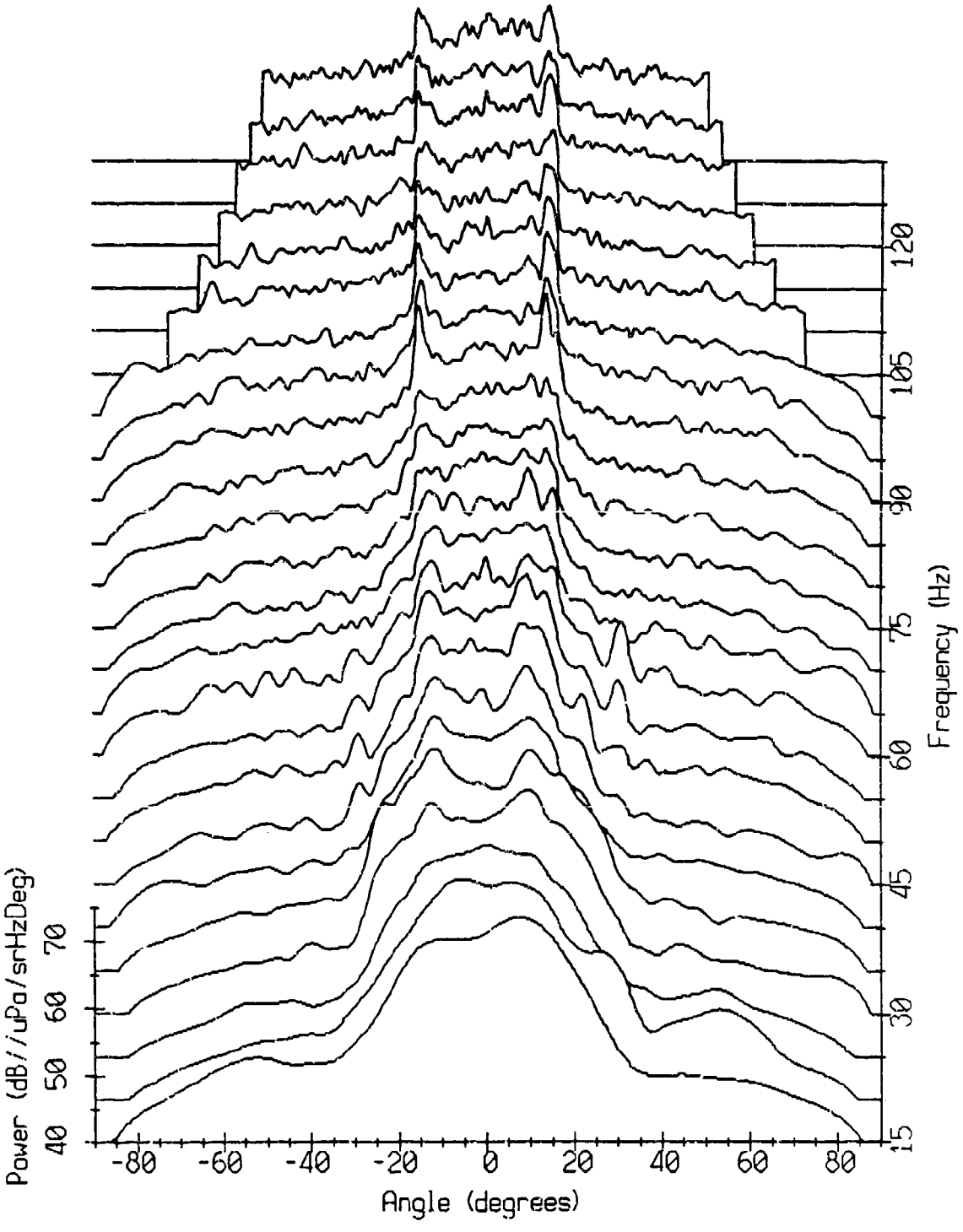

Spatial Distribution During Storm at 0100 GMT

wind speed: 4.1 m/s

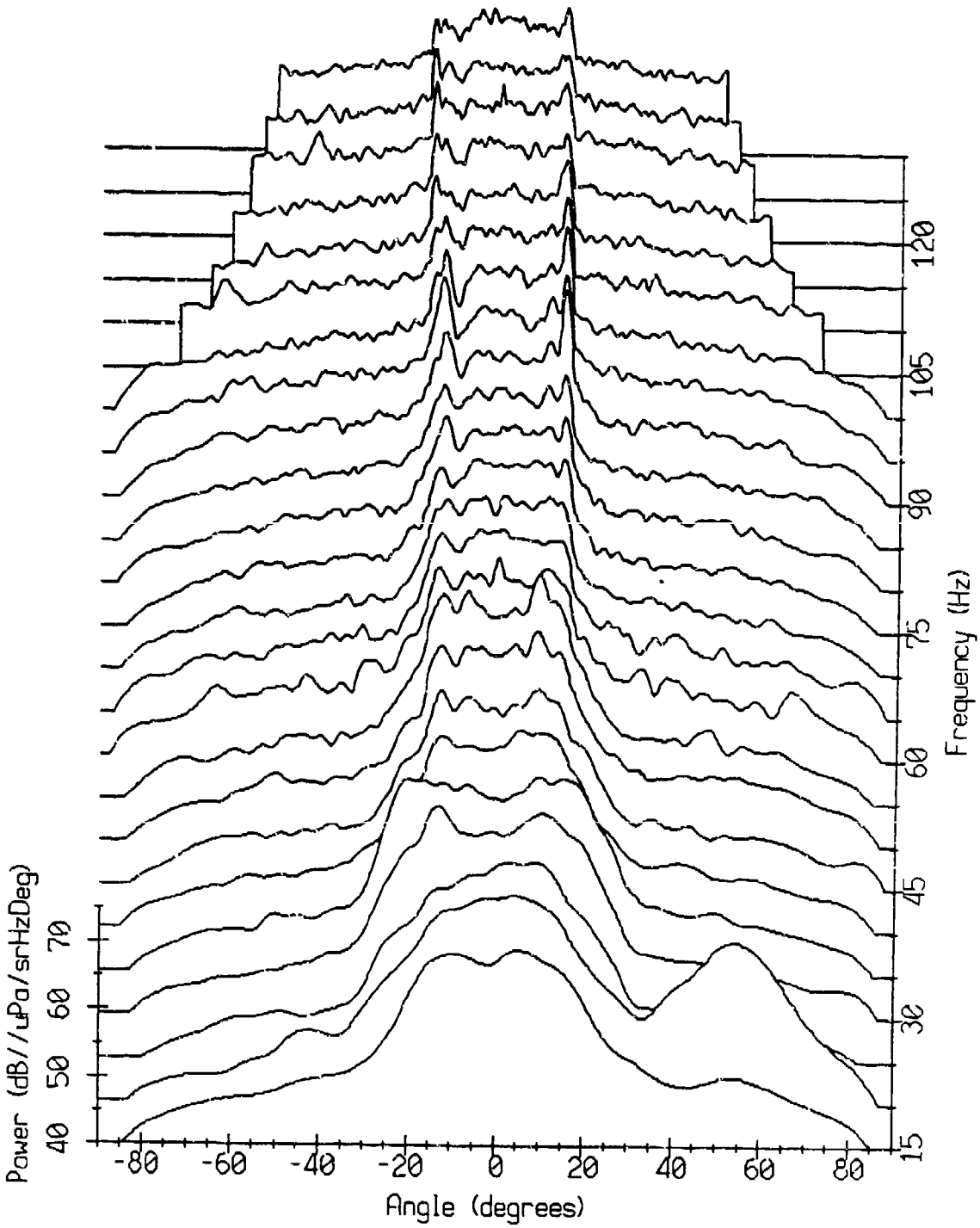

Spatial Distribution During Storm at 0120 GMT

wind speed: 4.4 m/s

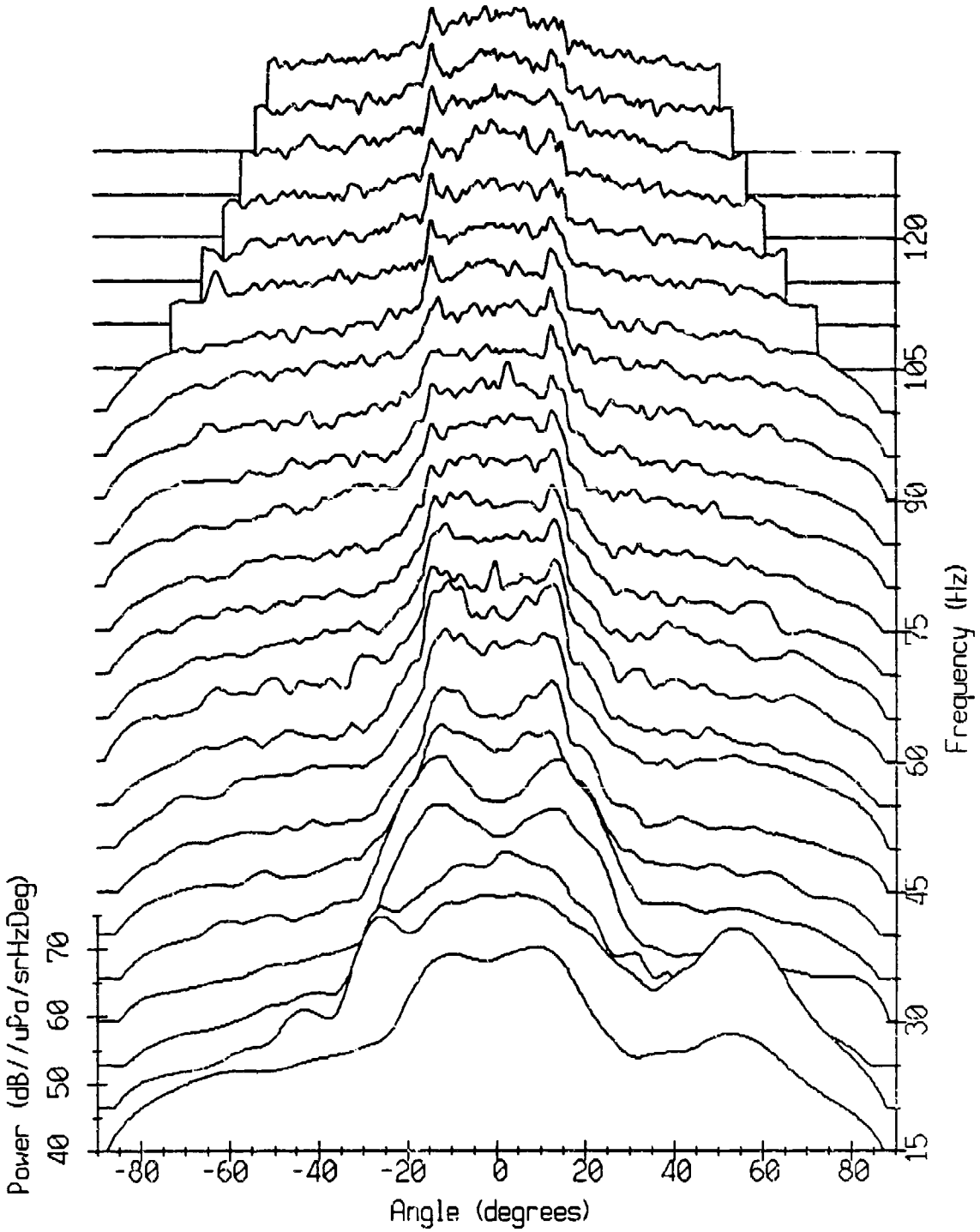

Spatial Distribution During Storm at 0140 GMT

wind speed: 4.6 m/s

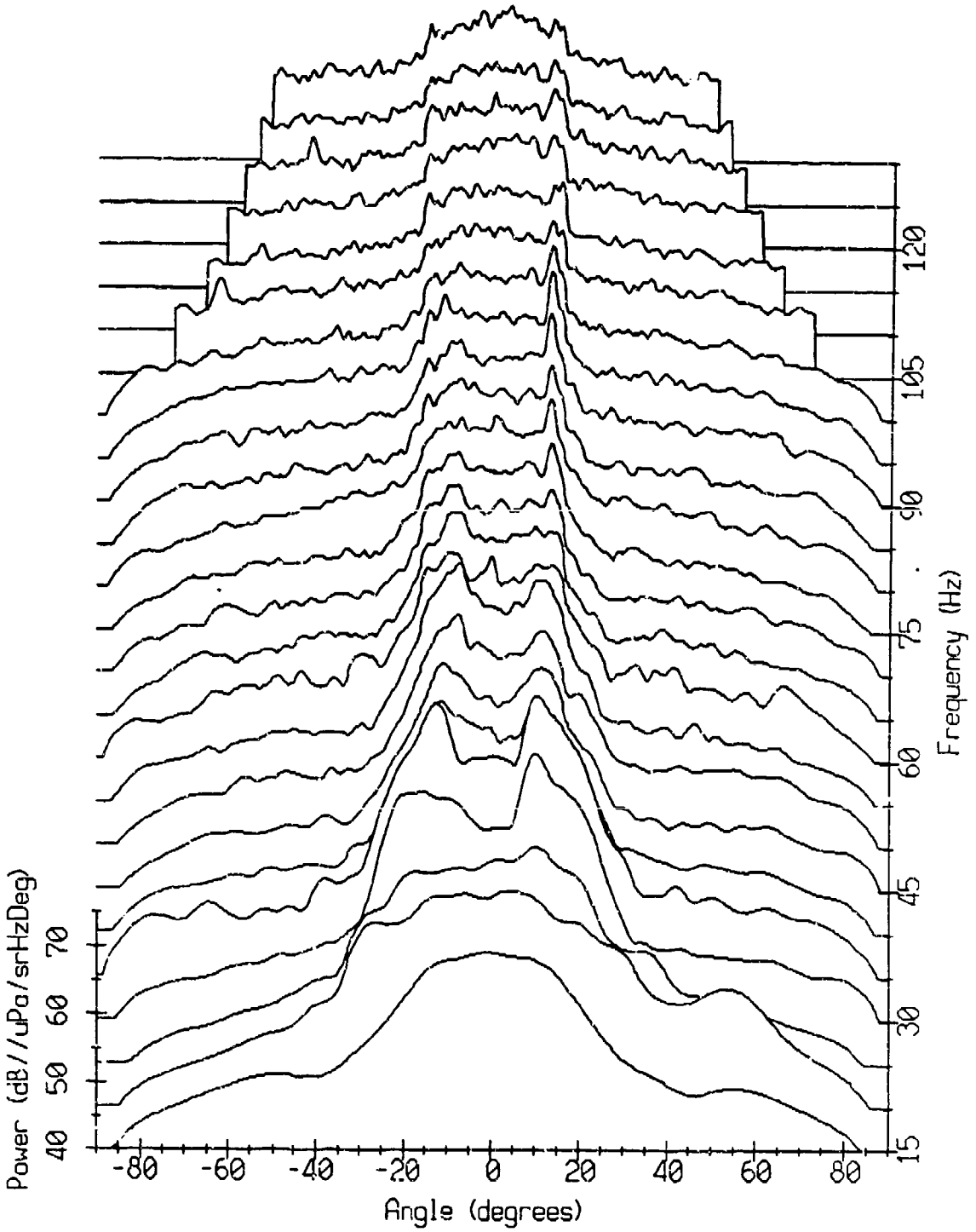

Spatial Distribution During Storm at 0200 GMT

wind speed: 4.9 m/s

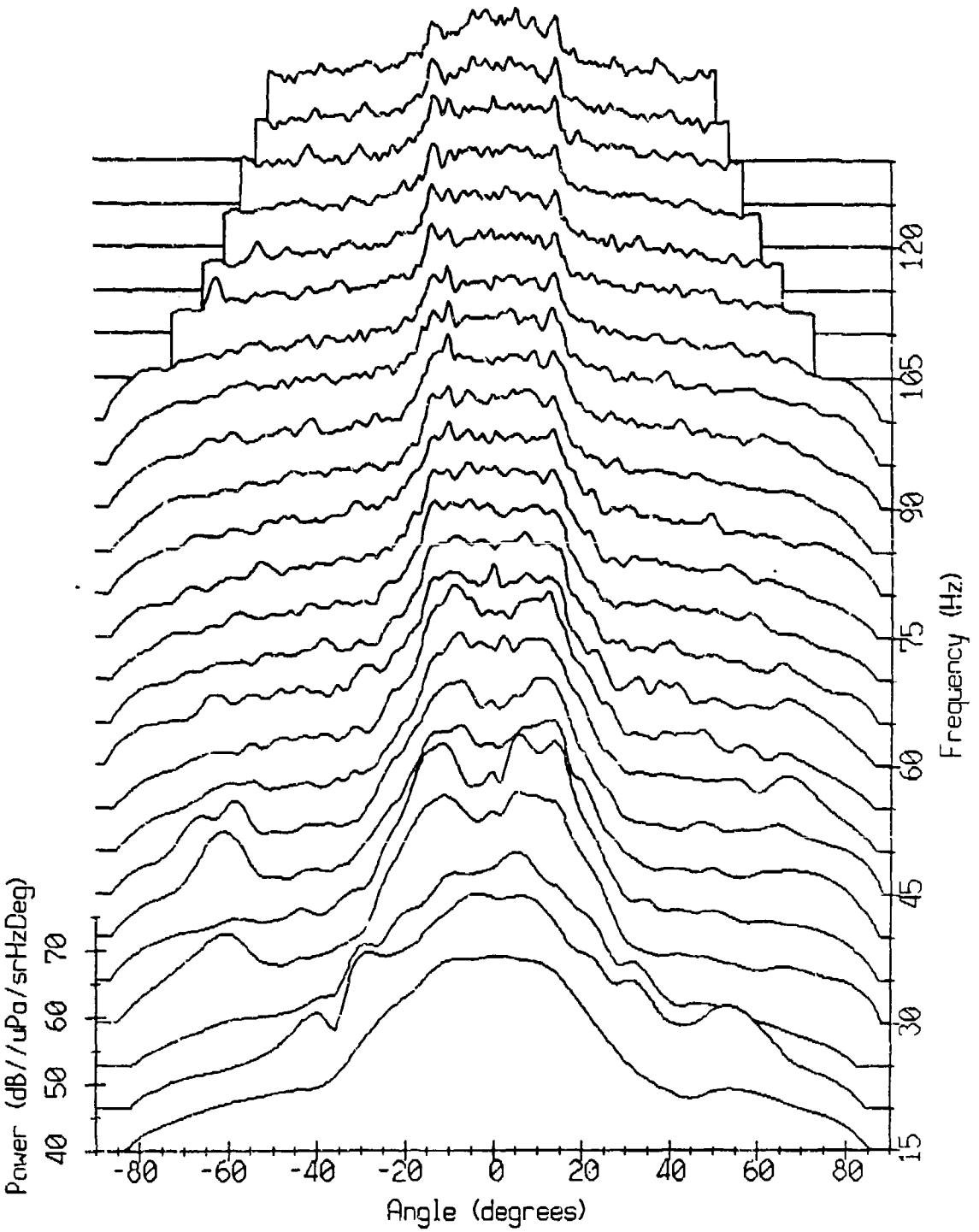

Spatial Distribution During Storm at 0220 GMT

wind speed: 4.8 m/s

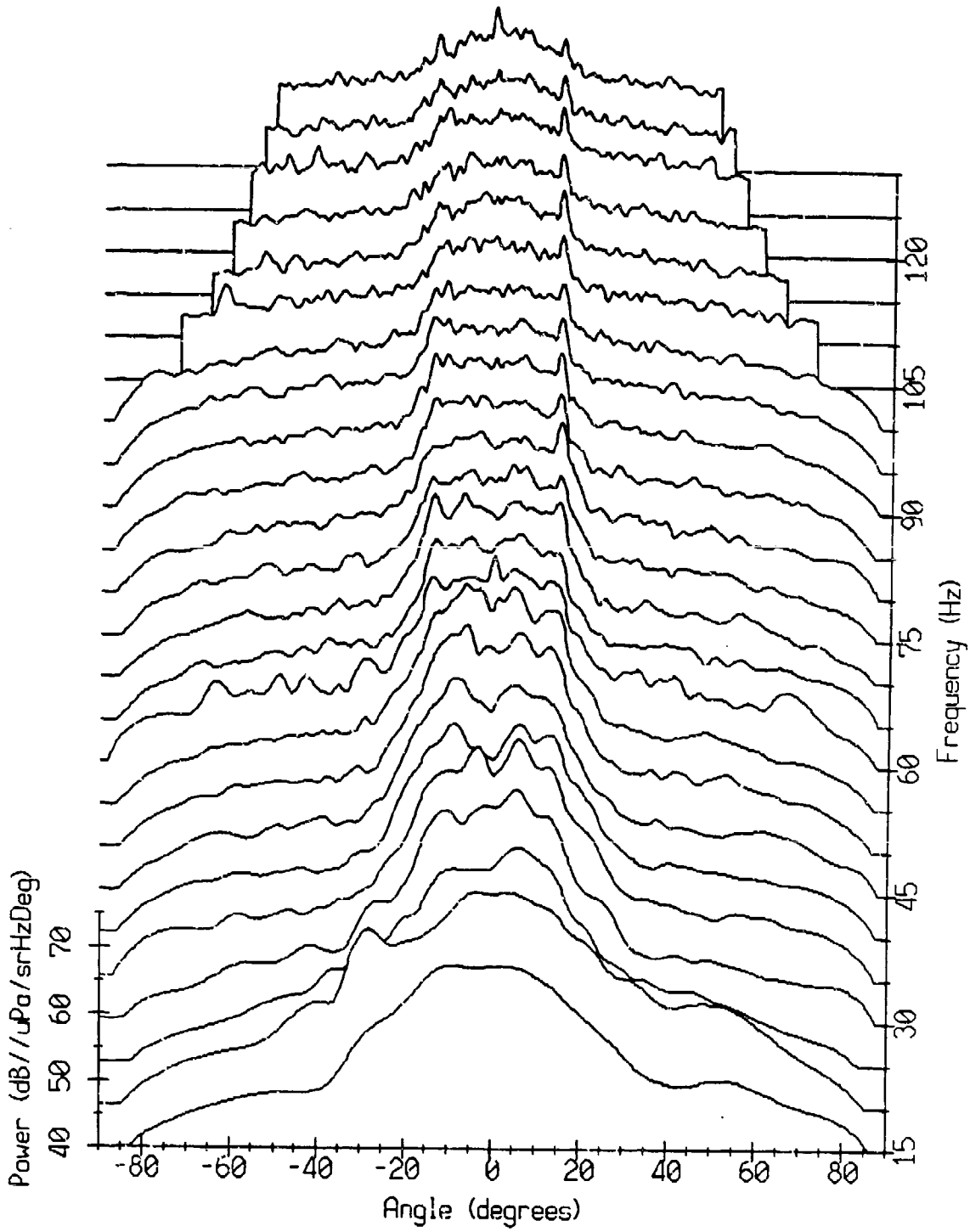

Spatial Distribution During Storm at 0240 GMT

wind speed: 4.7 m/s

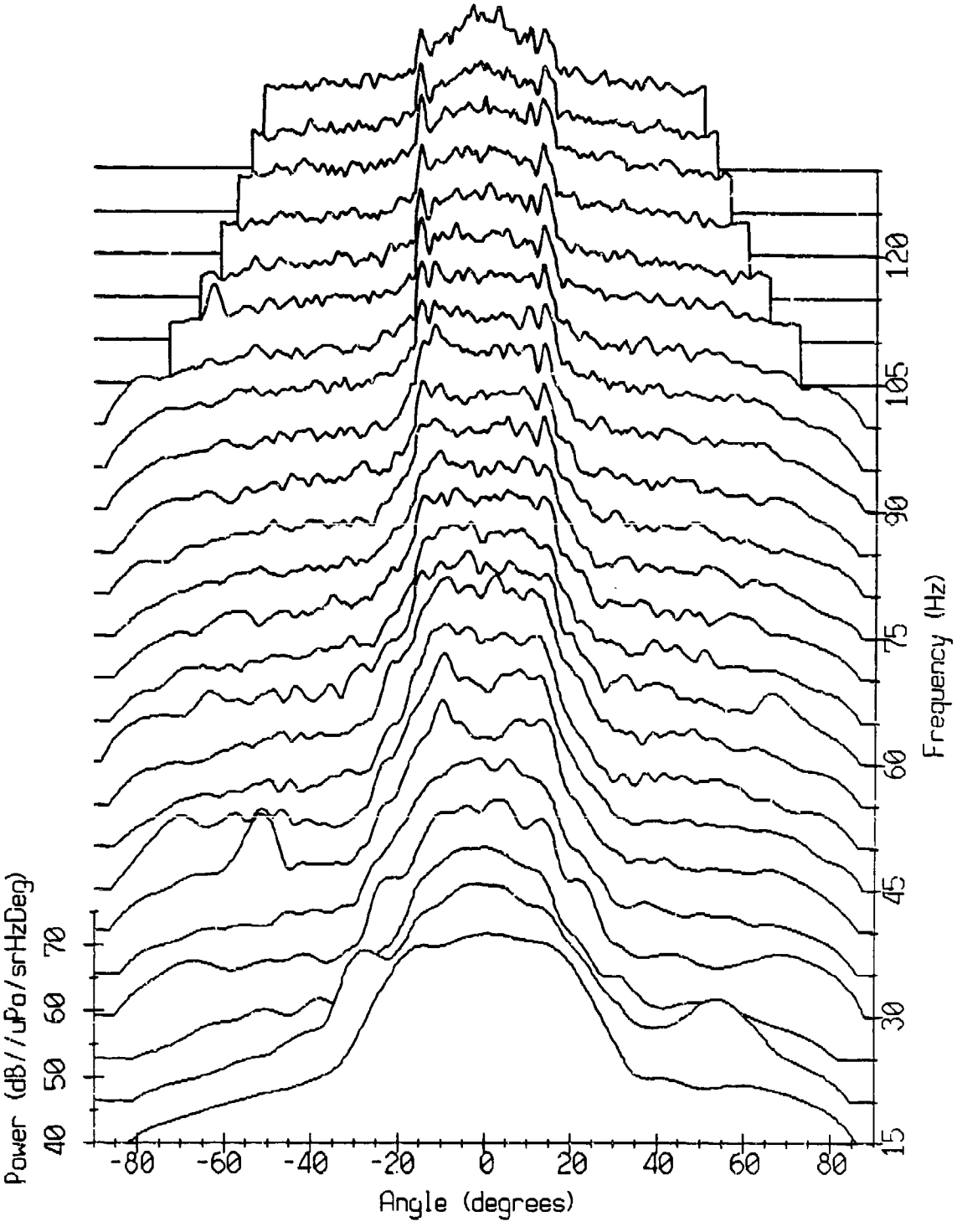

# Spatial Distribution During Storm at 0300 GMT

wind speed: 4.6 m/s

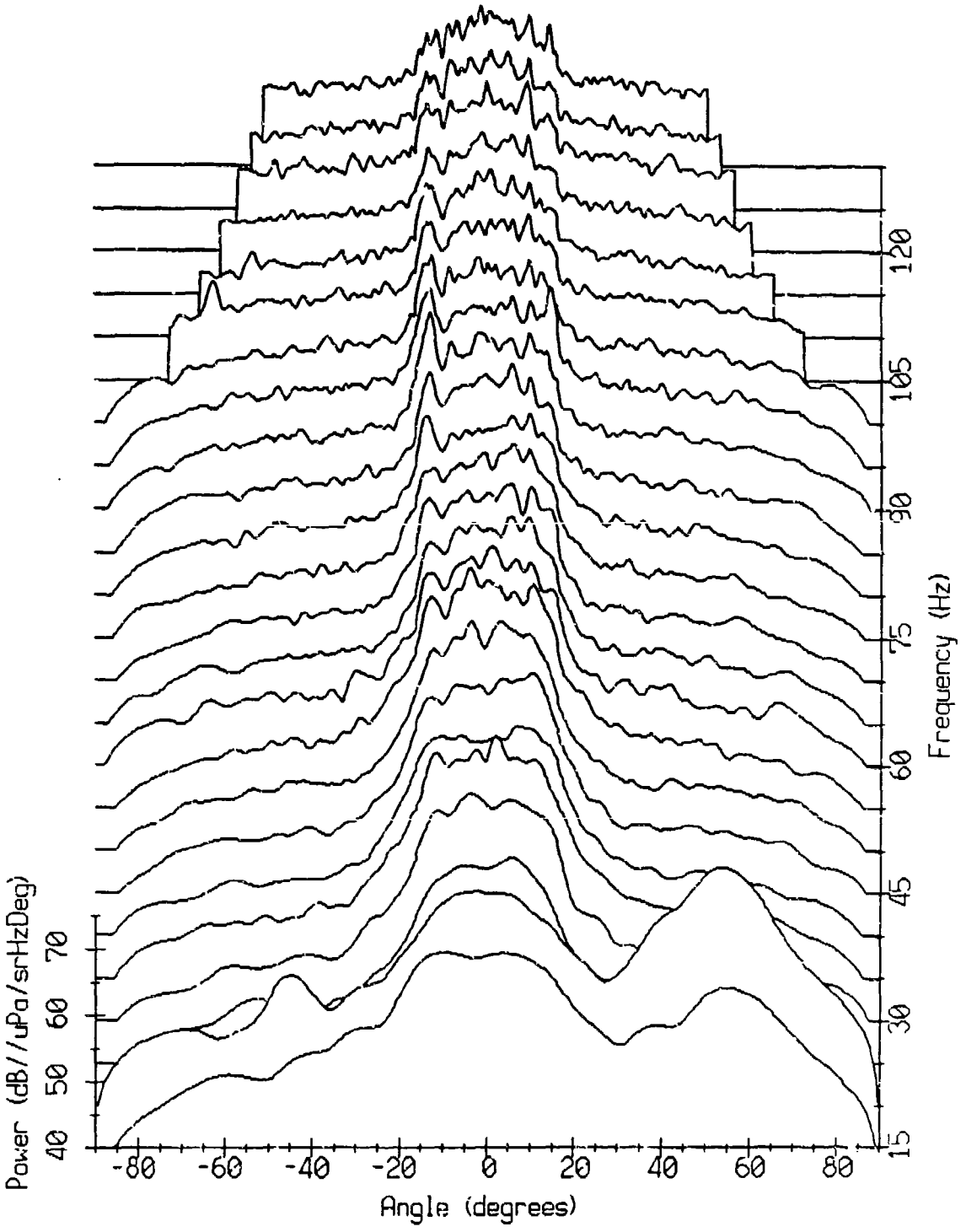

# Spatial Distribution During Storm at 0320 GMT

wind speed: 4.6 m/s

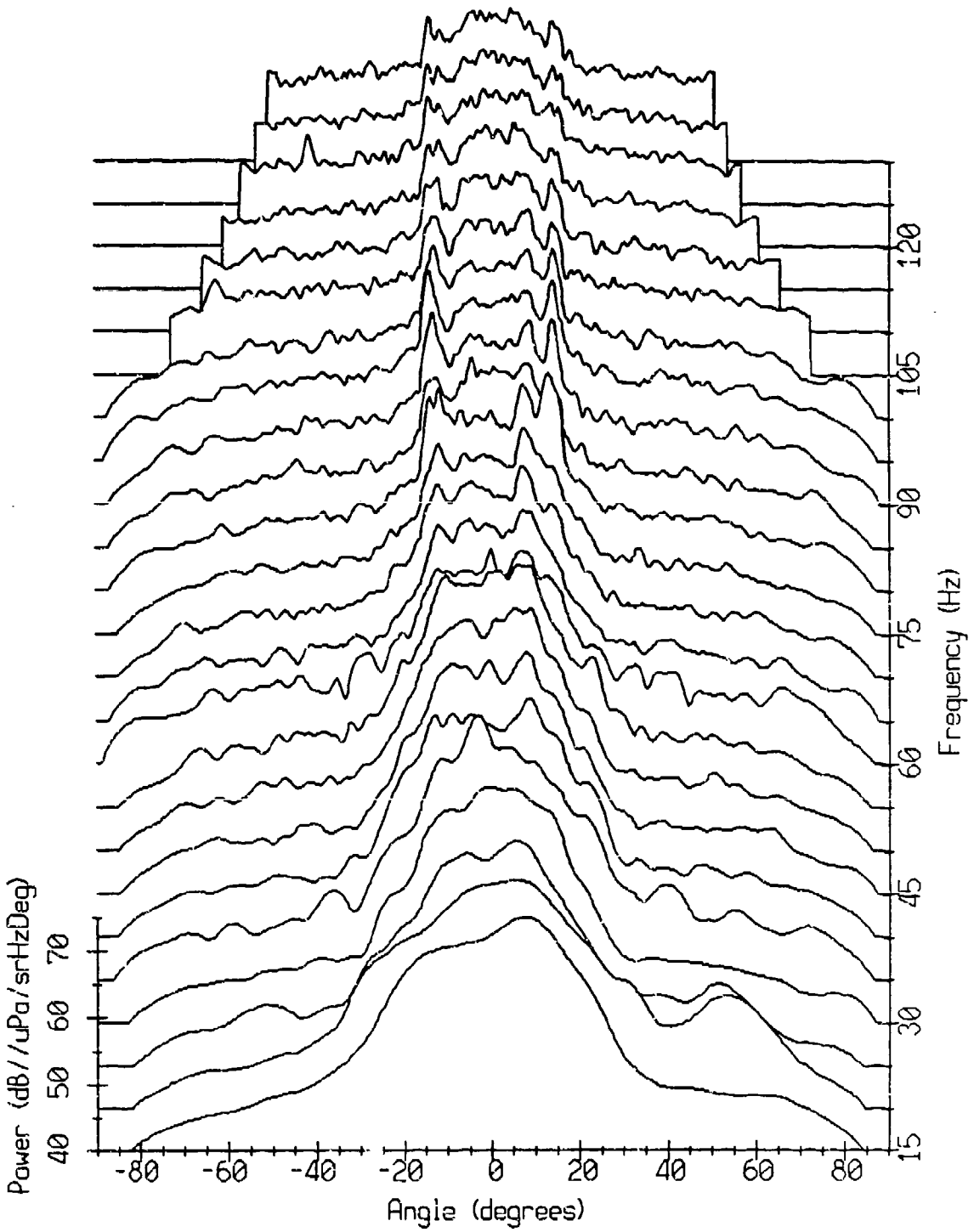

Spatial Distribution During Storm at 0340 GMT

wind speed: 4.6 m/s

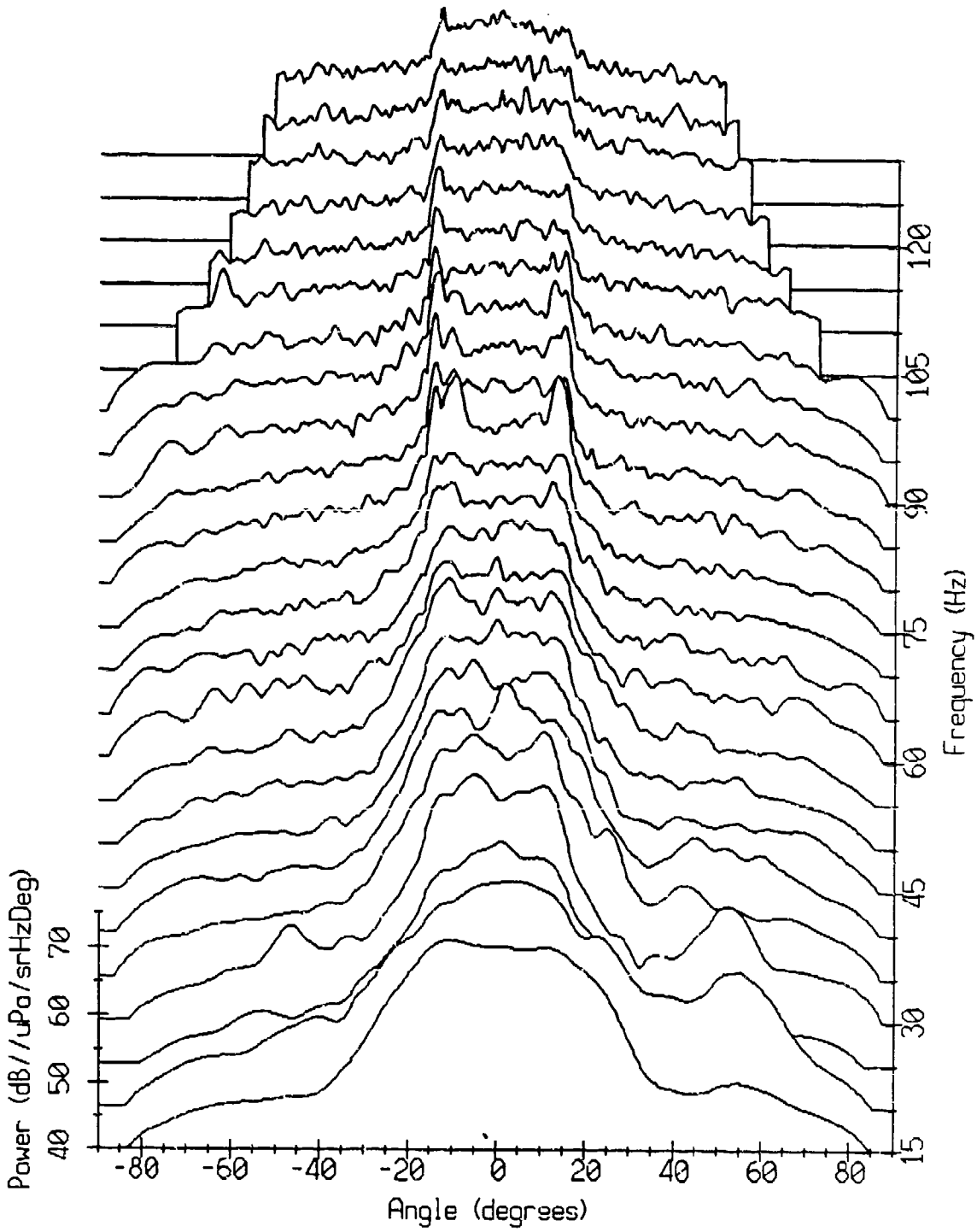

Spatial Distribution During Storm at 0400 GMT

wind speed: 4.6 m/s

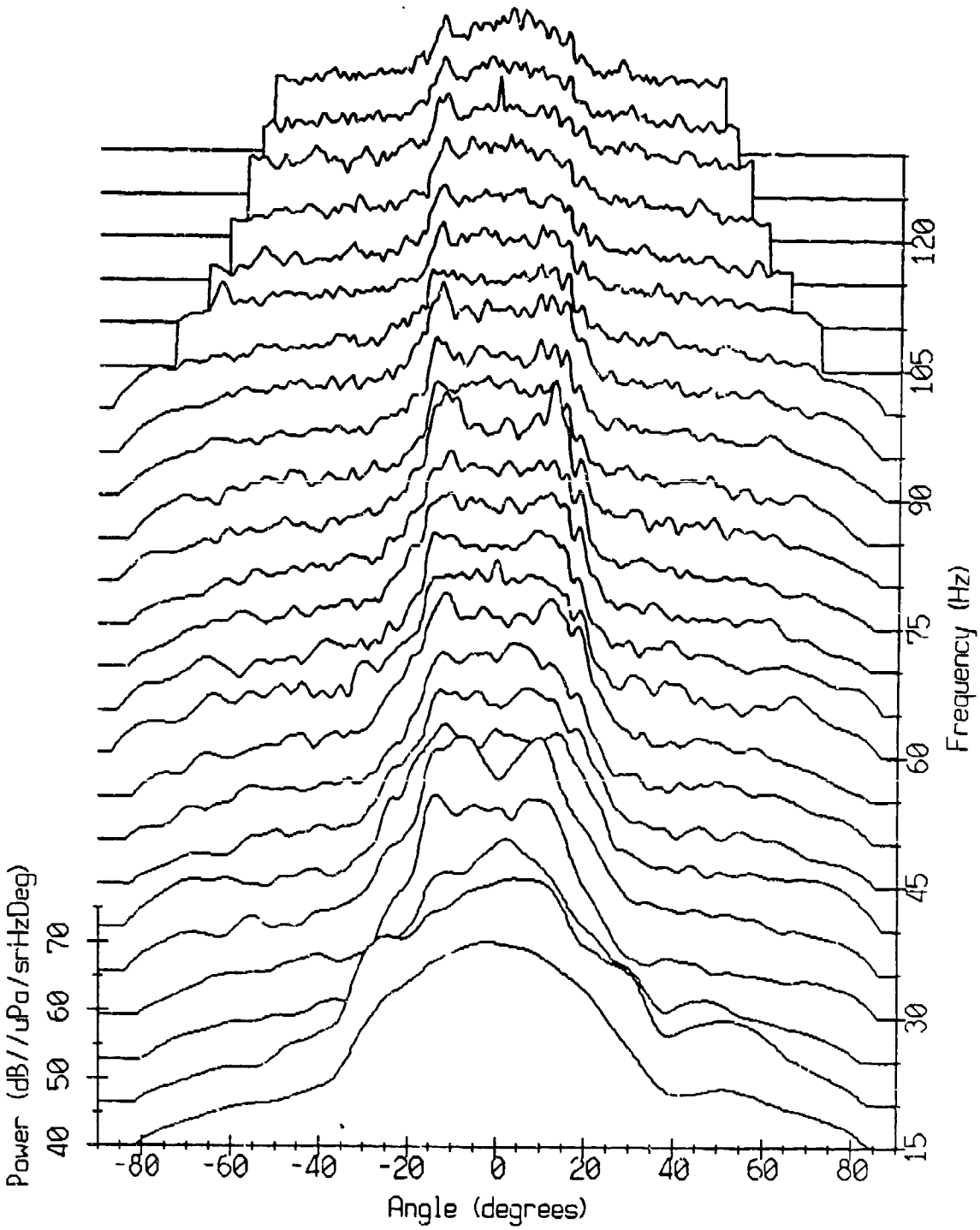

# Spatial Distribution During Storm at 0420 GMT

wind speed: 4.6 m/s

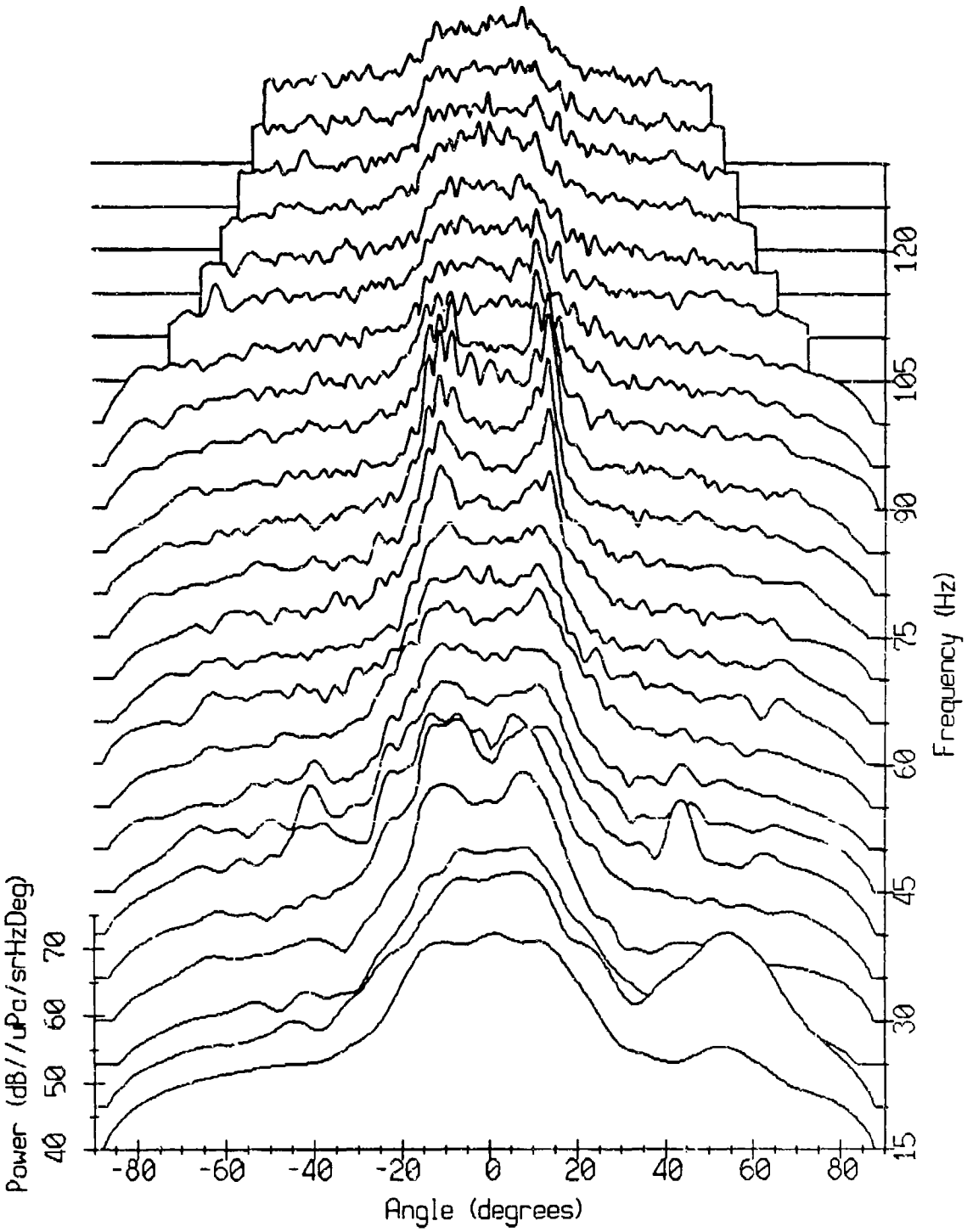

# Spatial Distribution During Storm at 0440 GMT

wind speed: 4.6 m/s

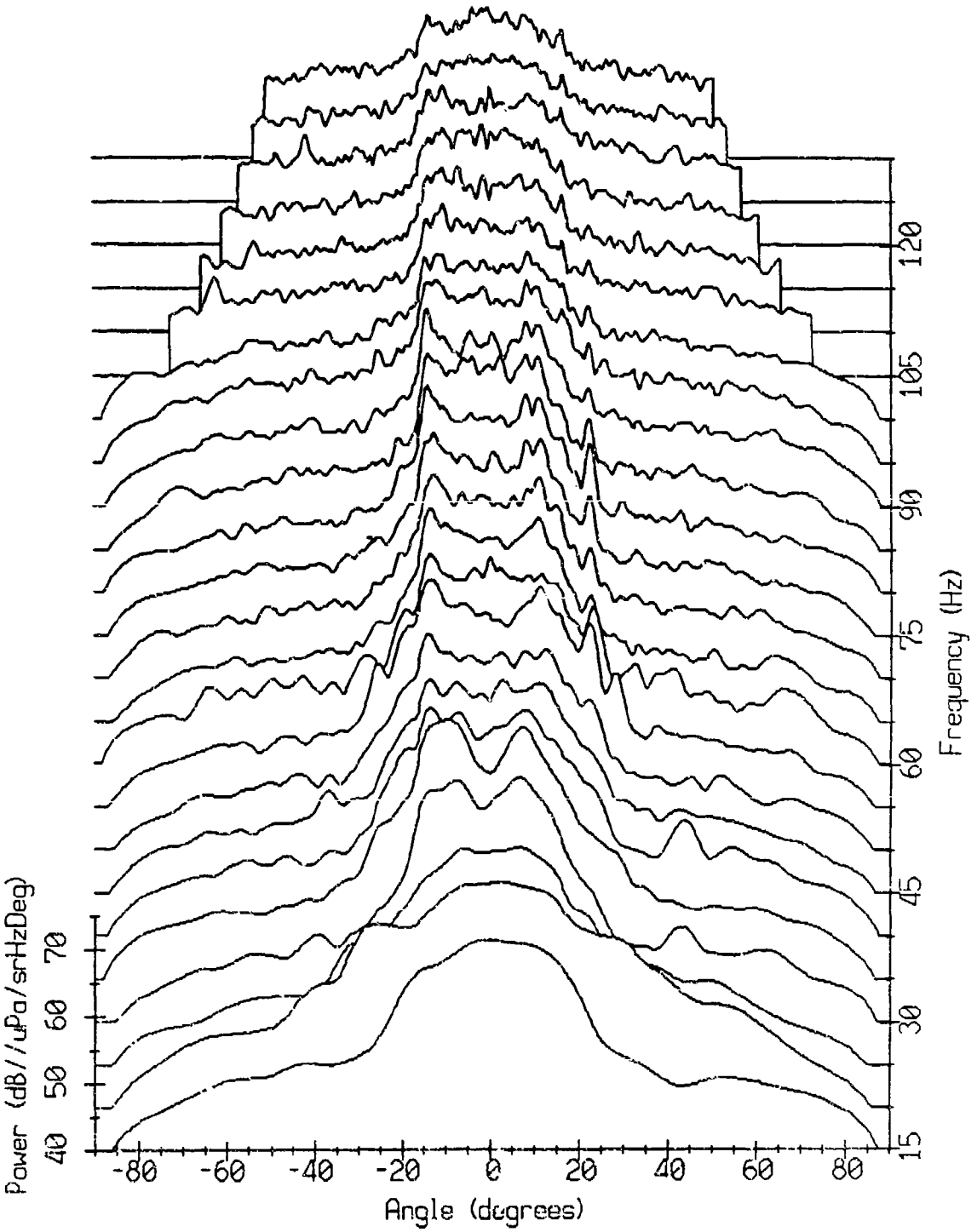

Spatial Distribution During Storm at 0500 GMT

wind speed: 4.6 m/s

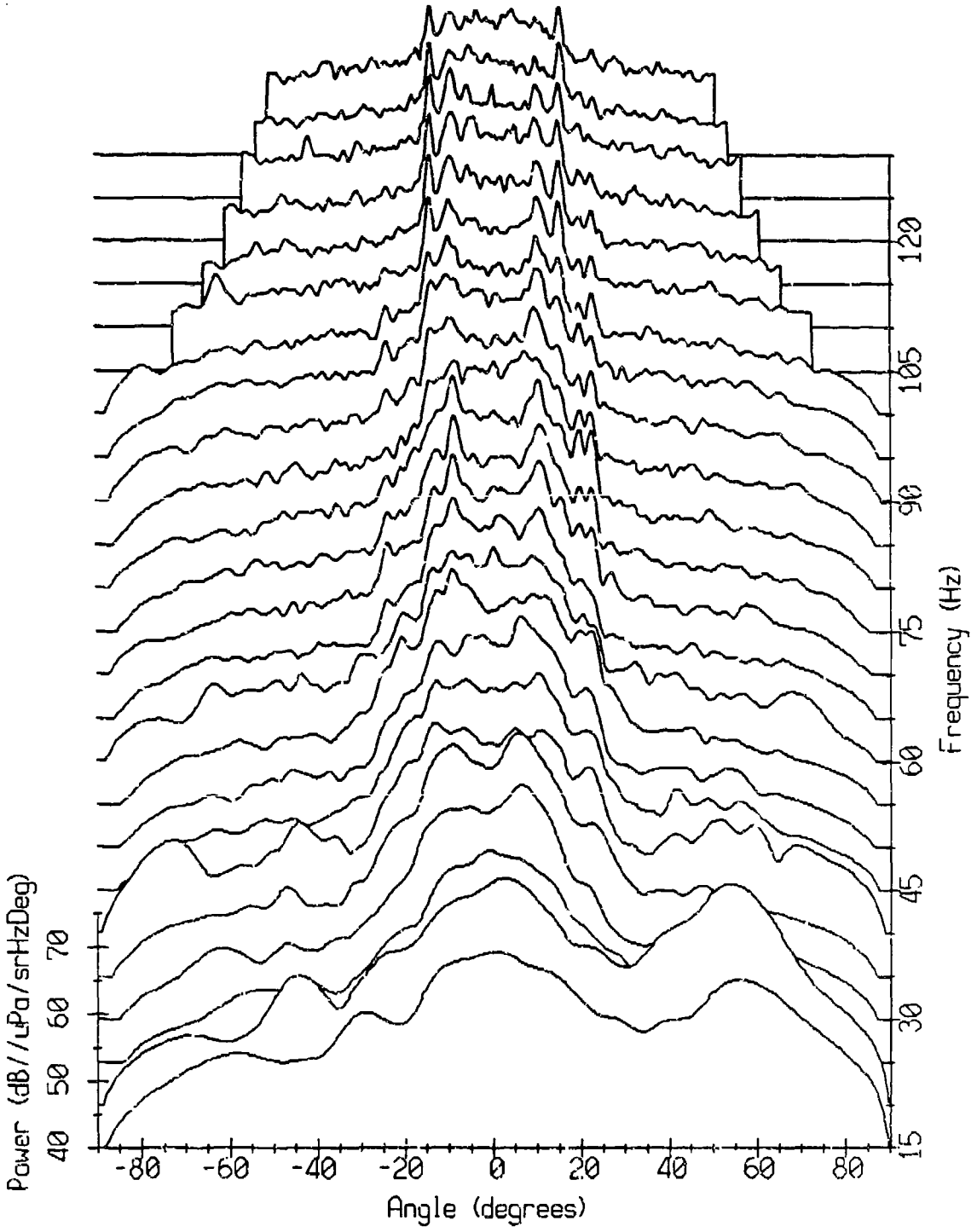

Spatial Distribution During Storm at 0520 GMT

wind speed: 4.3 m/s

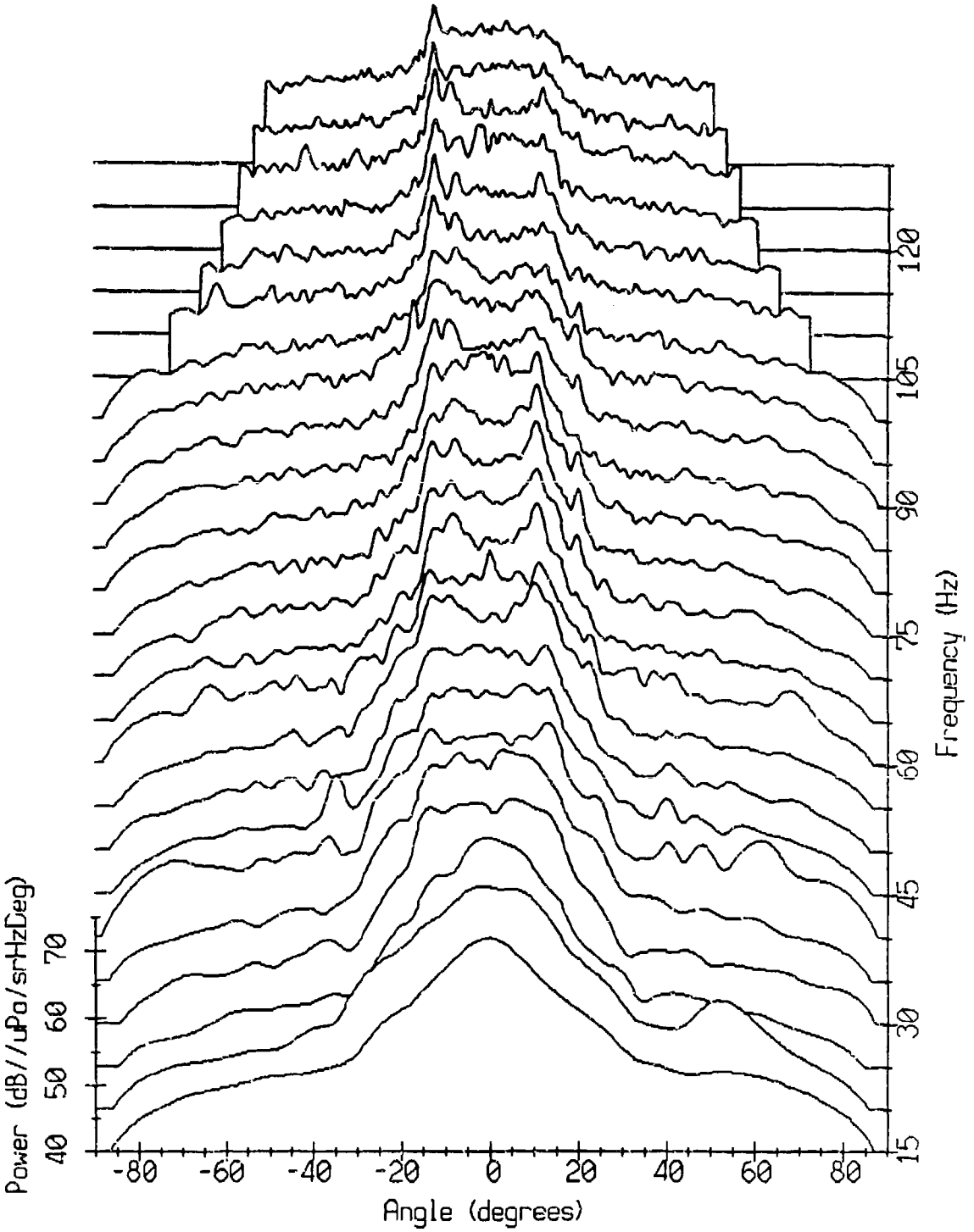

Spatial Distribution During Storm at 0540 GMT

wind speed: 4.0 m/s

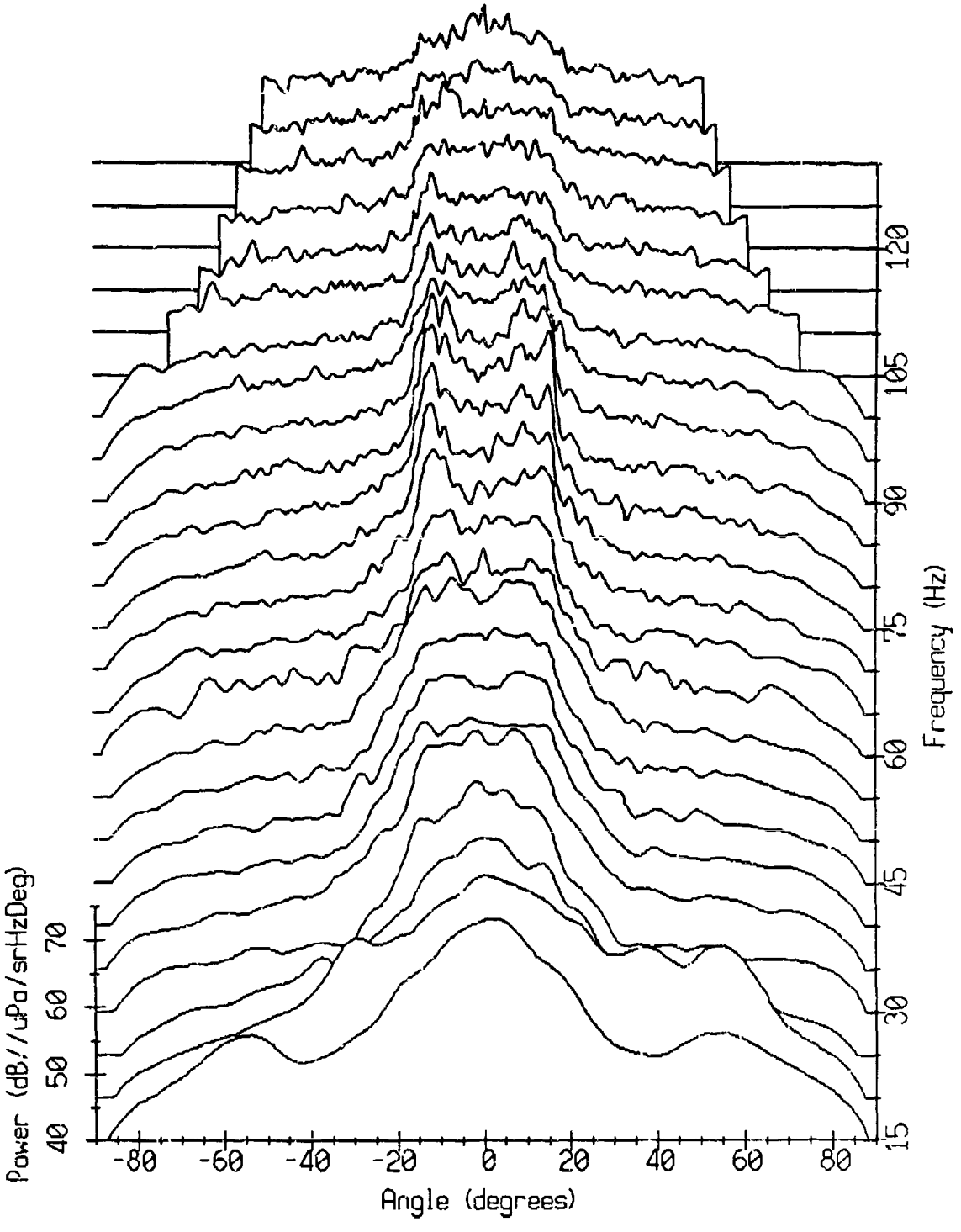

Spatial Distribution During Storm at 0600 GMT

wind speed: 3.6 m/s

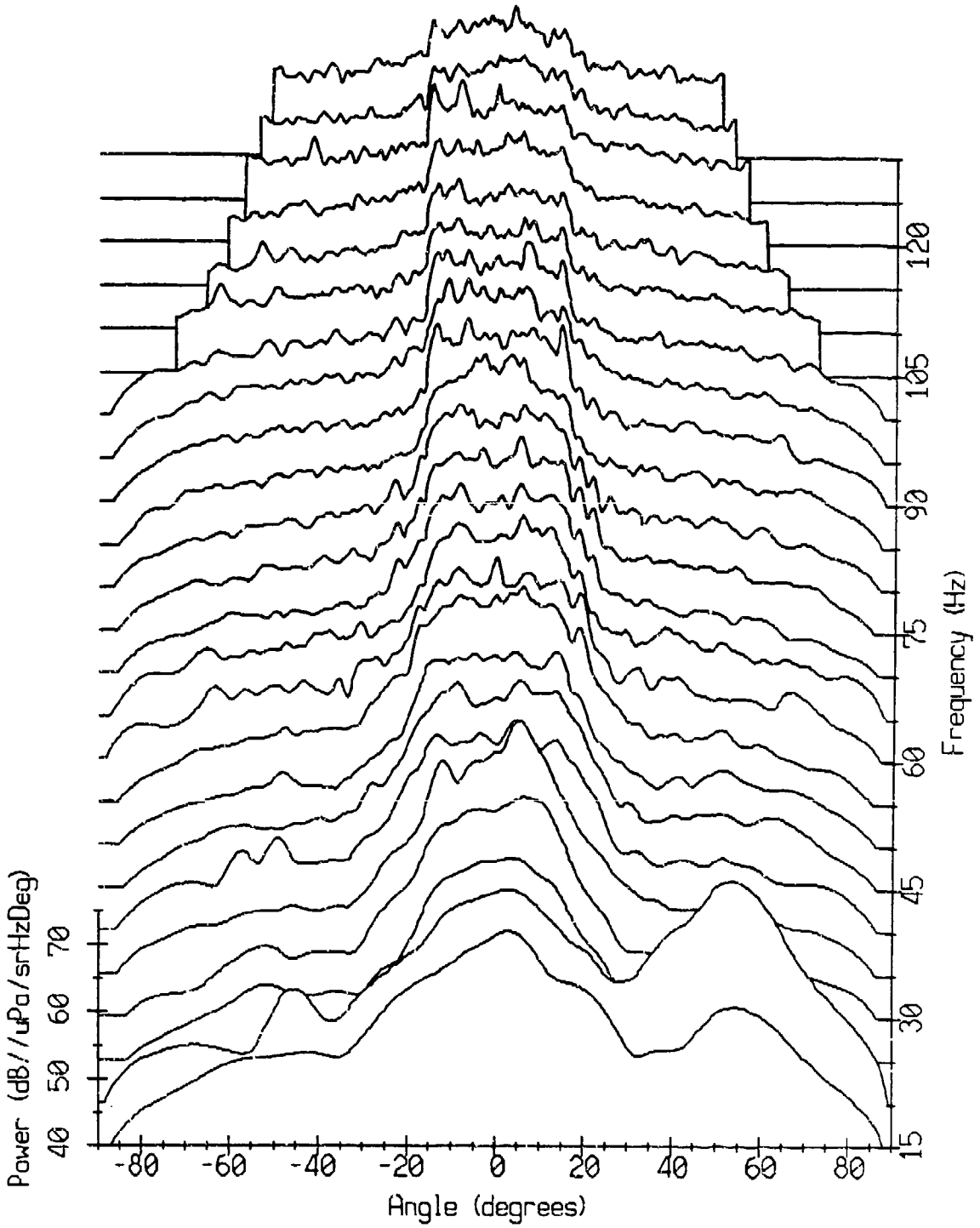

# Spatial Distribution During Storm at 0620 GMT

wind speed: 3.6 m/s

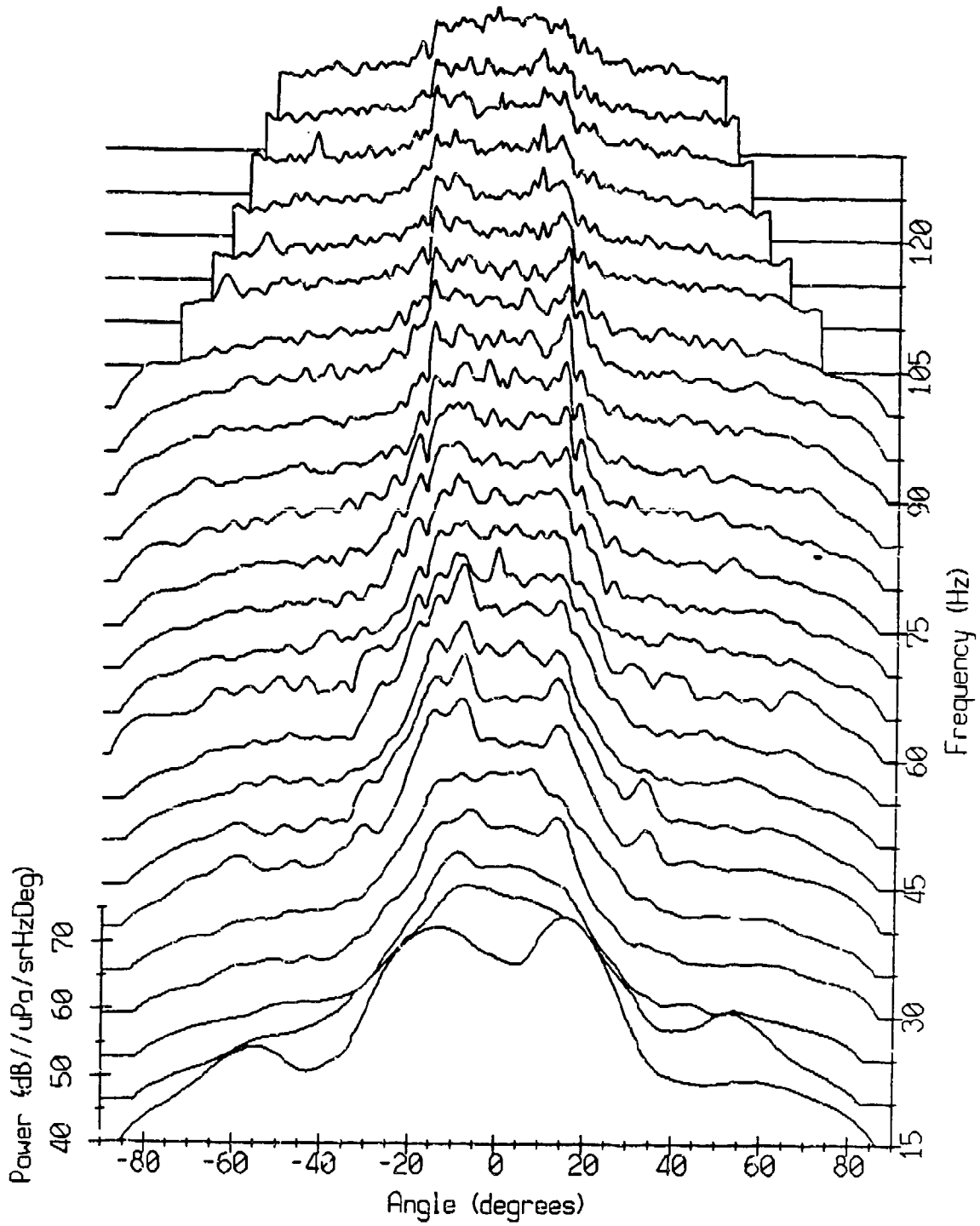

Spatial Distribution During Storm at 0640 GMT

wind speed: 3.6 m/s

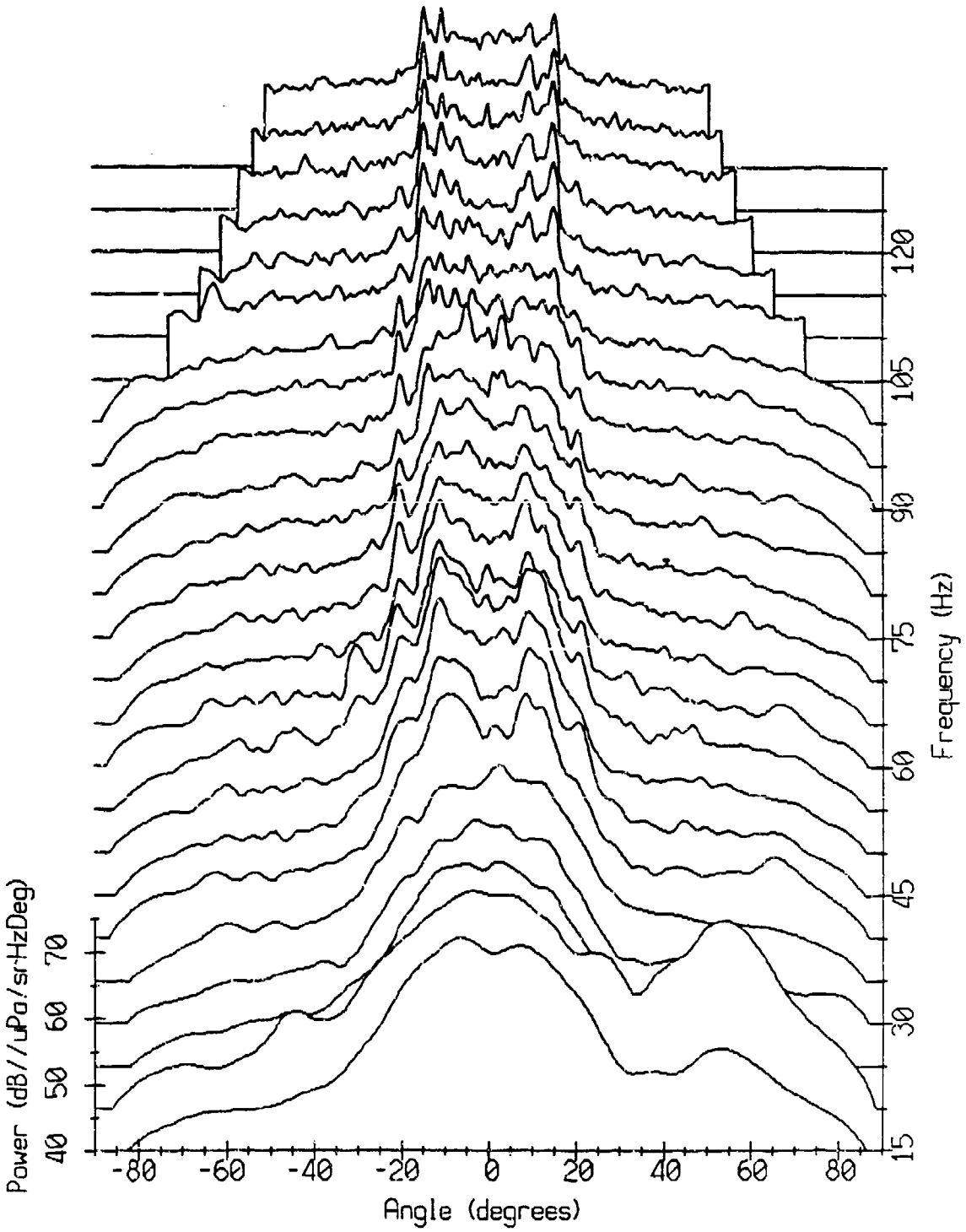

Spatial Distribution During Storm at 0700 GMT

wind speed: 3.6 m/s

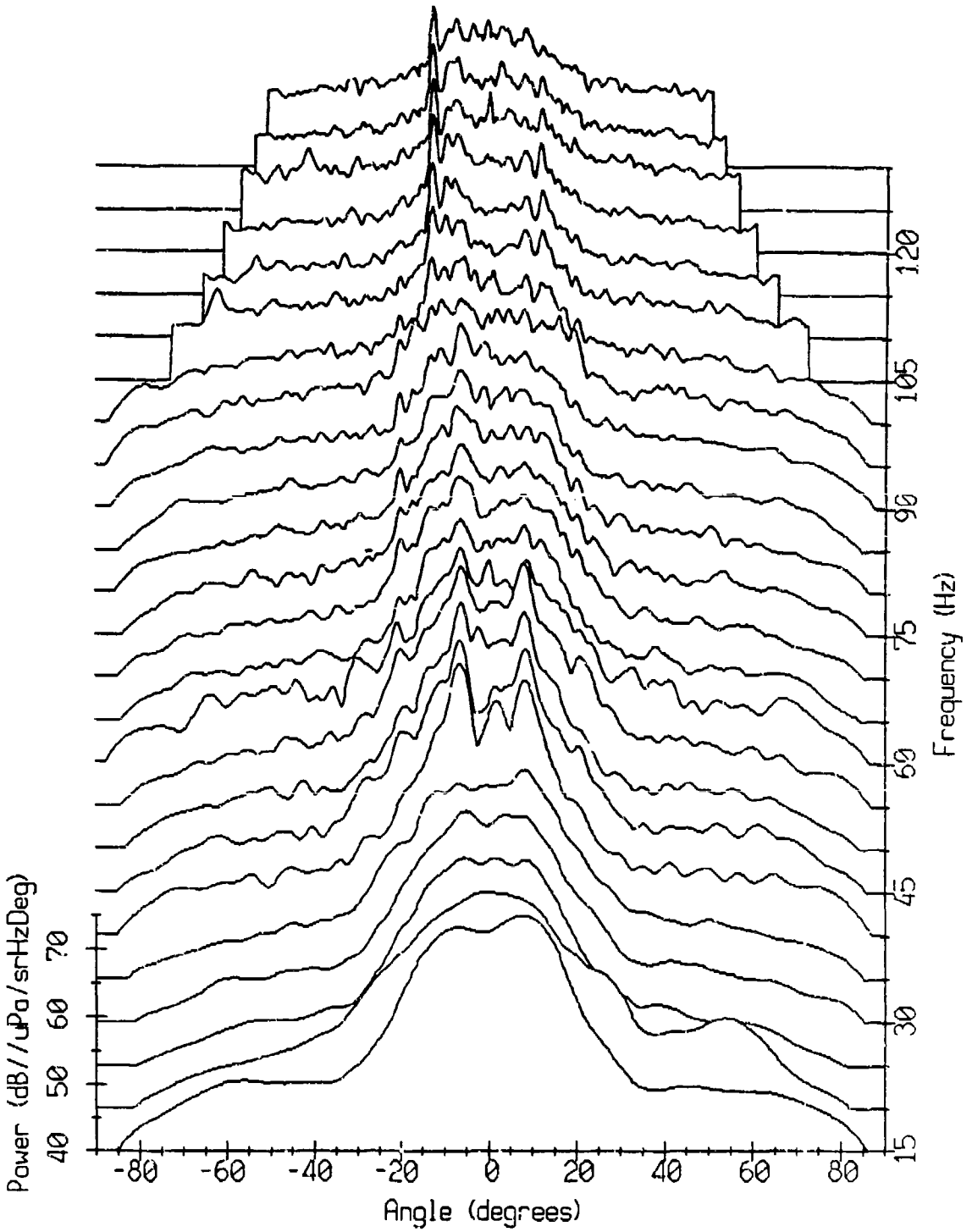

Spatial Distribution During Storm at 0720 GMT

wind speed: 3.8 m/s

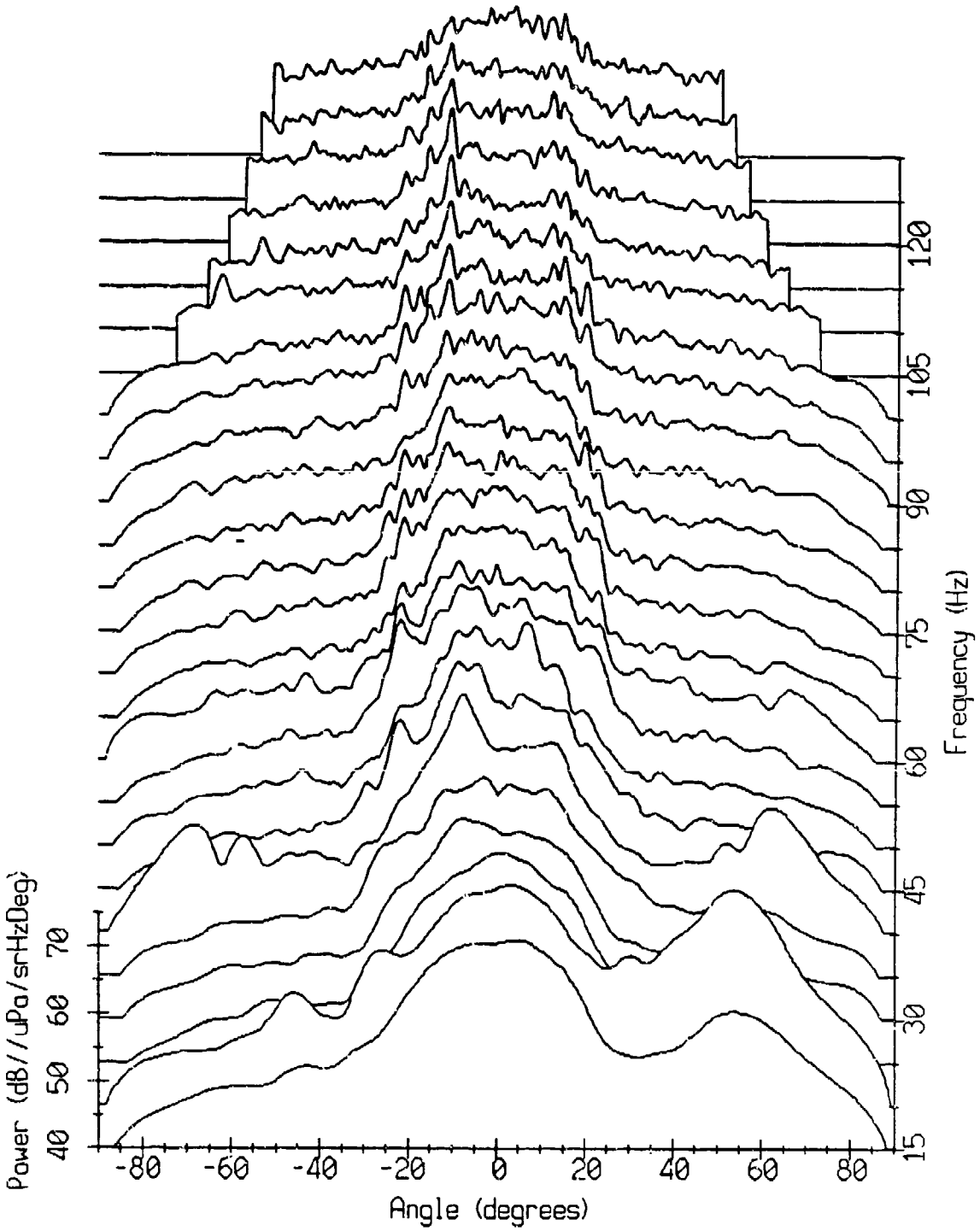

Spatial Distribution During Storm at 0740 GMT

wind speed: 4.0 m/s

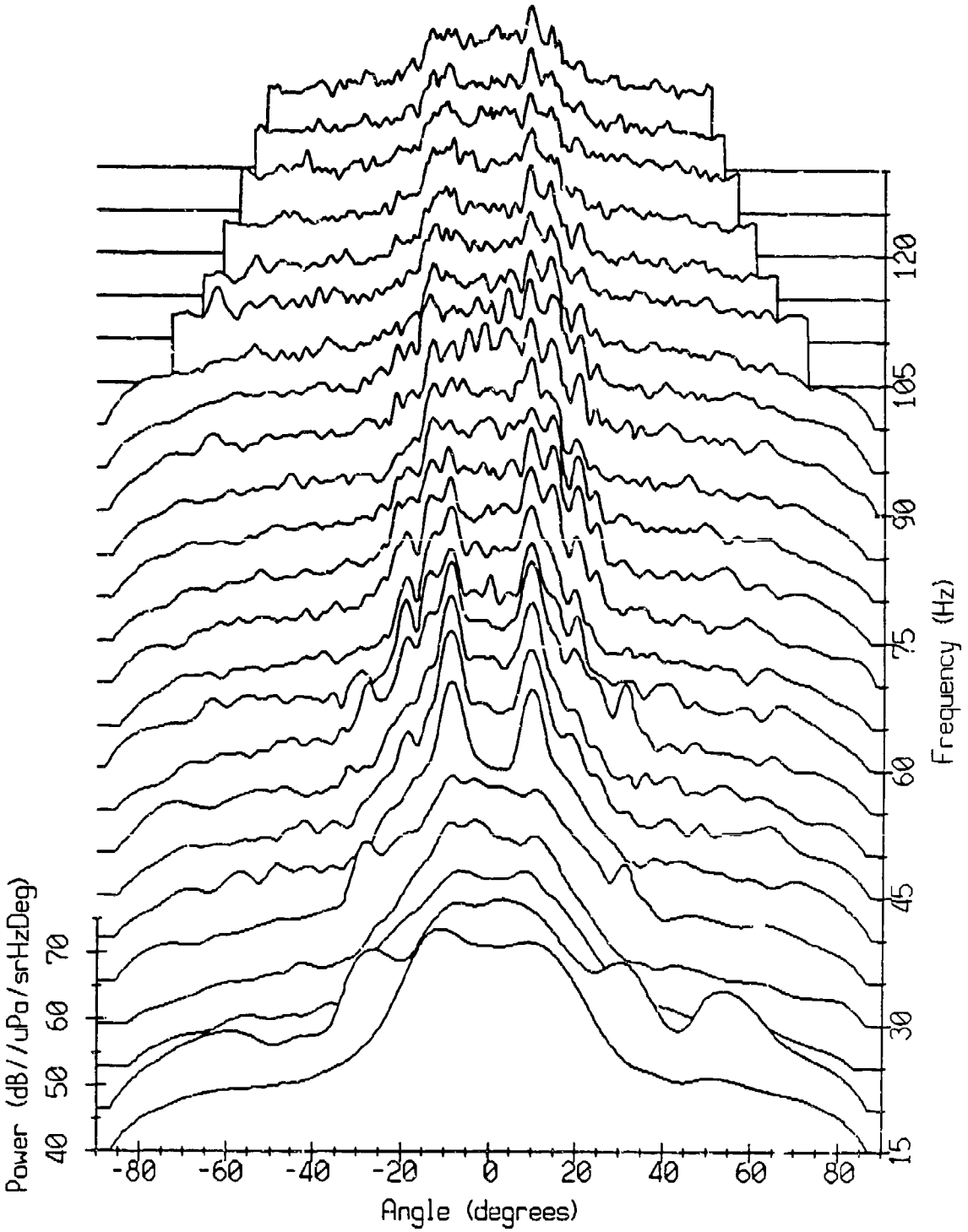

Spatial Distribution During Storm at 0800 GMT

wind speed: 4.1 m/s

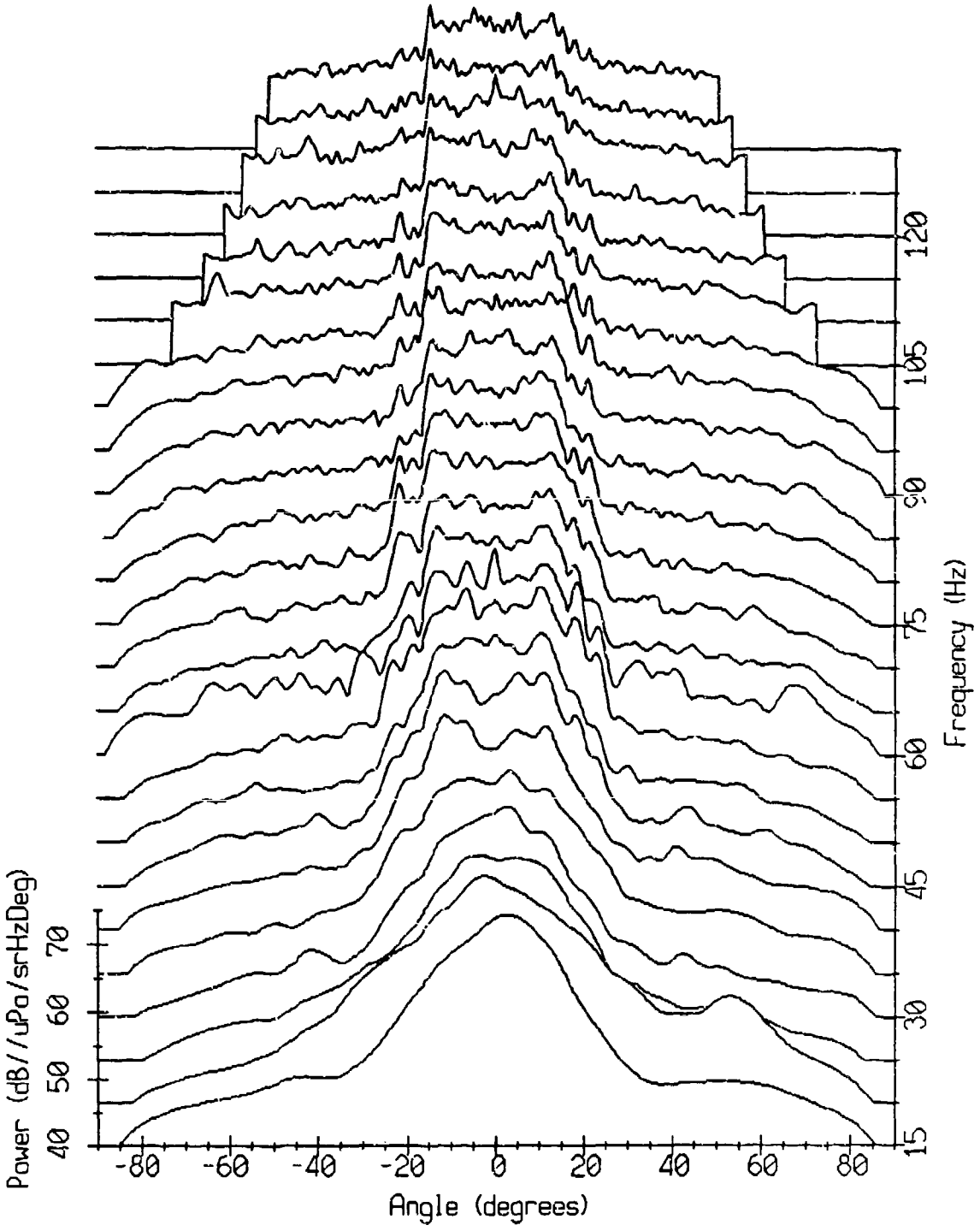

Spatial Distribution During Storm at 0820 GMT

wind speed: 5.0 m/s

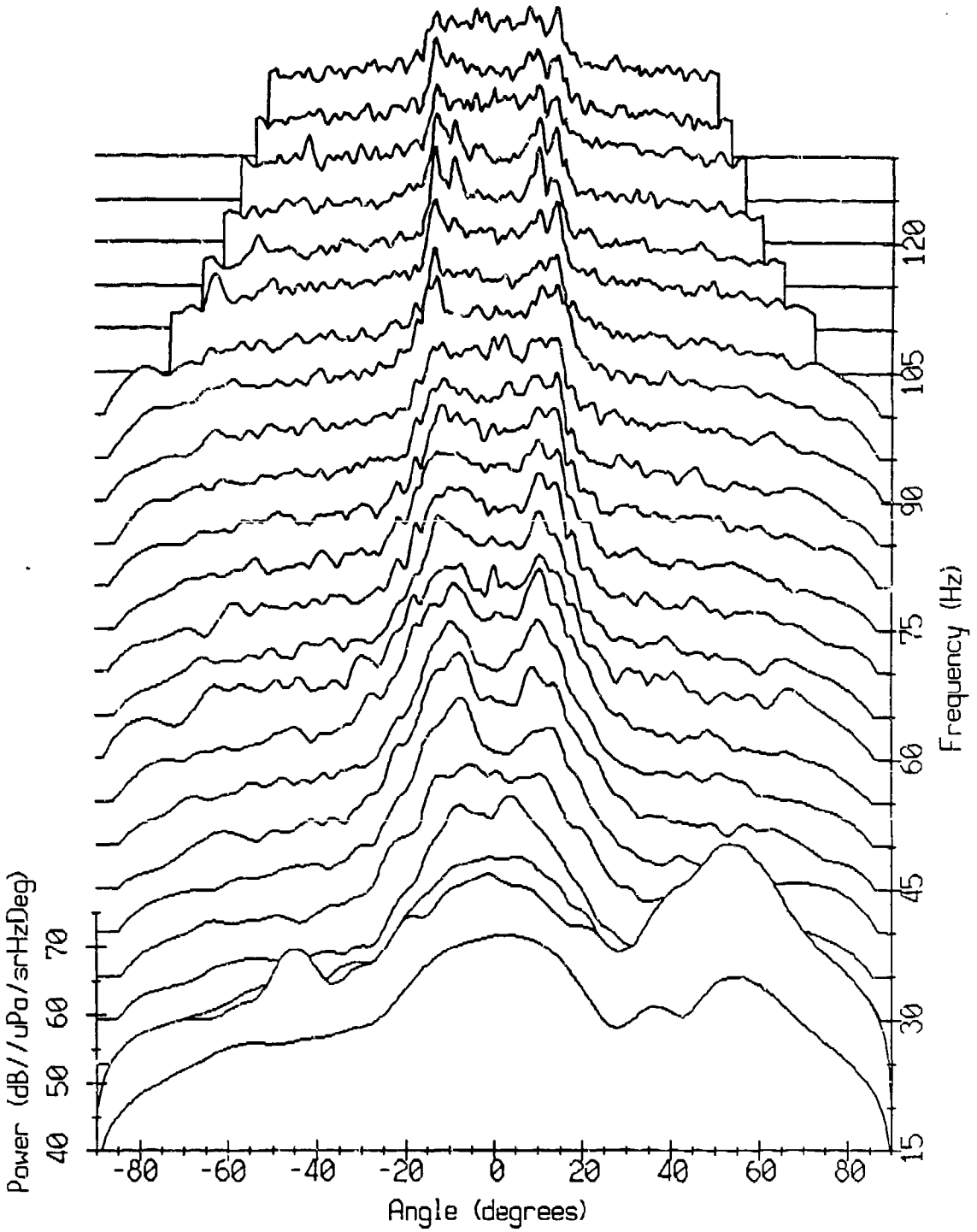

Spatial Distribution During Storm at 0840 GMT

wind speed: 5.8 m/s

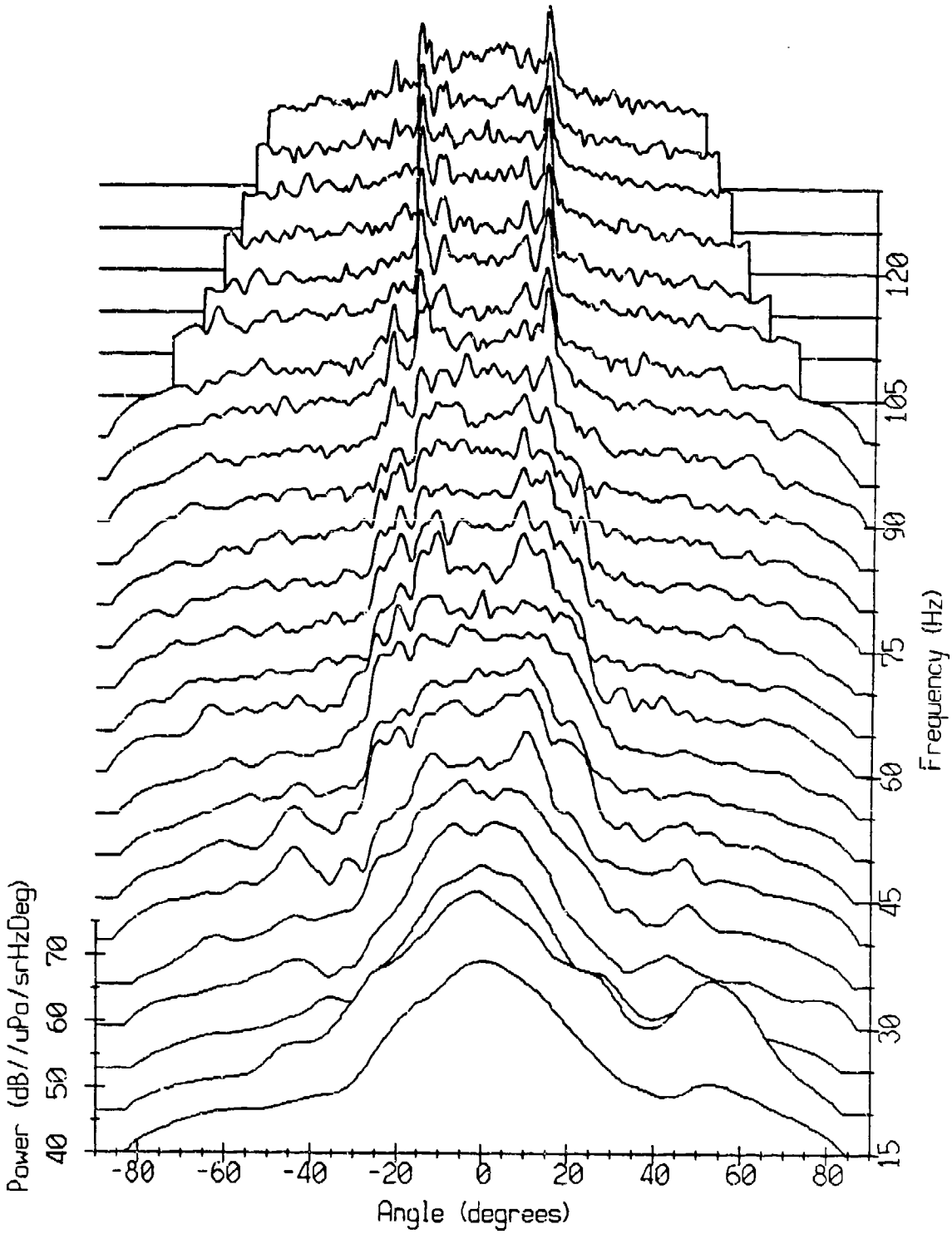

# Spatial Distribution During Storm at 0900 GMT

wind speed: 6.7 m/s

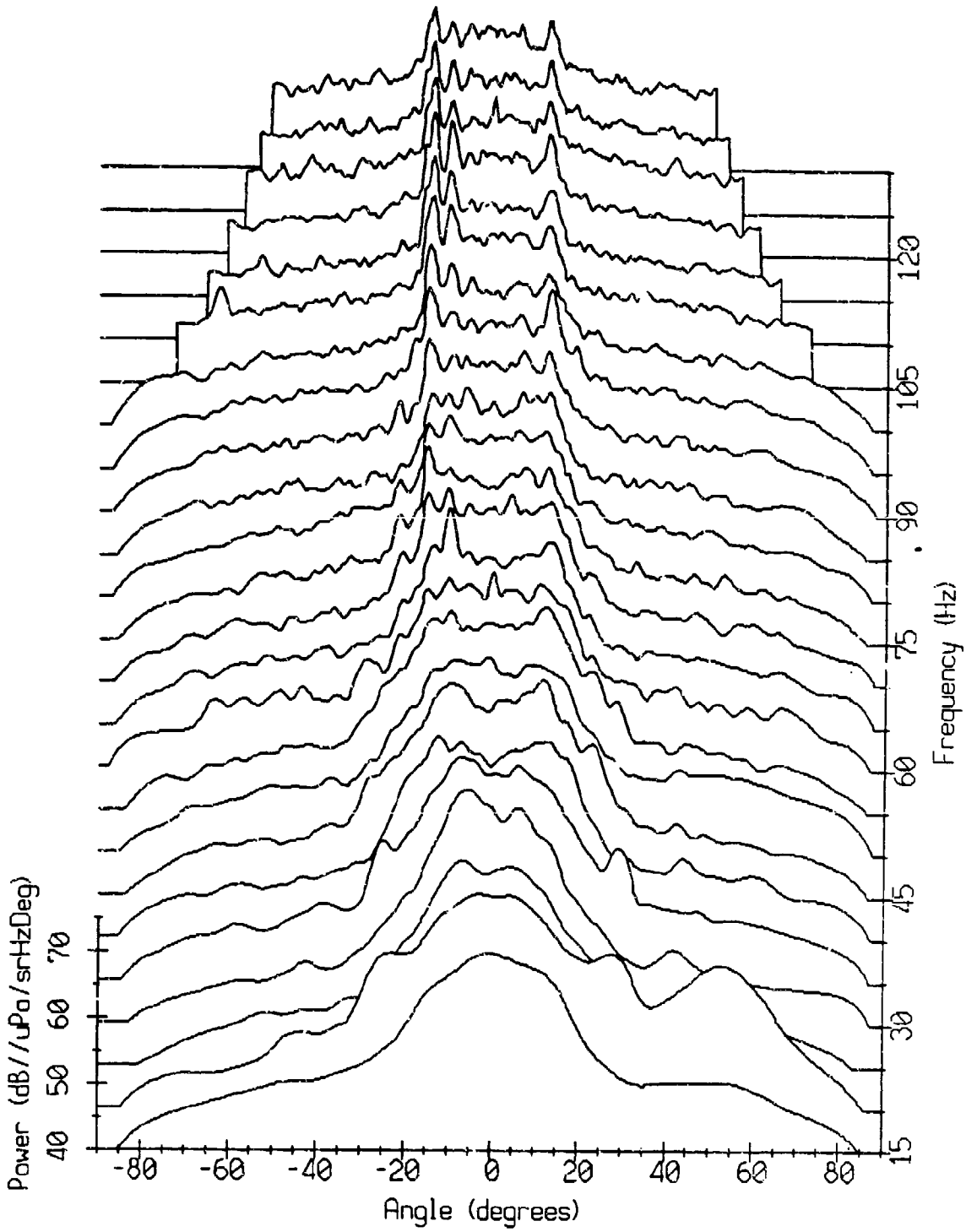

Spatial Distribution During Storm at 0920 GMT

wind speed: 7.6 m/s

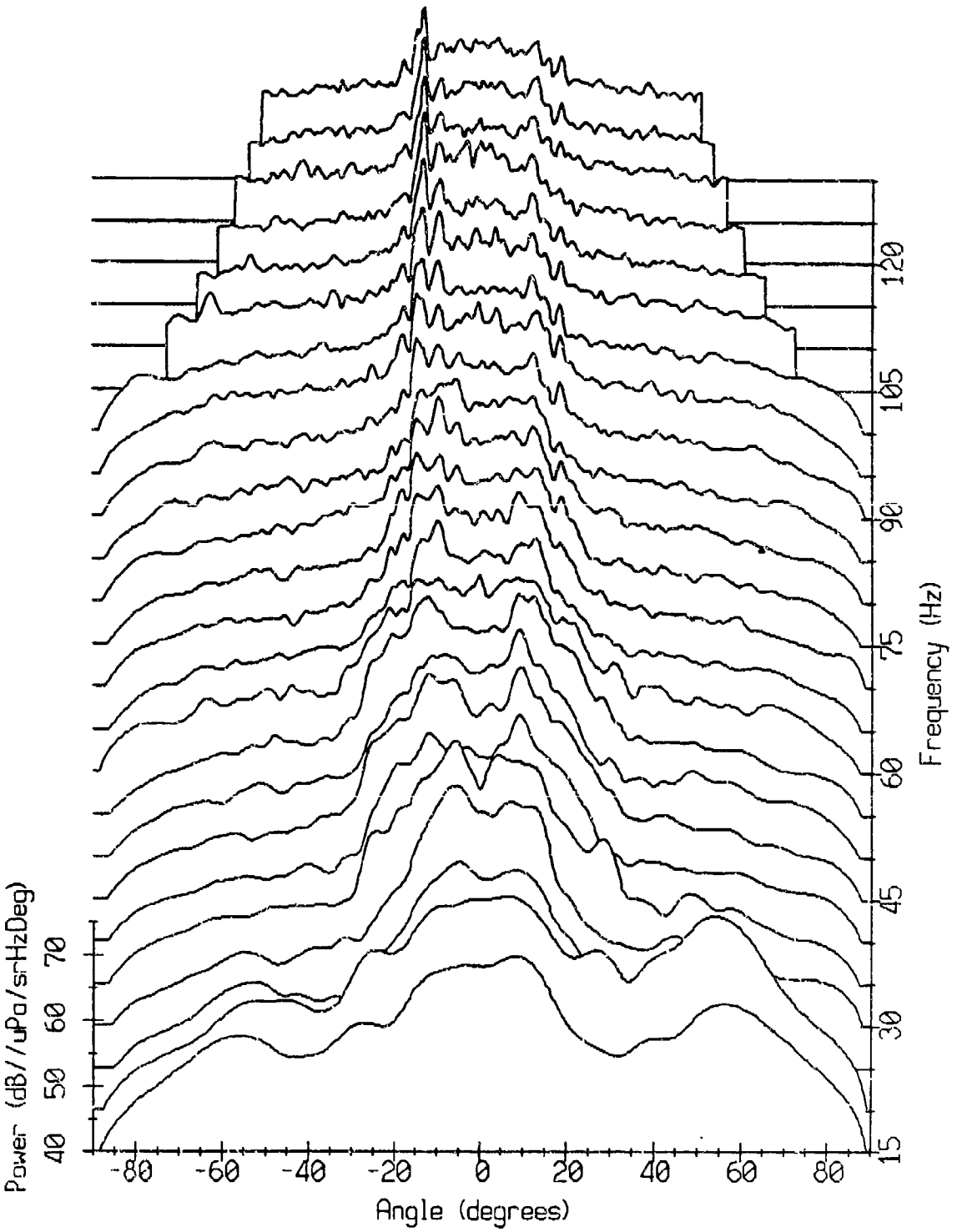

# Spatial Distribution During Storm at 0940 GMT

wind speed: 8.4 m/s

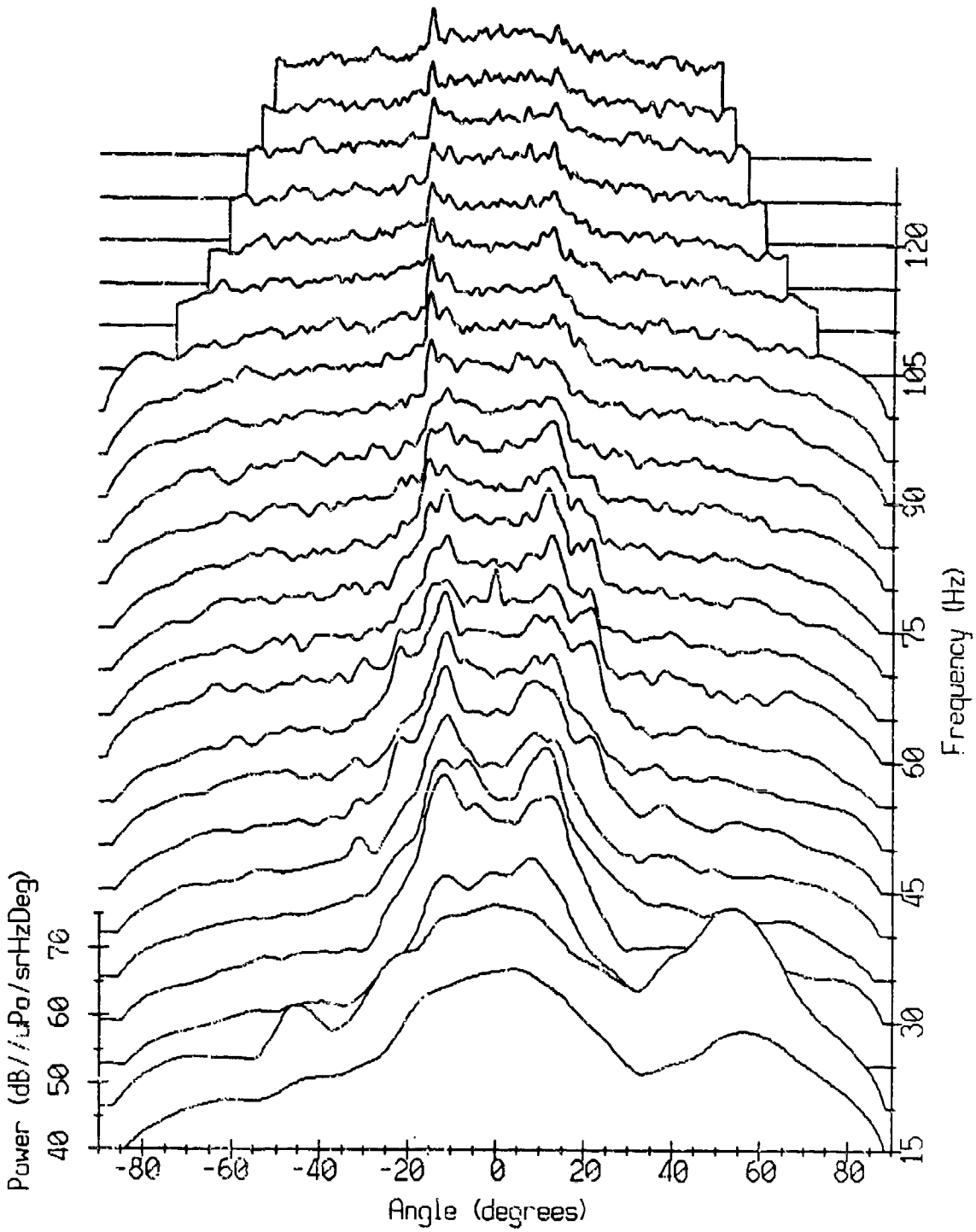

Spatial Distribution During Storm at 1000 GMT

wind speed: 9.3 m/s

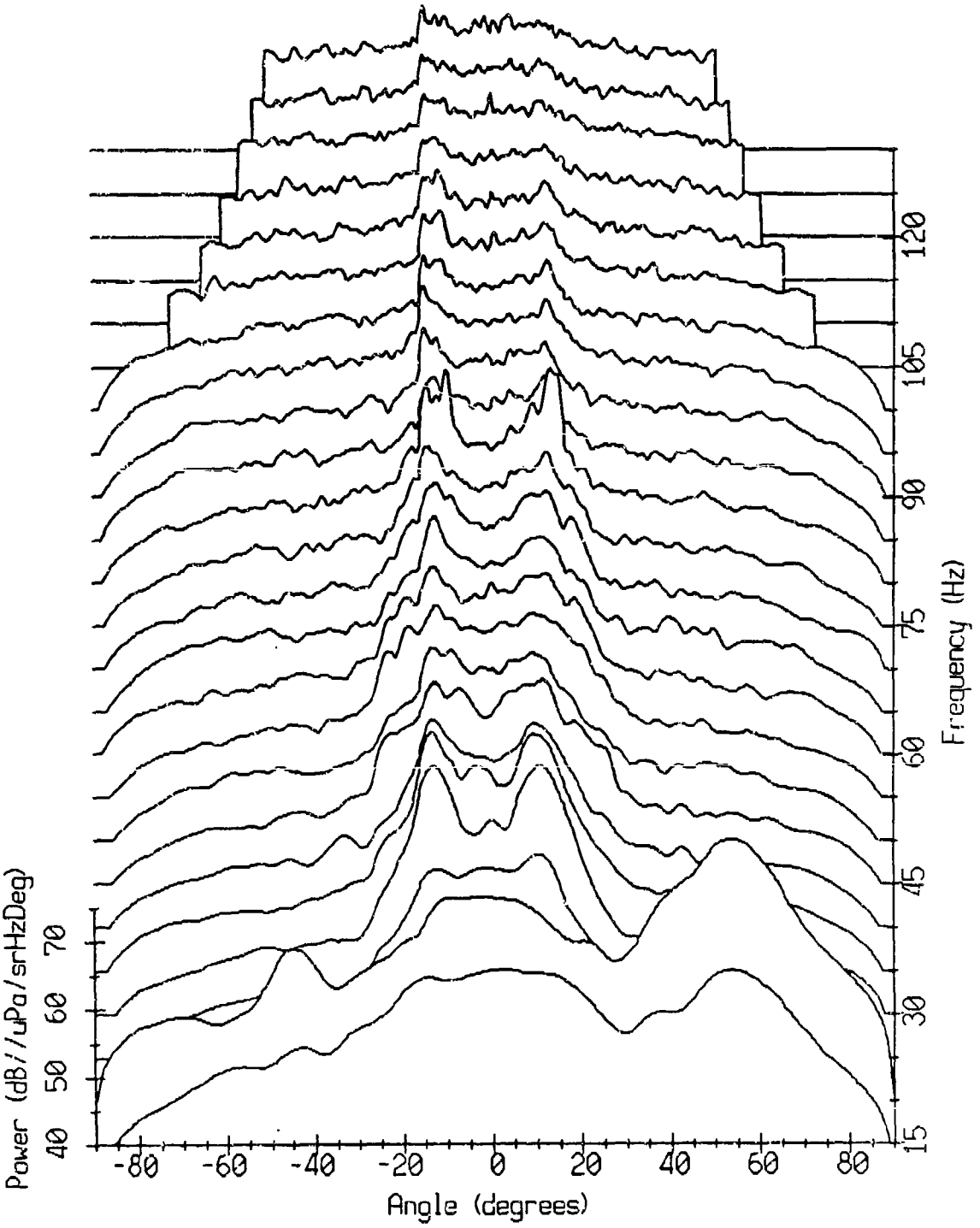

Spatial Distribution During Storm at 1020 GMT

wind speed: 8.4 m/s

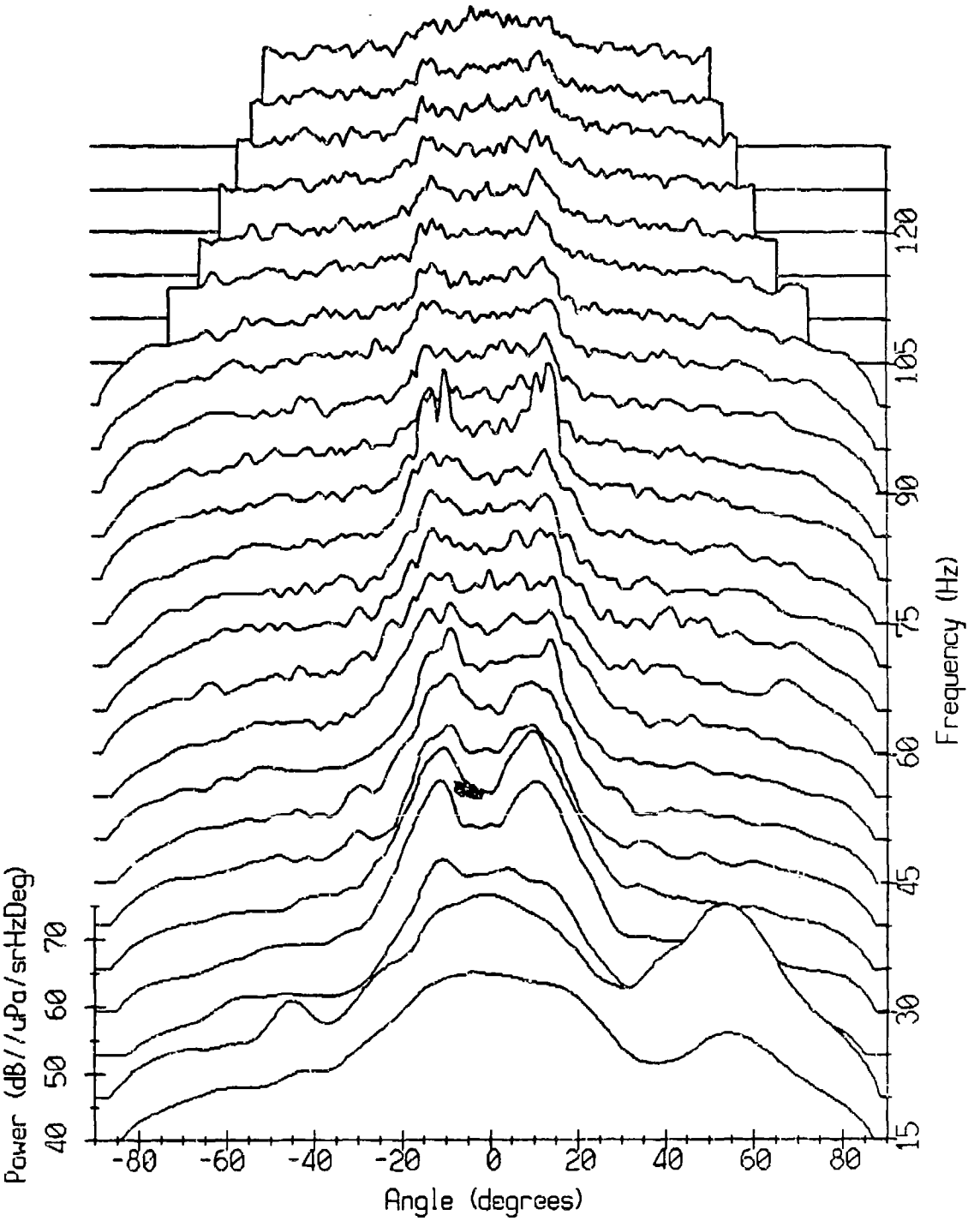

Spatial Distribution During Storm at 1040 GMT

wind speed: 7.6 m/s

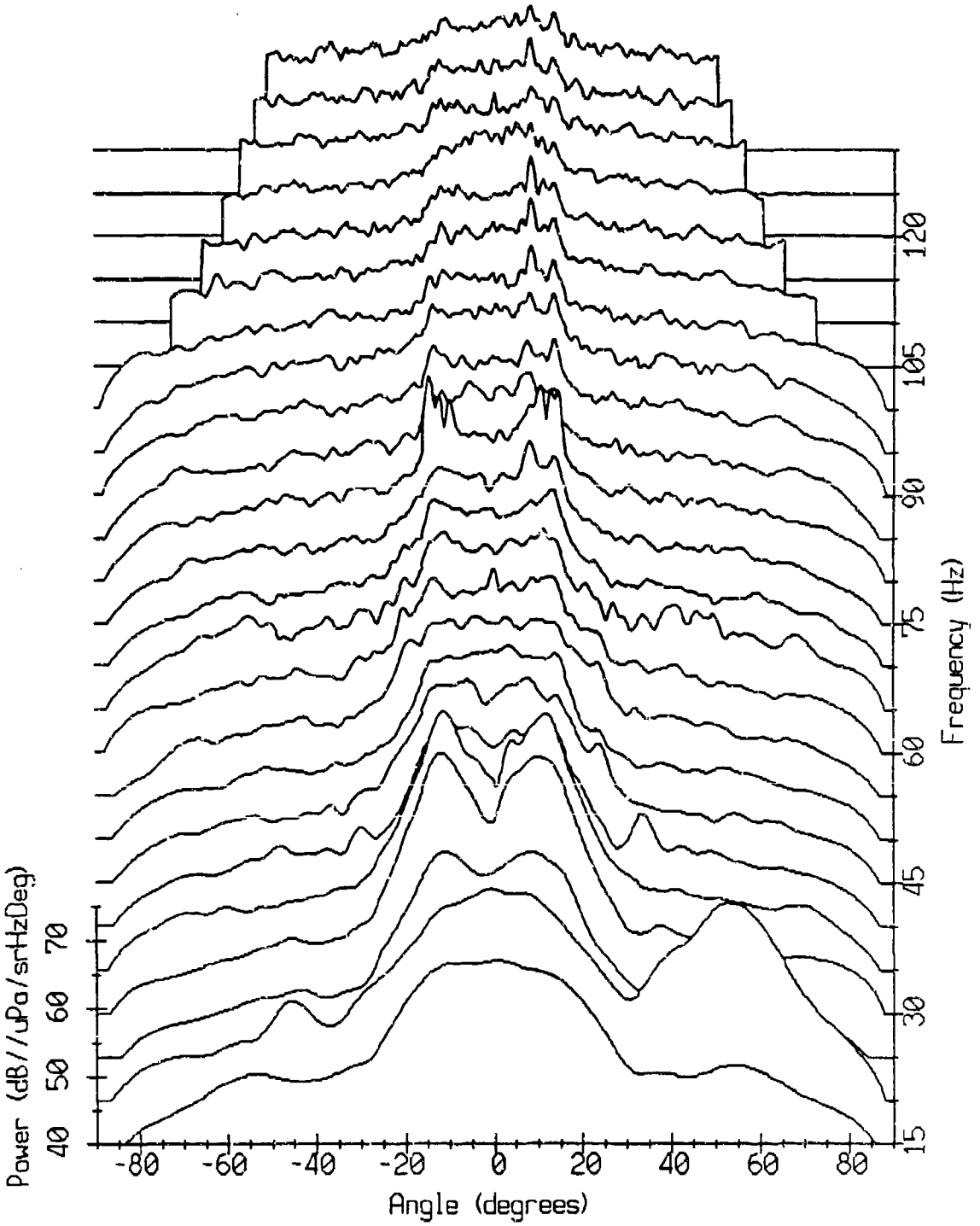

Spatial Distribution During Storm at 1100 GMT

wind speed: 6.7 m/s

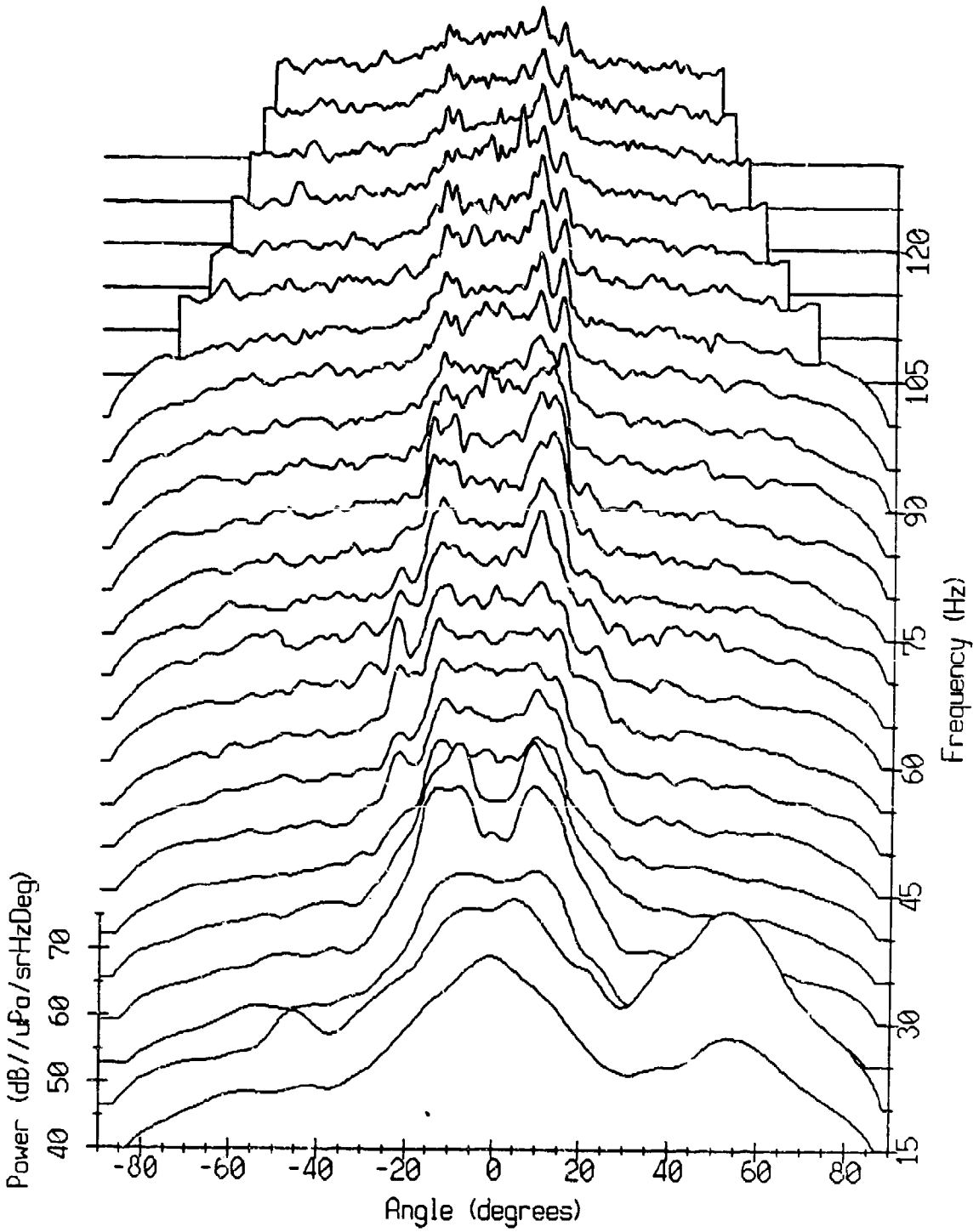

Spatial Distribution During Storm at 1120 GMT

wind speed: 7.4 m/s

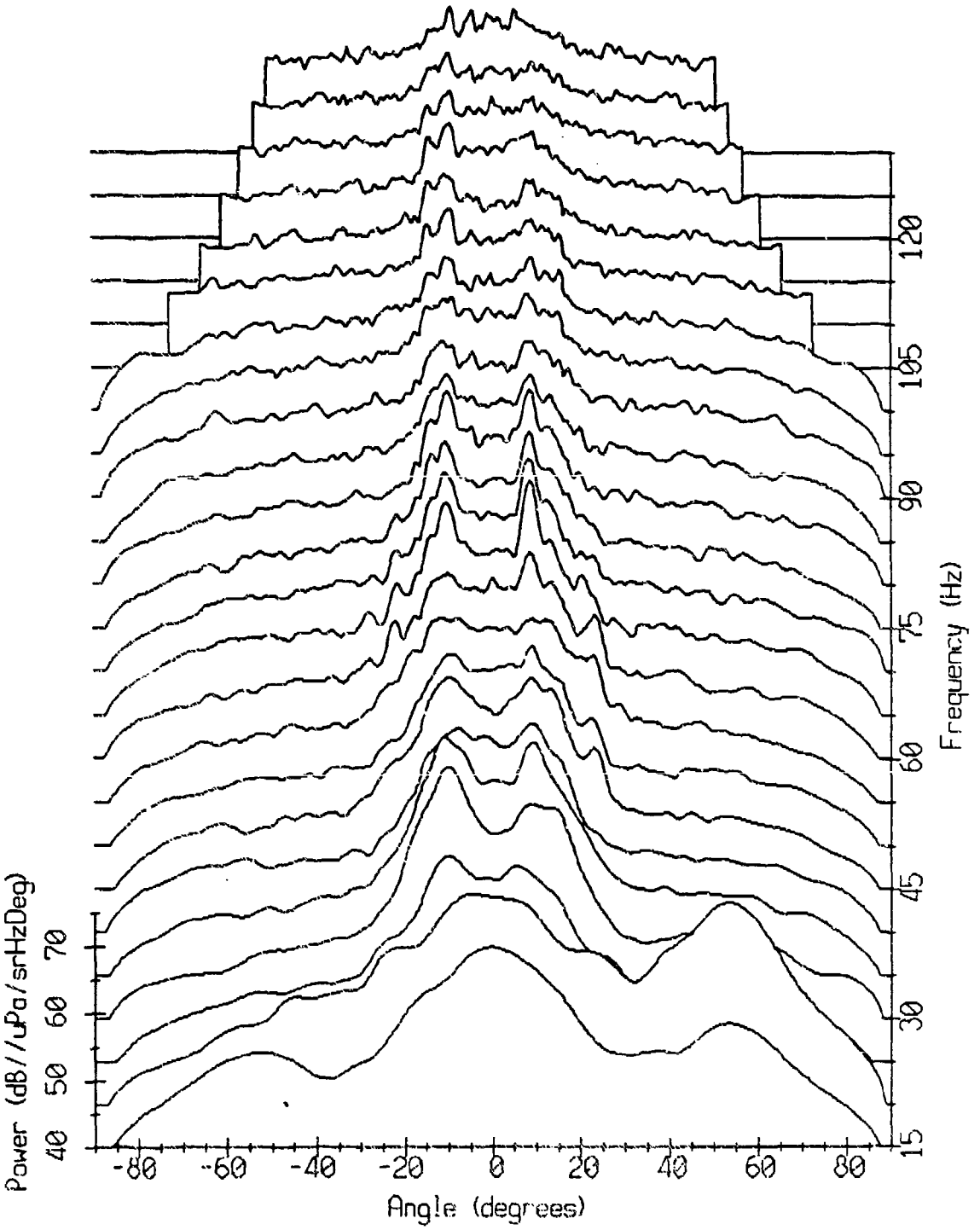

Spatial Distribution During Storm at 1140 GMT

wind speed: 8.1 m/s

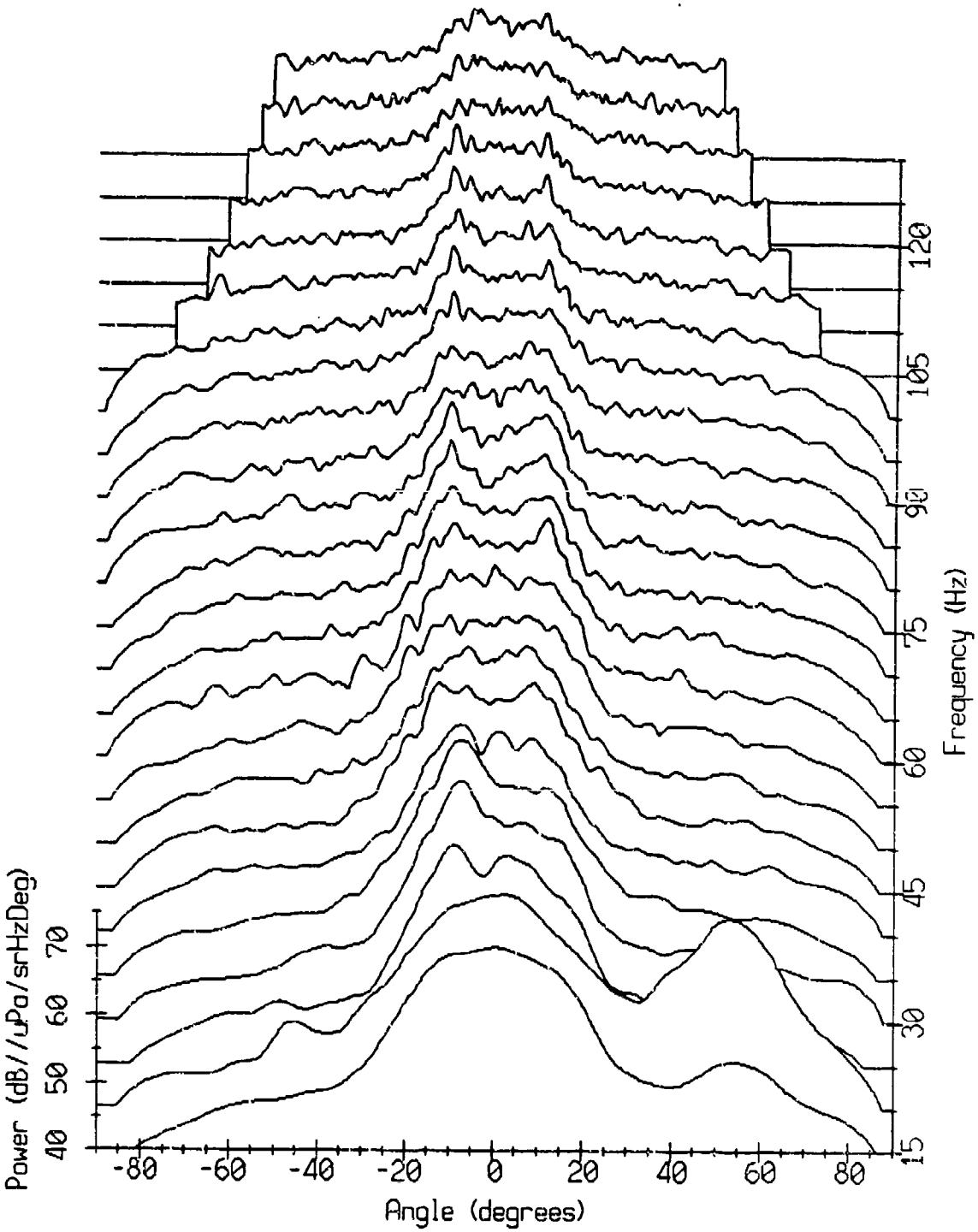

Spatial Distribution During Storm at 1200 GMT

wind speed: 8.8 m/s

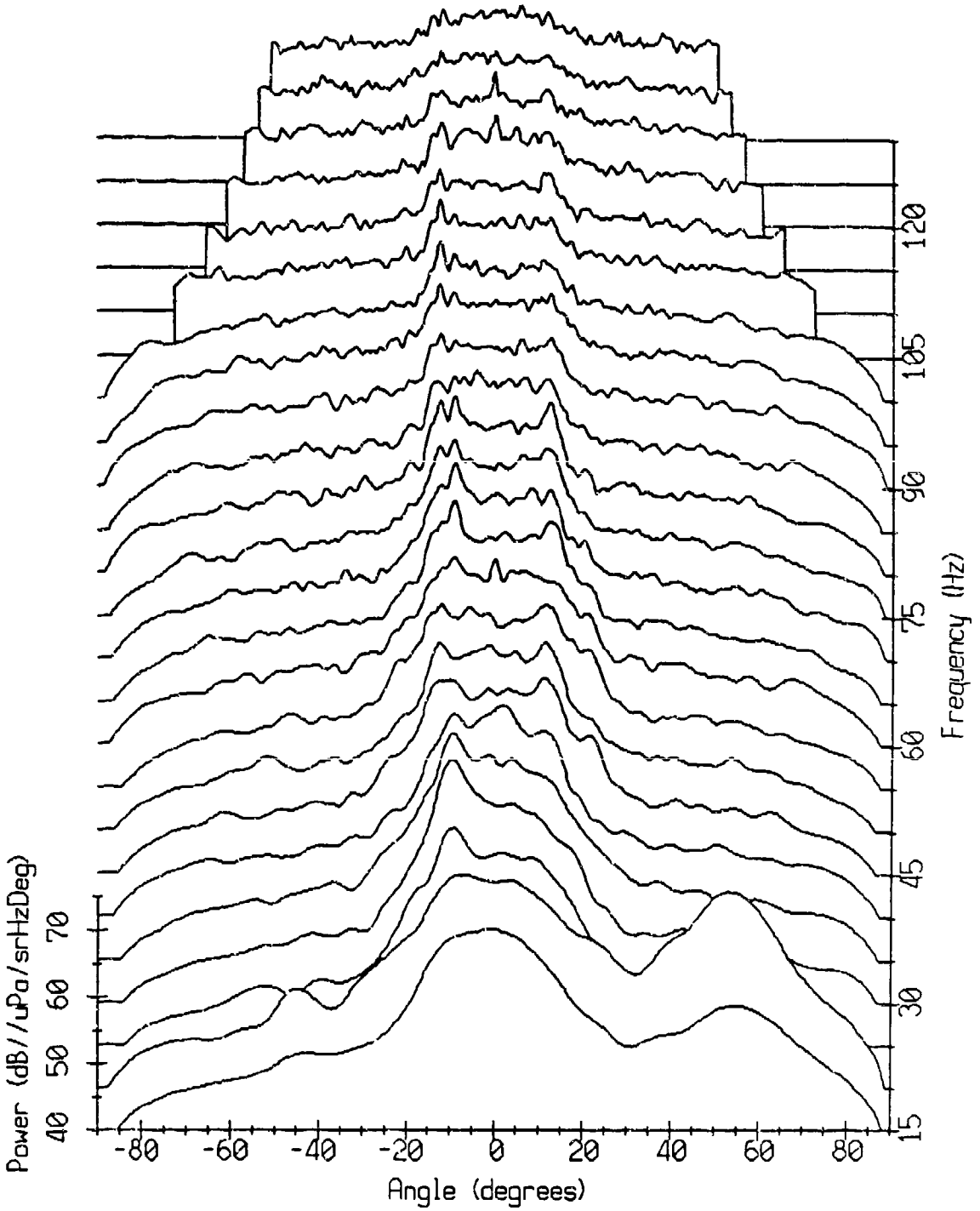

Spatial Distribution During Storm at 1220 GMT

wind speed: 9.1 m/s

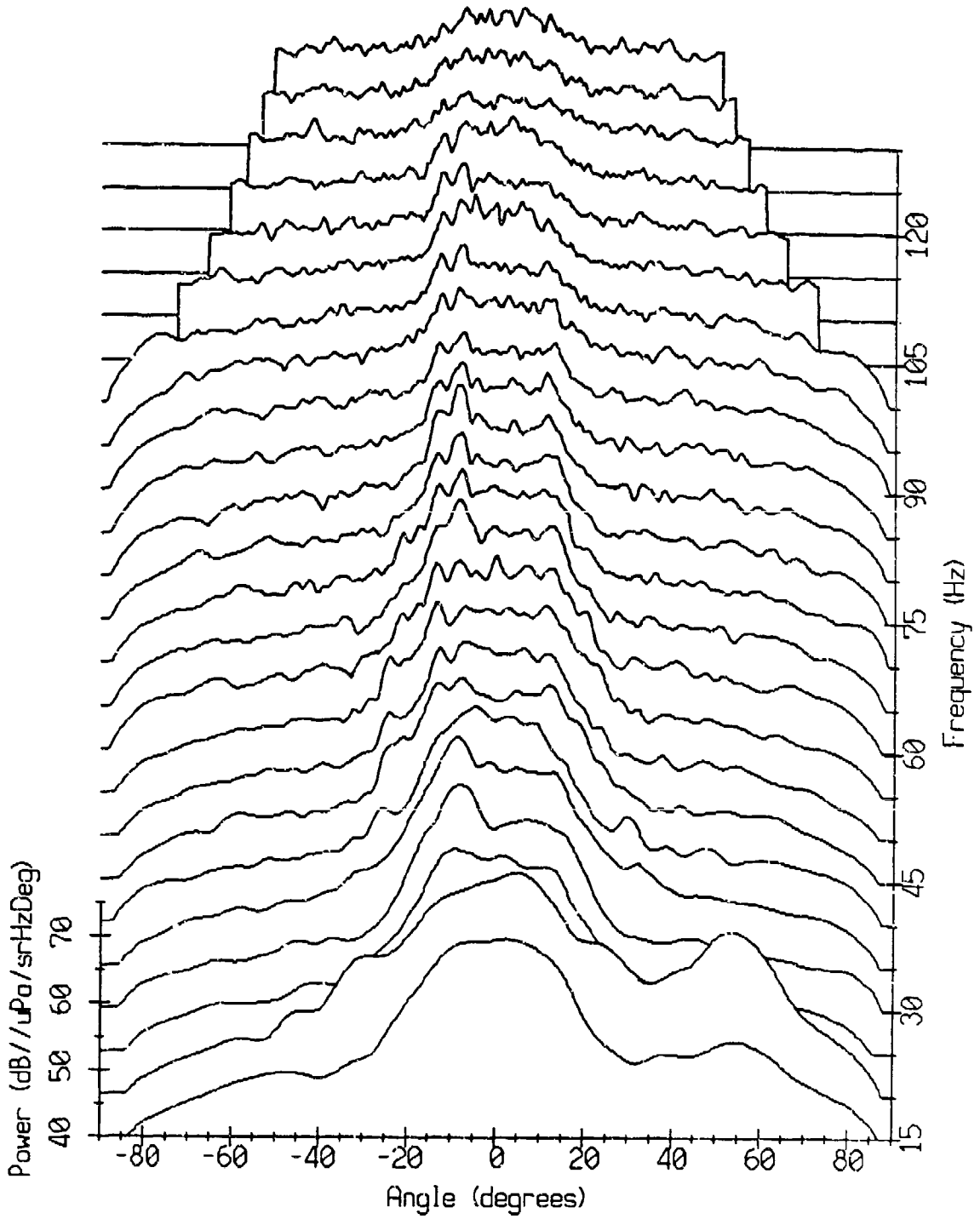

Spatial Distribution During Storm at 1240 GMT

wind speed: 9.4 m/s

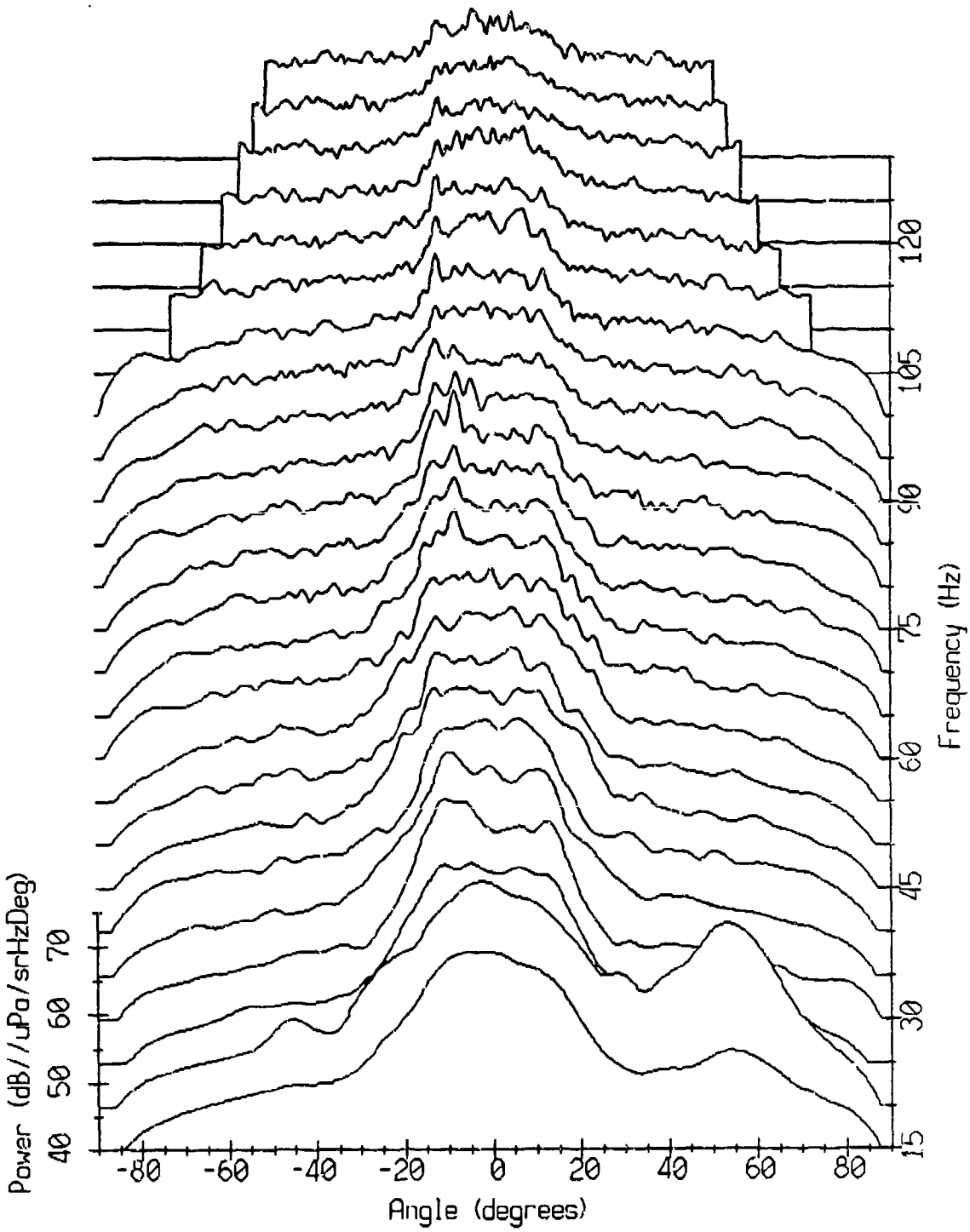

Spatial Distribution During Storm at 1300 GMT

wind speed: 9.8 m/s

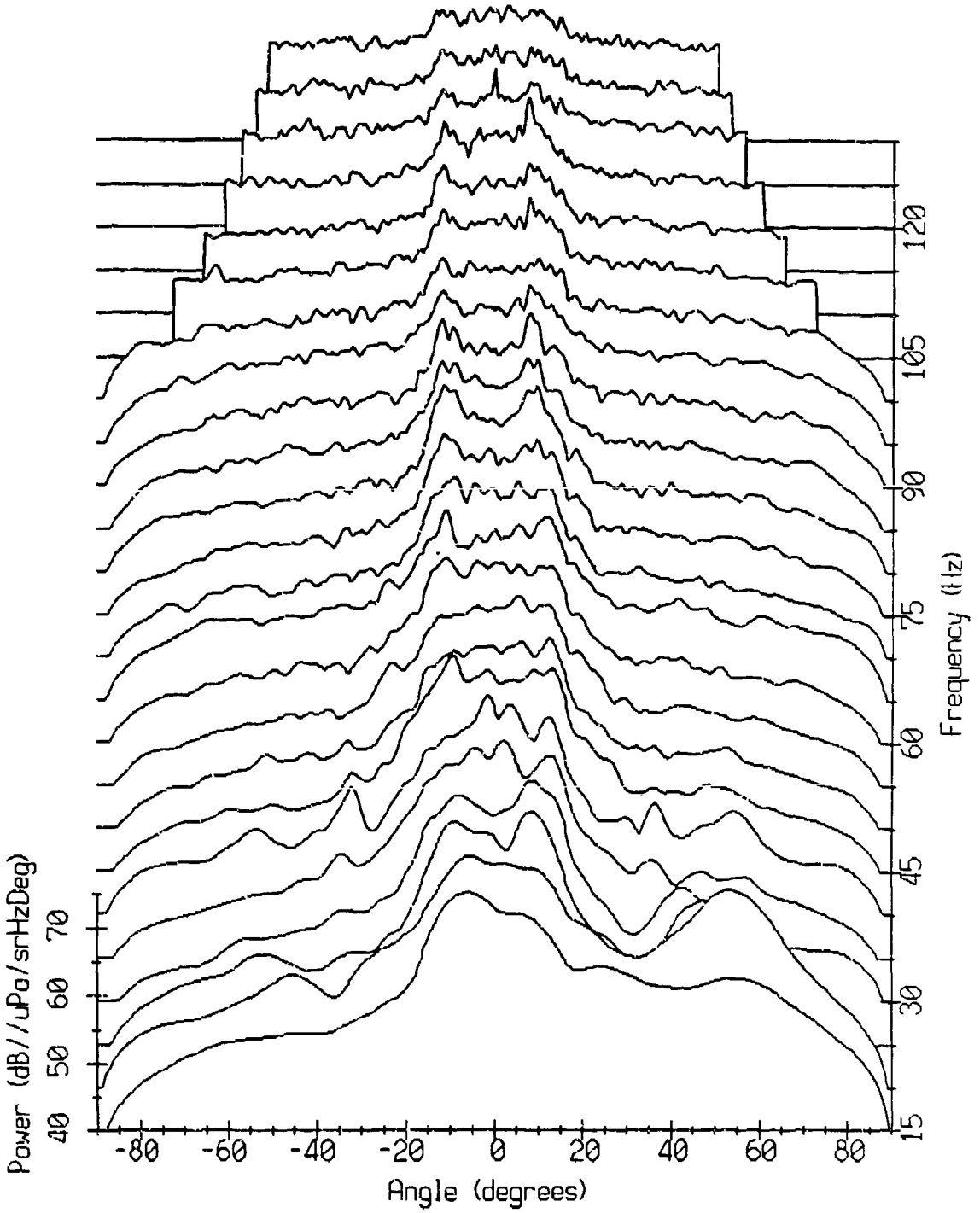

Spatial Distribution During Storm at 1320 GMT

wind speed: 9.9 m/s

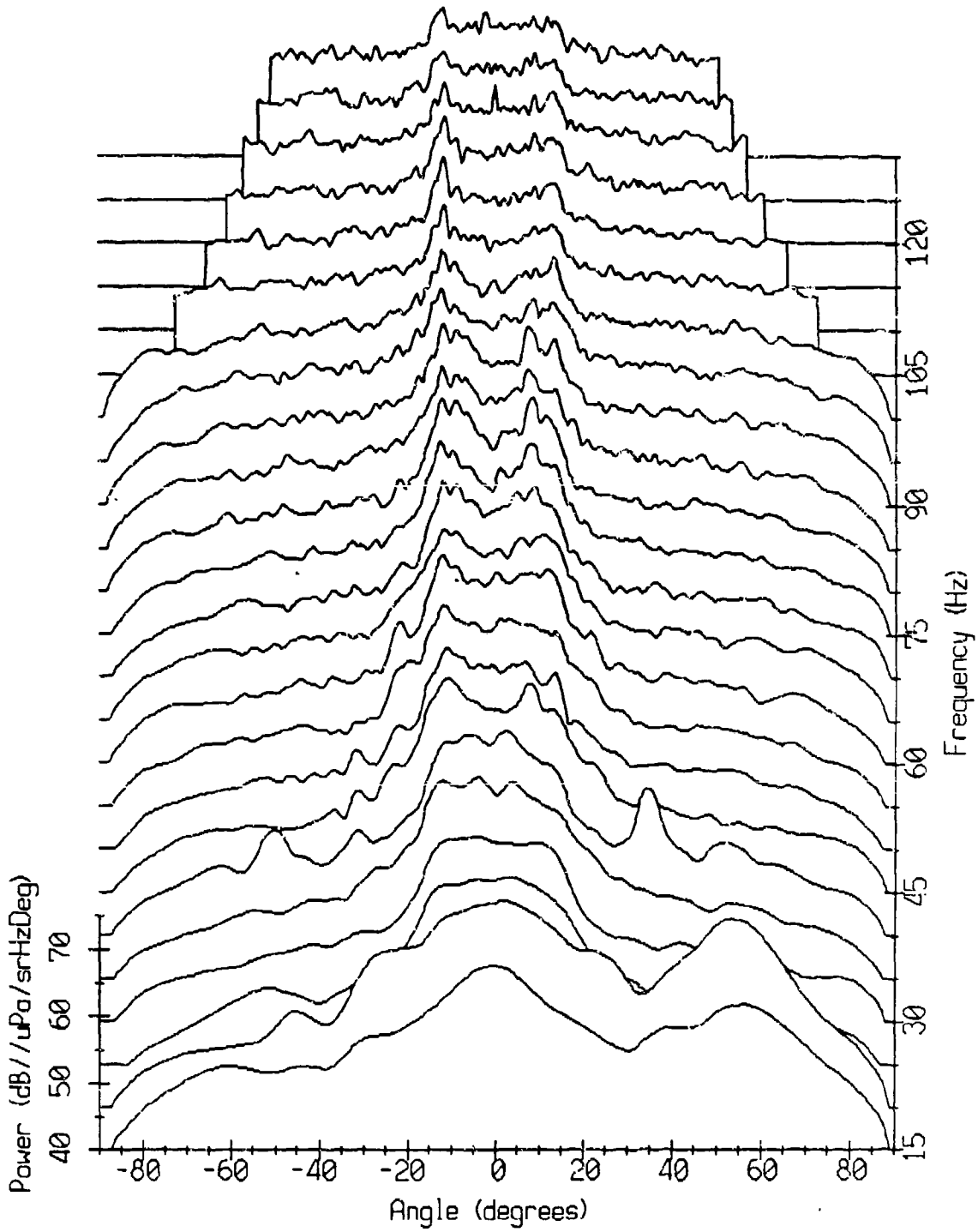

Spatial Distribution During Storm at 1340 GMT

wind speed: 10.1 m/s

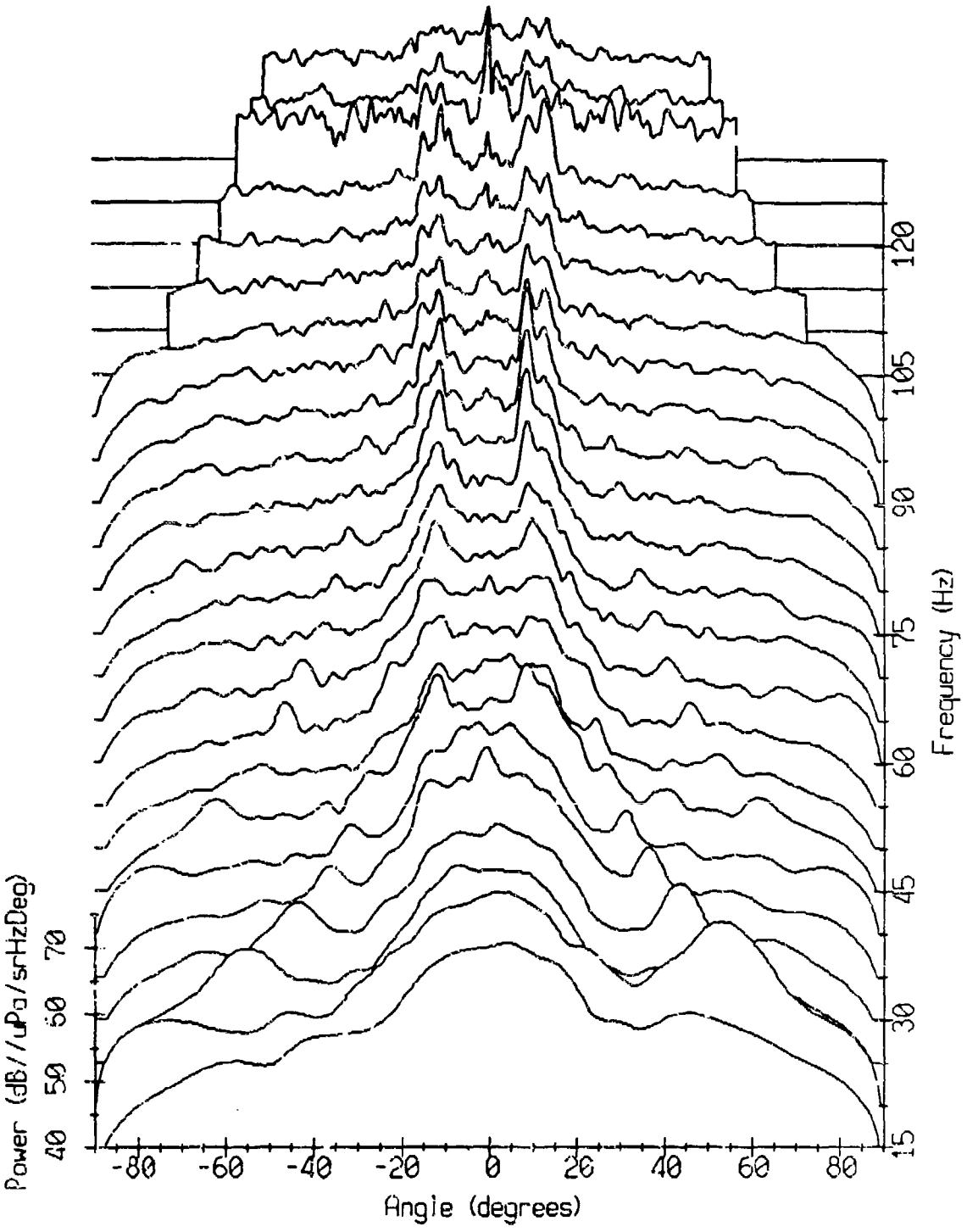

Spatial Distribution During Storm at 1400 GMT

wind speed: 10.3 m/s

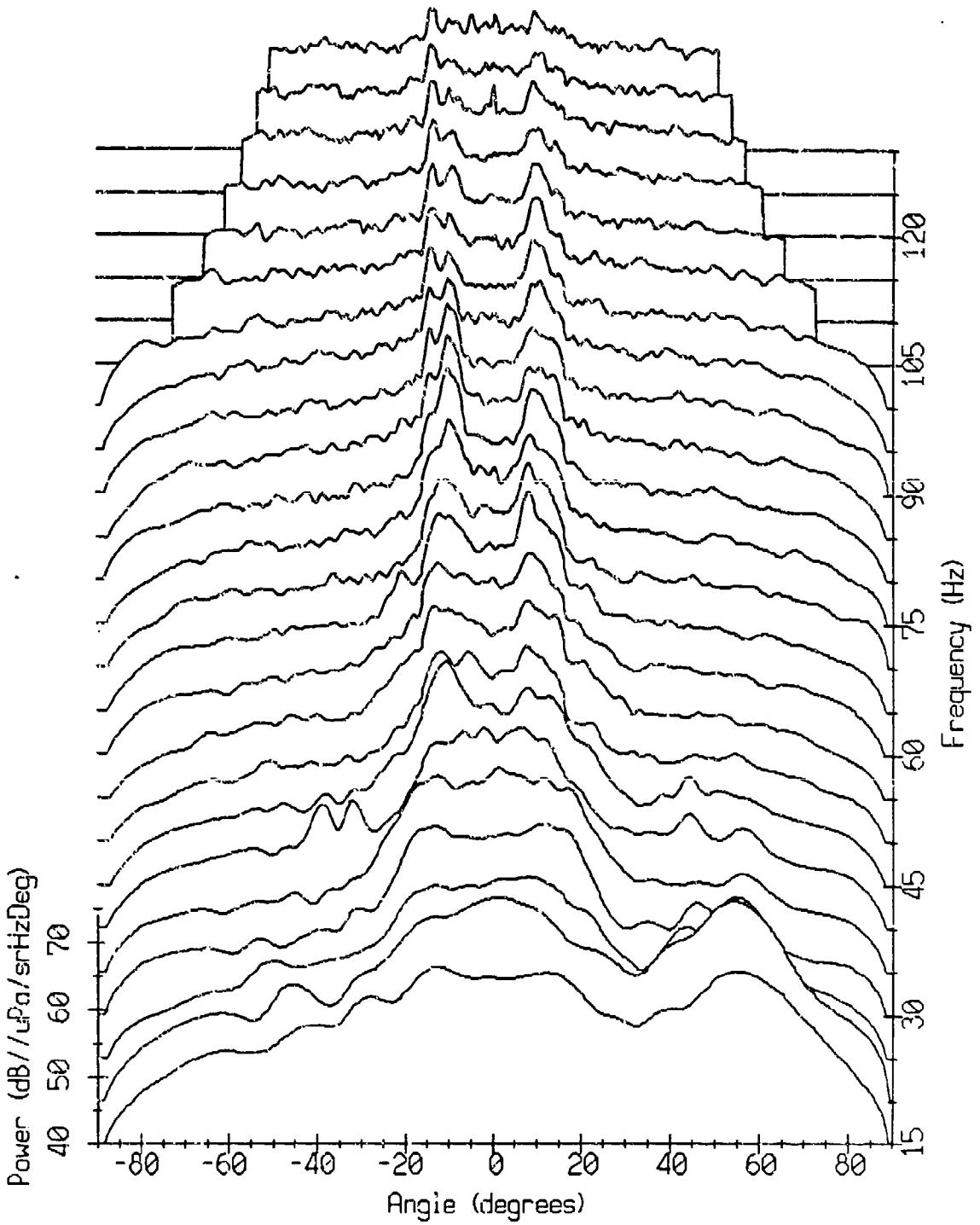

Spatial Distribution During Storm at 1420 GMT

wind speed: 10.4 m/s

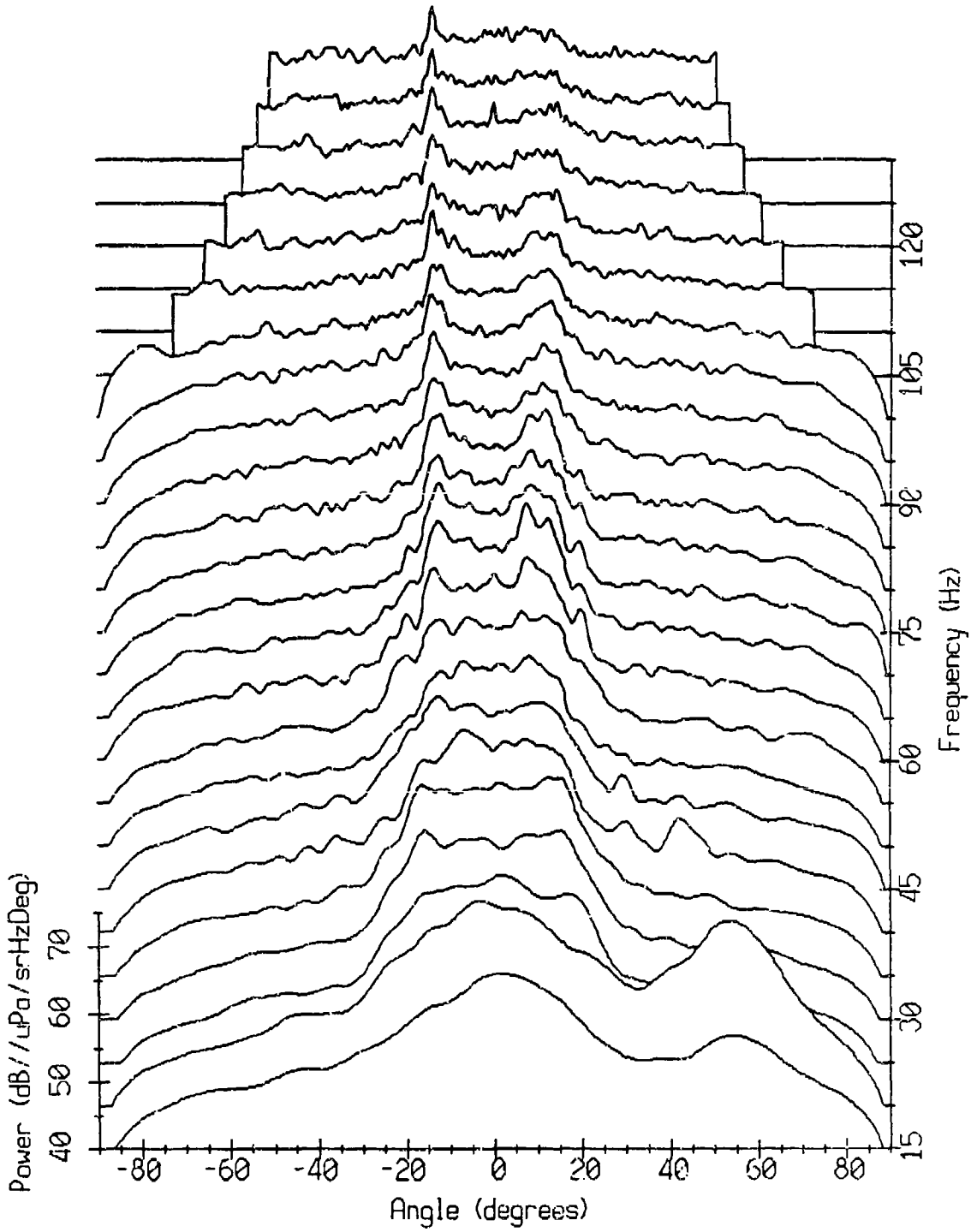

Spatial Distribution During Storm at 1440 GMT

wind speed: 10.7m/s

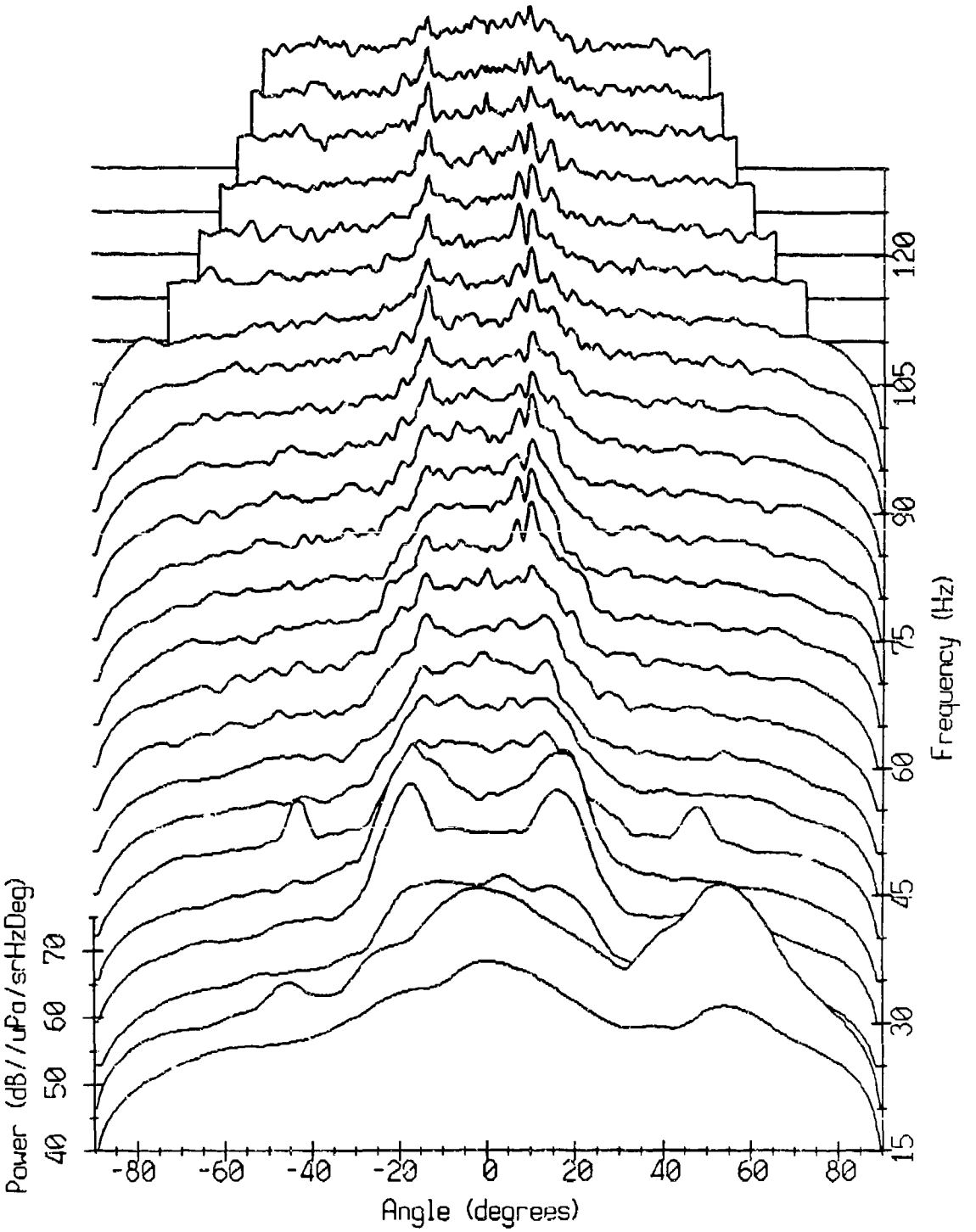

Spatial Distribution During Storm at 1500 GMT

wind speed: 10.8 m/s

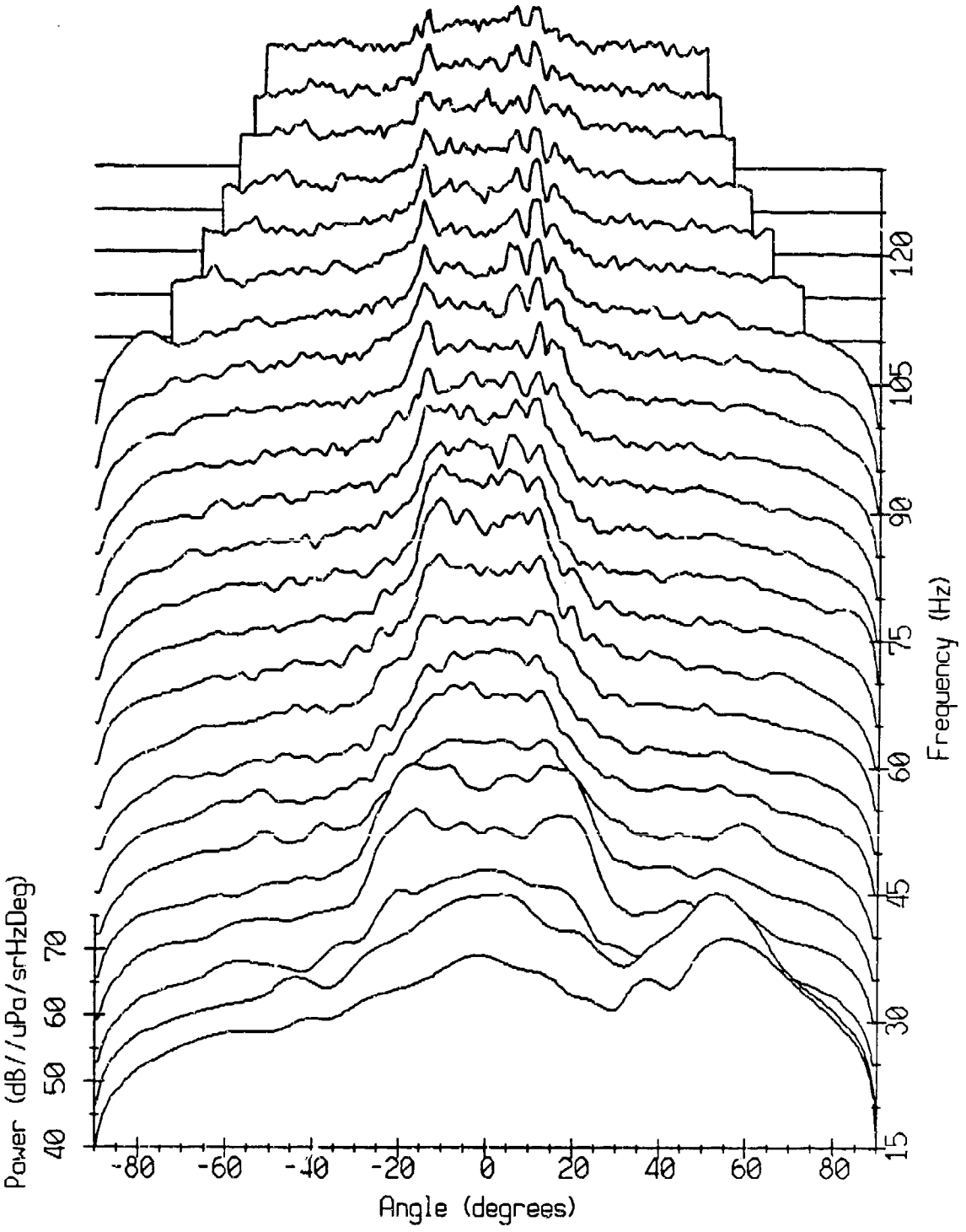

Spatial Distribution During Storm at 1520 GMT

wind speed: 11.0m/s

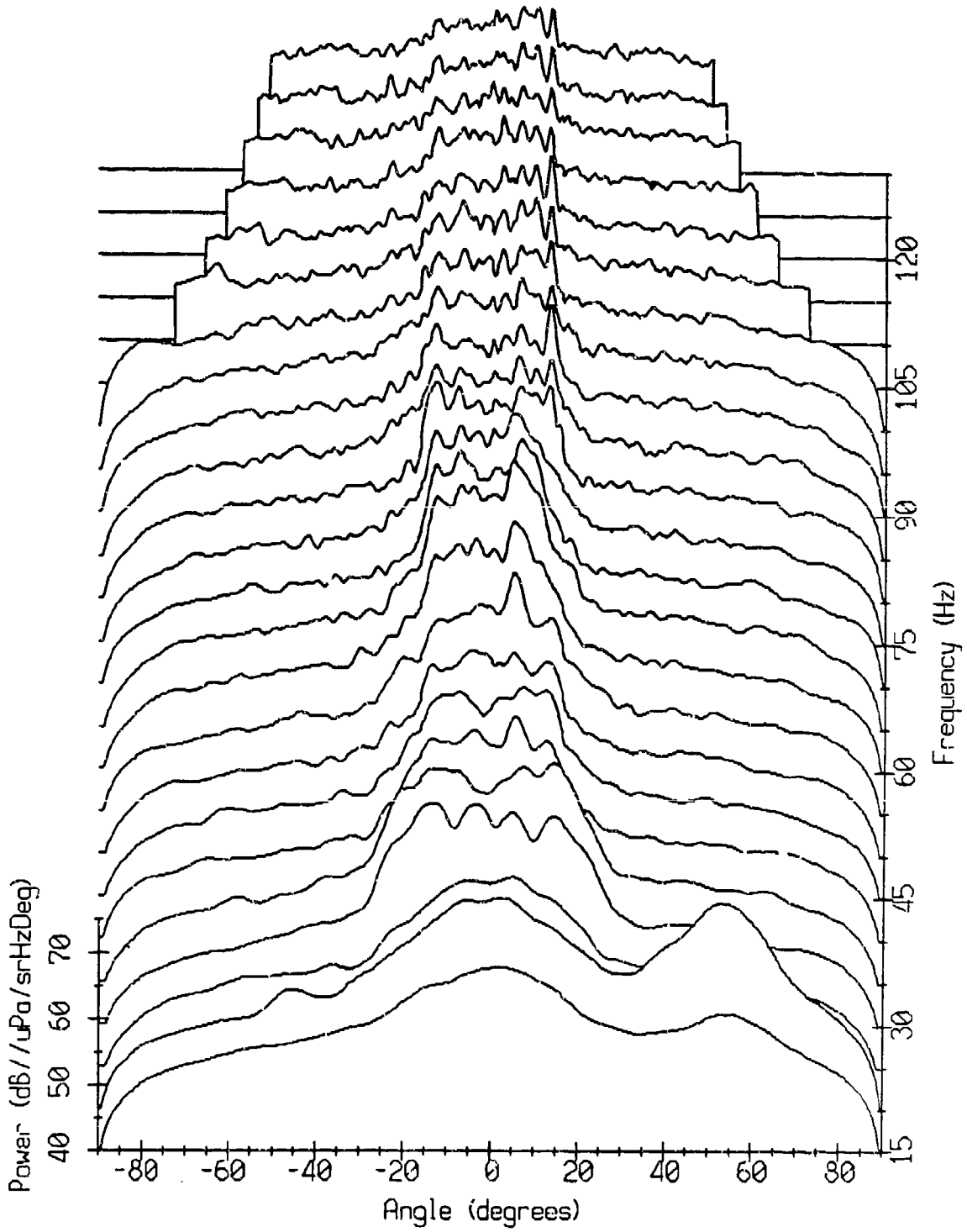

# Spatial Distribution During Storm at 1540 GMT

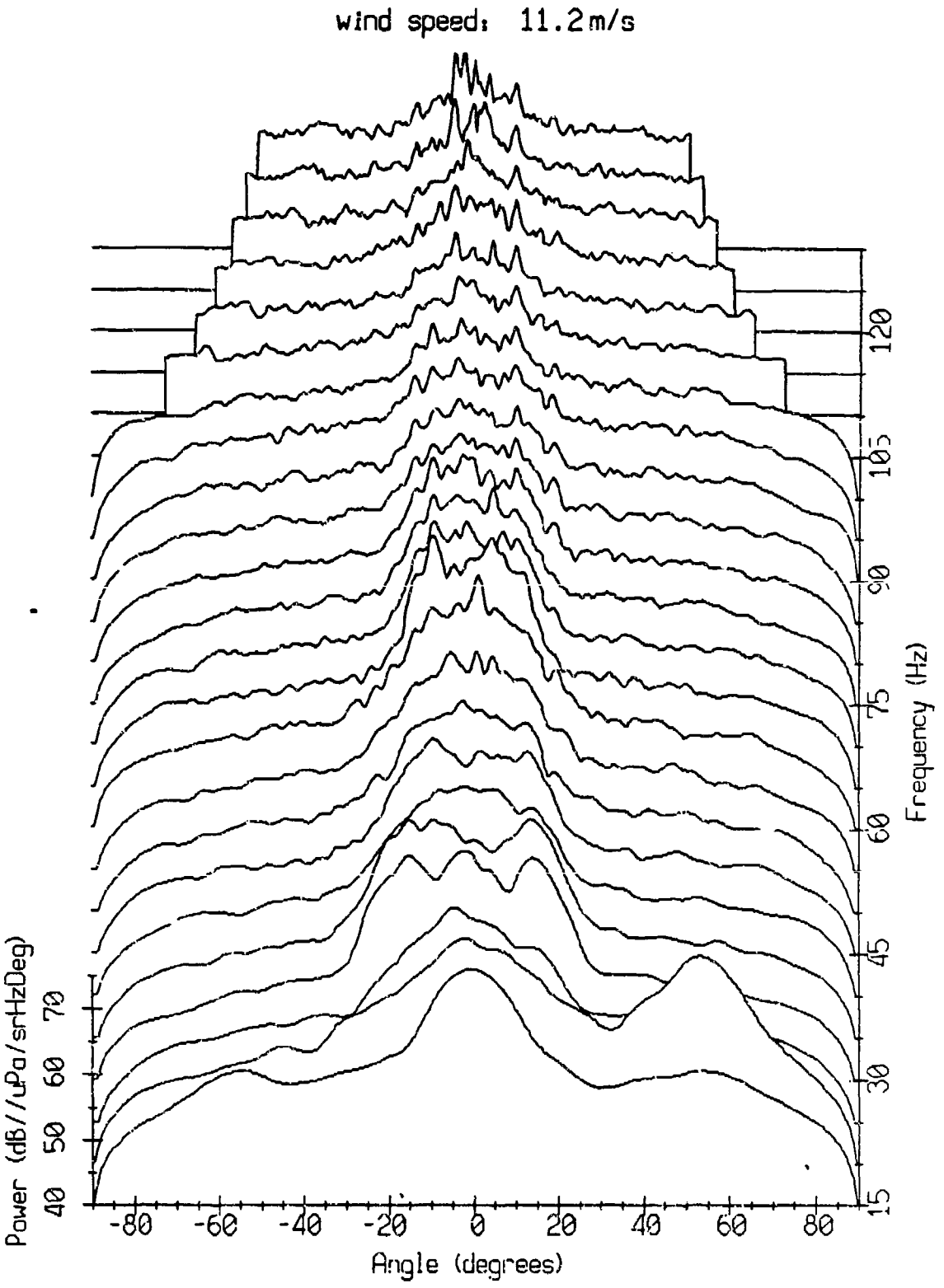

# Spatial Distribution During Storm at 1600 GMT

wind speed: 11.3 m/s

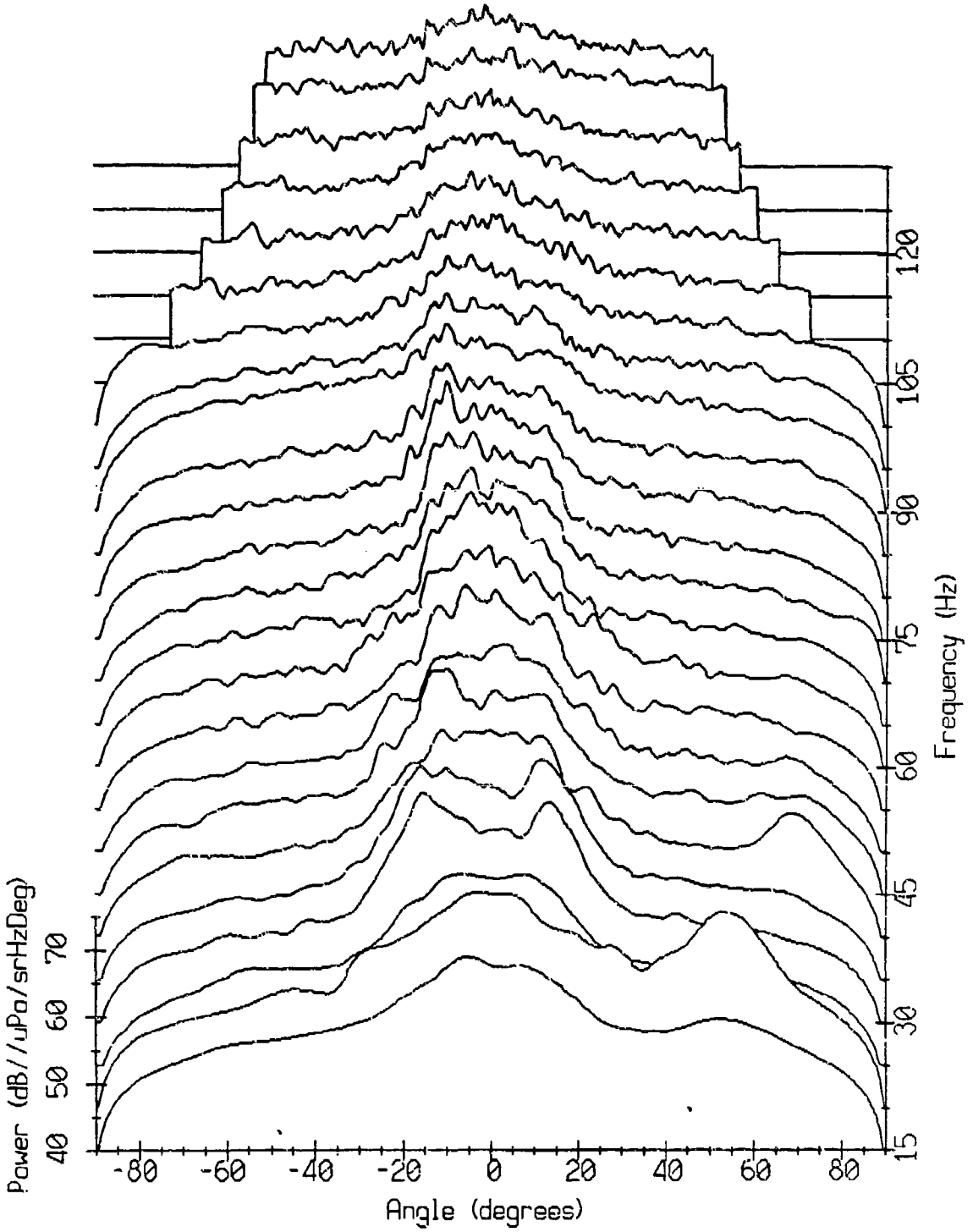

Spatial Distribution During Storm at 1620 GMT

wind speed: 11.0m/s

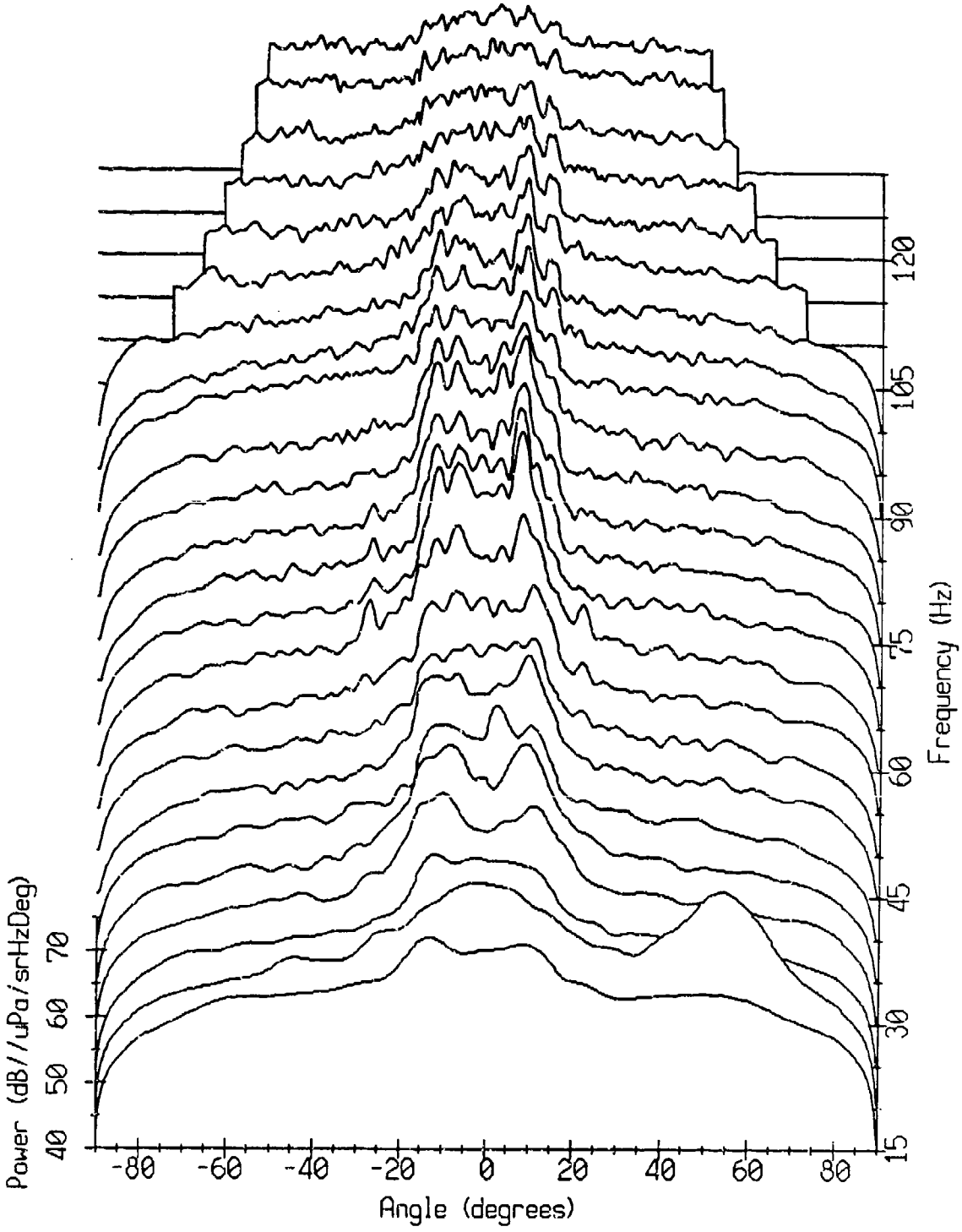

Spatial Distribution During Storm at 1640 GMT

wind speed: 10.7 m/s

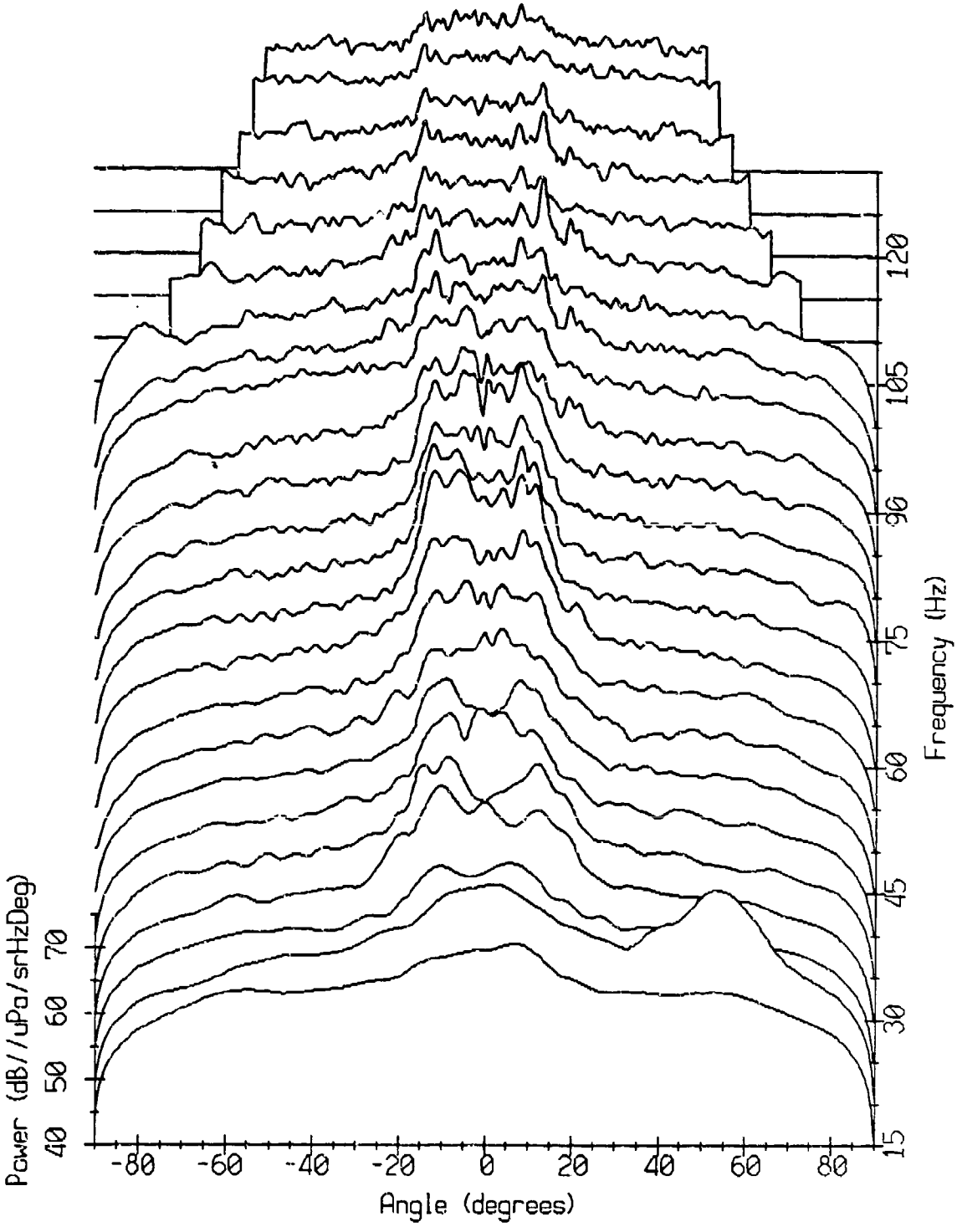

Spatial Distribution During Storm at 1700 GMT

wind speed: 10.3 m/s

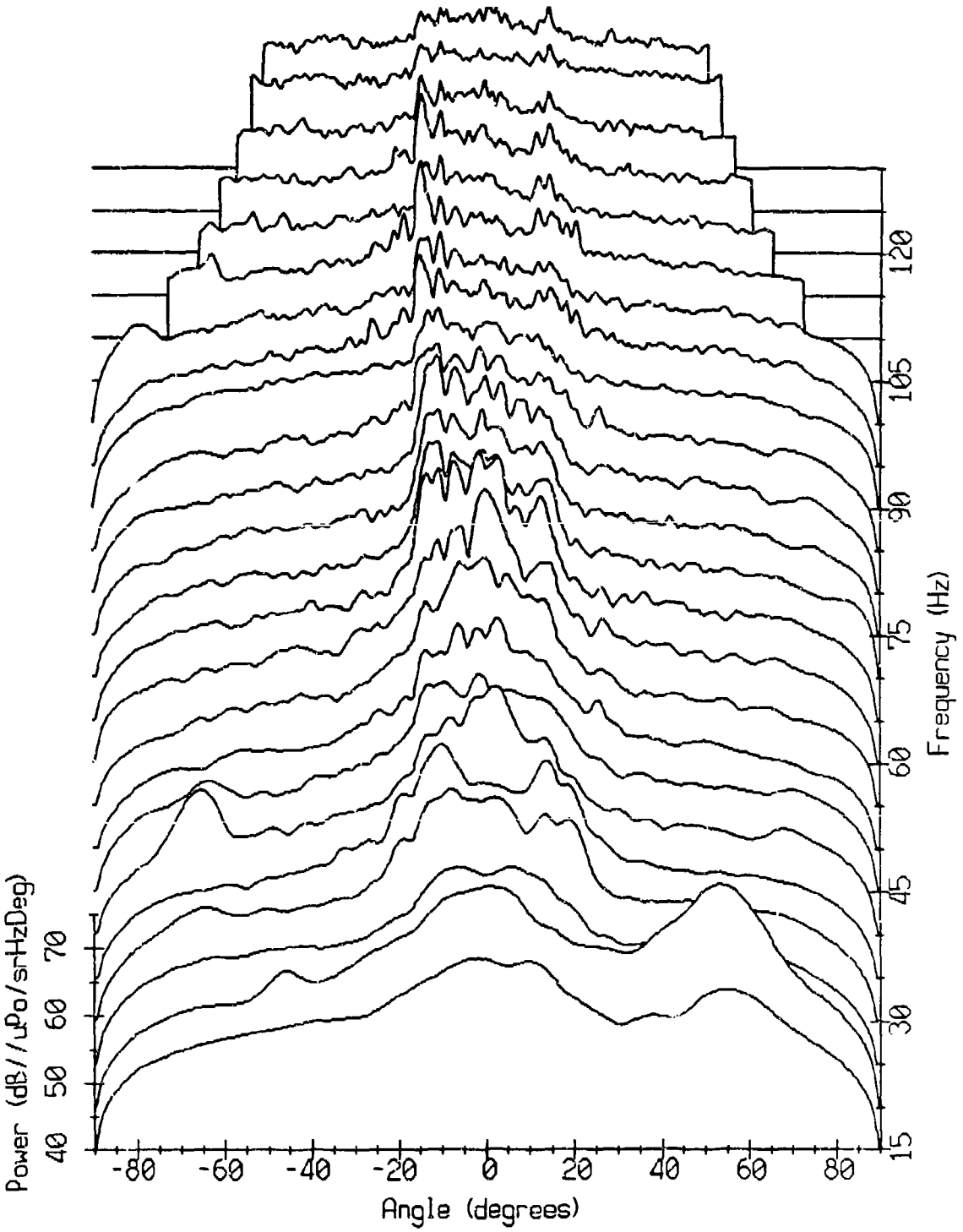

Spatial Distribution During Storm at 1720 GMT

wind speed: 10.4 m/s

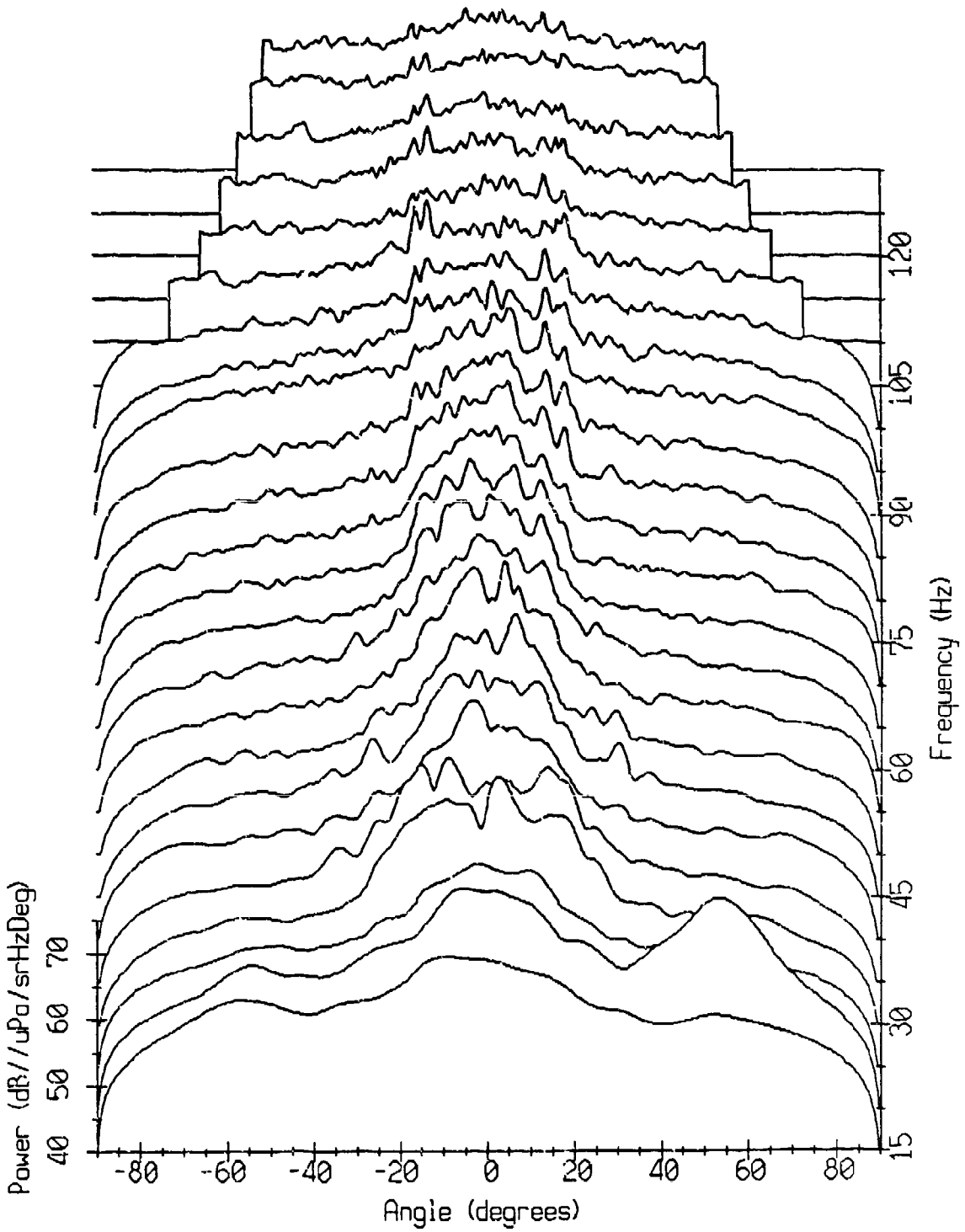

Spatial Distribution During Storm at 1740 GMT

wind speed: 10.7m/s

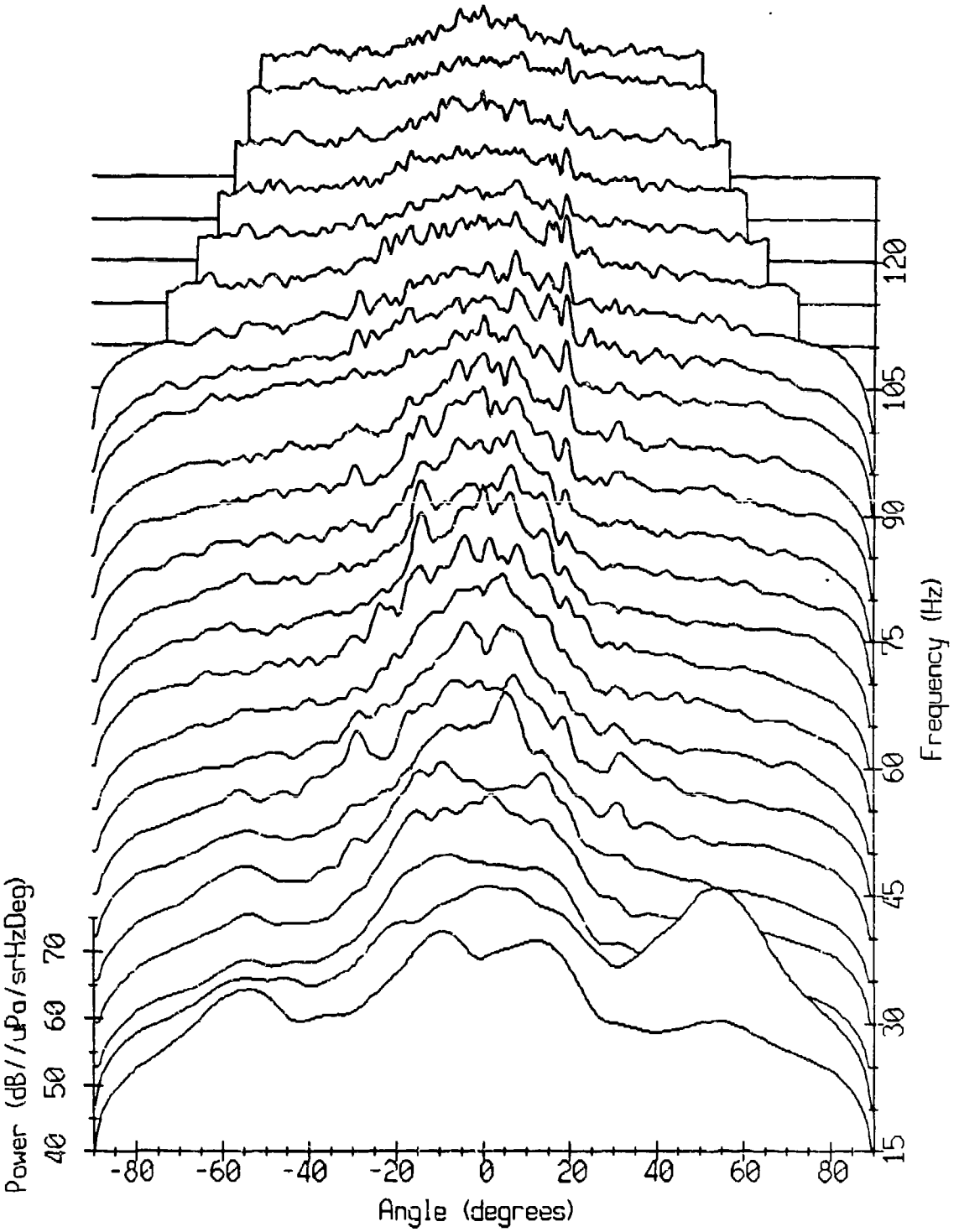

Spatial Distribution During Storm at 1800 GMT

wind speed: 10.8 m/s

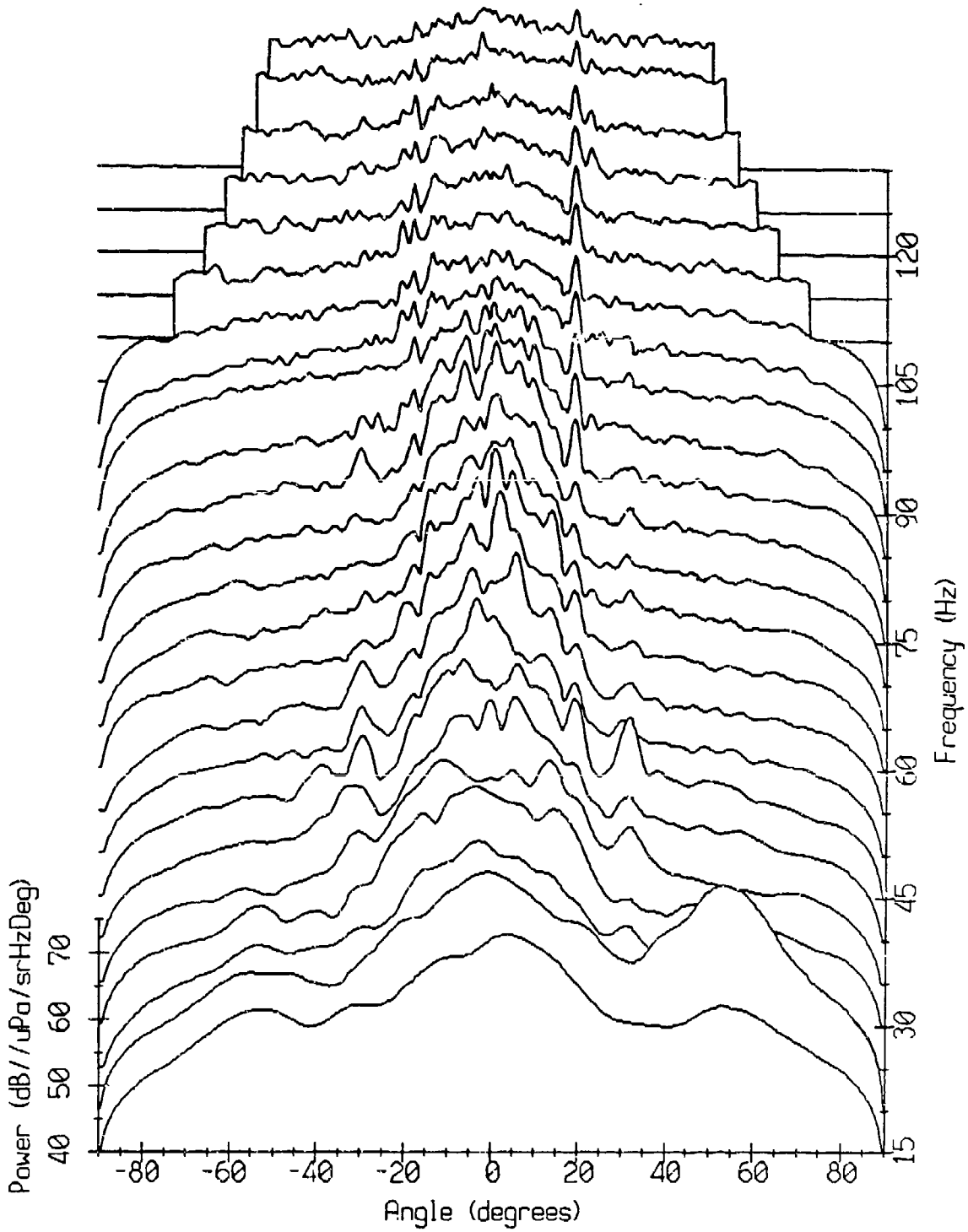

Spatial Distribution During Storm at 1820 GMT

wind speed: 11.2 m/s

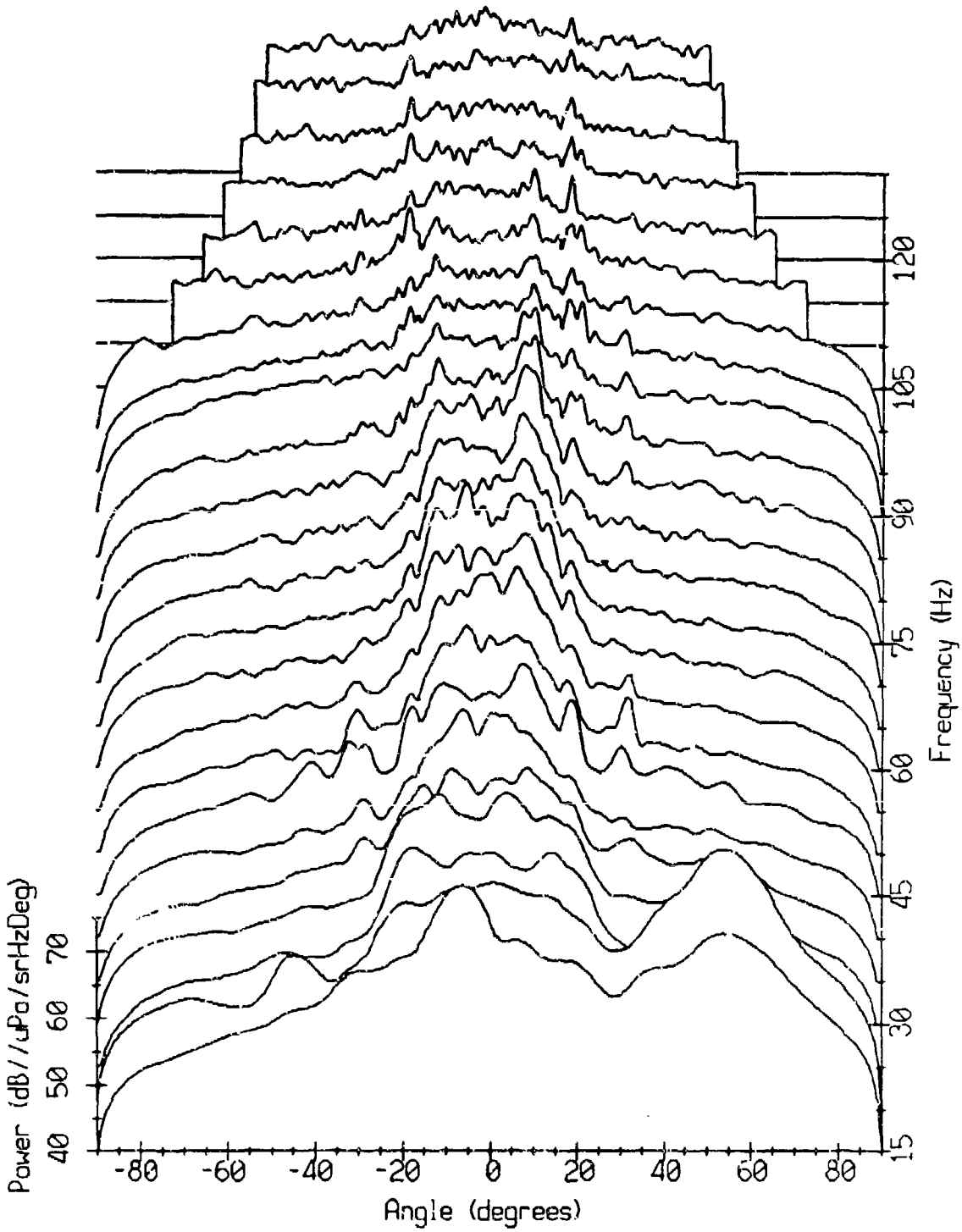

Spatial Distribution During Storm at 1840 GMT

wind speed: 11.5 m/s

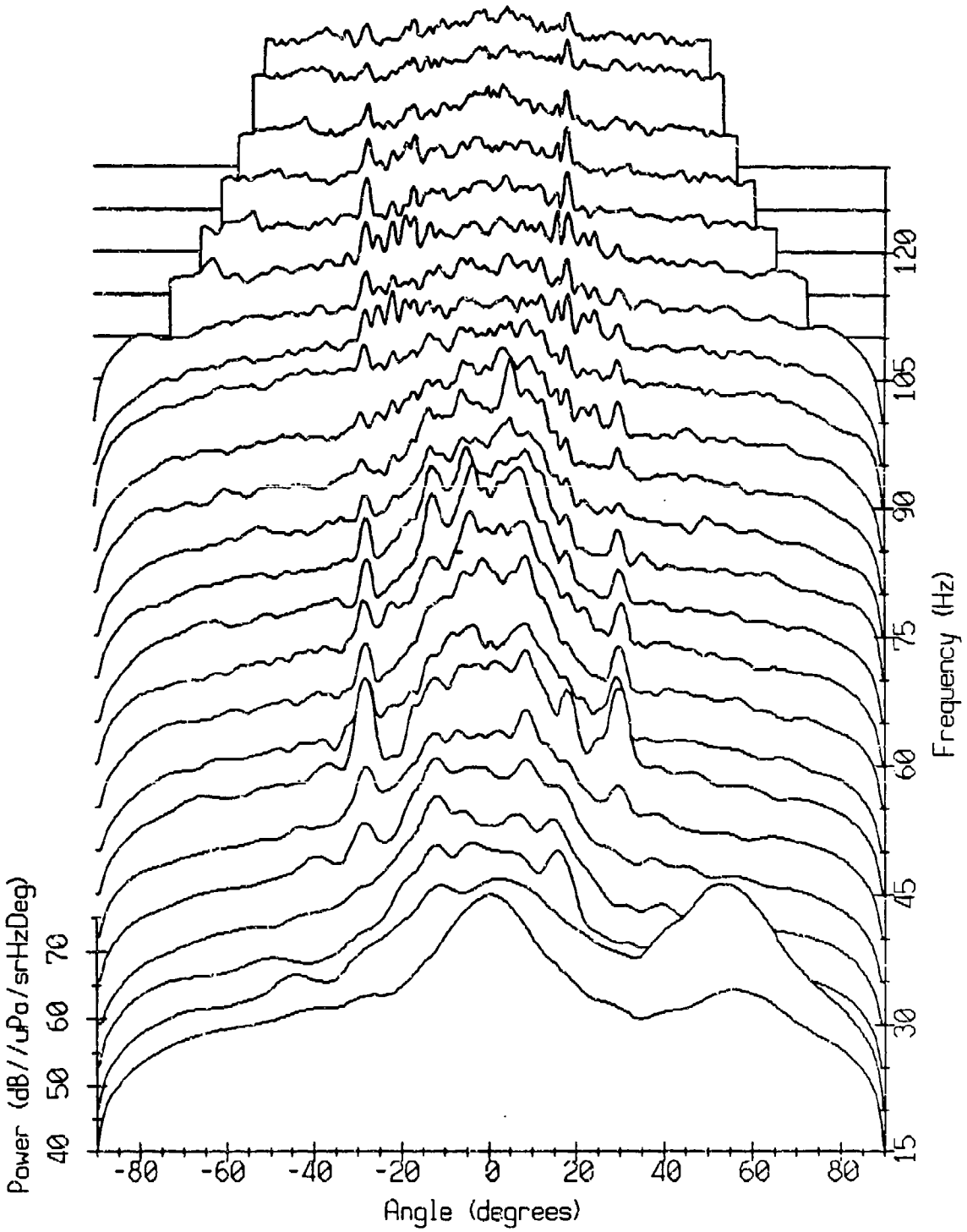

Spatial Distribution During Storm at 1900 GMT

wind speed: 11.8 m/s

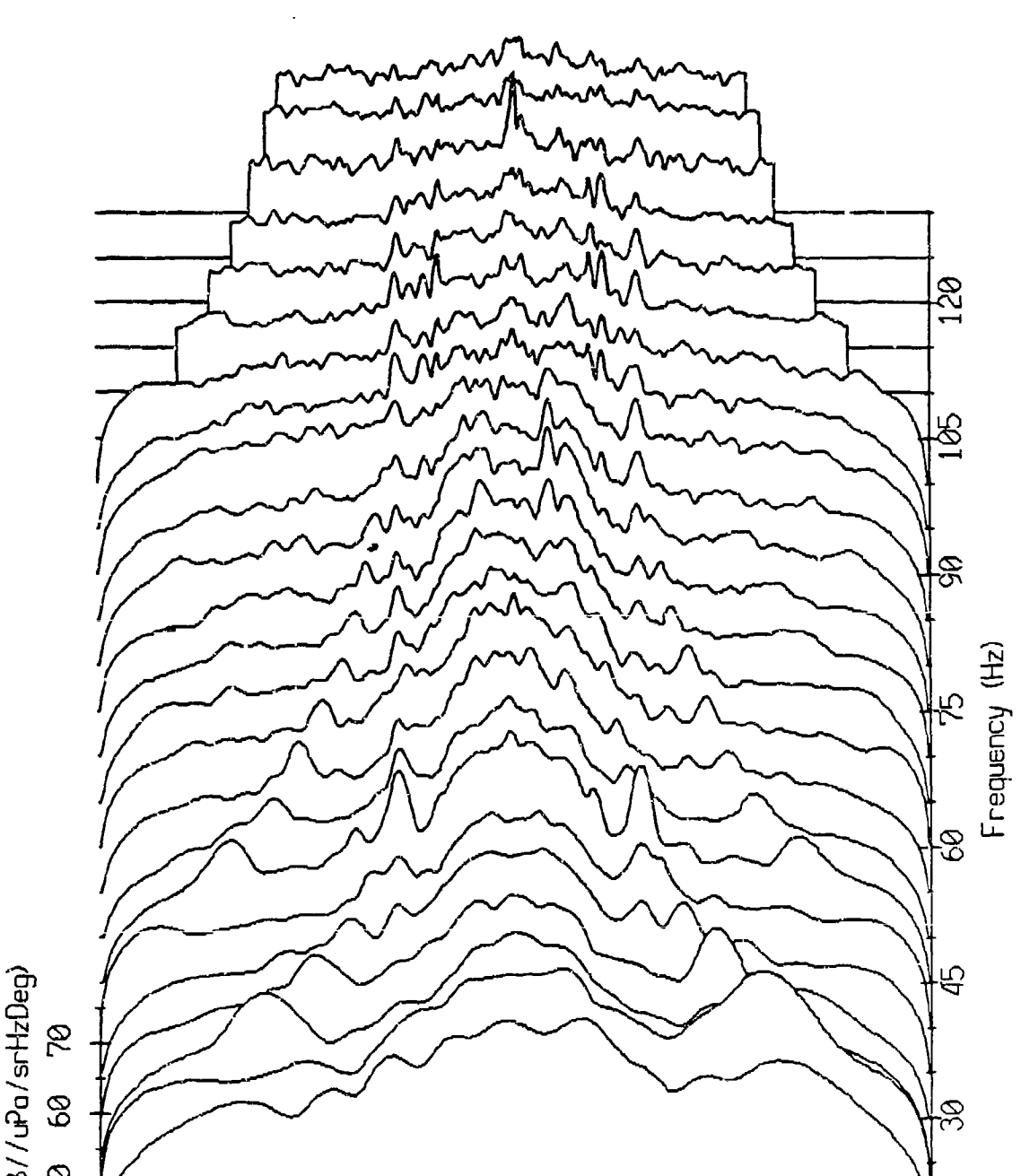

Spatial Distribution During Storm at 1920 GMT

wind speed: 11.7 m/s

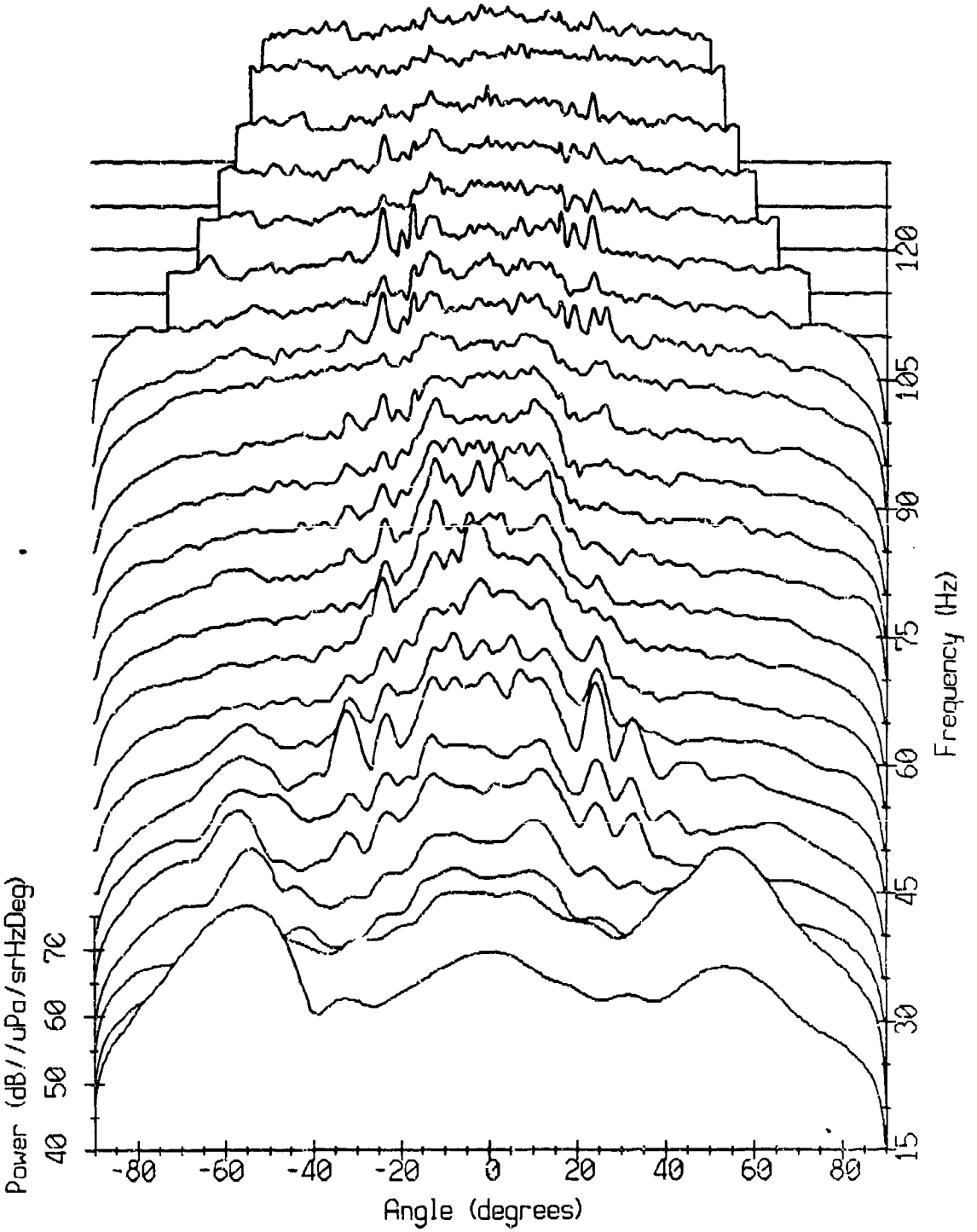

Spatial Distribution During Storm at 1940 GMT

wind speed: 11.5 m/s

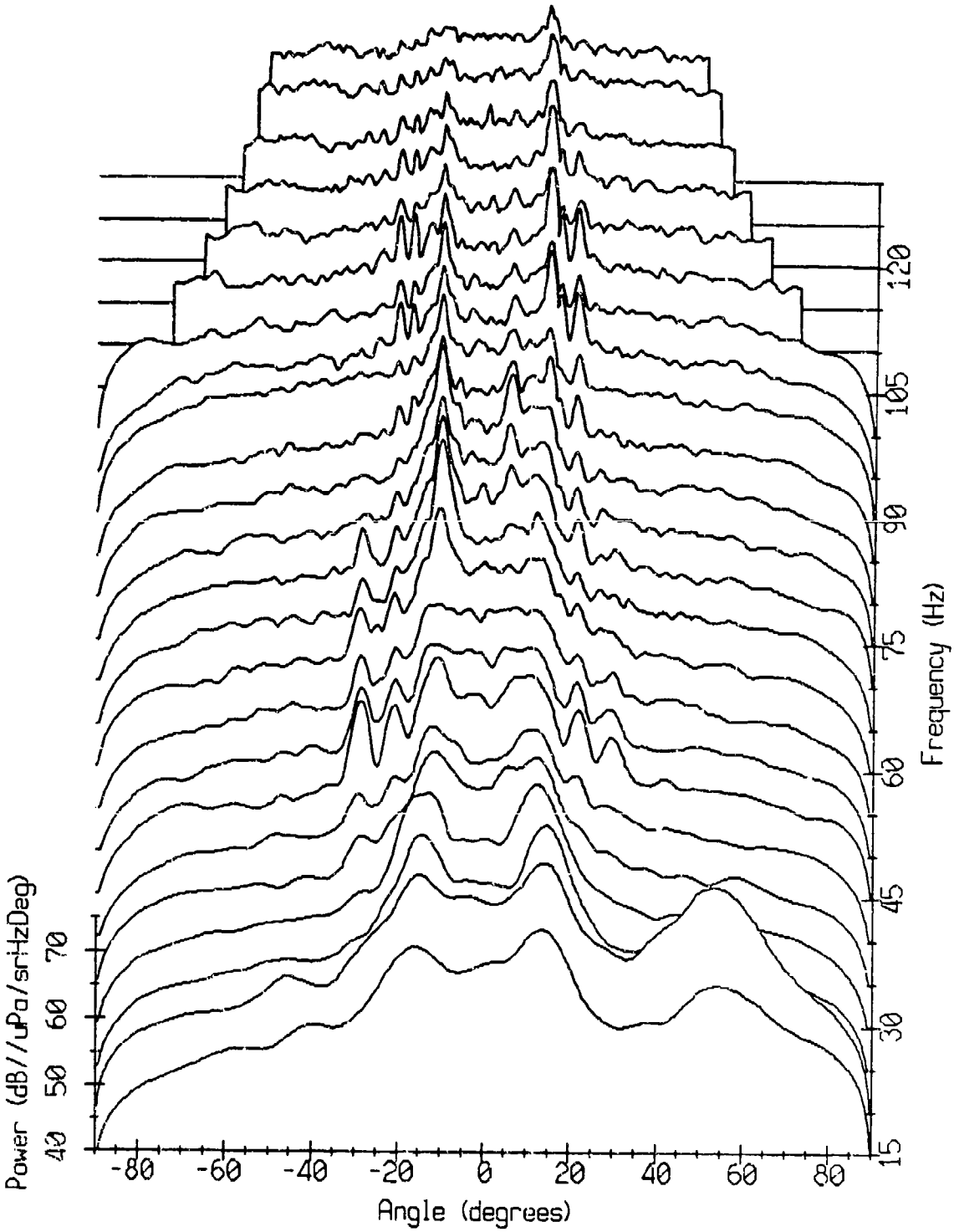

**Figure 3.**

**Spatial spectra 21 hour time series at specified frequencies.**

# Spatial Distribution with Increasing Wind at 15 Hz

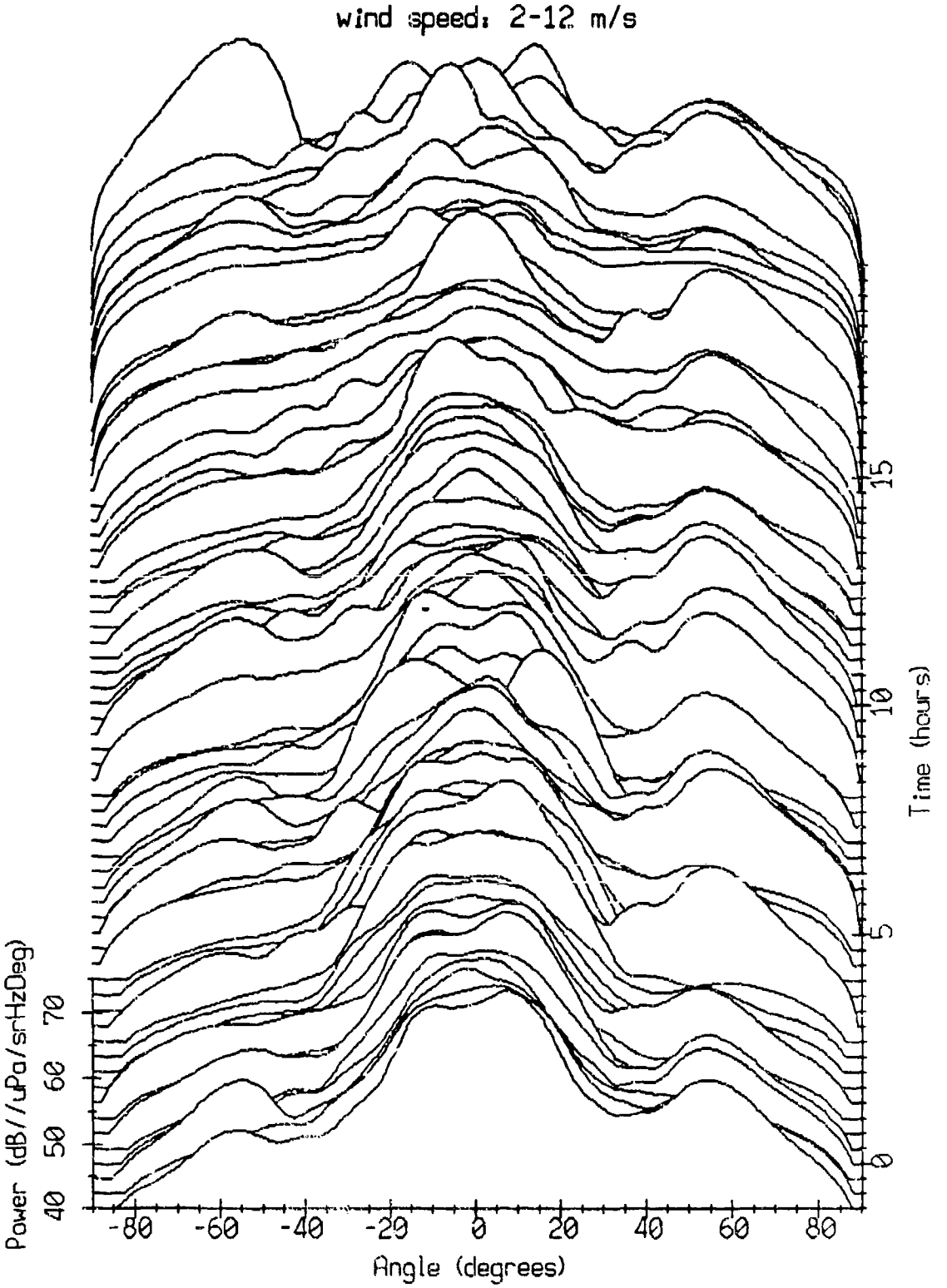

# Spatial Distribution with Increasing Wind at 20 Hz

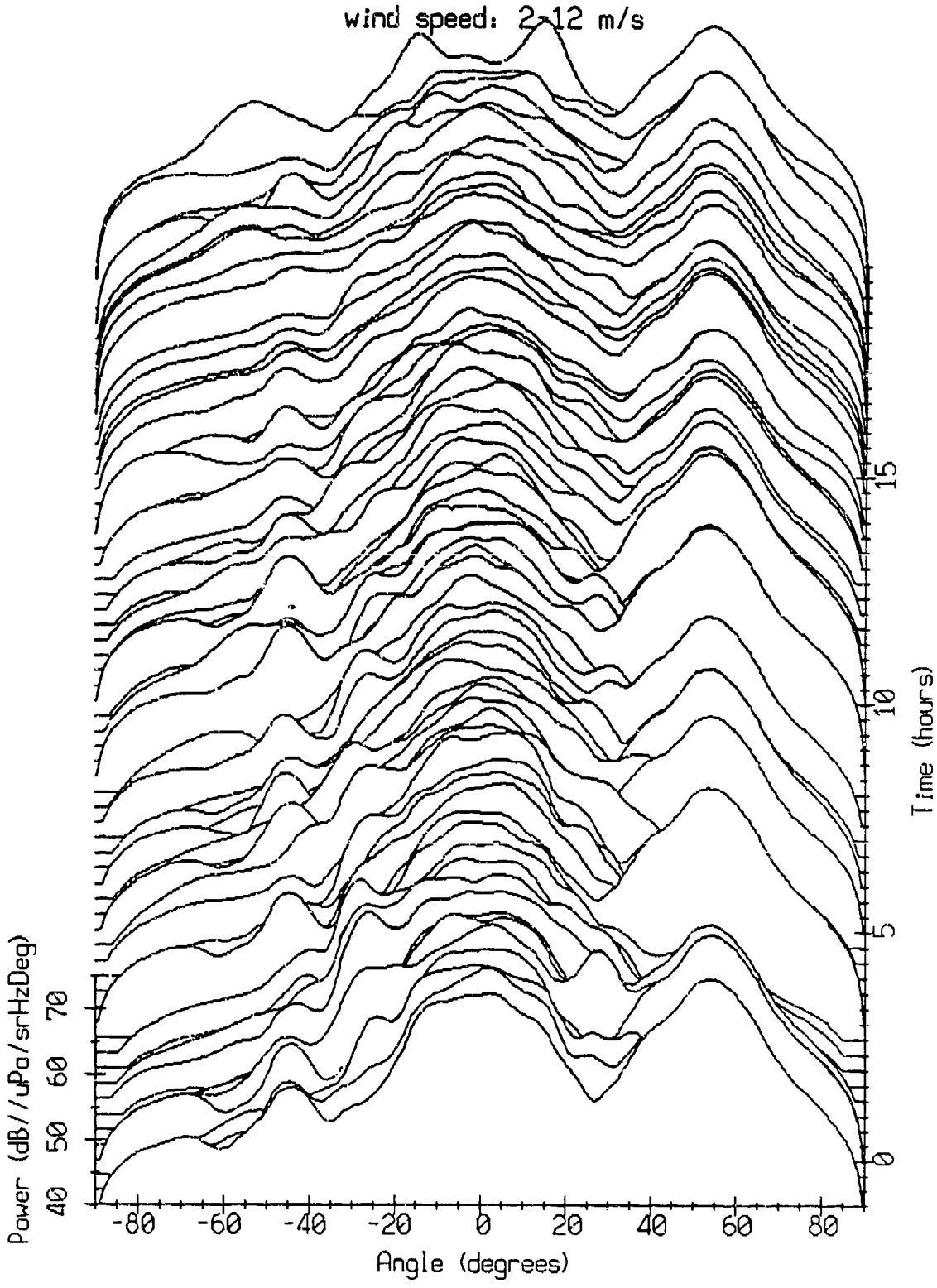

# Spatial Distribution with Increasing Wind at 25 Hz

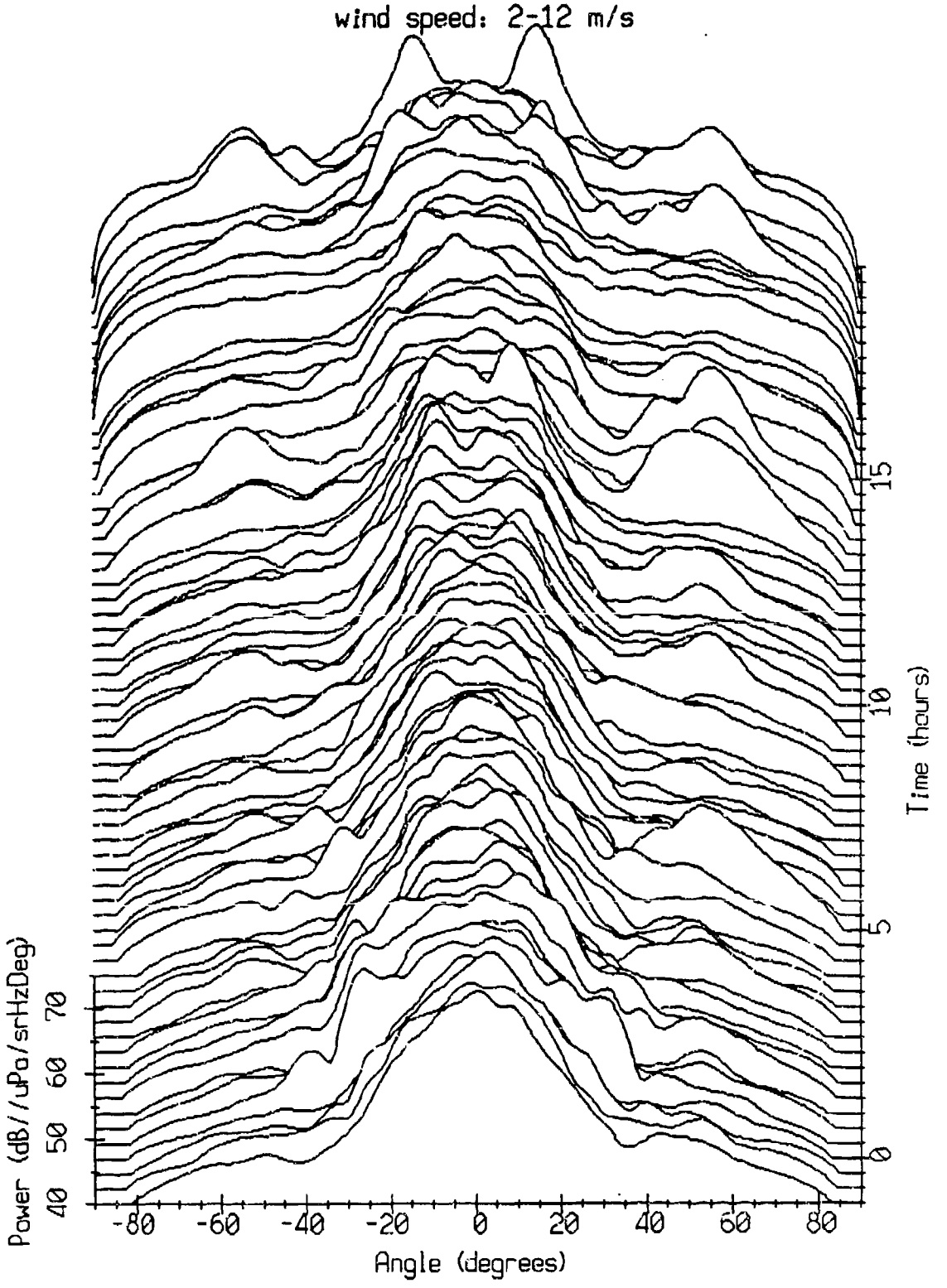

Spatial Distribution with Increasing Wind at 30 Hz

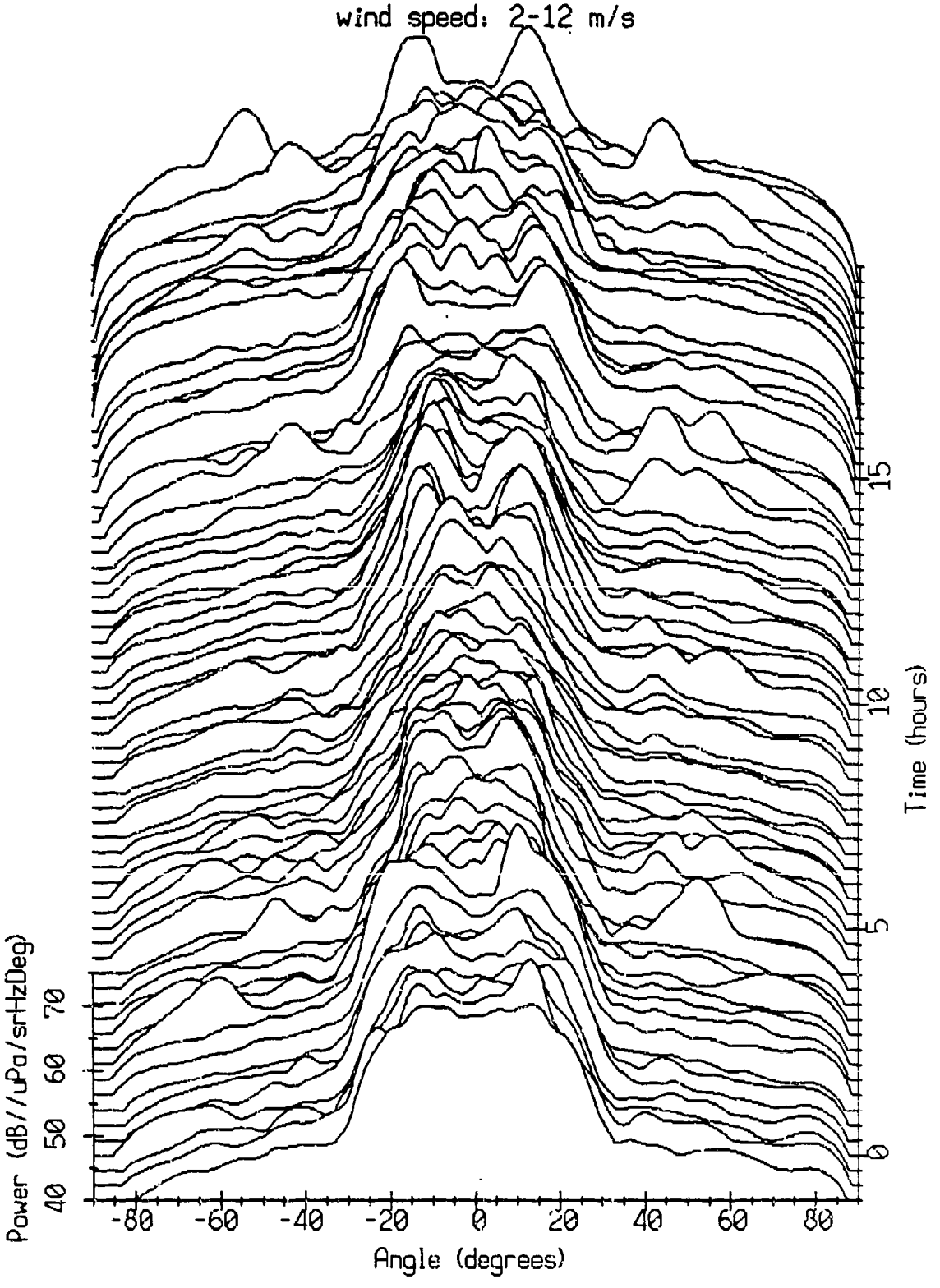

# Spatial Distribution with Increasing Wind at 35 Hz

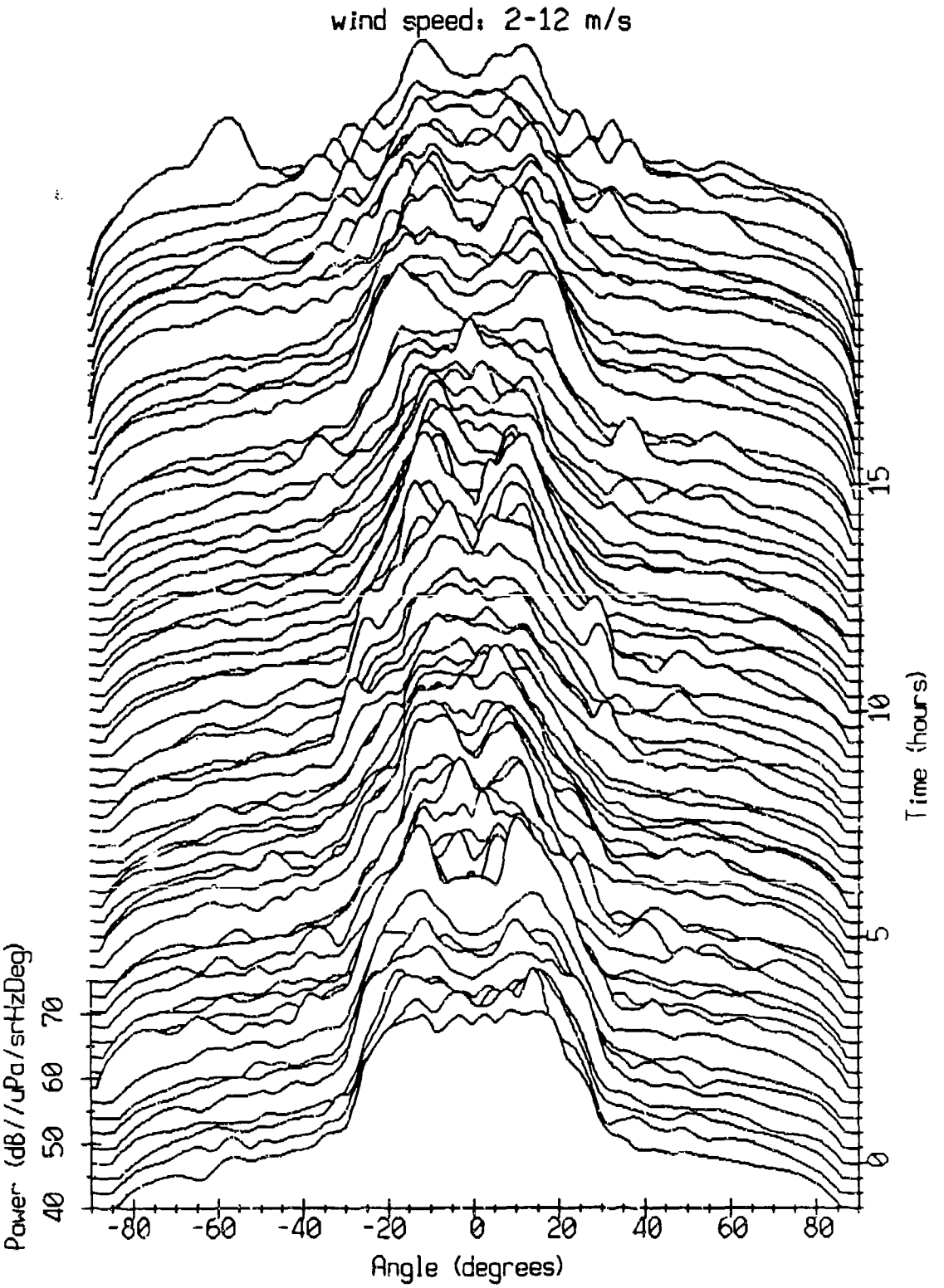

# Spatial Distribution with Increasing Wind at 40 Hz

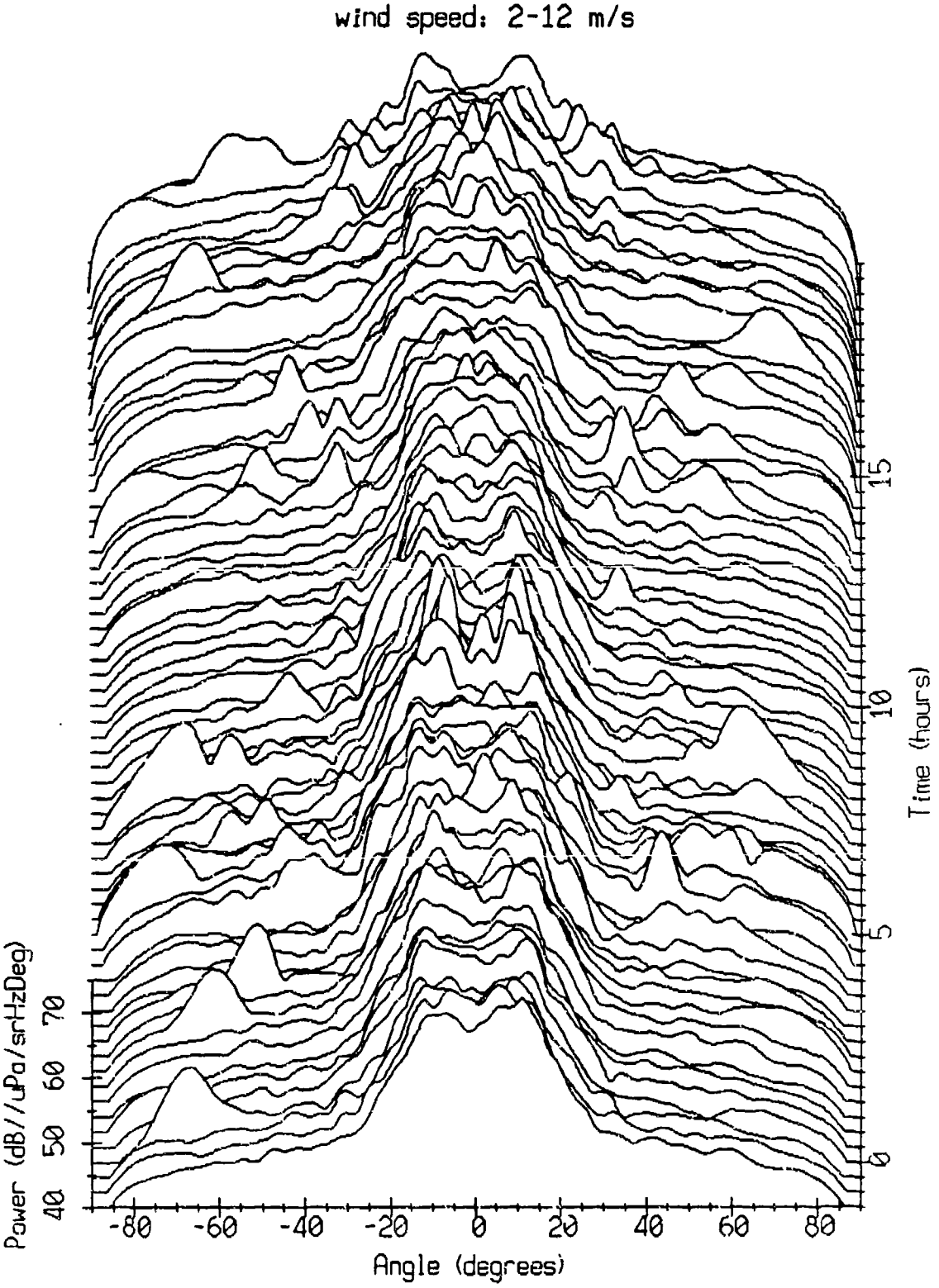

# Spatial Distribution with Increasing Wind at 45 Hz

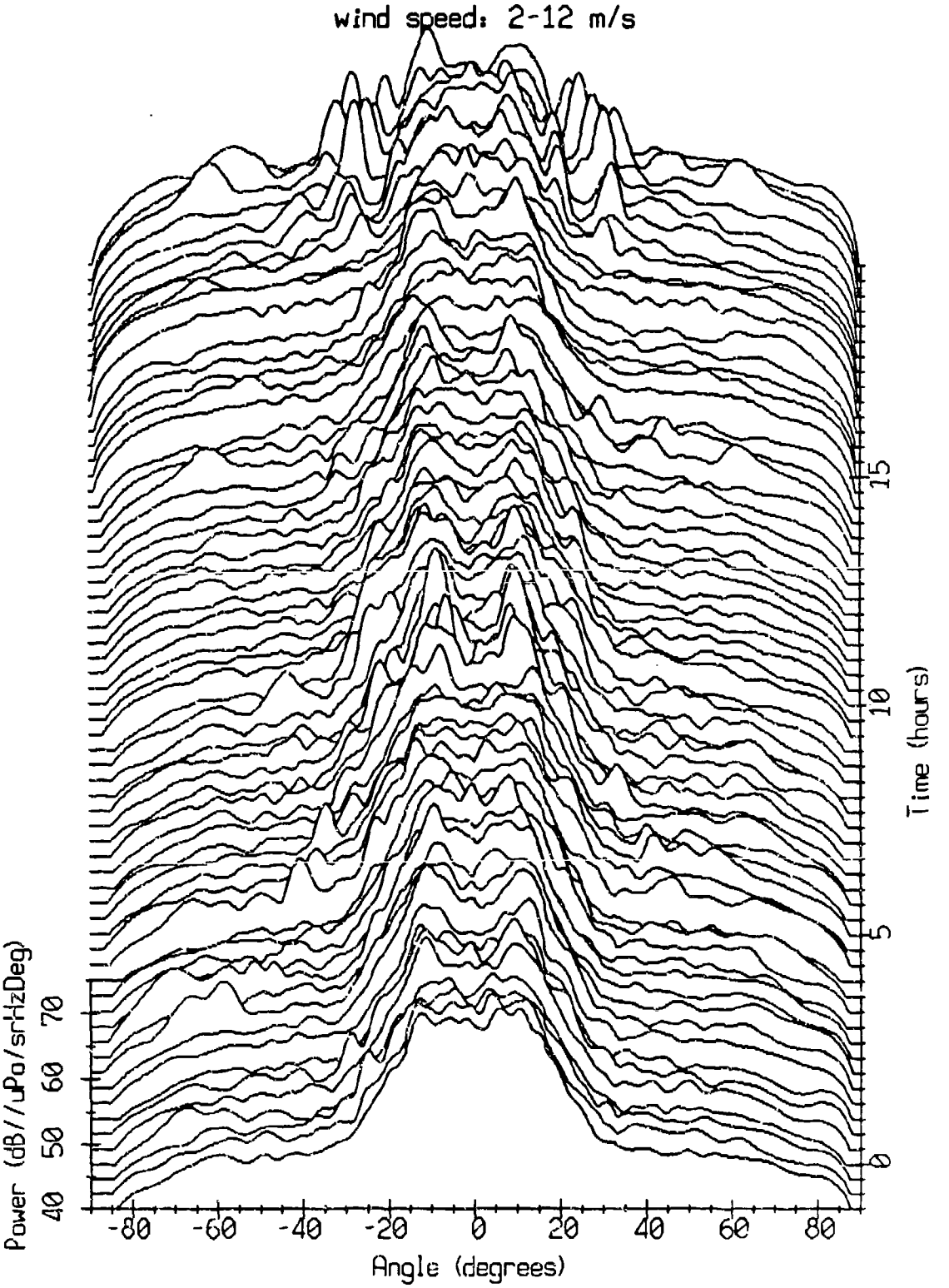

Spatial Distribution with Increasing Wind at 50 Hz

wind speed: 2-12 m/s

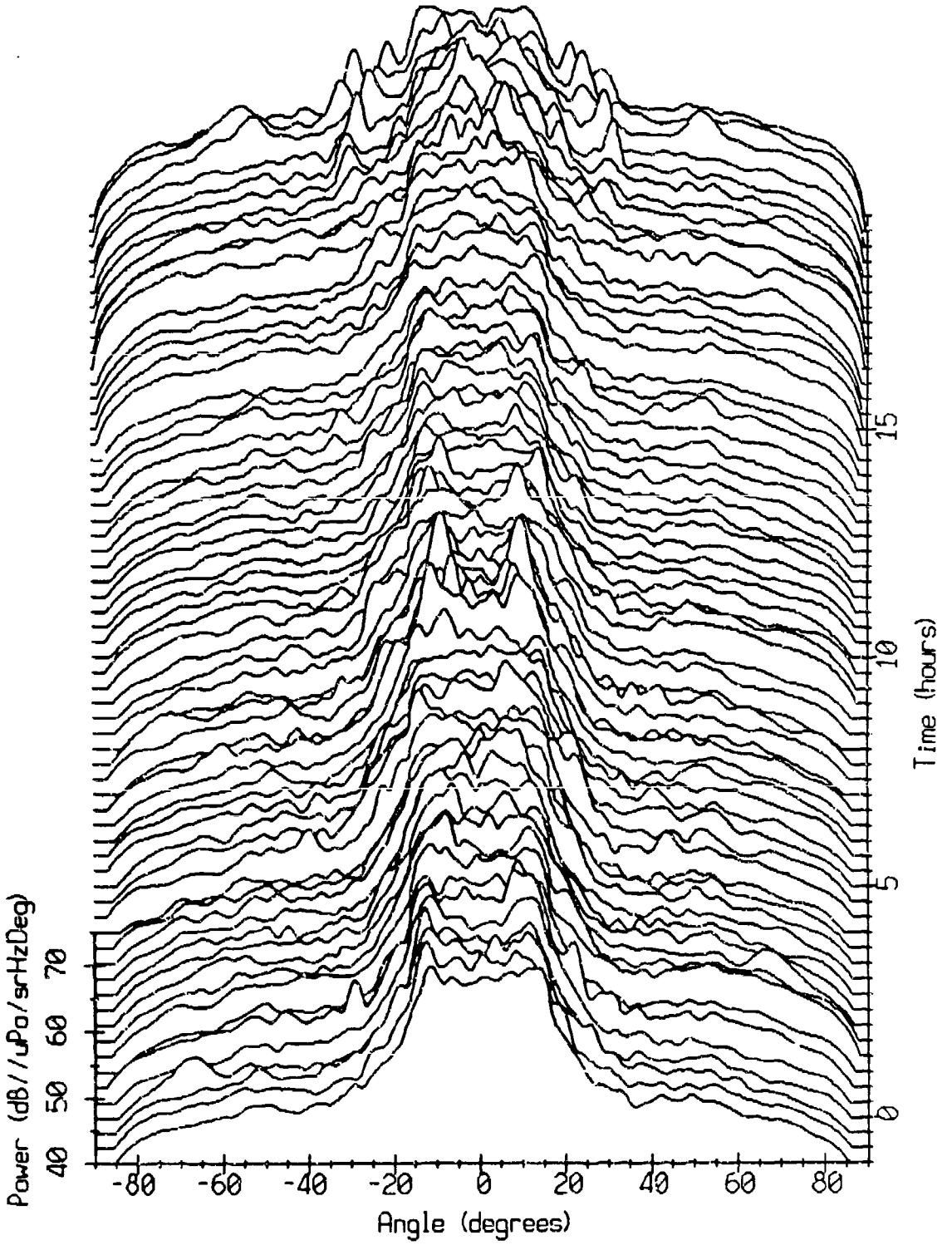

# Spatial Distribution with Increasing Wind at 55 Hz

wind speed: 2-12 m/s

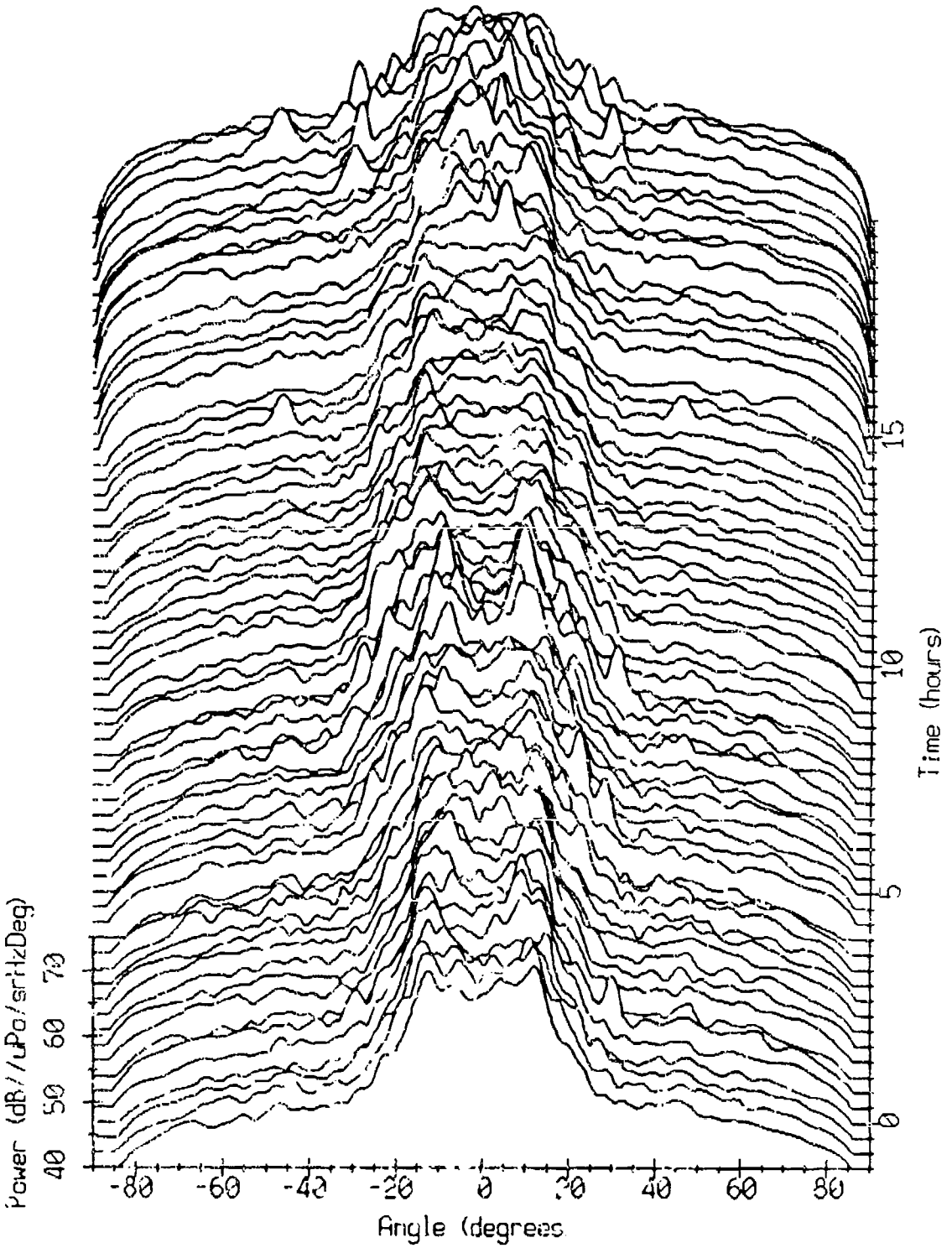

Spatial Distribution with Increasing Wind at 60 Hz

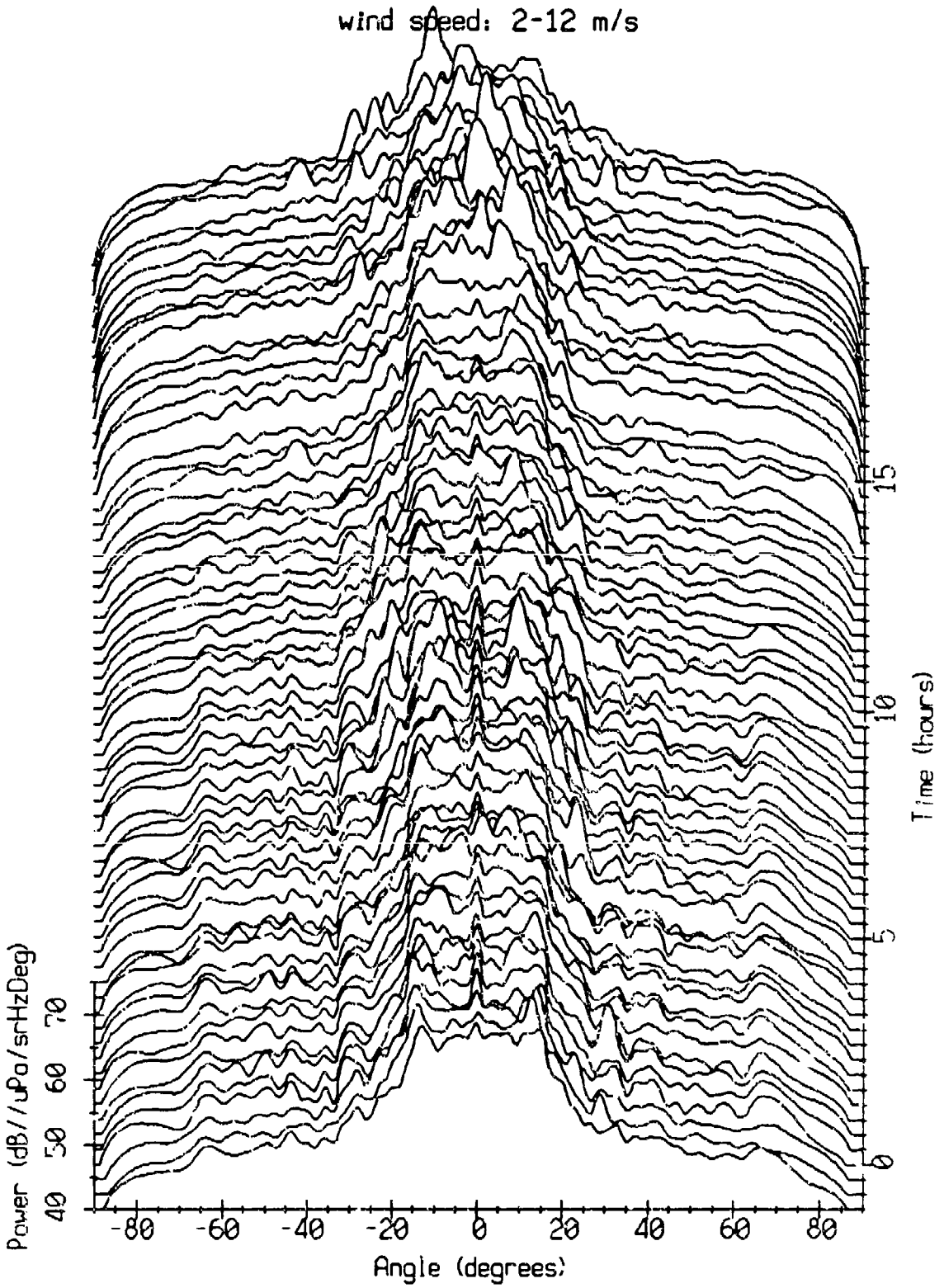

Spatial Distribution with Increasing Wind at 65 Hz

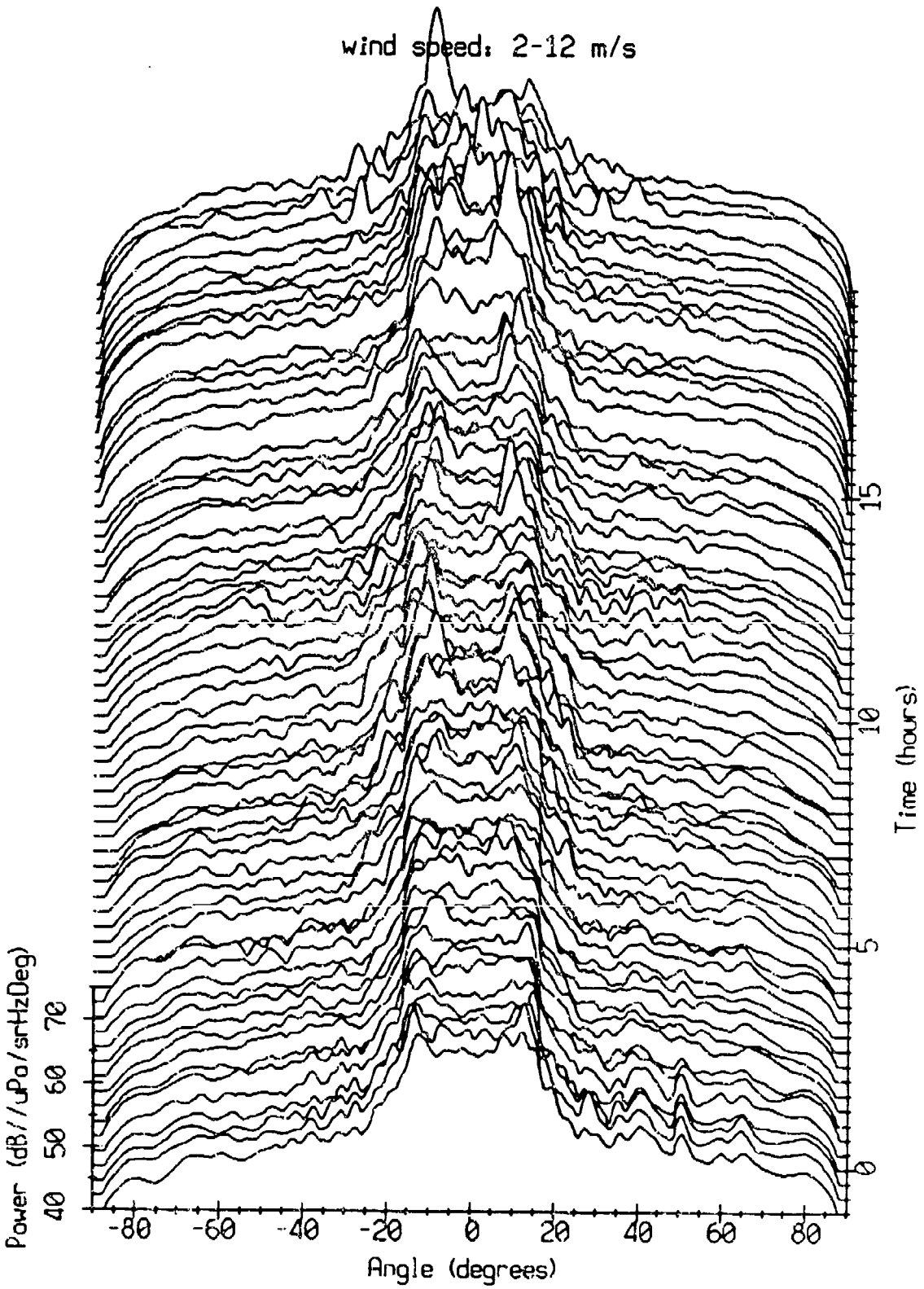

Spatial Distribution with Increasing Wind at 70 Hz

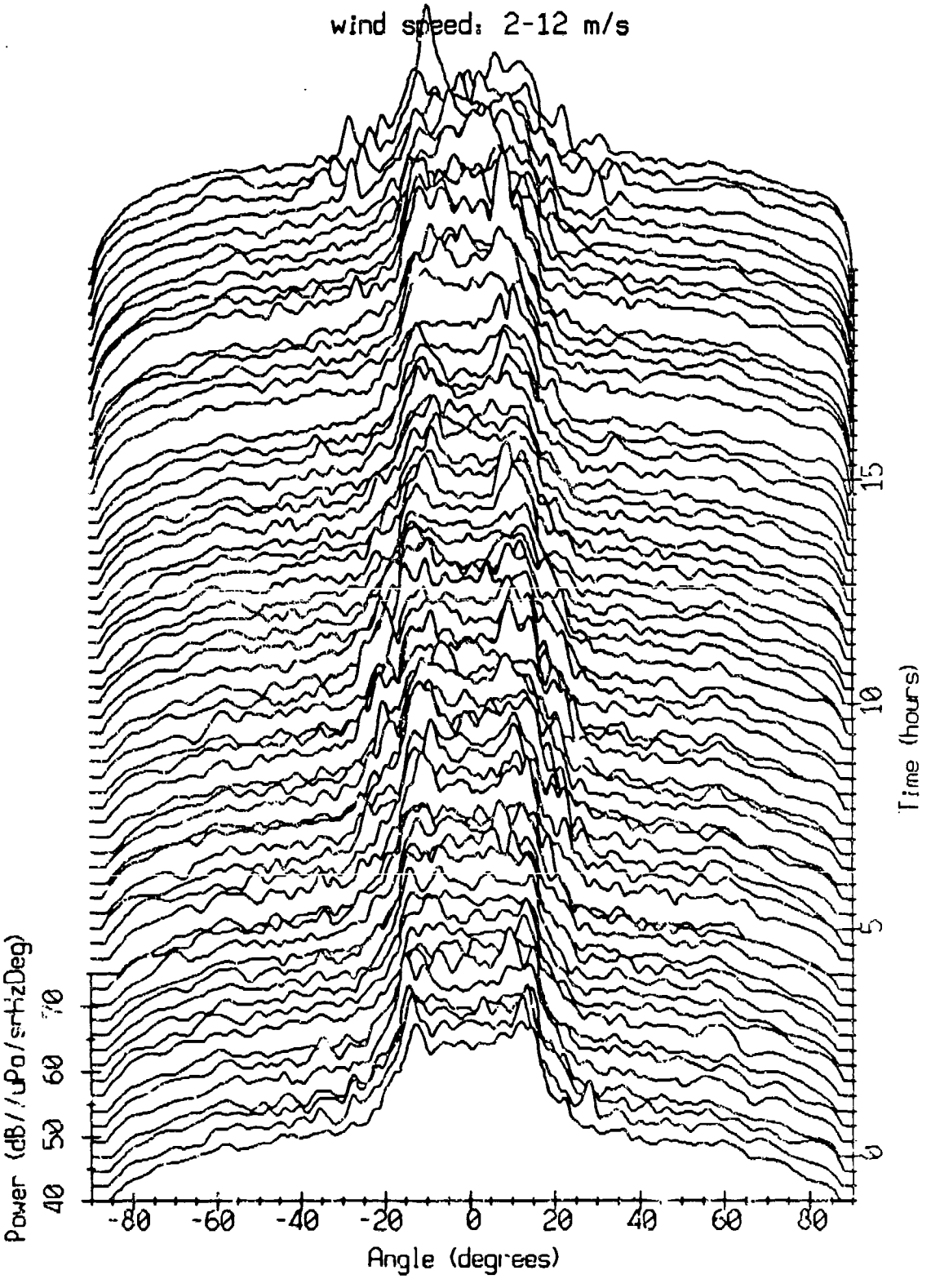

# Spatial Distribution with Increasing Wind at 75 Hz

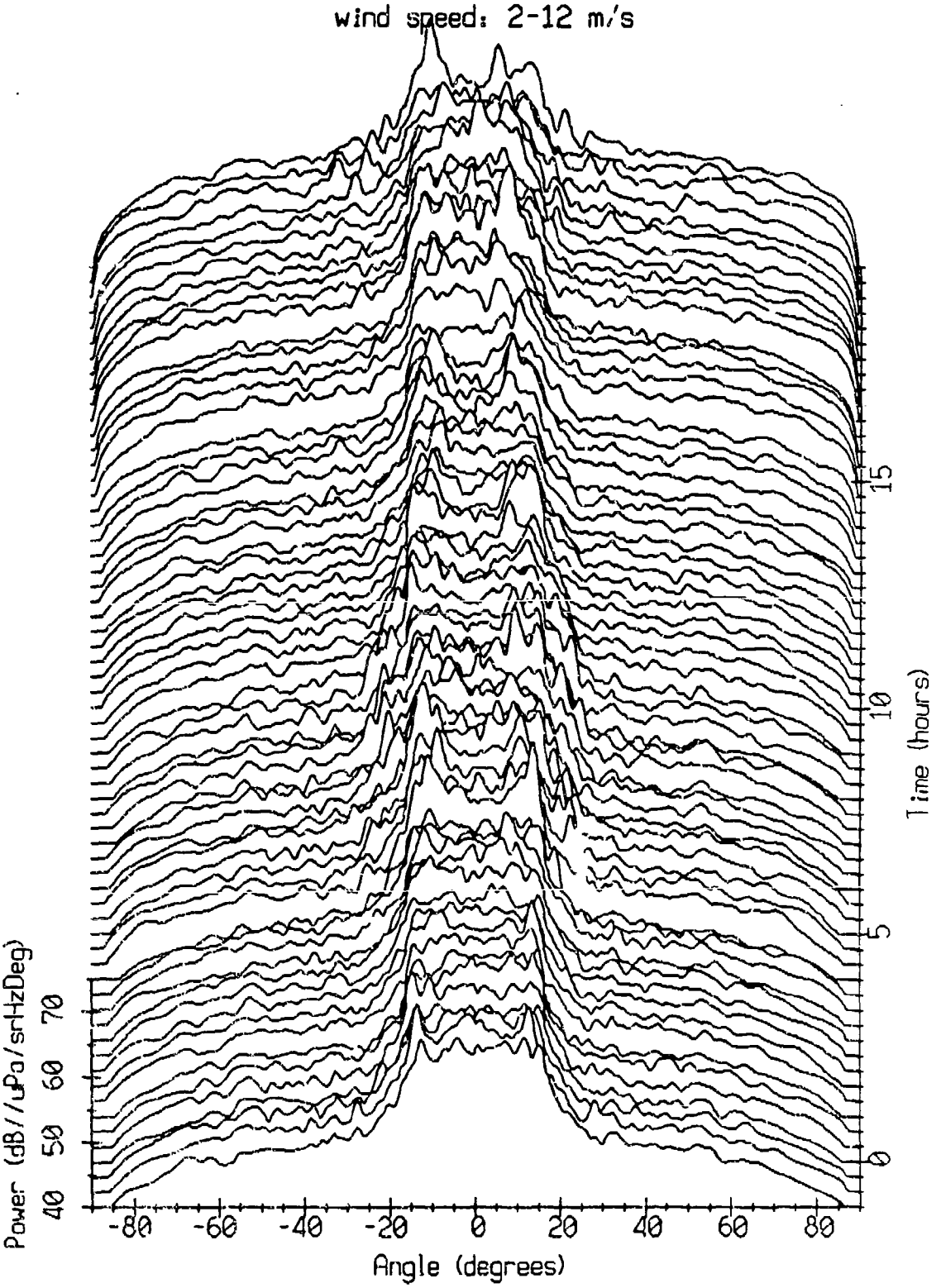

# Spatial Distribution with Increasing Wind at 80 Hz

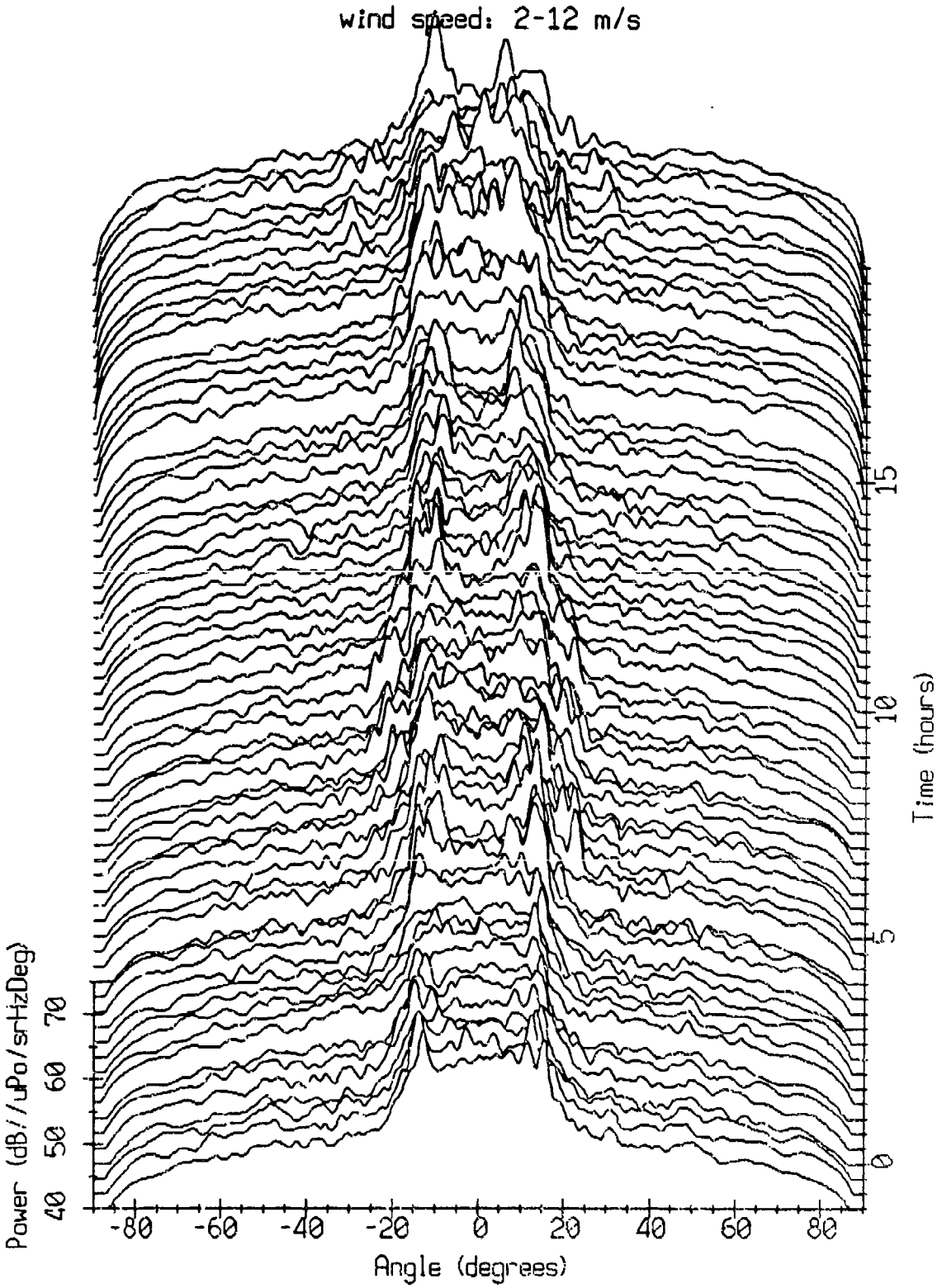

# Spatial Distribution with Increasing Wind at 85 Hz

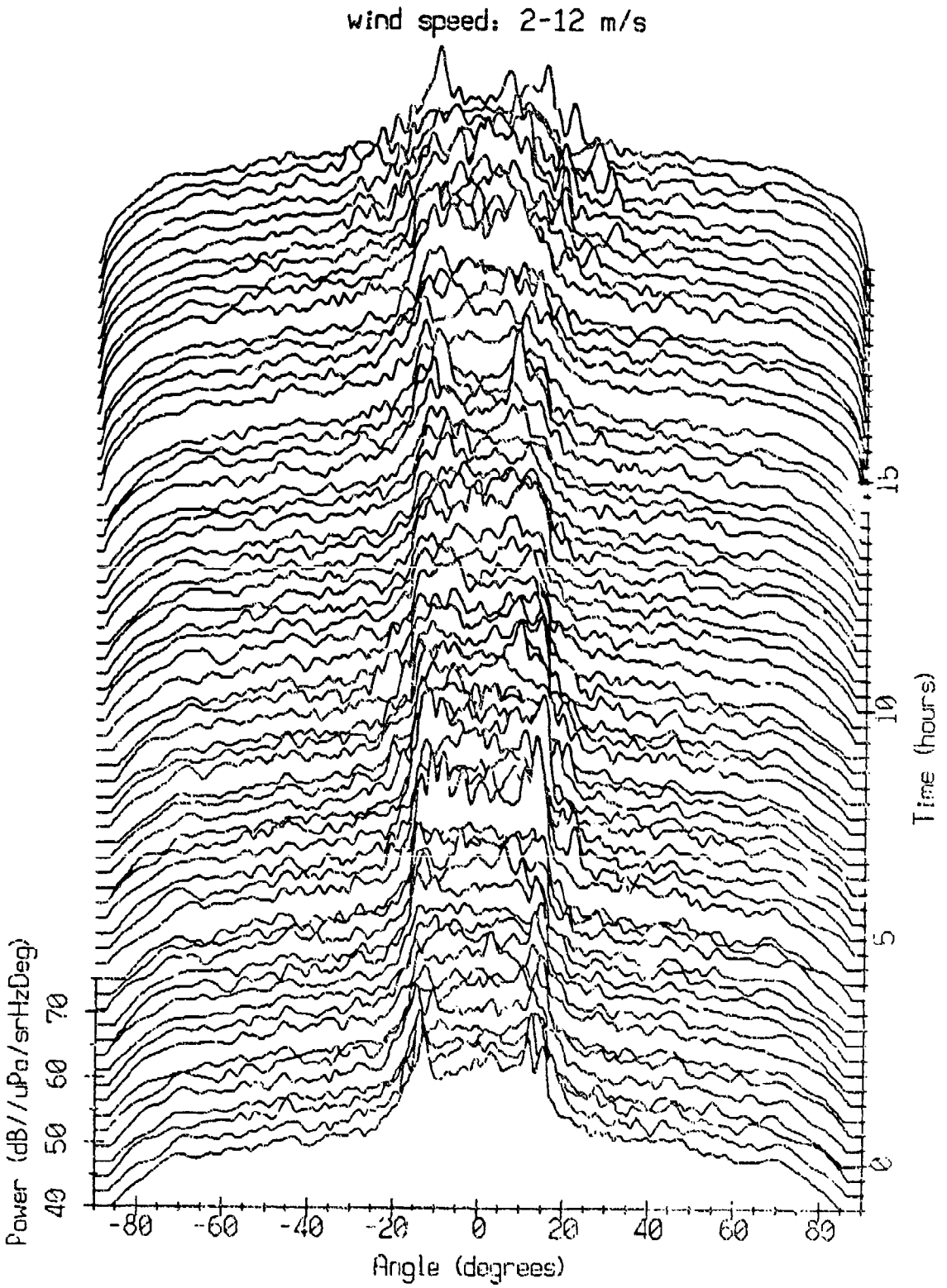

Spatial Distribution with Increasing Wind at 90 Hz

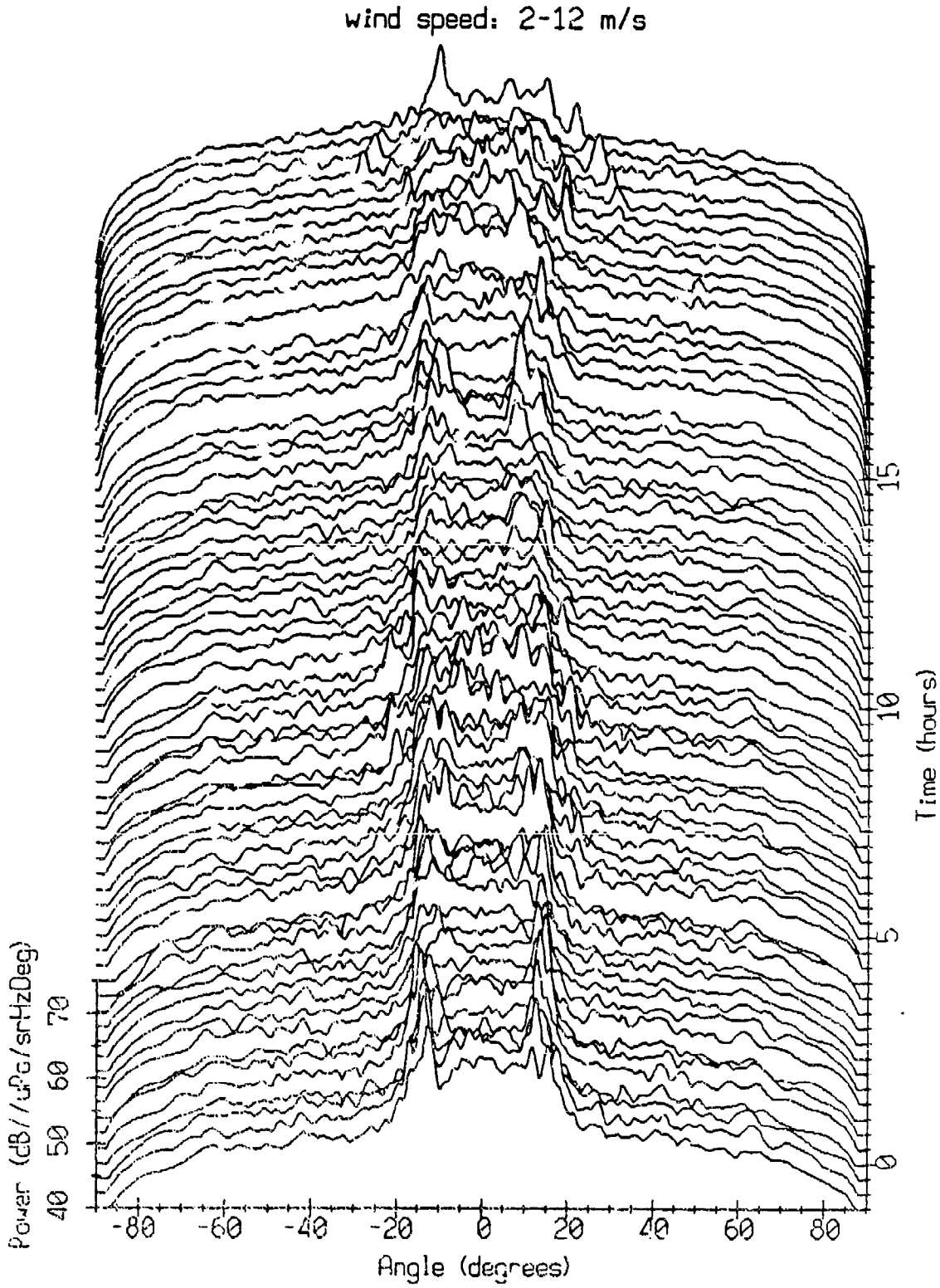

# Spatial Distribution with Increasing Wind at 95 Hz

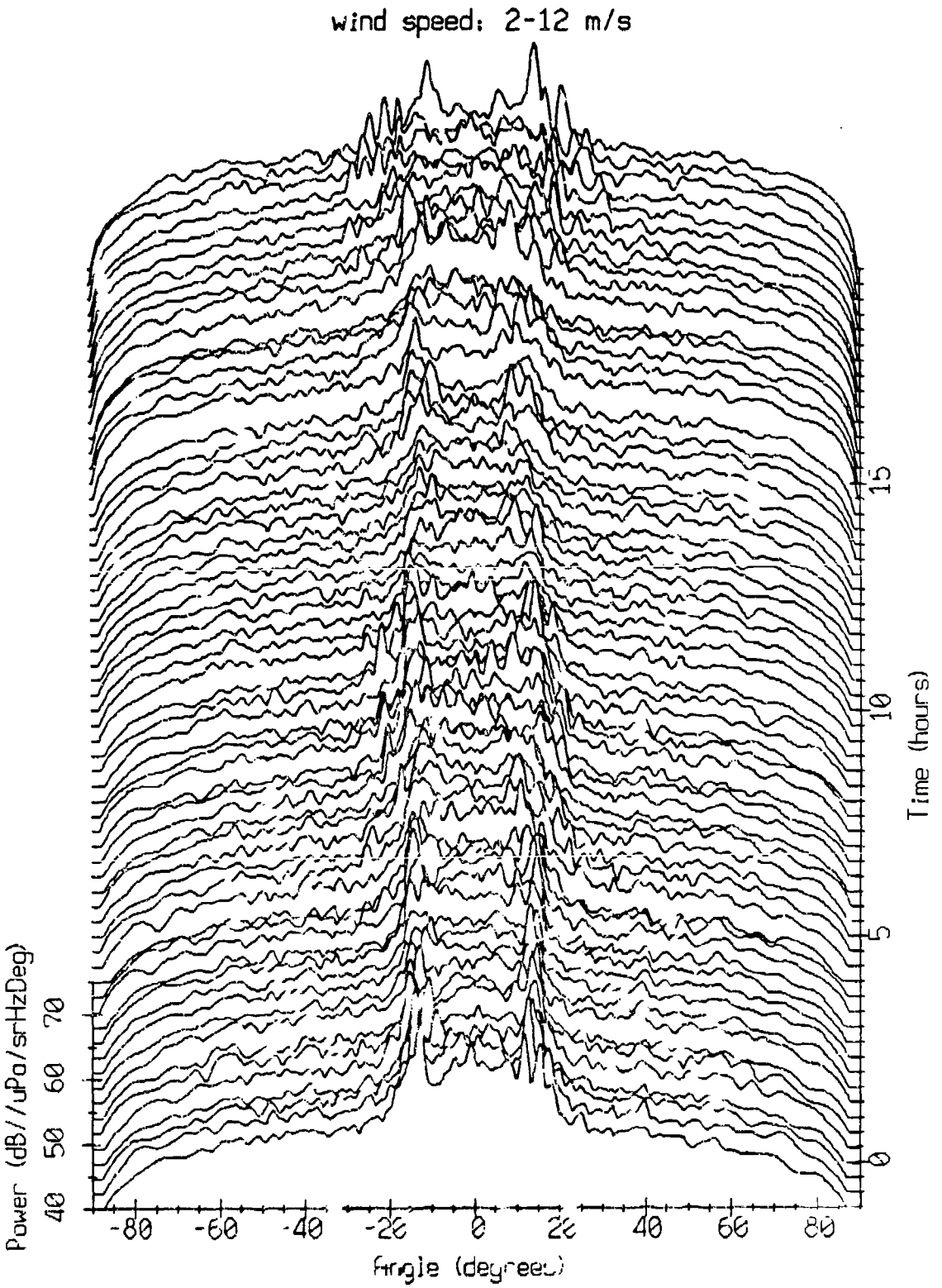

Spatial Distribution with Increasing Wind at 100 Hz

wind speed: 2-12 m/s

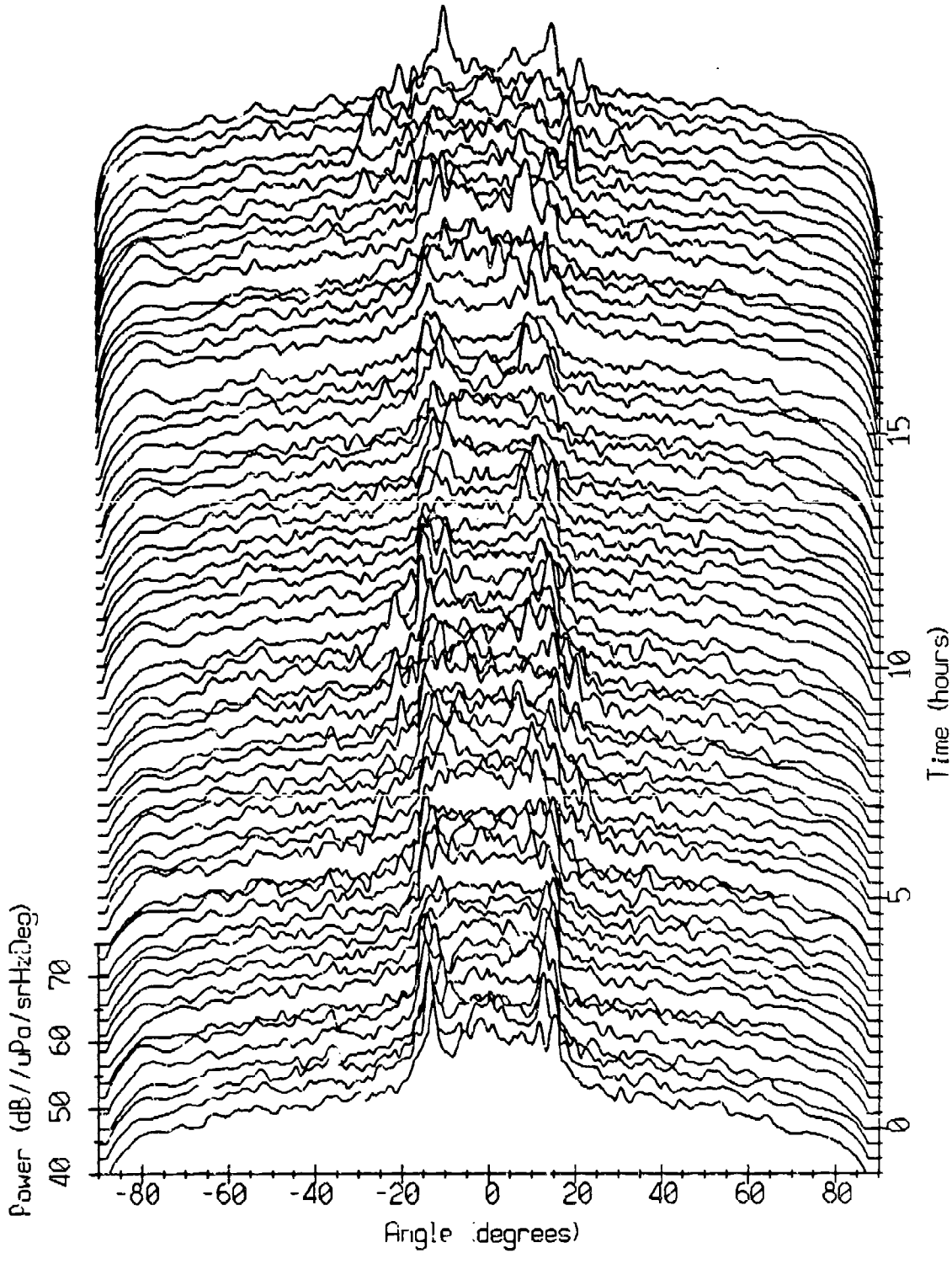

# Spatial Distribution with Increasing Wind at 105 Hz

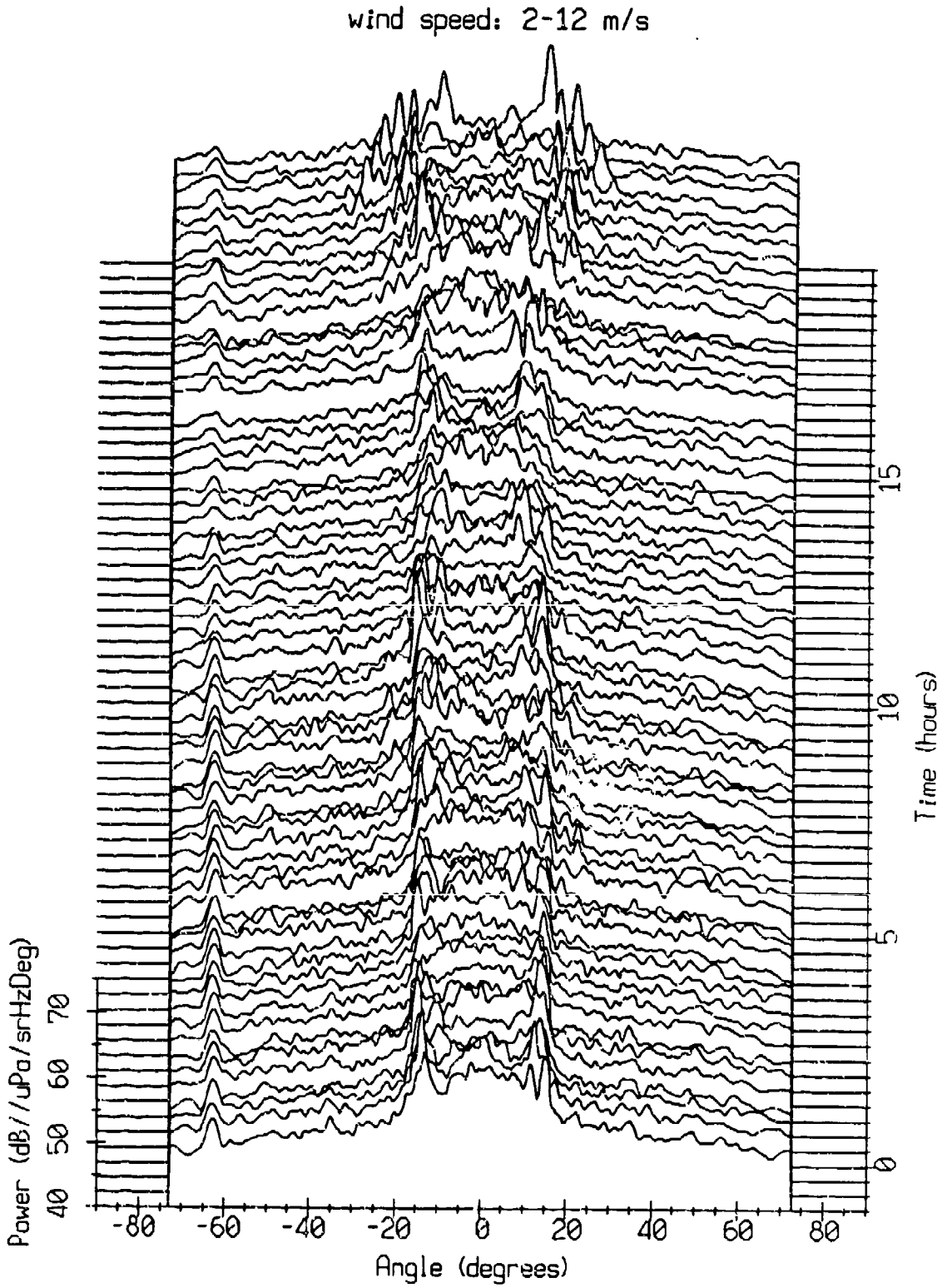

Spatial Distribution with Increasing Wind at 110 Hz

wind speed: 2-12 m/s

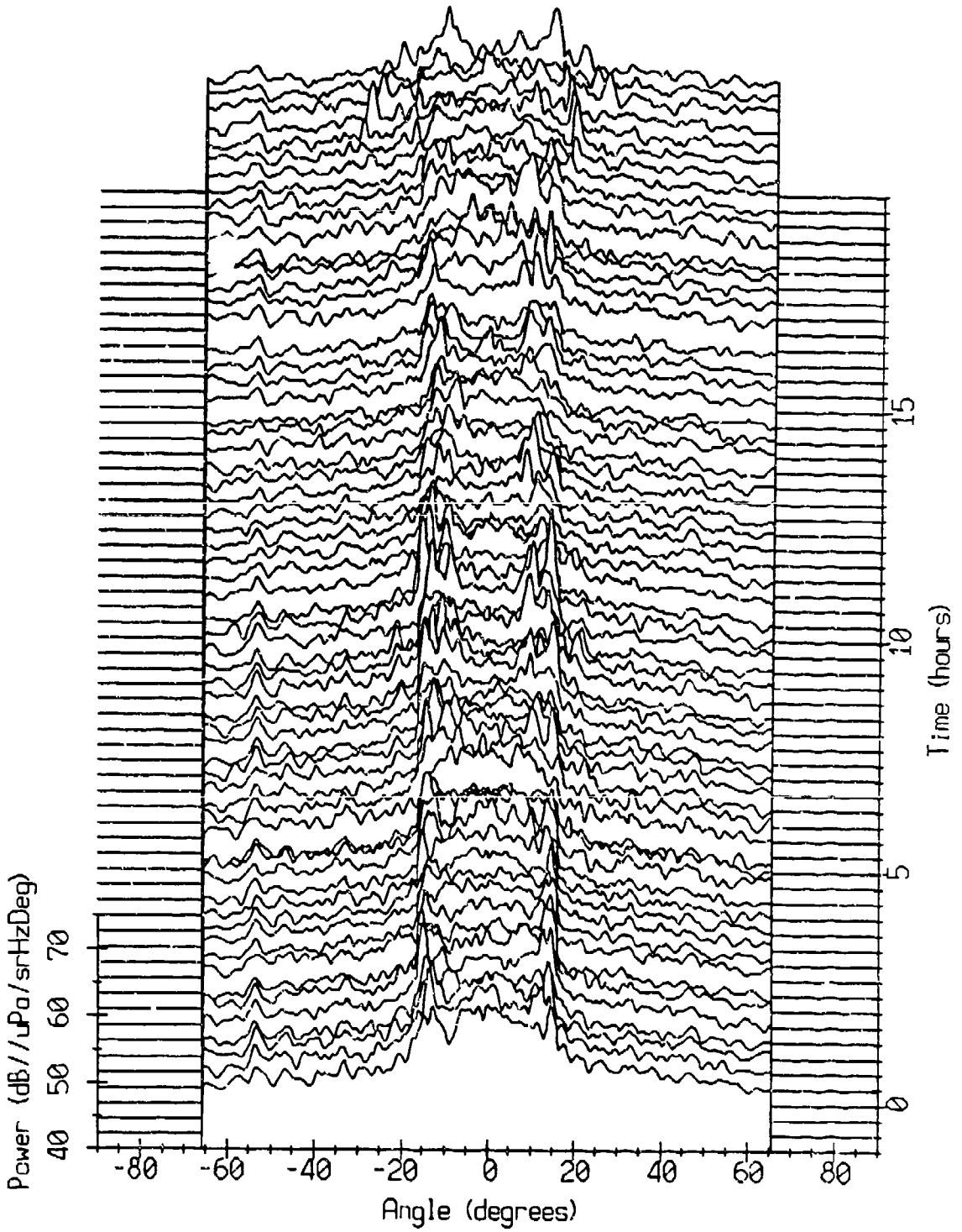

# Spatial Distribution with Increasing Wind at 115 Hz

wind speed: 2-12 m/s

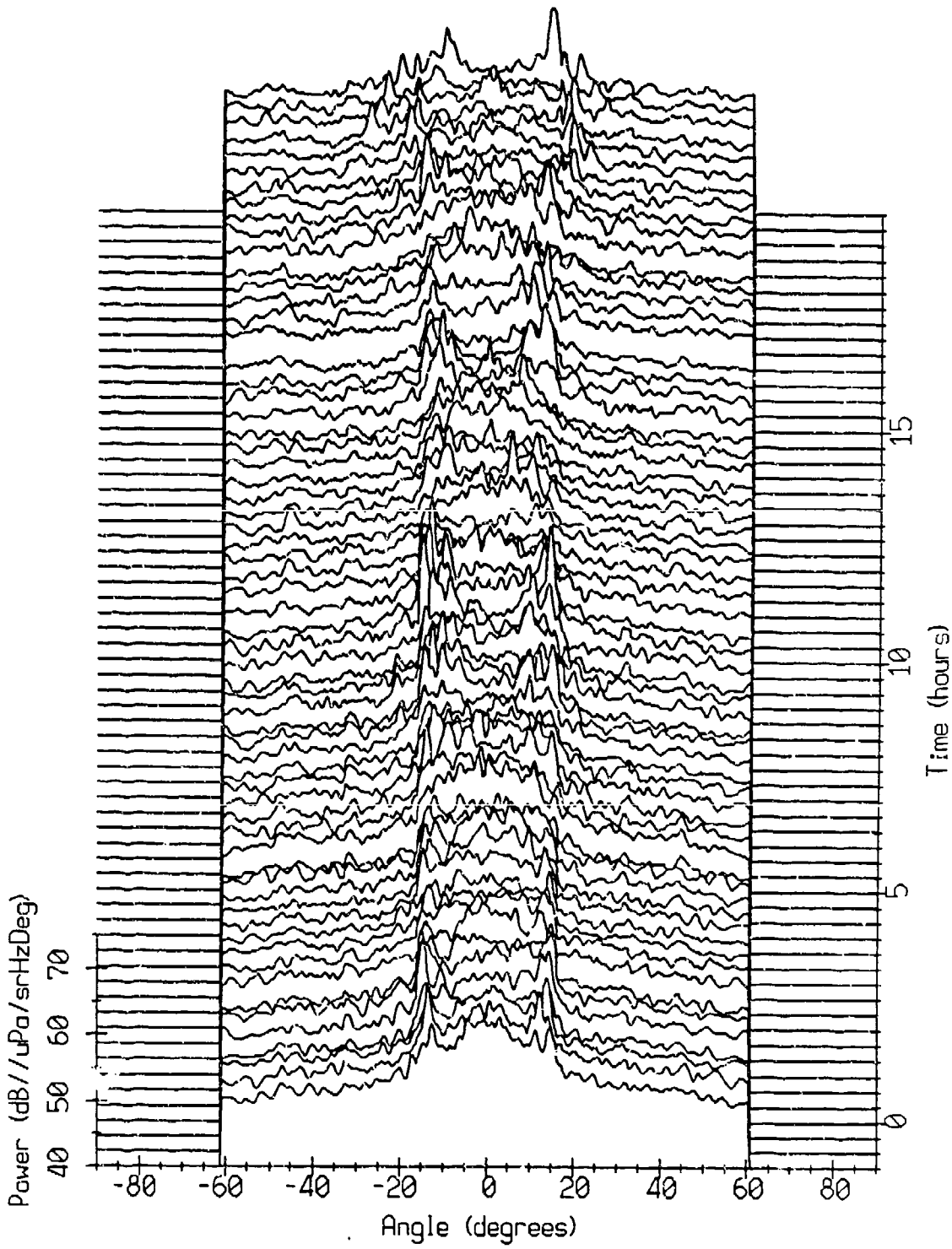

Spatial Distribution with Increasing Wind at 120 Hz

wind speed: 2-12 m/s

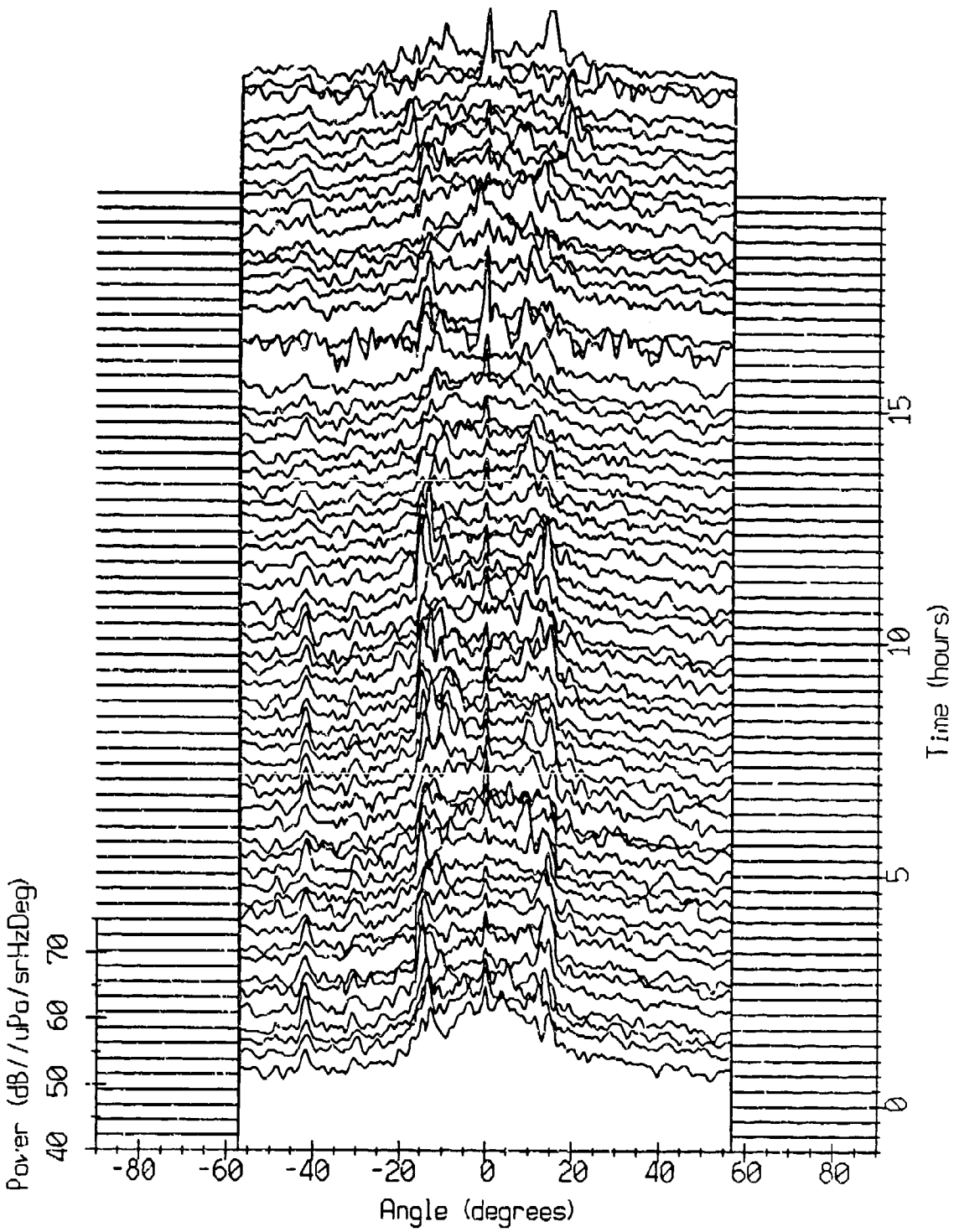

# Spatial Distribution with Increasing Wind at 125 Hz

wind speed: 2-12 m/s

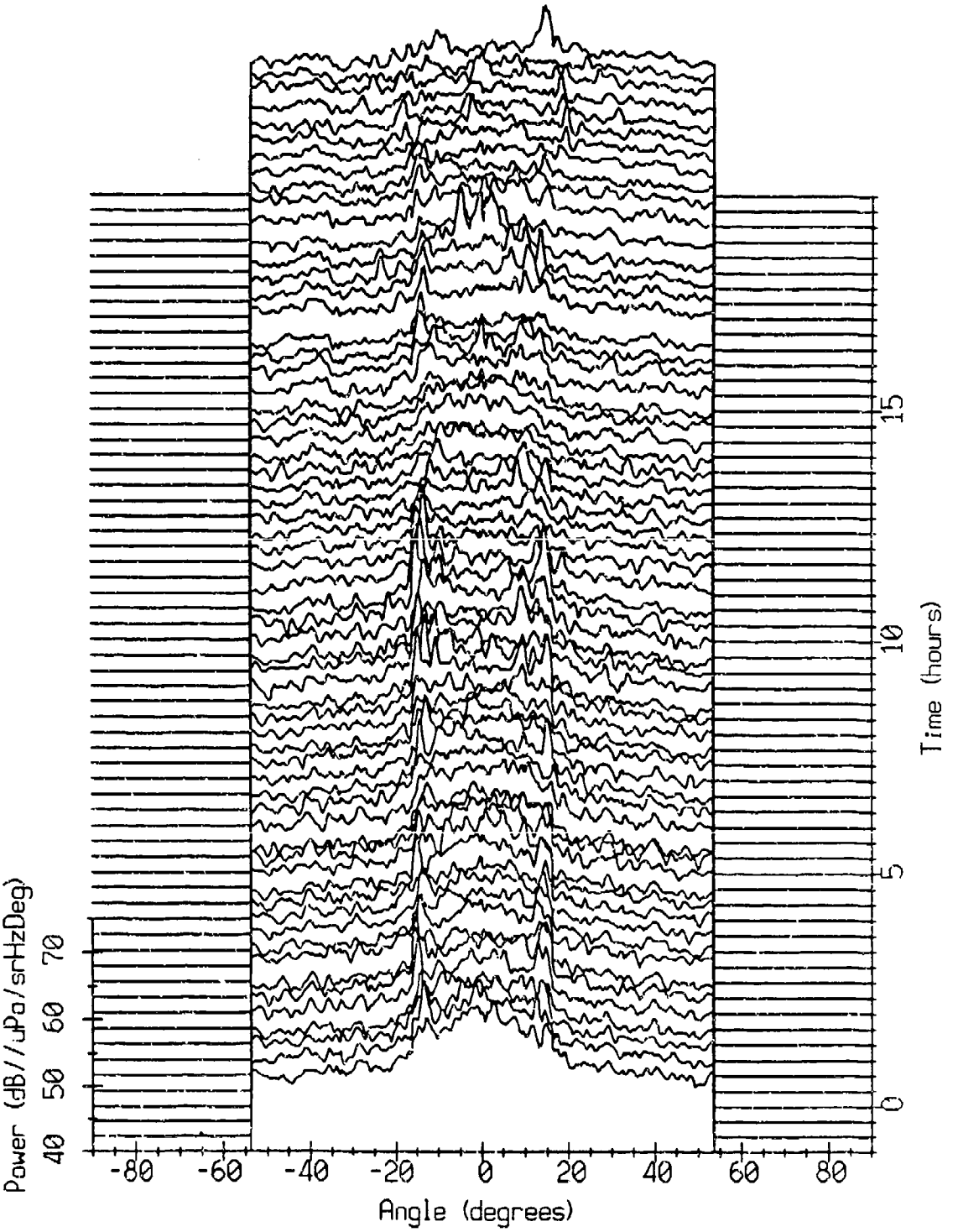

Spatial Distribution with Increasing Wind at 130 Hz

wind speed: 2-12 m/s

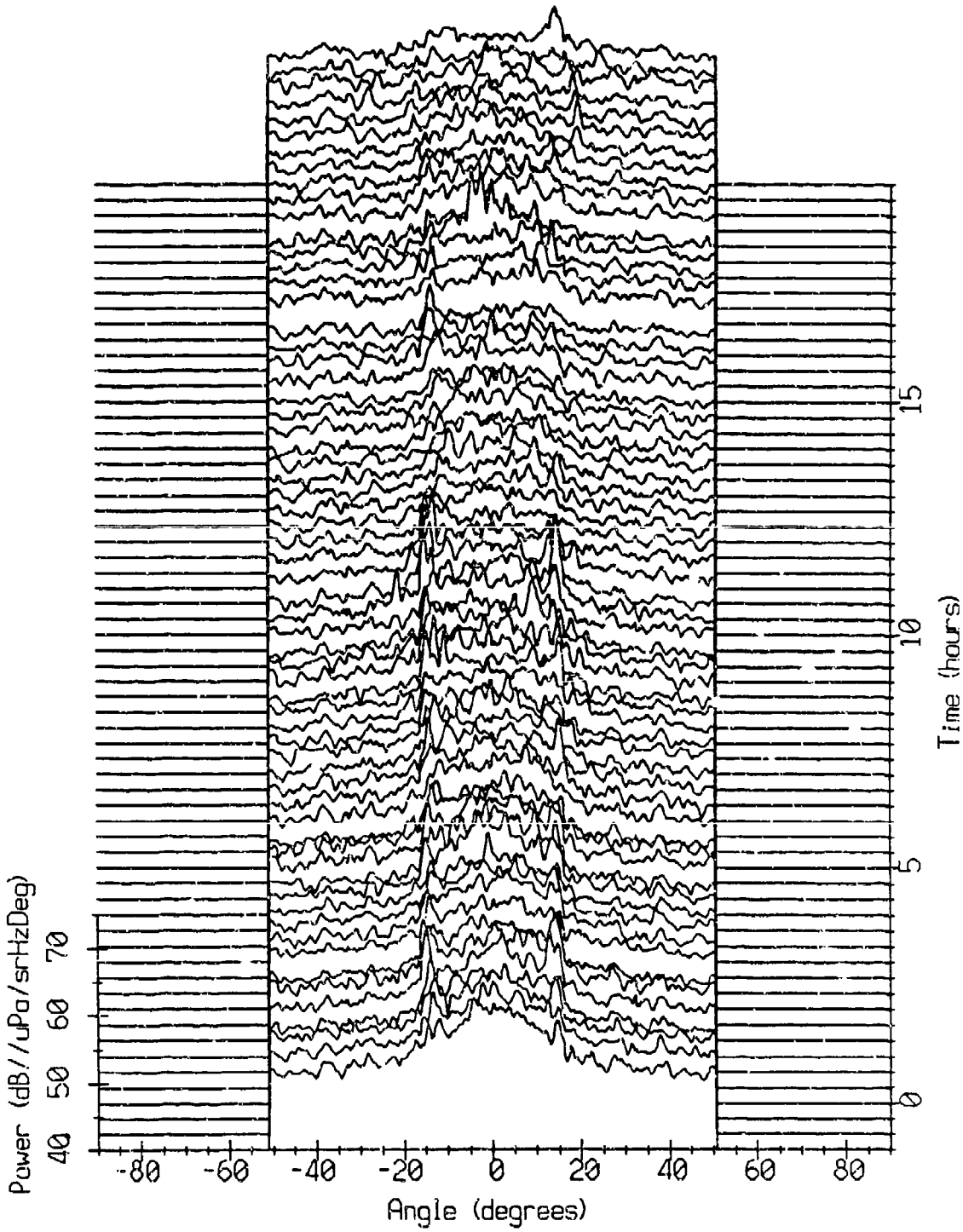

**Figure 4.**

**Directional 21 hour time series at specified frequencies.**

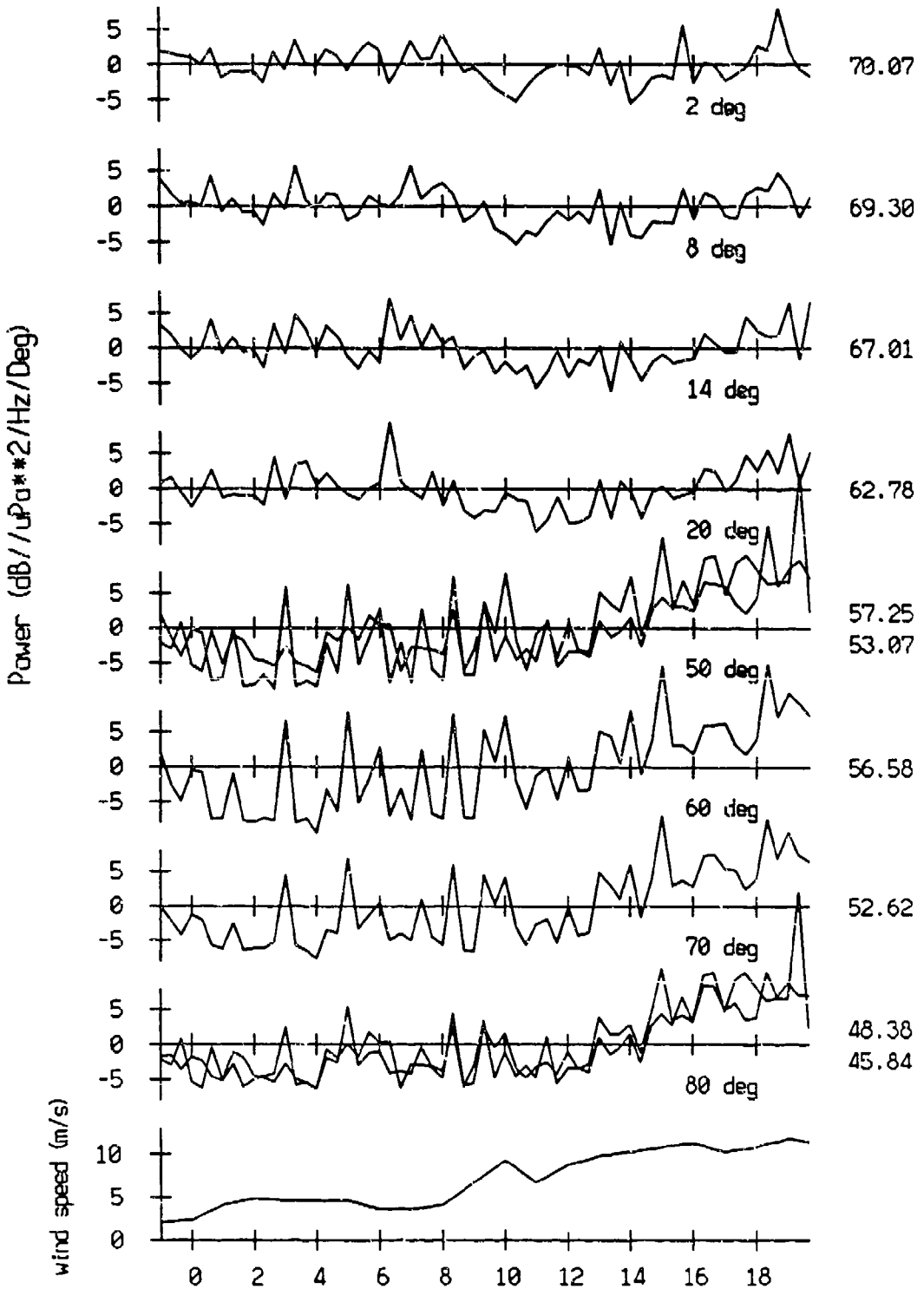


Directional time series : 15 Hz

Time (hours) from Jday 258, increasing wind speed

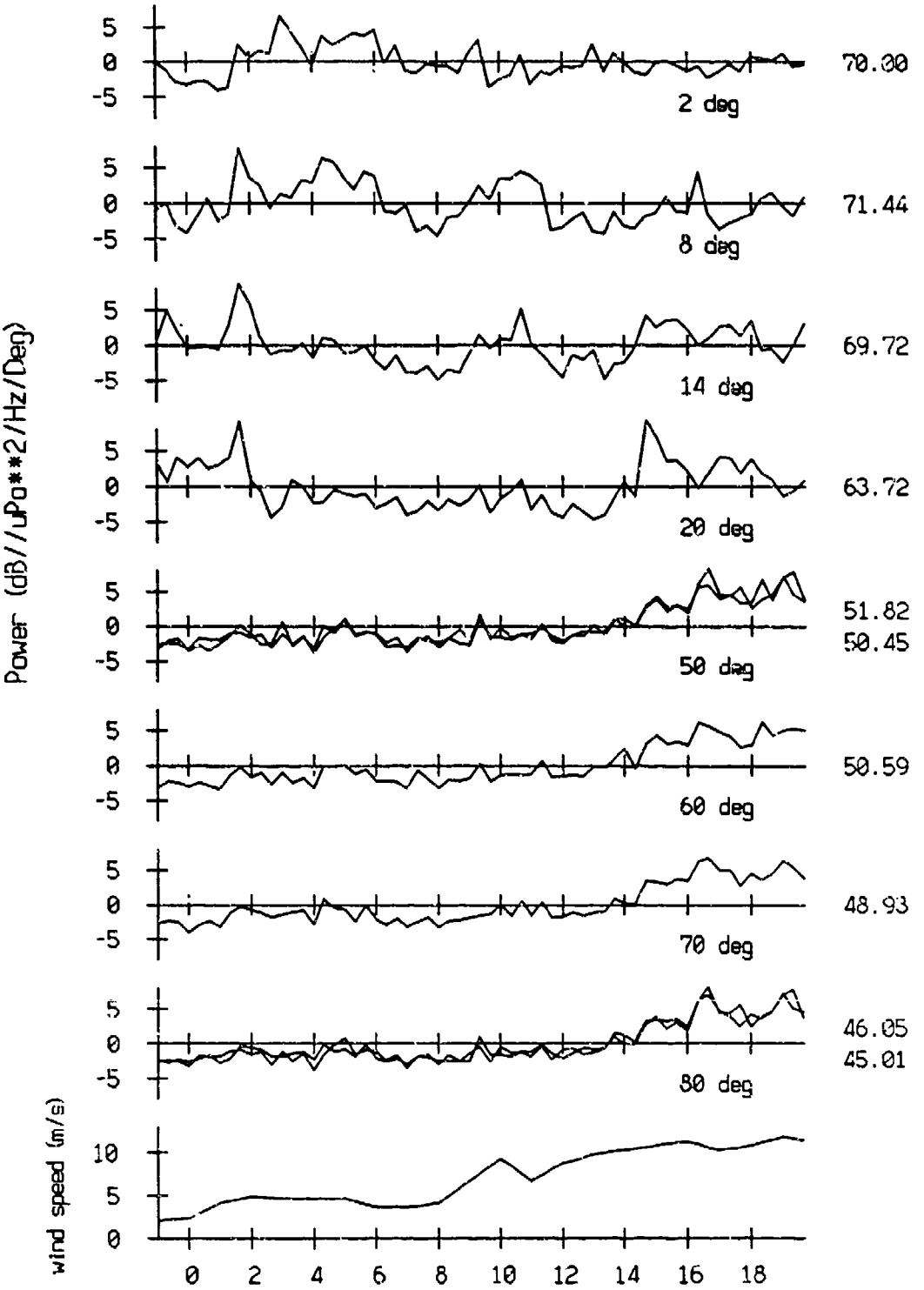
Power (dB//uPa**2/Hz/Deg)
5
0
-5
2 deg
70.00
8 deg
71.44
14 deg
69.72
20 deg
63.72
50 deg
51.82
50.45
60 deg
50.59
70 deg
48.93
80 deg
46.05
45.01
wind speed (m/s)
10
5
0
0 2 4 6 8 10 12 14 16 18
Directional time series : 35 Hz
Time (hours) from Jday 258, increasing wind speed

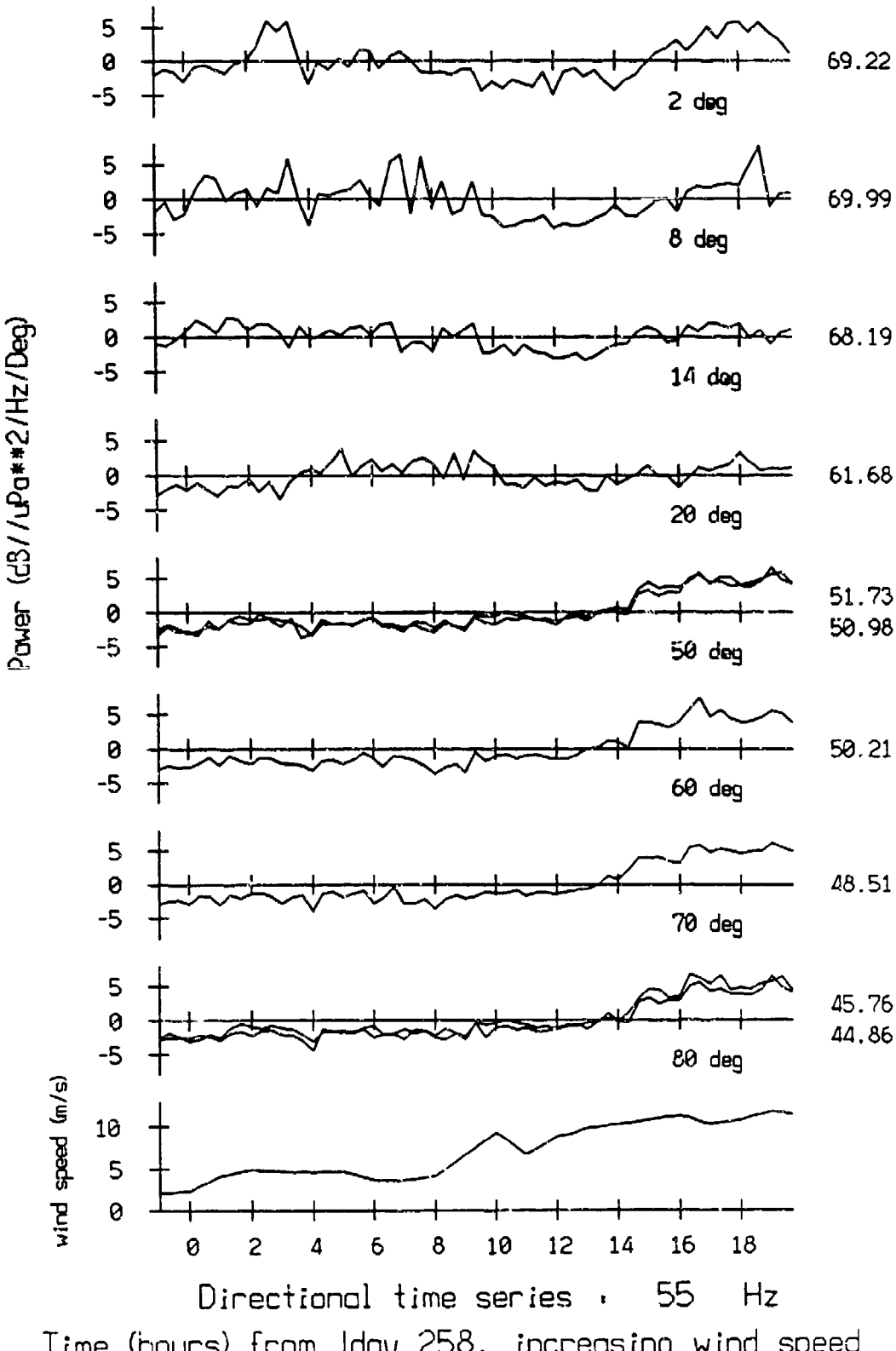
Power (dB//uPa**2/Hz/Deg)
5
0
-5
2 deg
69.22
8 deg
69.99
14 deg
68.19
20 deg
61.68
50 deg
51.73
50.98
60 deg
50.21
70 deg
48.51
80 deg
45.76
44.86
wind speed (m/s)
10
5
0
0
2
4
6
8
10
12
14
16
18
Directional time series . 55 Hz
Time (hours) from Jday 258, increasing wind speed

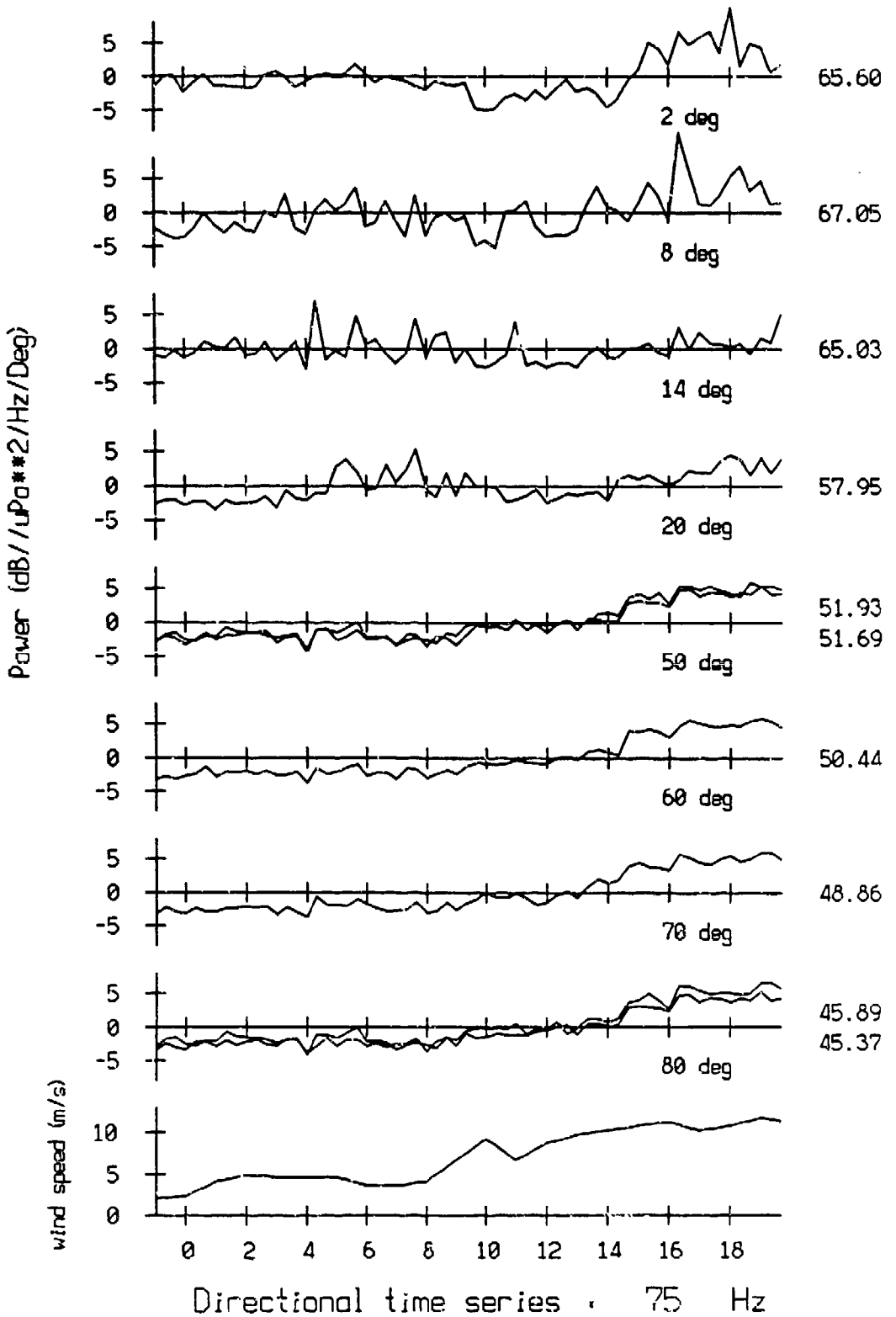
Power (dB//uPa**2/Hz/Deg)
5
0
-5
2 deg
65.60
8 deg
67.05
14 deg
65.03
20 deg
57.95
50 deg
51.93
51.69
60 deg
50.44
70 deg
48.86
80 deg
45.89
45.37
wind speed (m/s)
10
5
0
0 2 4 6 8 10 12 14 16 18
Directional time series . 75 Hz
Time (hours) from Jday 258, increasing wind speed

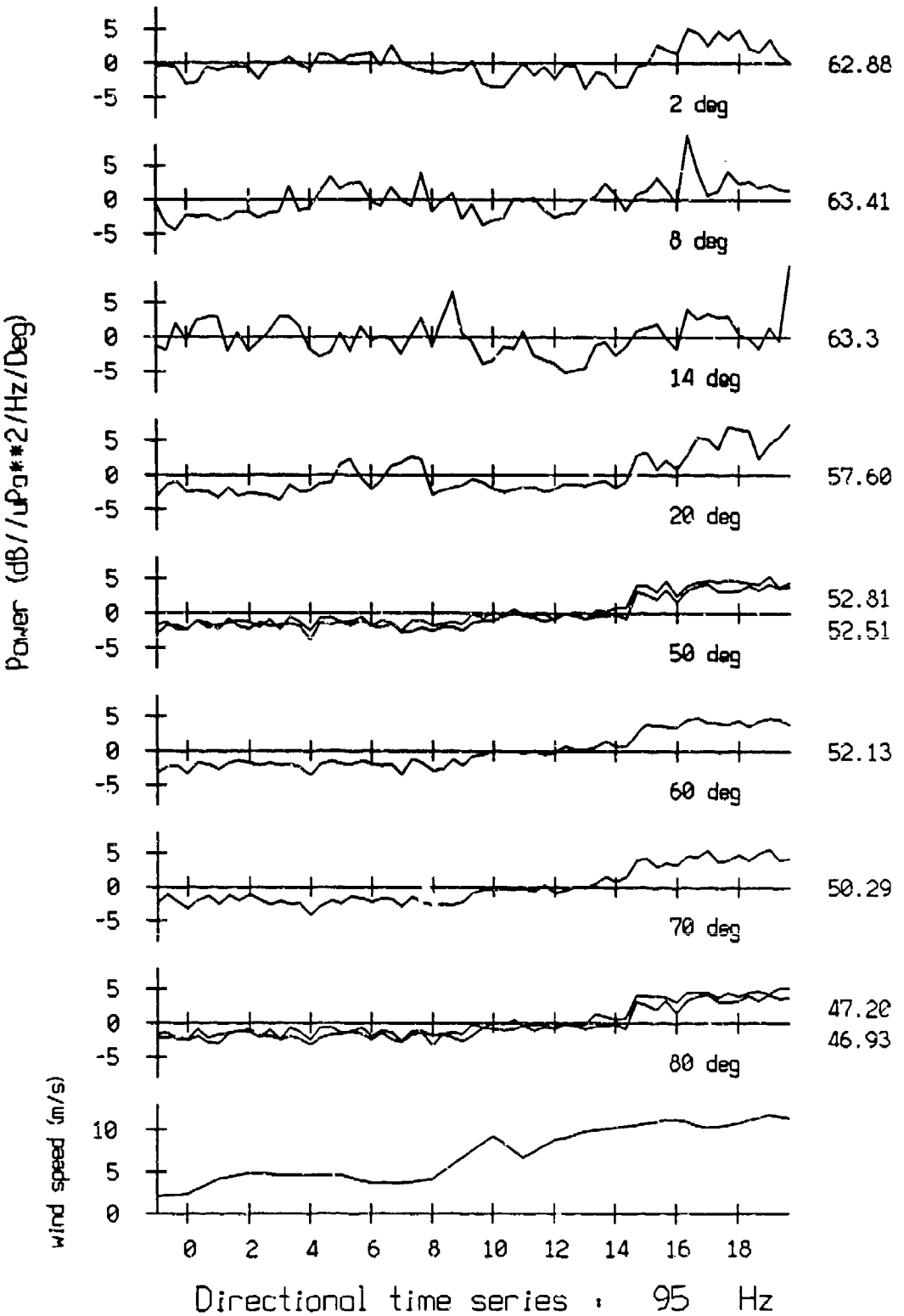
Power (dB//uPa**2/Hz/Deg)
5
0
-5
2 deg
62.88
8 deg
63.41
14 deg
63.3
20 deg
57.60
50 deg
52.81
52.51
60 deg
52.13
70 deg
50.29
80 deg
47.20
46.93
wind speed (m/s)
10
0
0 2 4 6 8 10 12 14 16 18
Directional time series : 95 Hz
Time (hours) from Jday 258, increasing wind speed

**Figure 5.**

**Spatial spectra 1 hour time series at low wind speeds.**

Spatial Distribution at Low Wind Speed, 15 Hz

268/1000, 120 elements, KB window, 512 pt

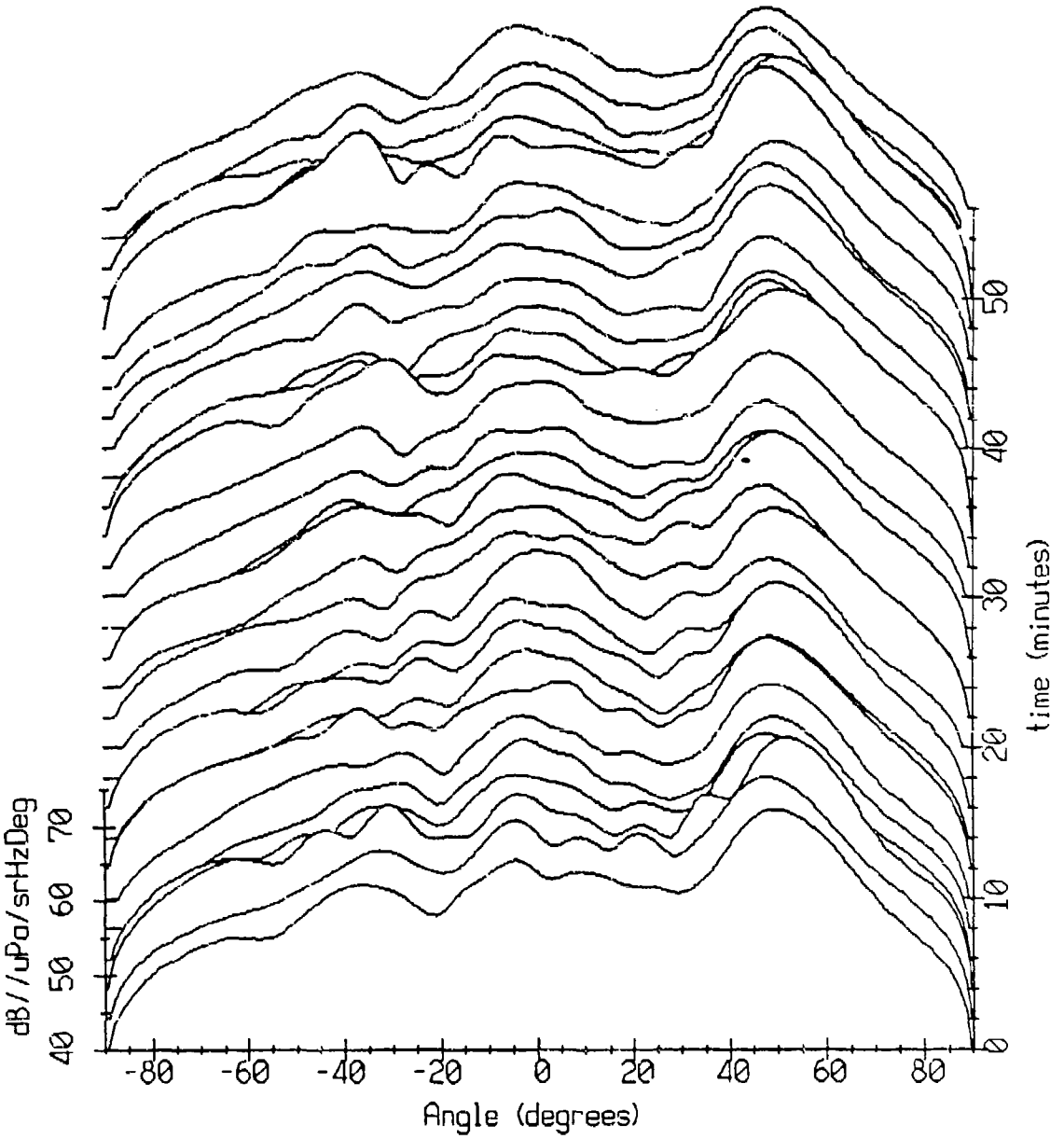

Spatial Distribution at Low Wind Speed, 35 Hz

268/1000, 120 elements, KB window, 512 pt

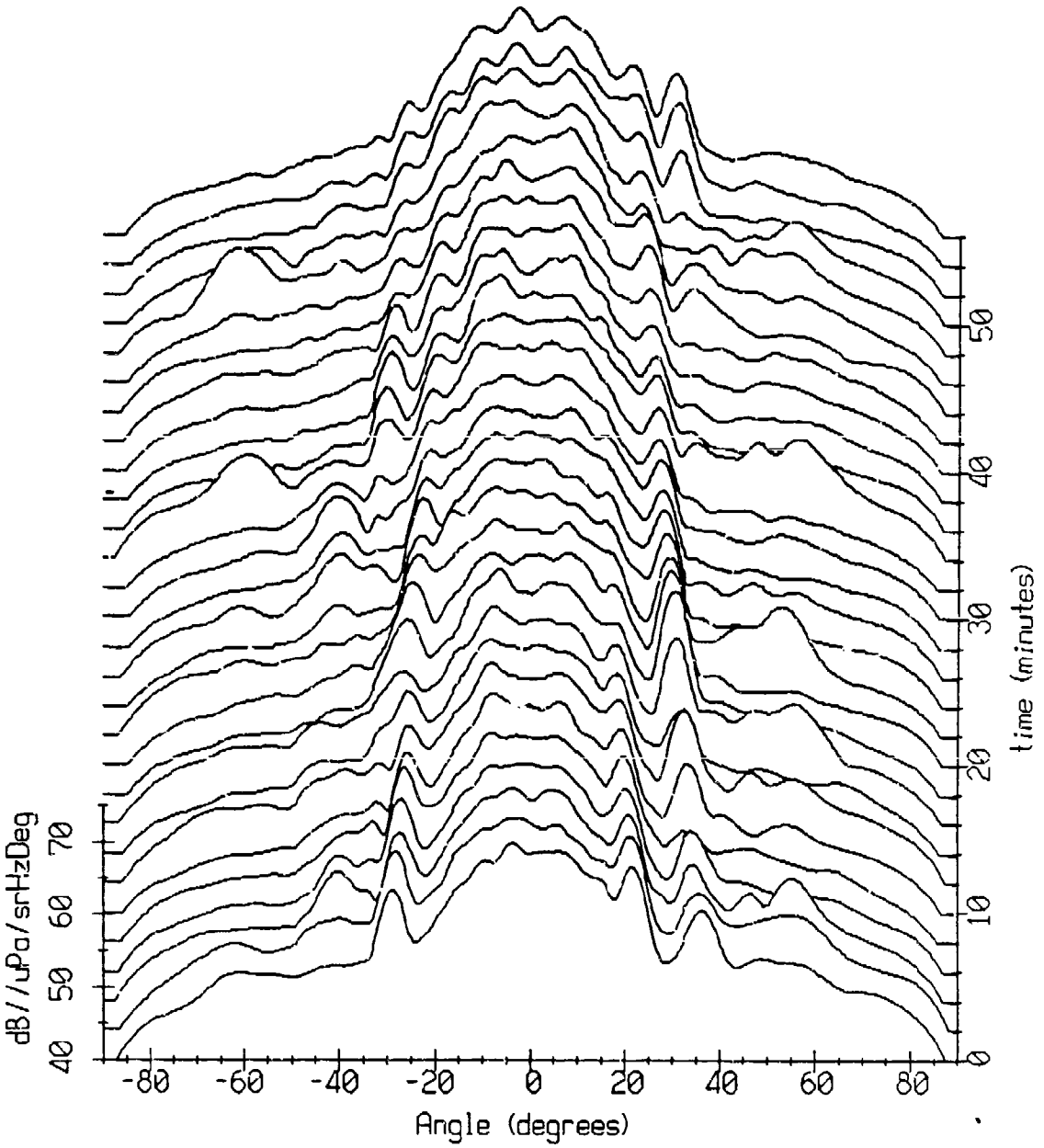

Spatial Distribution at Low Wind Speed, 55 Hz

268/1000, 120 elements, KB window, 512 pt

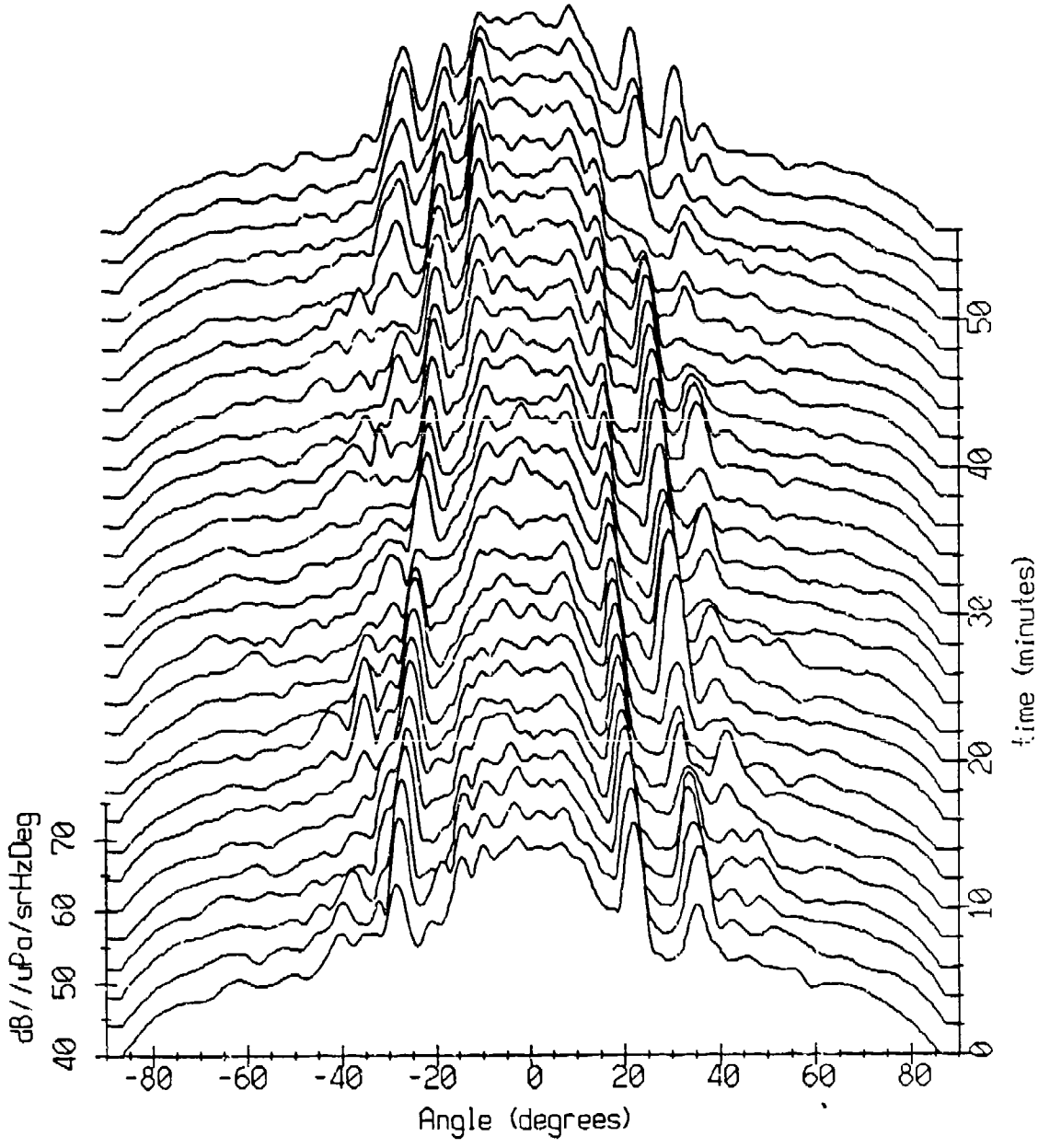

Spatial Distribution at Low Wind Speed, 75 Hz

268/1000, 120 elements, KB window, 512 pt

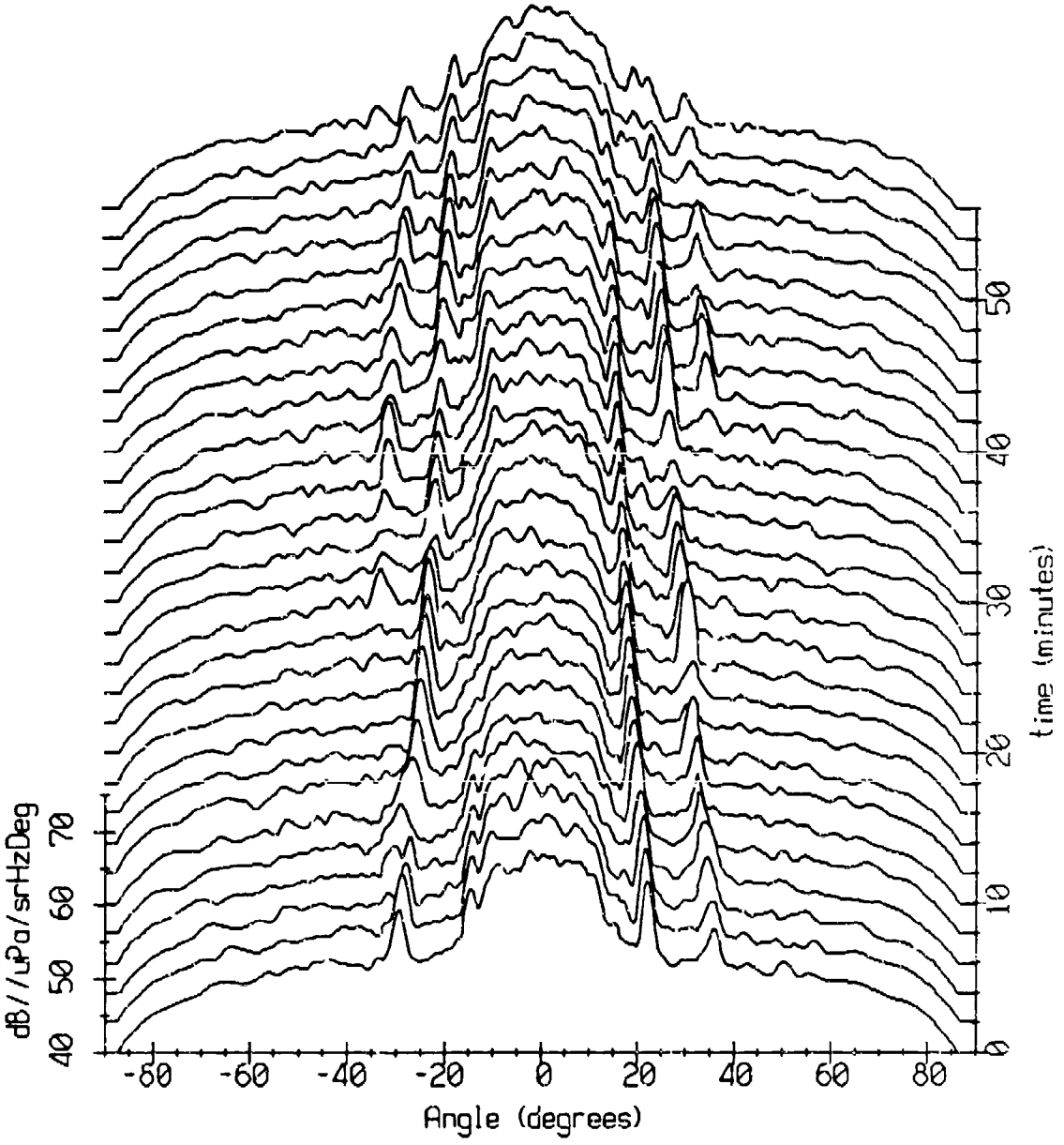

Spatial Distribution at Low Wind Speed, 95 Hz

268/1000, 120 elements, KB window, 512 pt

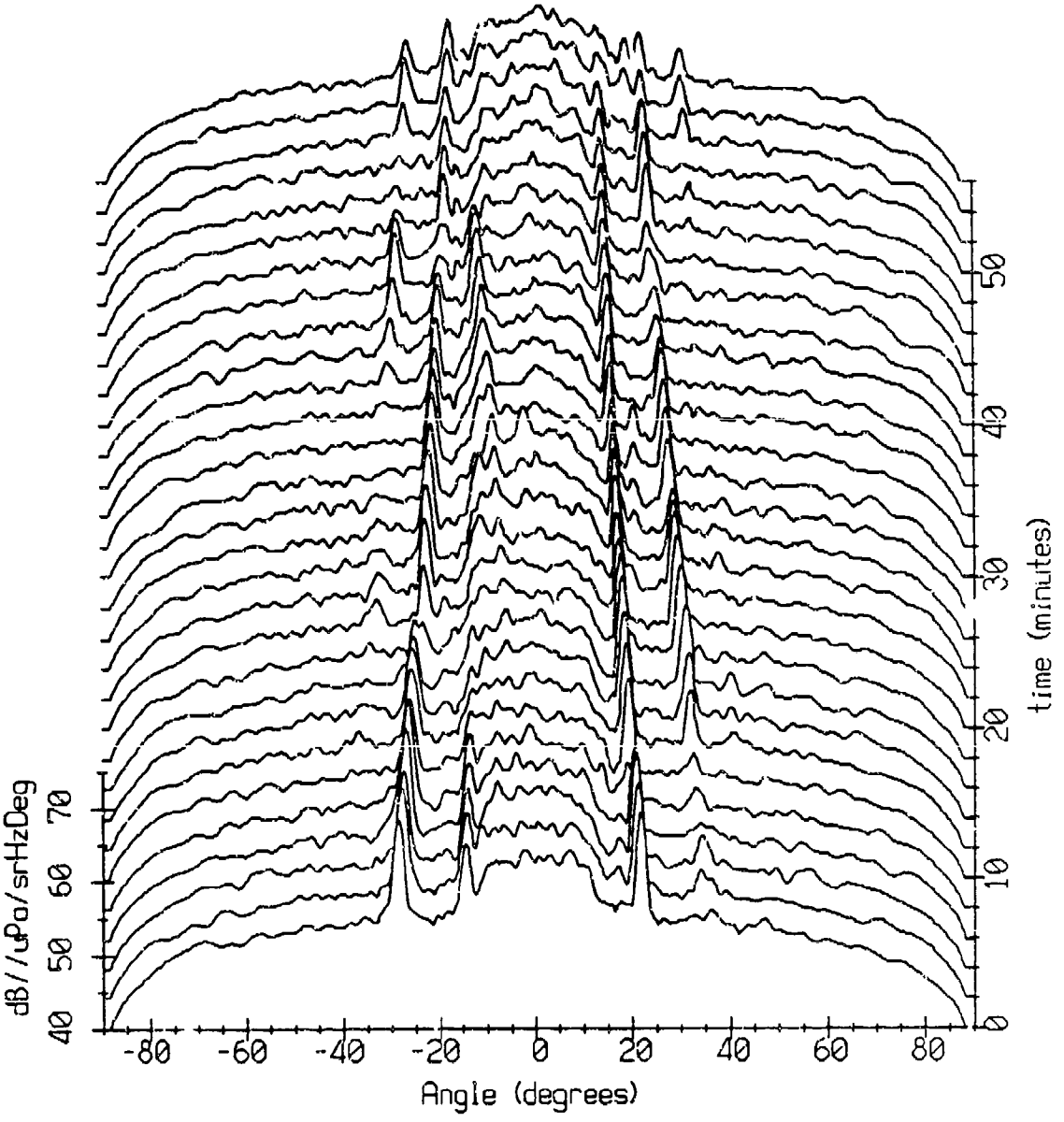

Spatial Distribution at Low Wind Speed, 115Hz

268/1000, 120 elements, KB window, 512 pt

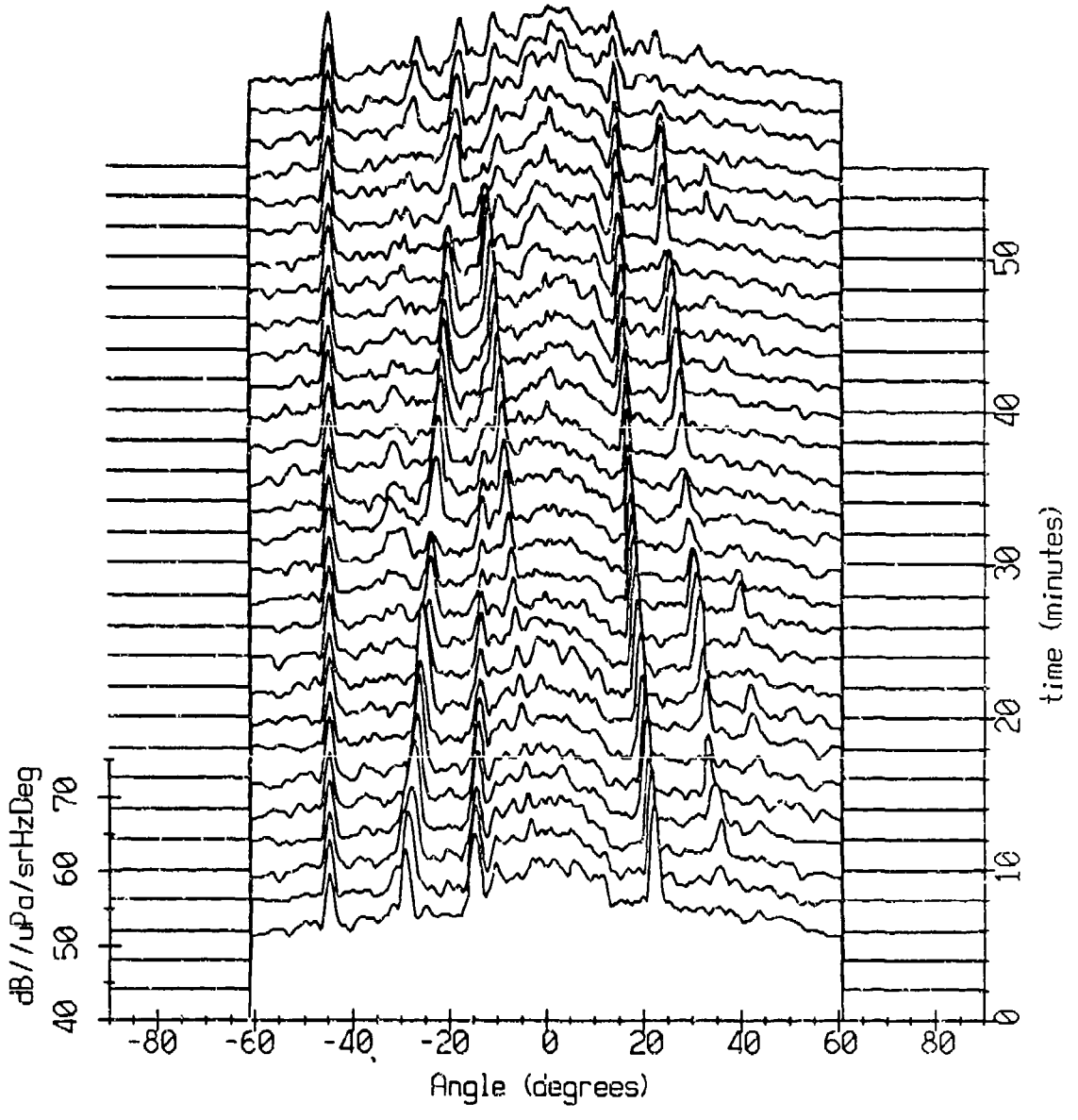

**Figure 6.**

**Spatial spectra 1 hour time series at high wind speeds.**

Spatial Distribution at High Wind Speed, 15 Hz

258/1430, 120 elements, KB window, 512 pt

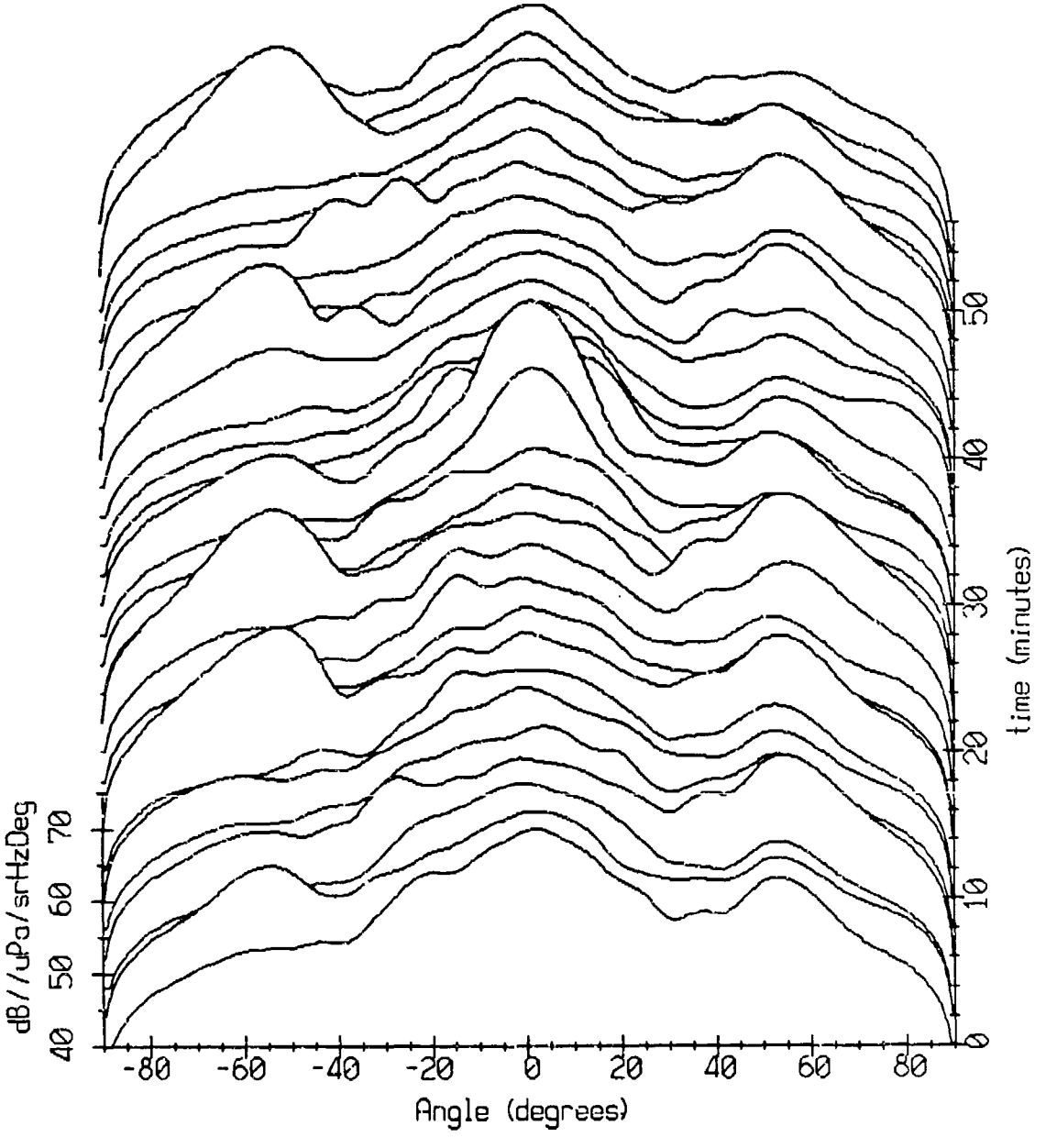

Spatial Distribution at High Wind Speed, 35 Hz

258/1430, 120 elements, KB window, 512 pt

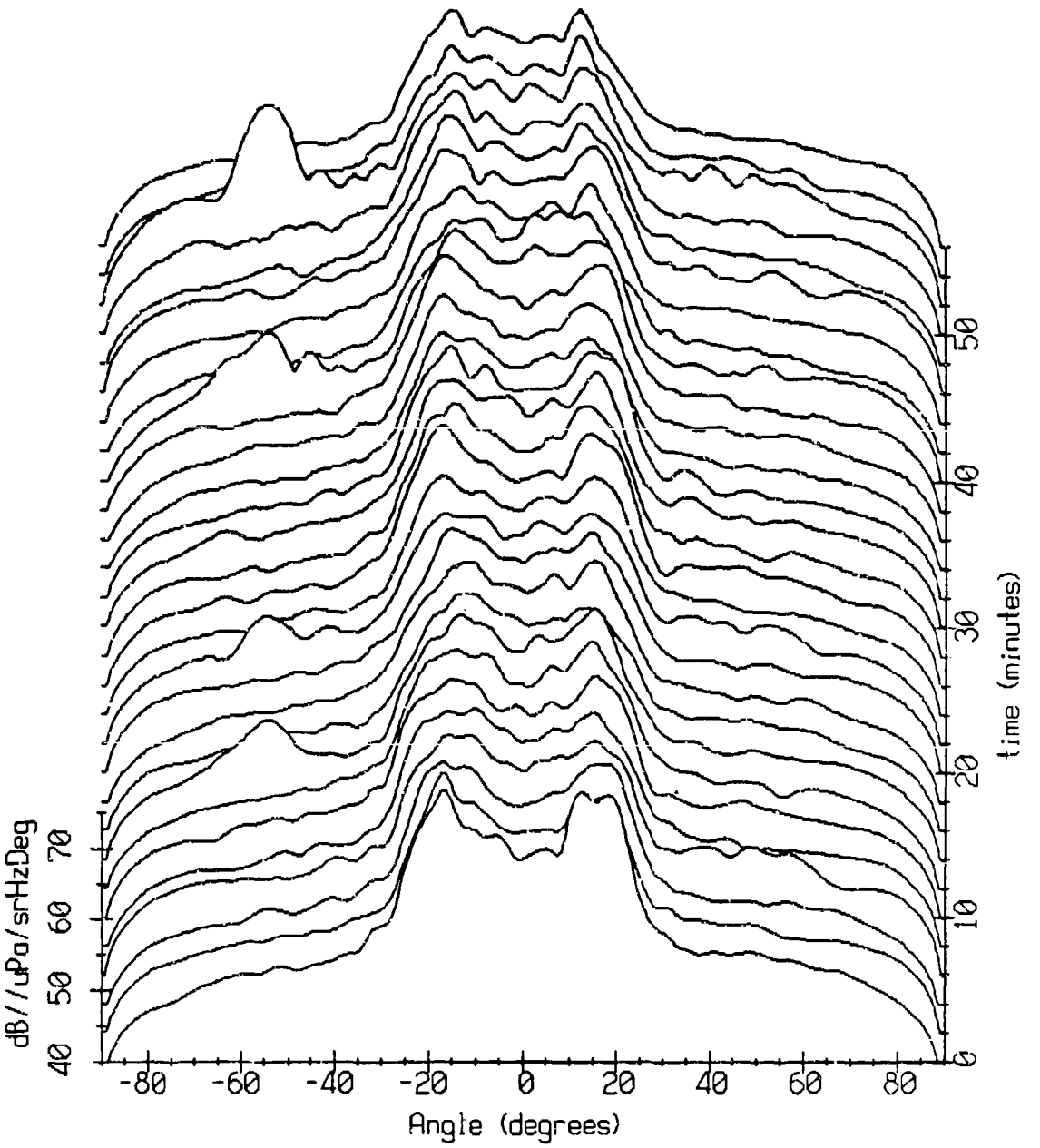

Spatial Distribution at High Wind Speed, 55 Hz

258/1430, 120 elements, KB window, 512 pt

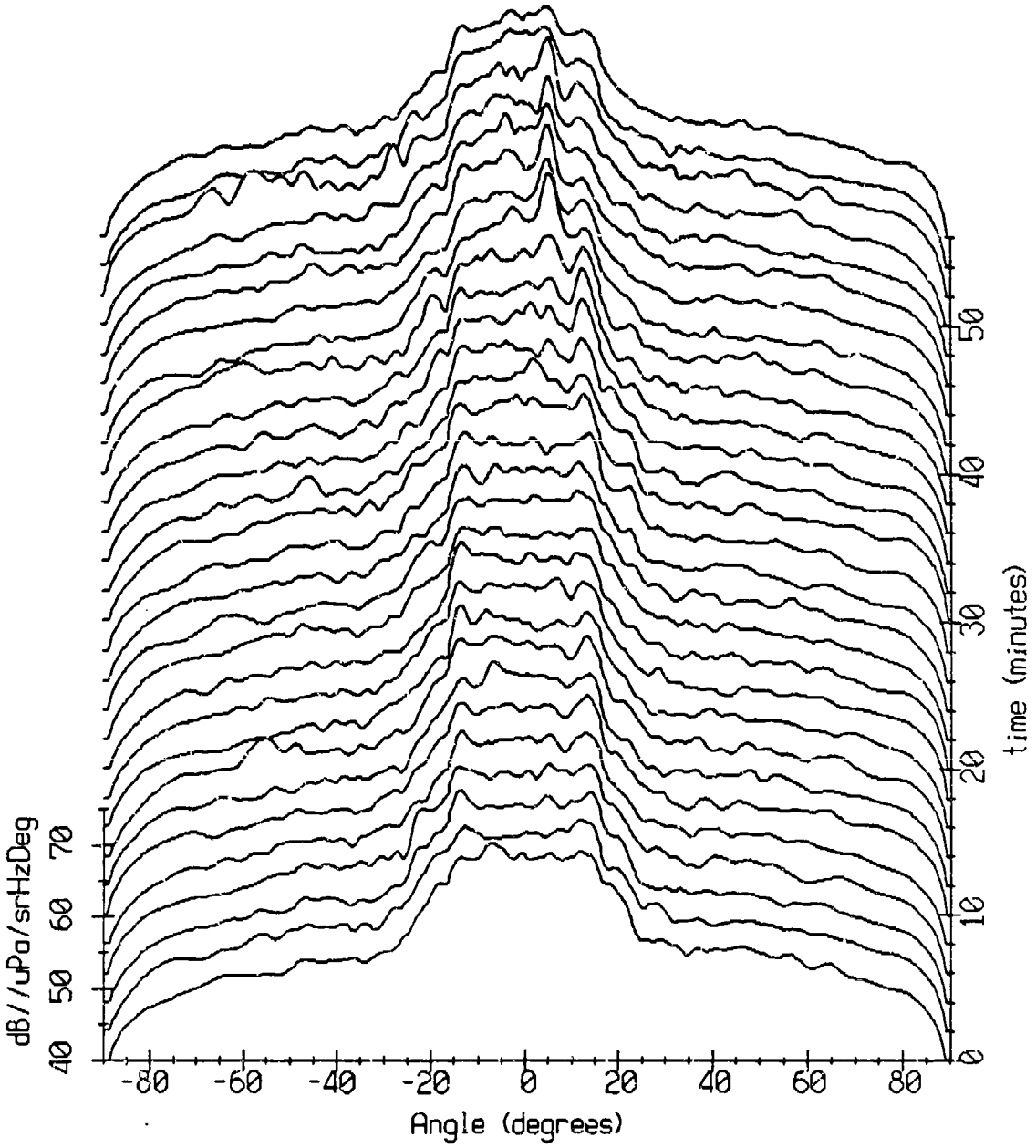

Spatial Distribution at High Wind Speed, 75 Hz

258/1430, 120 elements, KB window, 512 pt

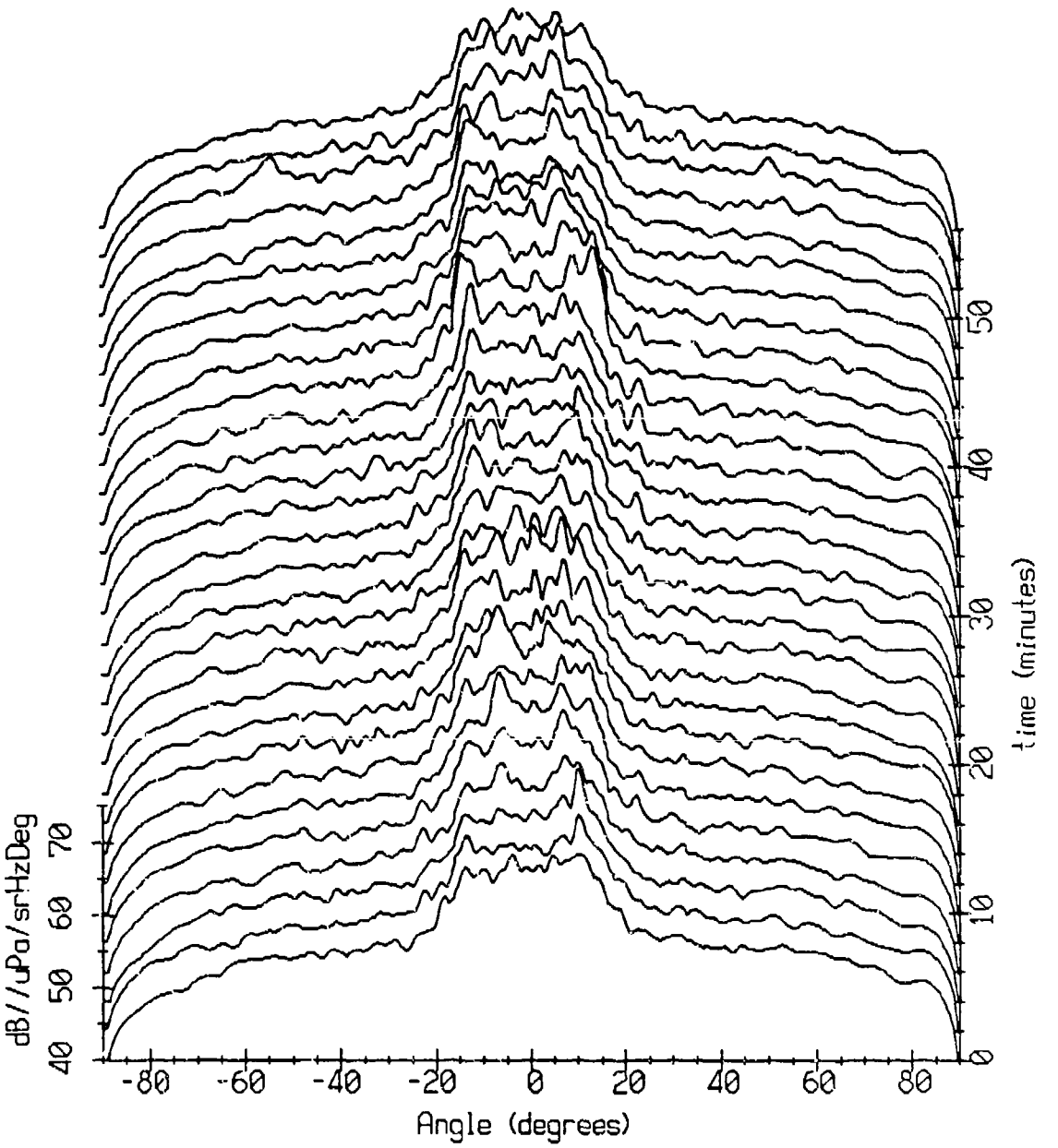

Spatial Distribution at High Wind Speed, 95 Hz

258/1430, 120 elements, KB window, 512 pt

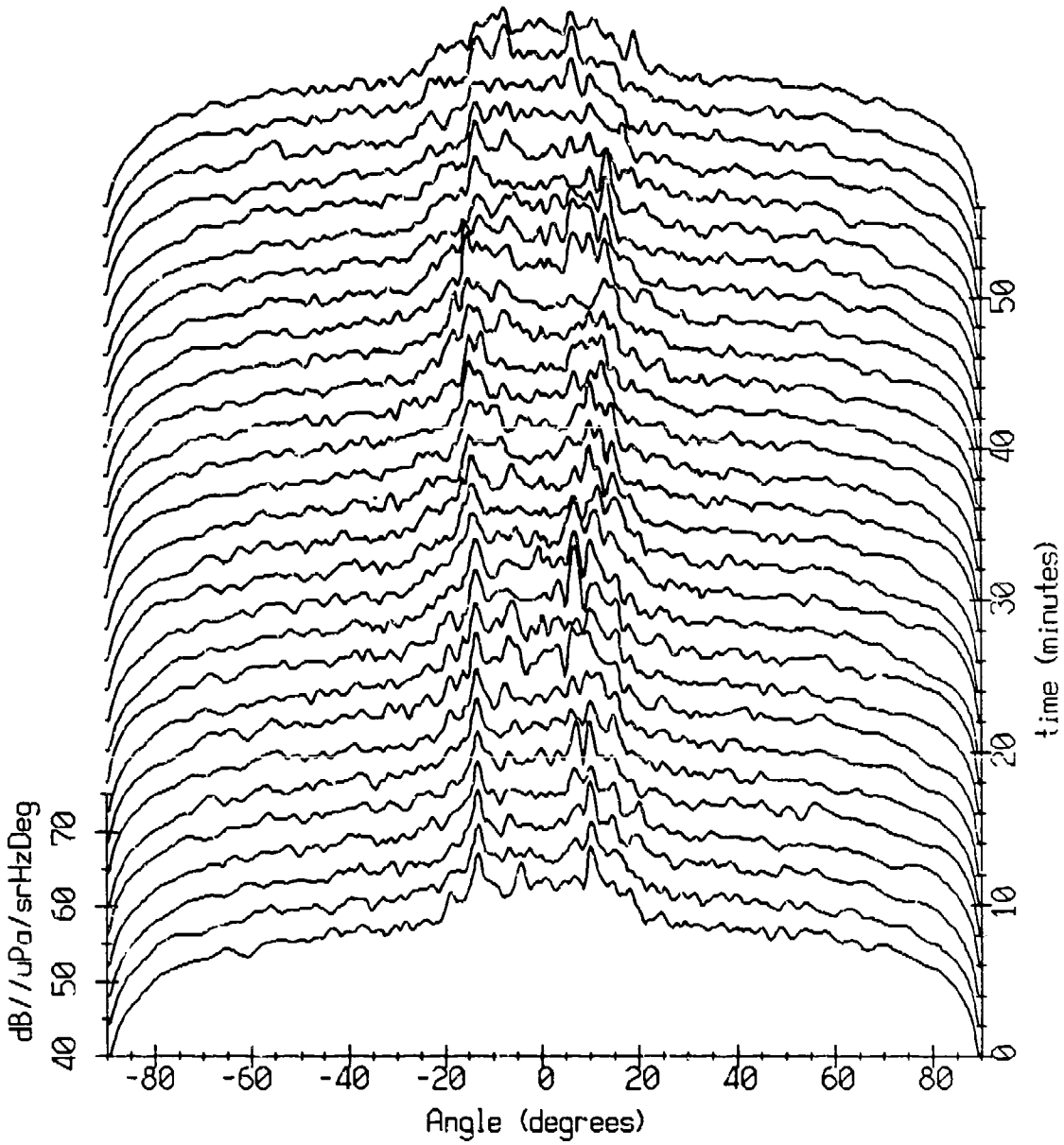

Spatial Distribution at High Wind Speed, 115Hz

258/1430, 120 elements, KB window, 512 pt

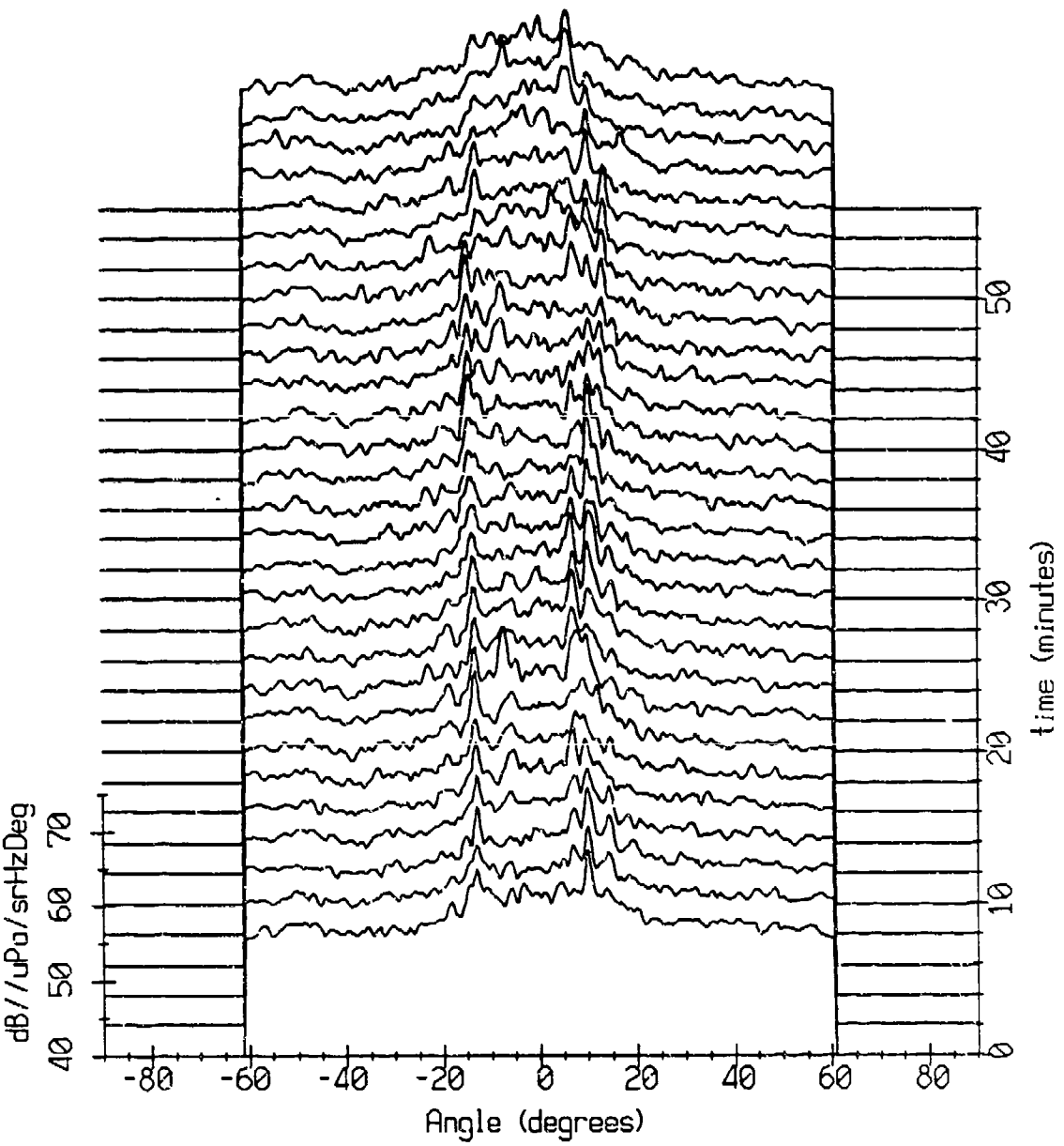

**Figure 7.**

**Spatial spectra versus array depth at specified frequencies and wind speeds.**

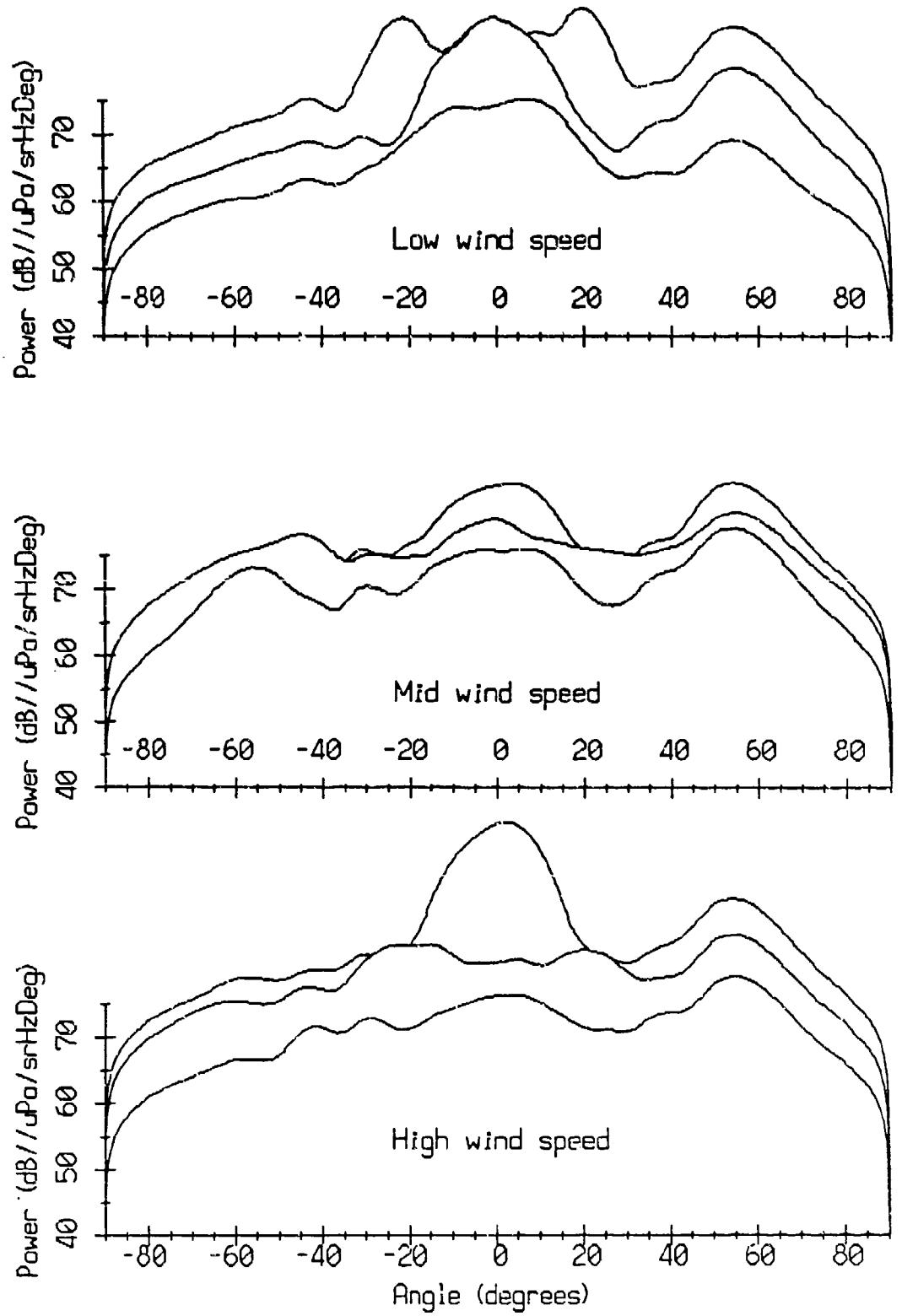
Spatial Distribution vs. Depth at 15 Hz
Power (dB//uPa/srHzDeg)
40
50
60
70
Low wind speed
-80
-60
-40
-20
0
20
40
60
80
Mid wind speed
High wind speed
Angle (degrees)

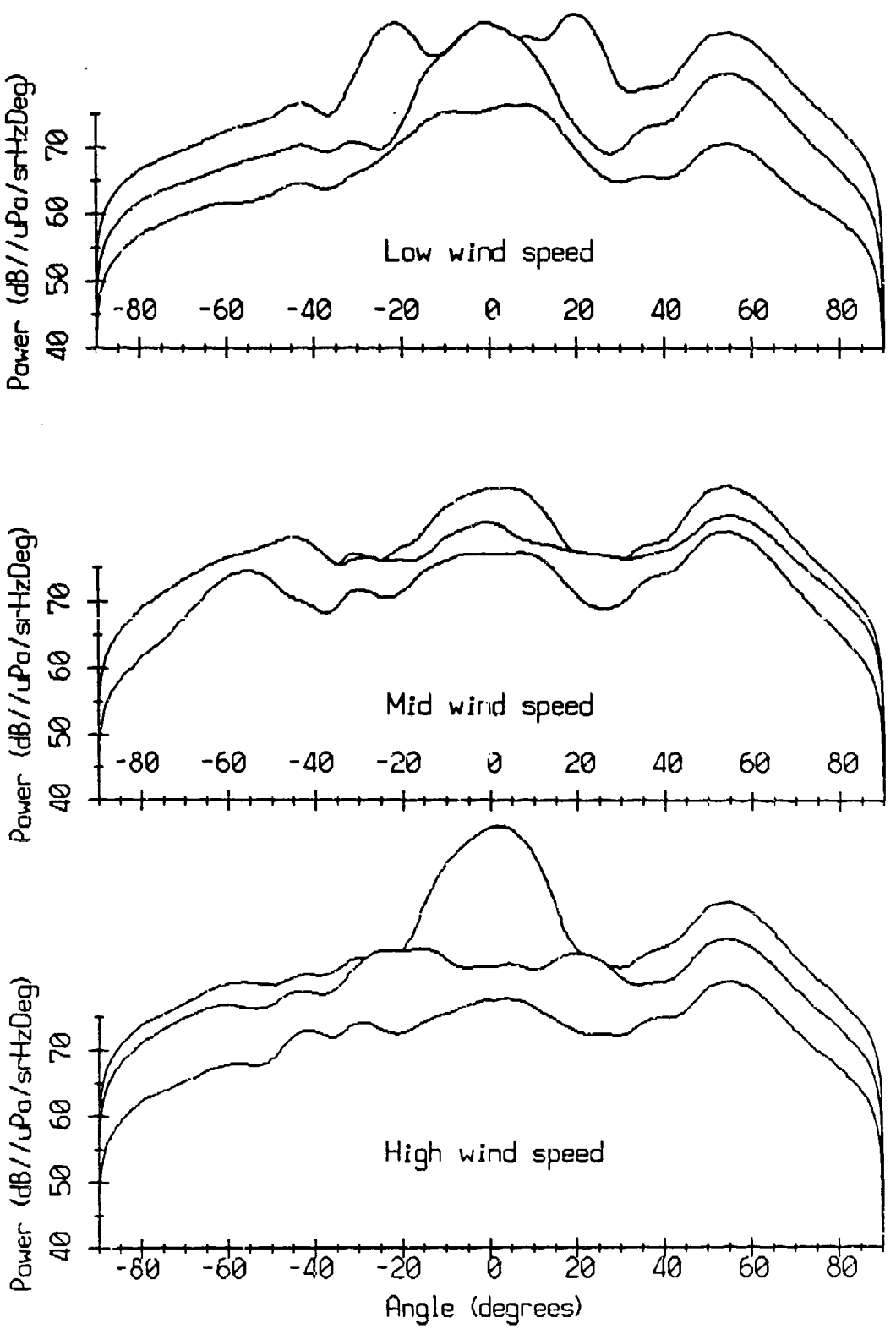
Spatial Distribution vs. Depth at 20 Hz
Power (dB//uPa/srHzDeg)
40
50
60
70
Low wind speed
-80
-60
-40
-20
0
20
40
60
80
Mid wind speed
High wind speed
Angle (degrees)

# Spatial Distribution vs. Depth at 25 Hz

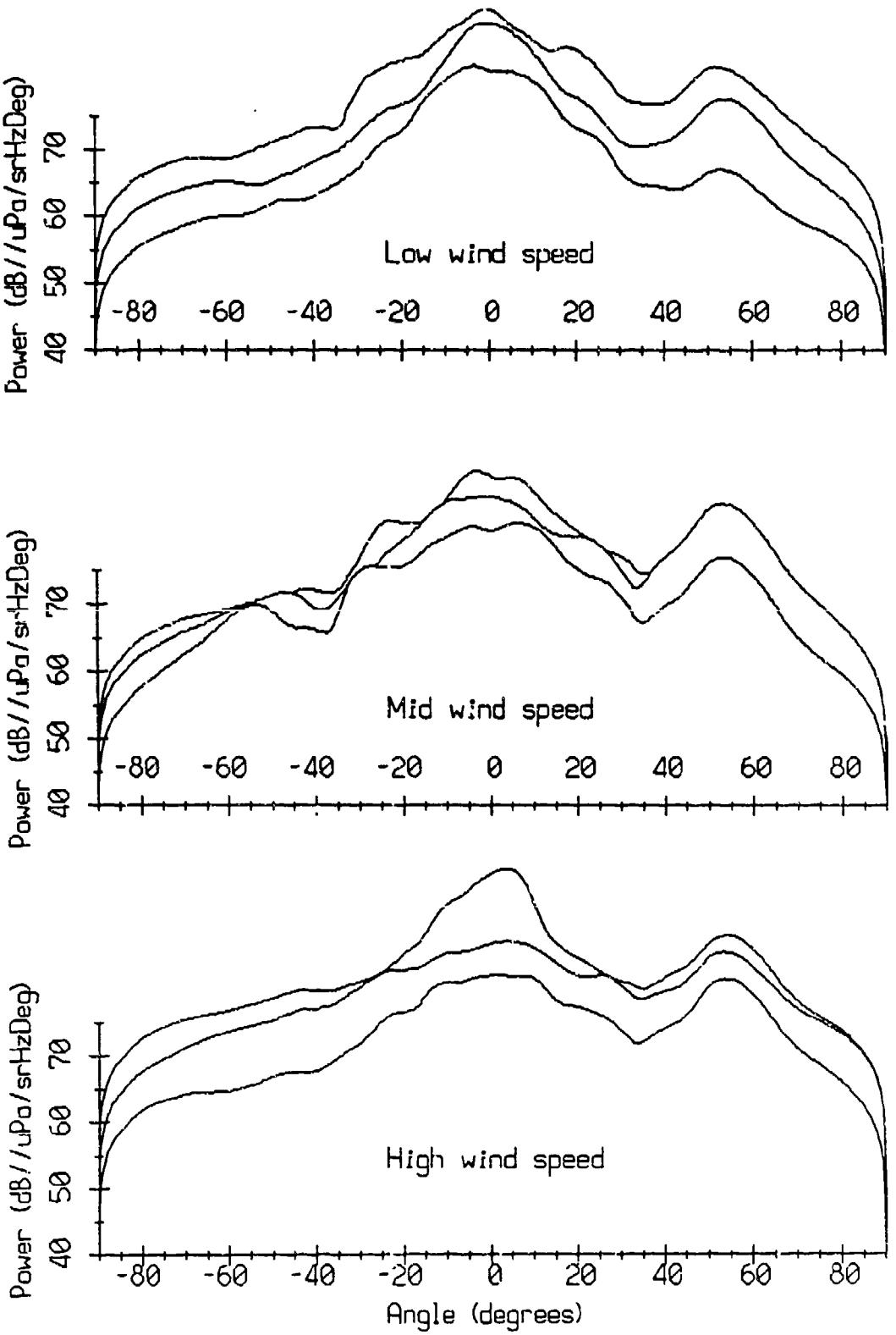

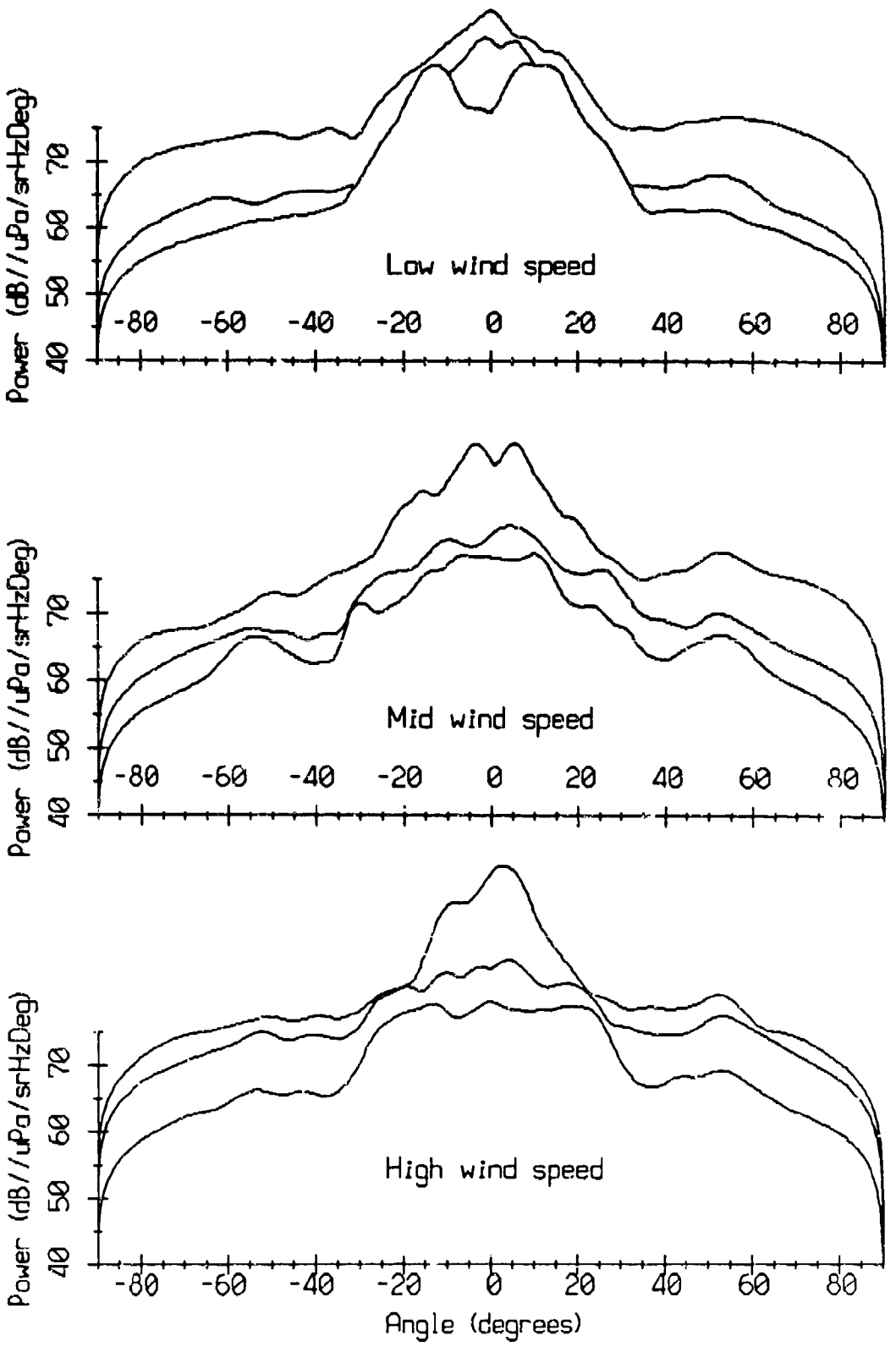
Spatial Distribution vs. Depth at 30 Hz
Power (dB//uPa/srHzDeg)
40
50
60
70
Low wind speed
-80
-60
-40
-20
0
20
40
60
80
Mid wind speed
High wind speed
Angle (degrees)

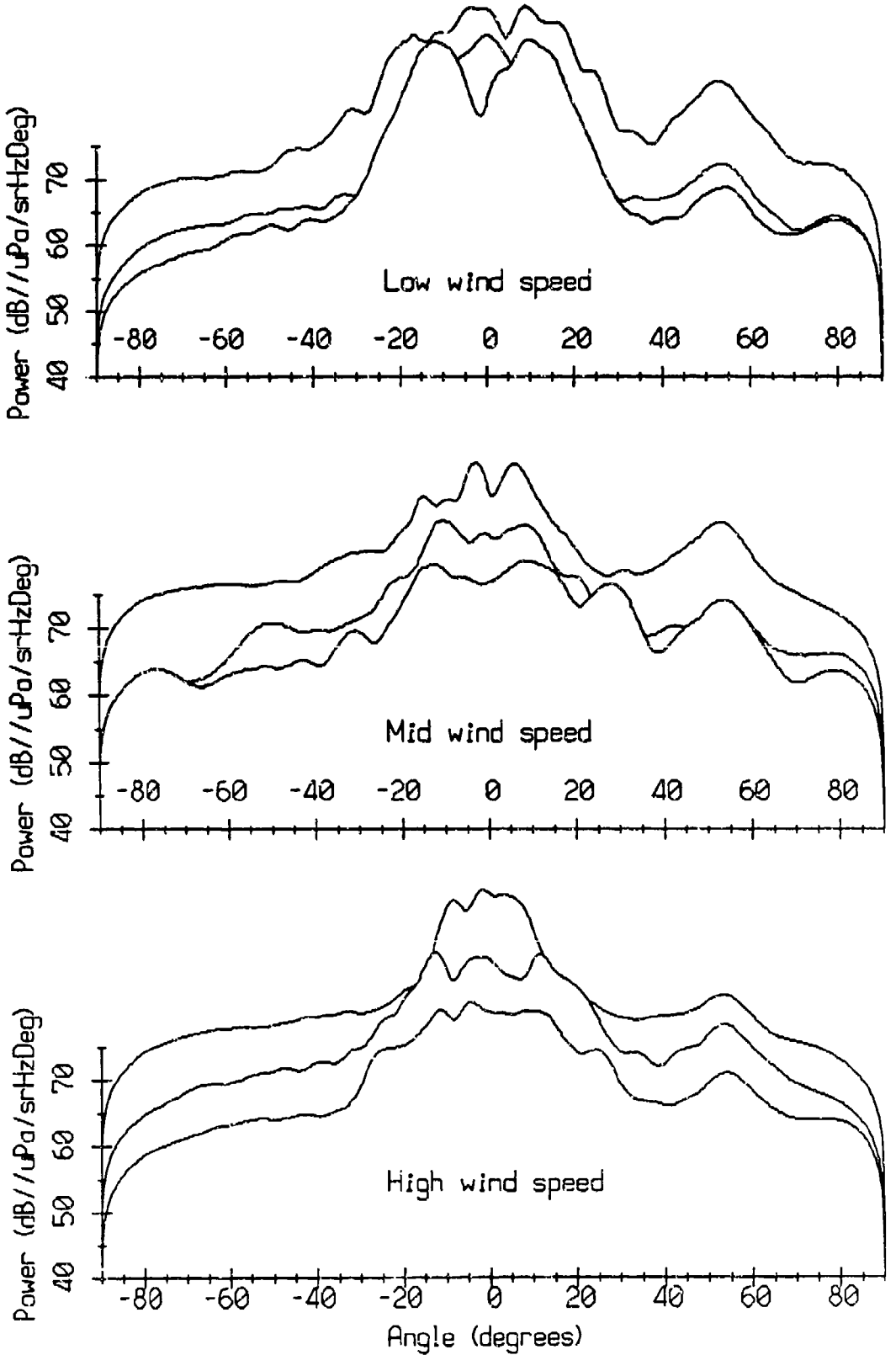
Spatial Distribution vs. Depth at 35 Hz
Power (dB//uPa/srHzDeg)
40
50
60
70
Low wind speed
-80
-60
-40
-20
0
20
40
60
80
Mid wind speed
High wind speed
Angle (degrees)

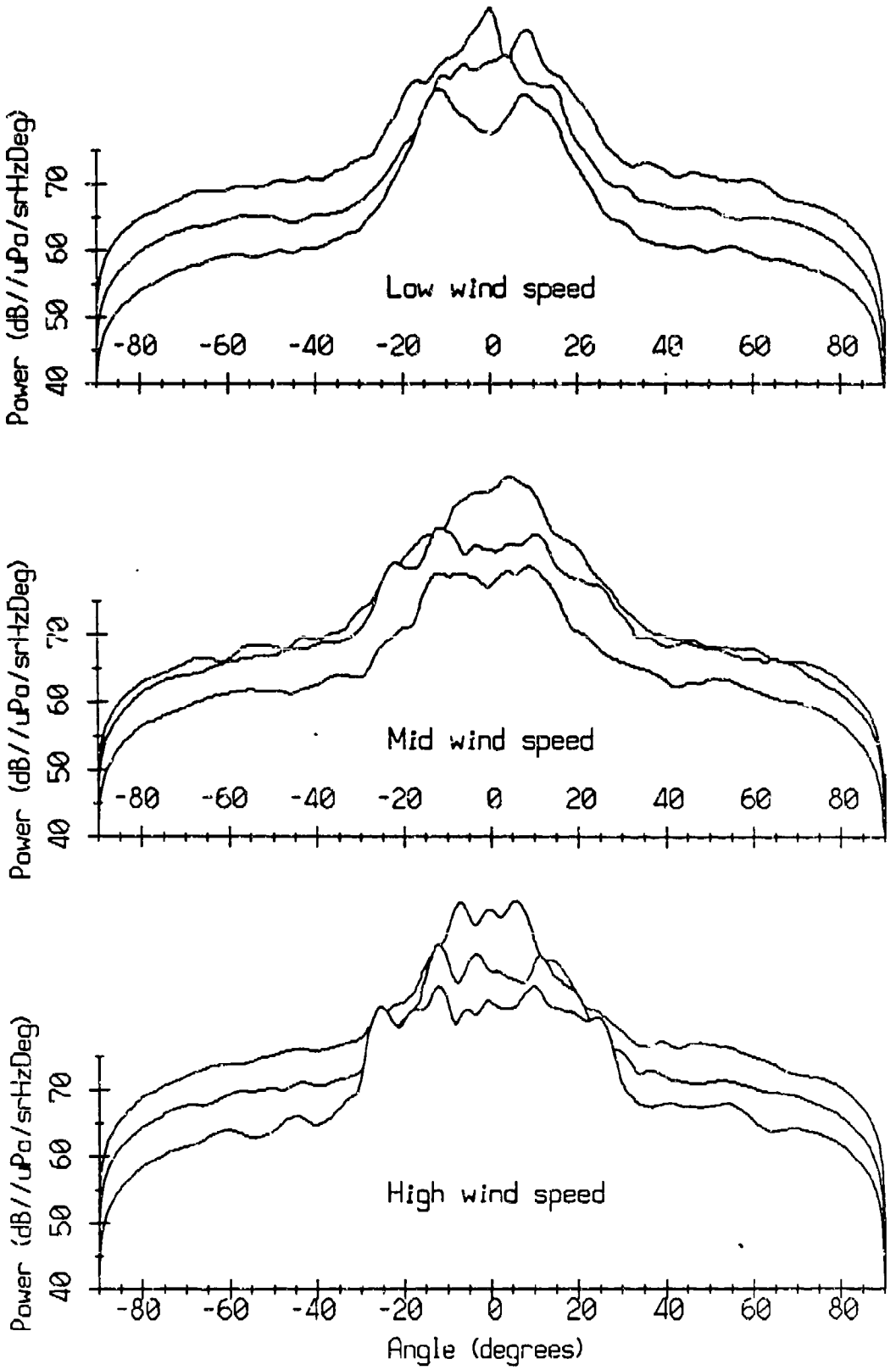
Spatial Distribution vs. Depth at 40 Hz
Power (dB//uPa/srHzDeg)
40
50
60
70
Low wind speed
-80
-60
-40
-20
0
20
40
60
80
Power (dB//uPa/srHzDeg)
40
50
60
70
Mid wind speed
-80
-60
-40
-20
0
20
40
60
80
Power (dB//uPa/srHzDeg)
40
50
60
70
High wind speed
-80
-60
-40
-20
0
20
40
60
80
Angle (degrees)

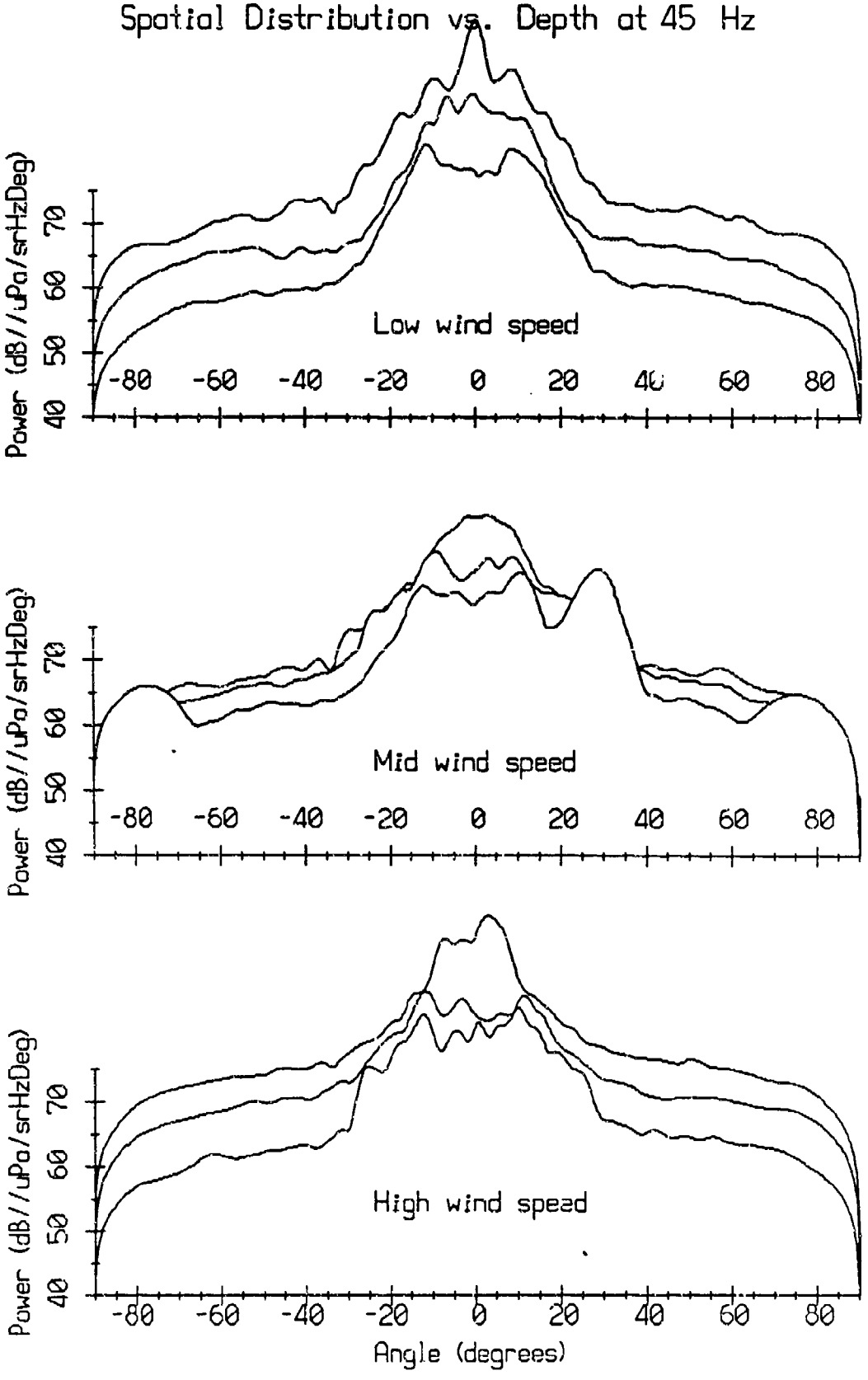
Spatial Distribution vs. Depth at 45 Hz
Power (dB//uPa/srHzDeg)
40
50
60
70
Low wind speed
-80
-60
-40
-20
0
20
40
60
80
Mid wind speed
High wind speed
Angle (degrees)

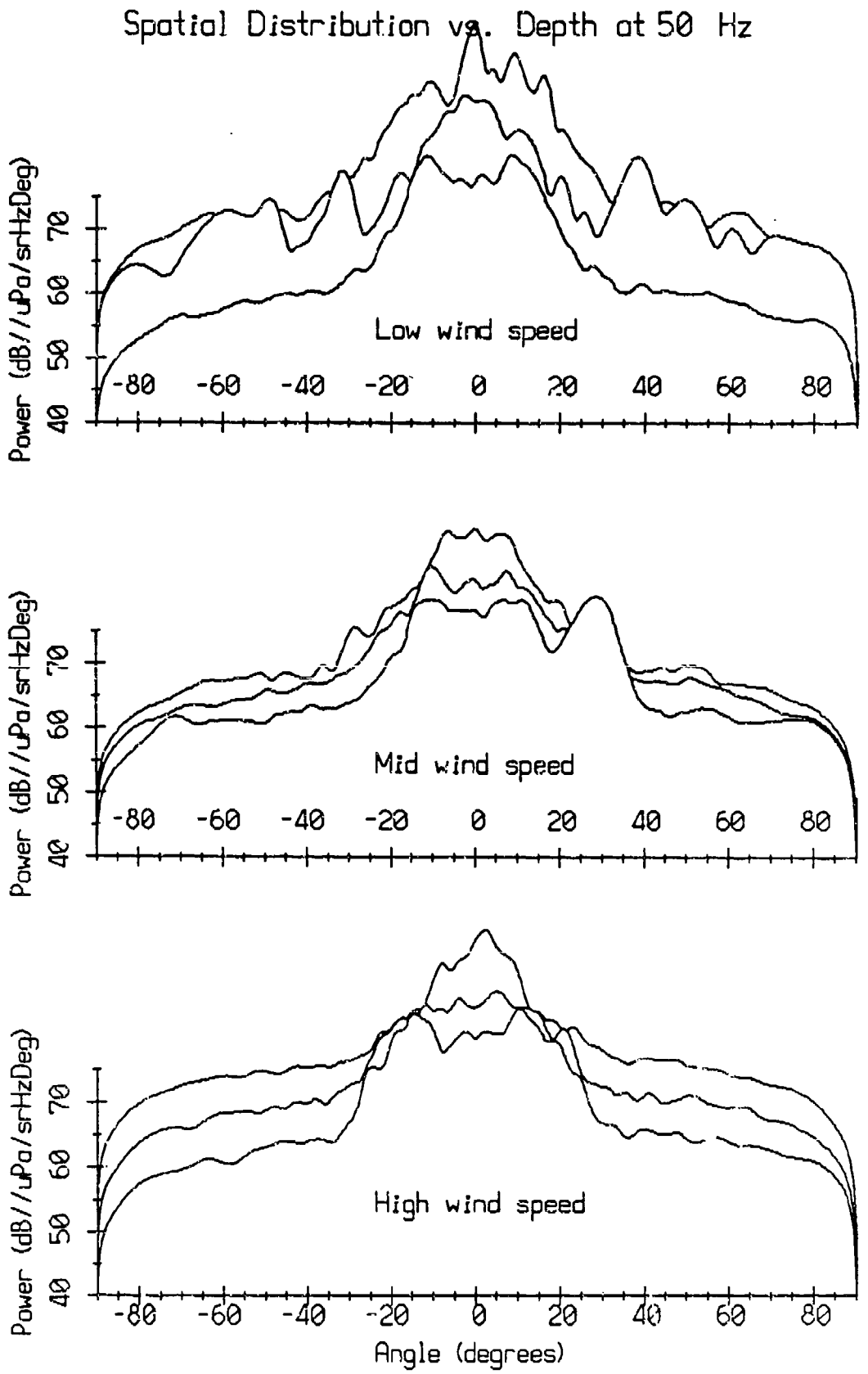
Spatial Distribution vs. Depth at 50 Hz
Power (dB//uPa/srHzDeg)
40
50
60
70
Low wind speed
-80
-60
-40
-20
0
20
40
60
80
Mid wind speed
High wind speed
Angle (degrees)

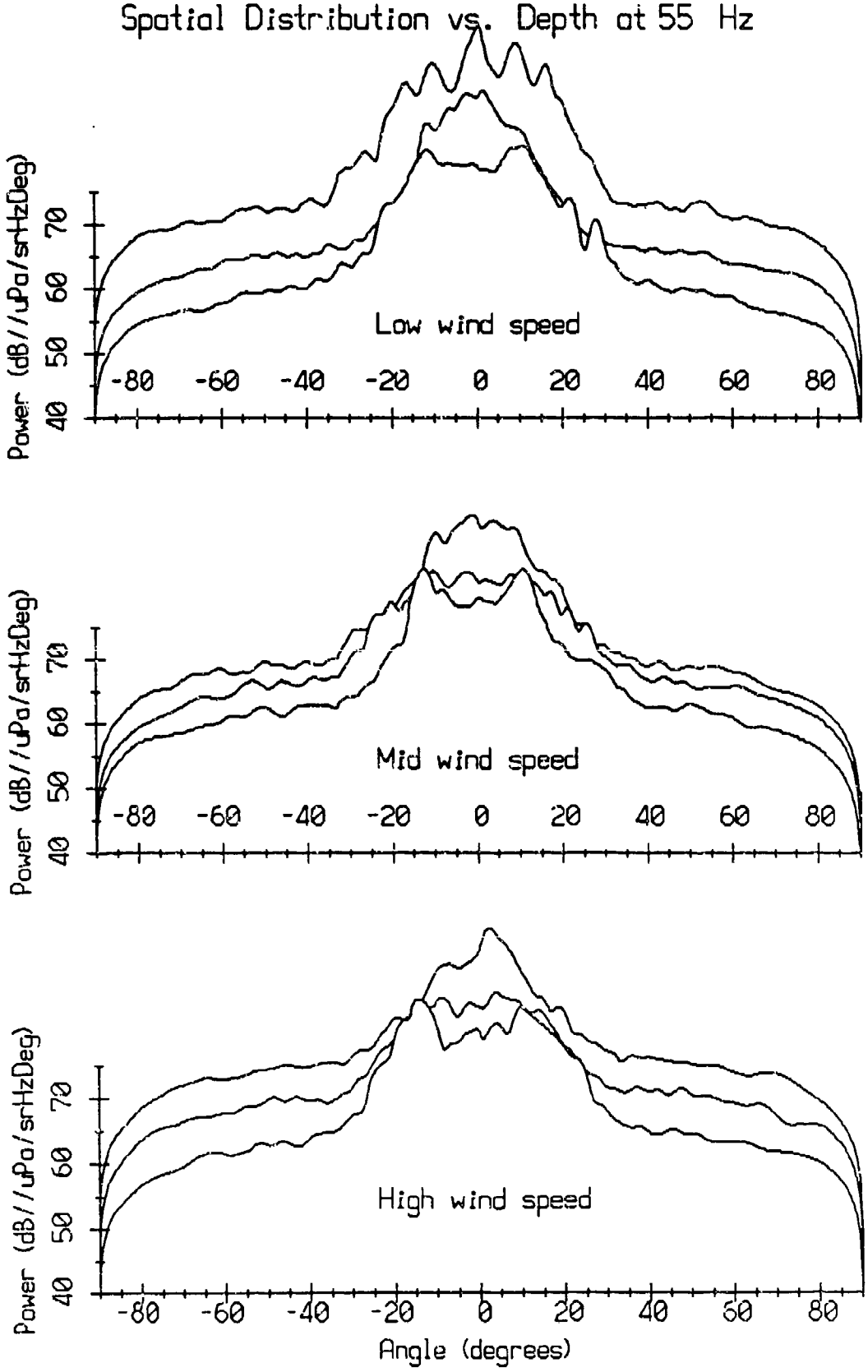
Spatial Distribution vs. Depth at 55 Hz
Power (dB//uPa/srHzDeg)
40
50
60
70
Low wind speed
-80
-60
-40
-20
0
20
40
60
80
Mid wind speed
High wind speed
Angle (degrees)

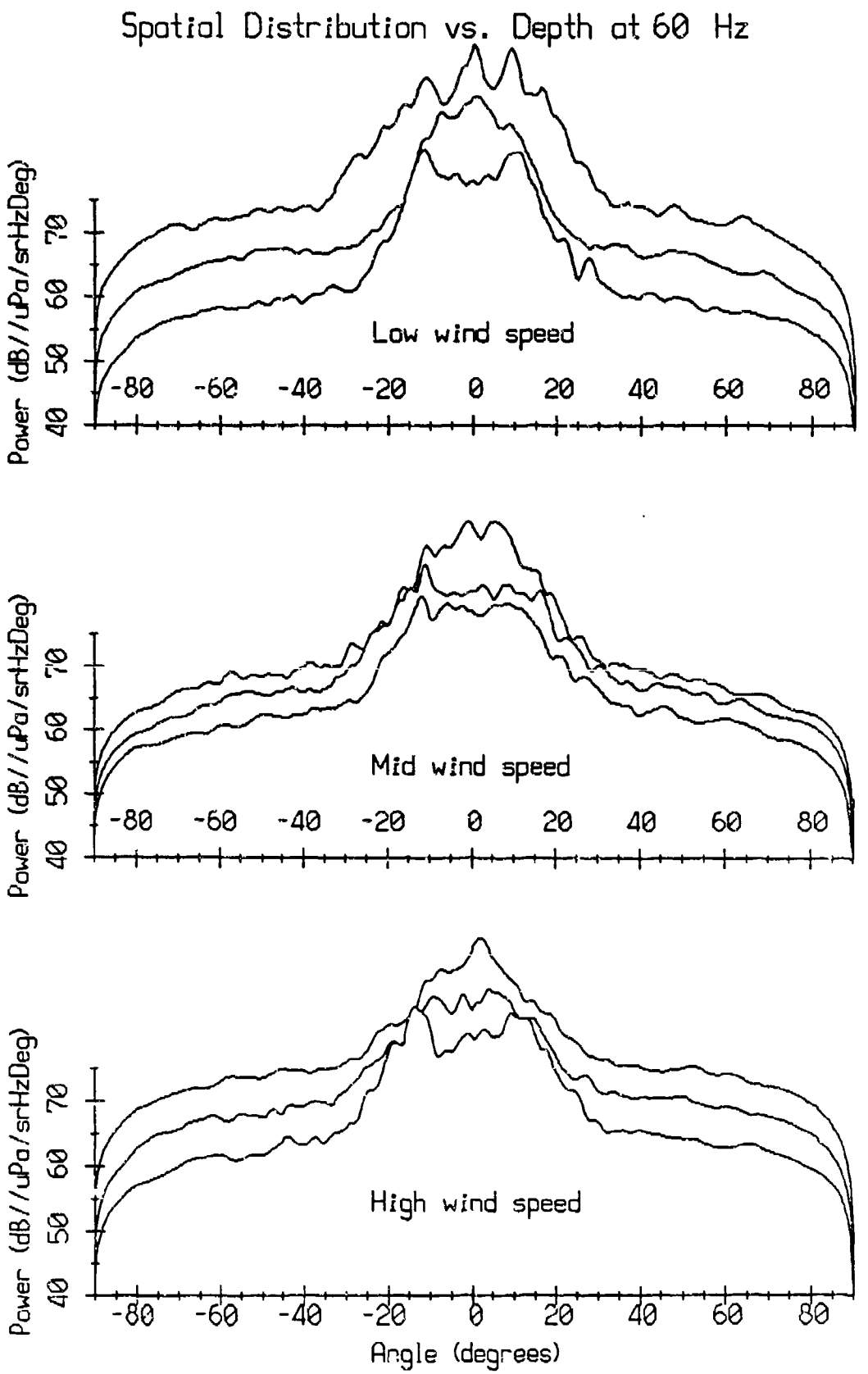
Spatial Distribution vs. Depth at 60 Hz
Power (dB//uPa/srHzDeg)
40
50
60
70
Low wind speed
-80
-60
-40
-20
0
20
40
60
80
Mid wind speed
High wind speed
Angle (degrees)

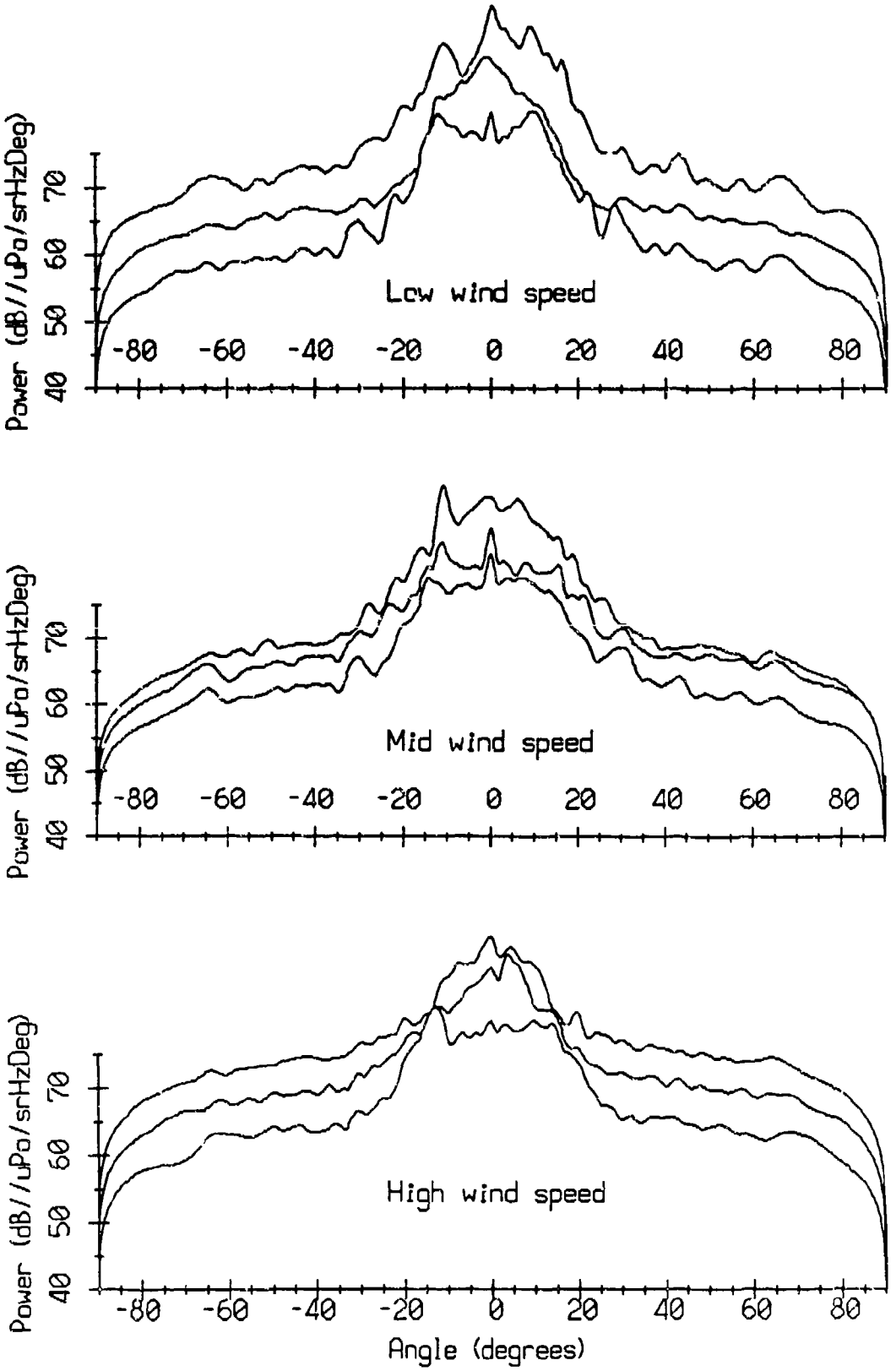
Spatial Distribution vs. Depth at 65 Hz
Power (dB//uPa/srHzDeg)
40
50
60
70
Low wind speed
-80
-60
-40
-20
0
20
40
60
80
Mid wind speed
High wind speed
Angle (degrees)

Spatial Distribution vs. Depth at 70 Hz

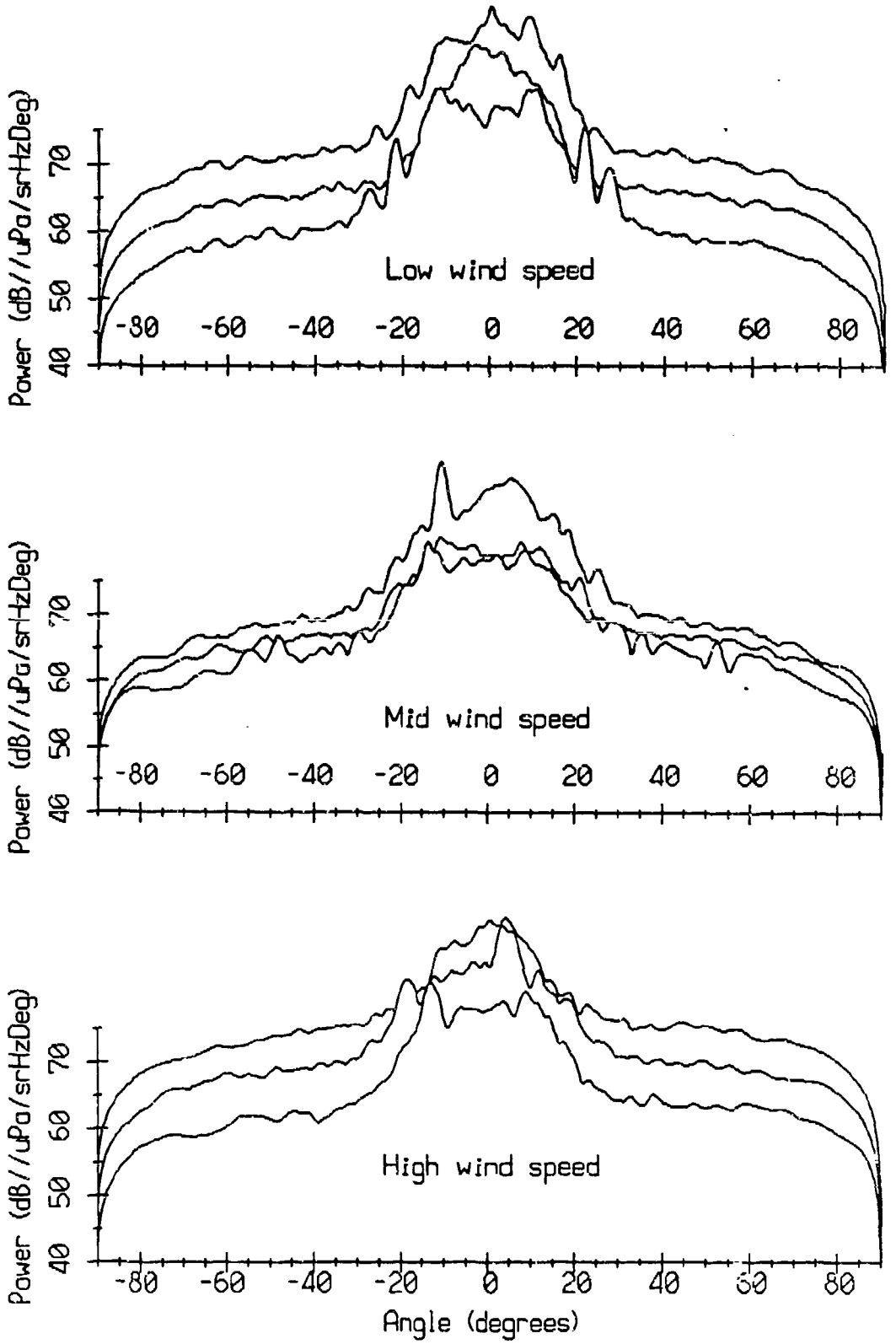

# Spatial Distribution vs. Depth at 75 Hz

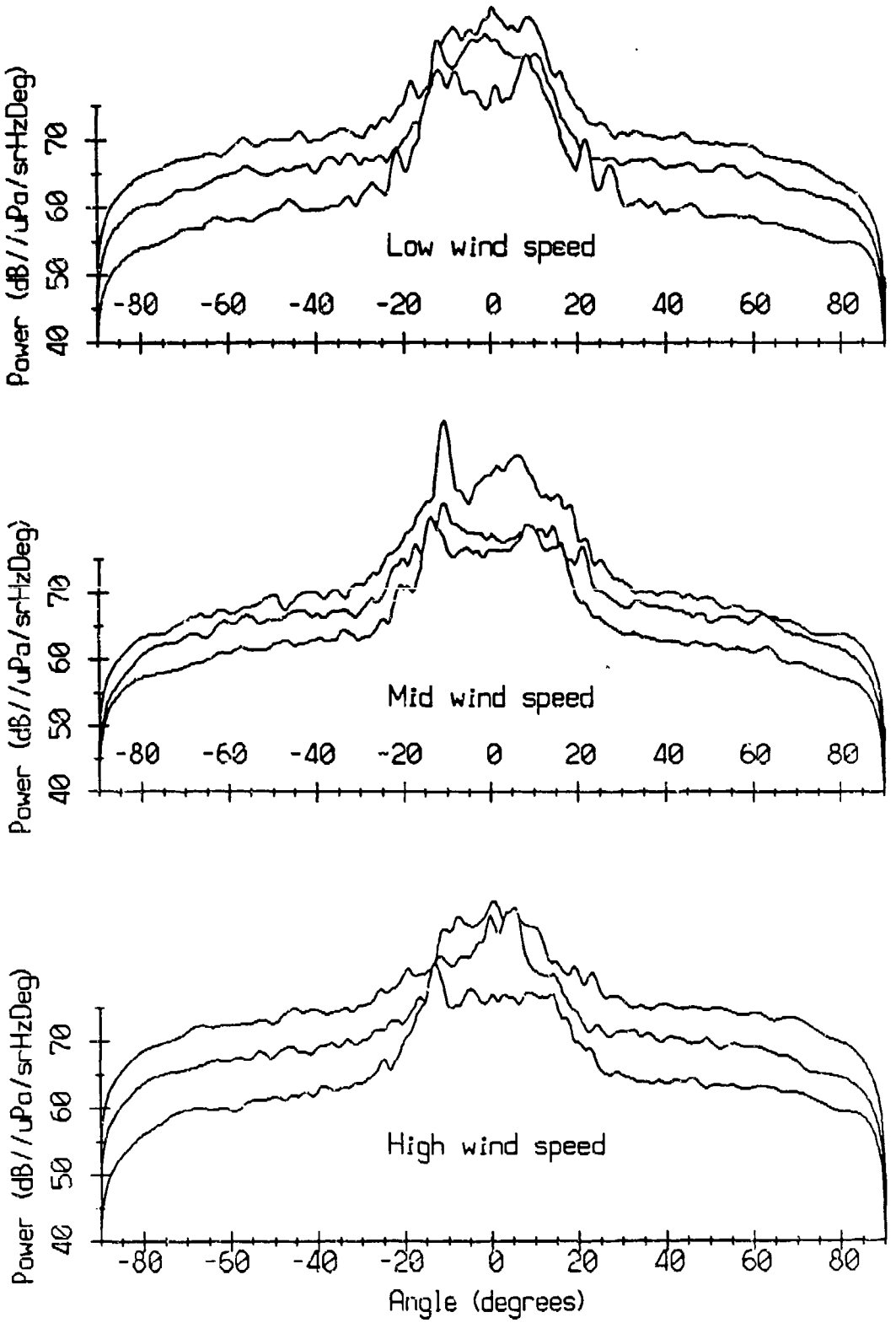

# Spatial Distribution vs. Depth at 80 Hz

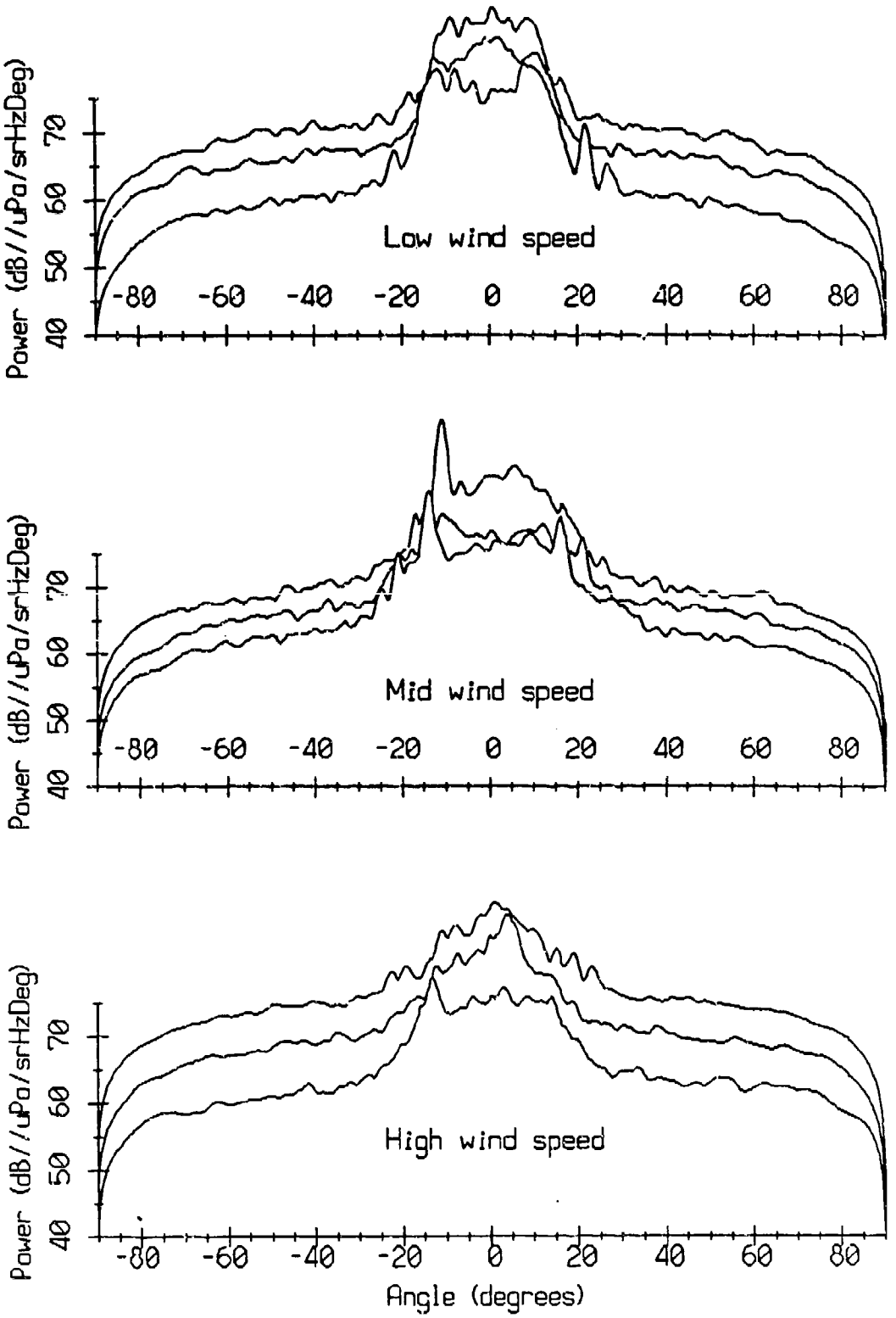

# Spatial Distribution vs. Depth at 85 Hz

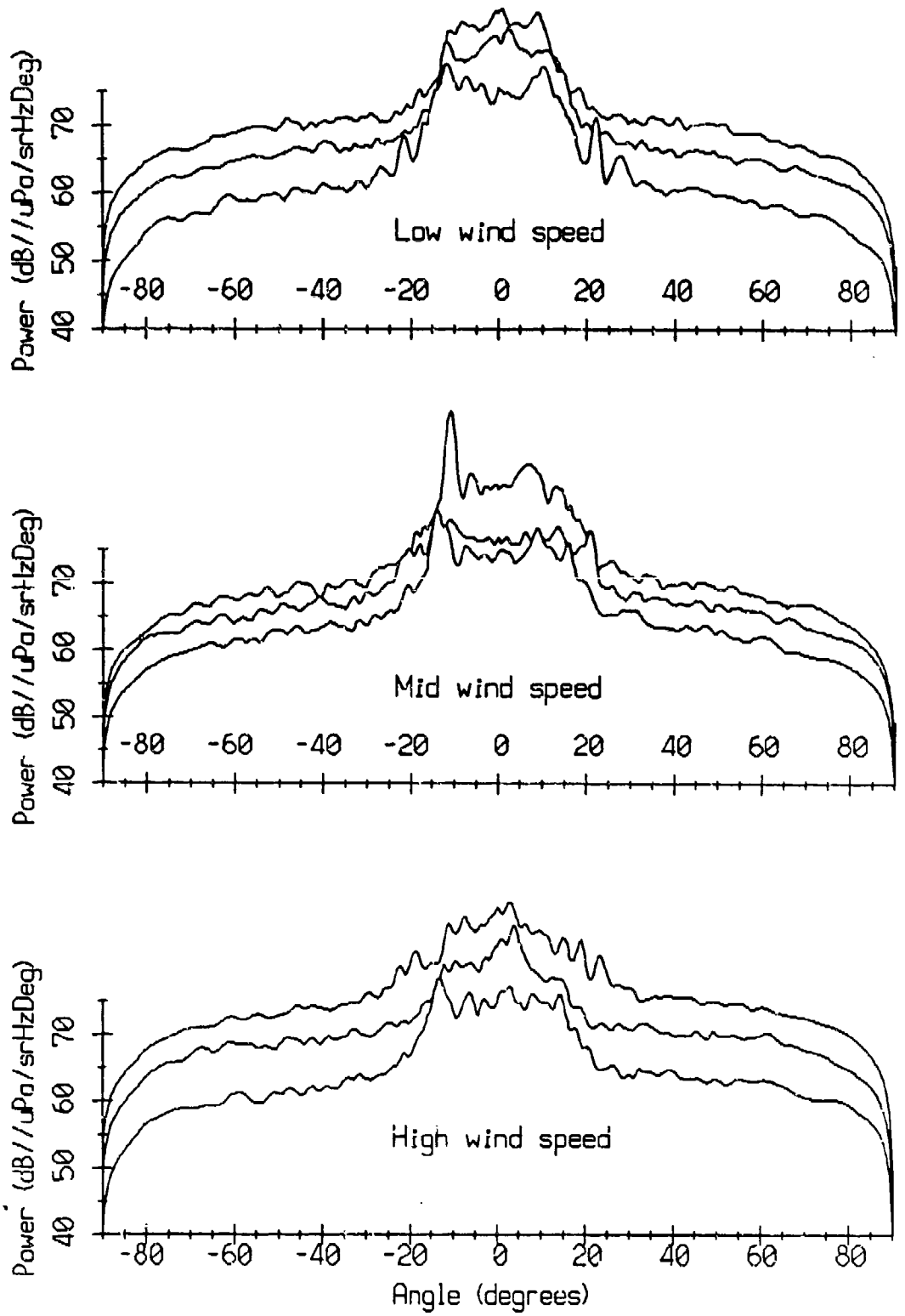

# Spatial Distribution vs. Depth at 90 Hz

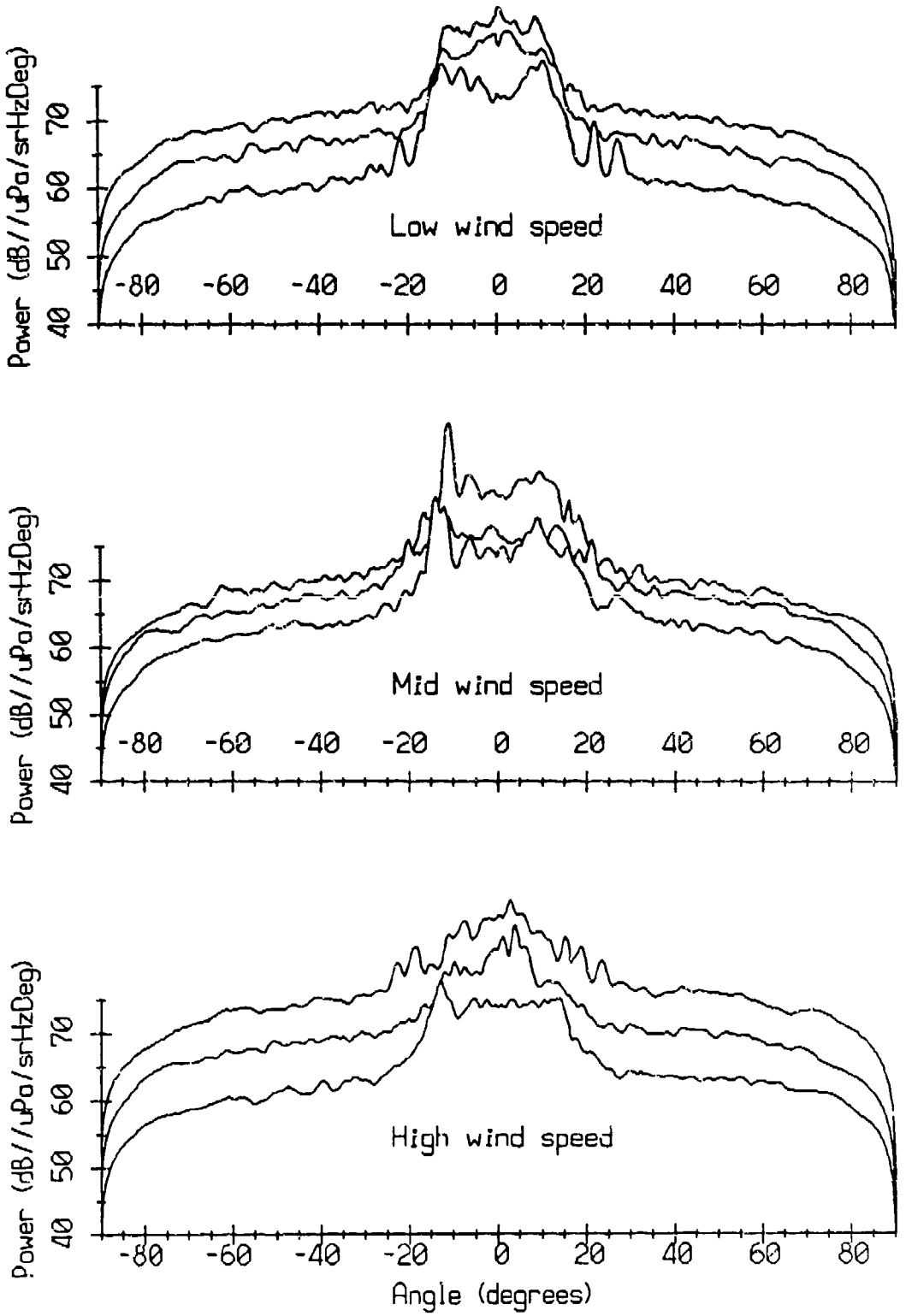

# Spatial Distribution vs. Depth at 95 Hz

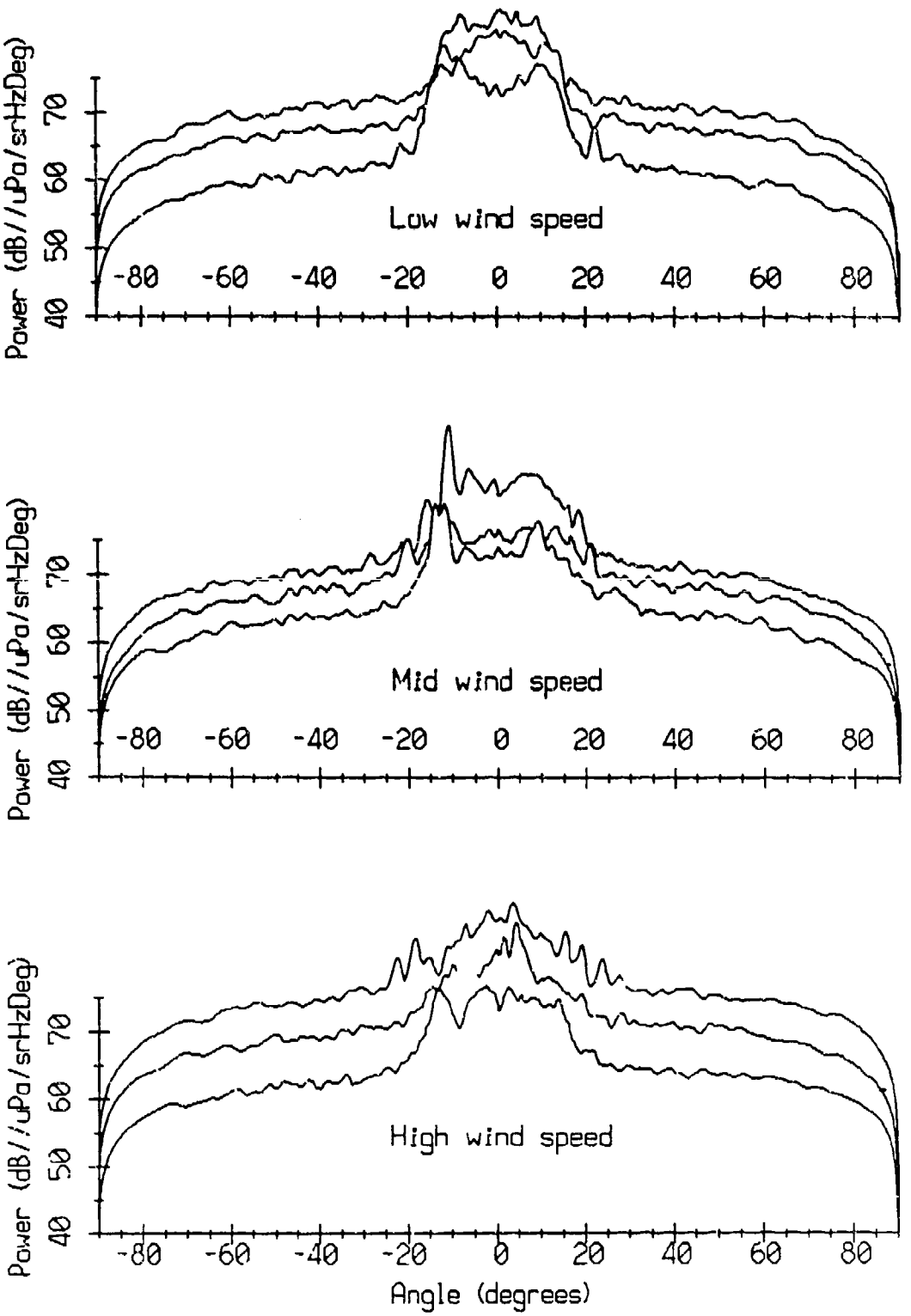

# Spatial Distribution vs. Depth at 100 Hz

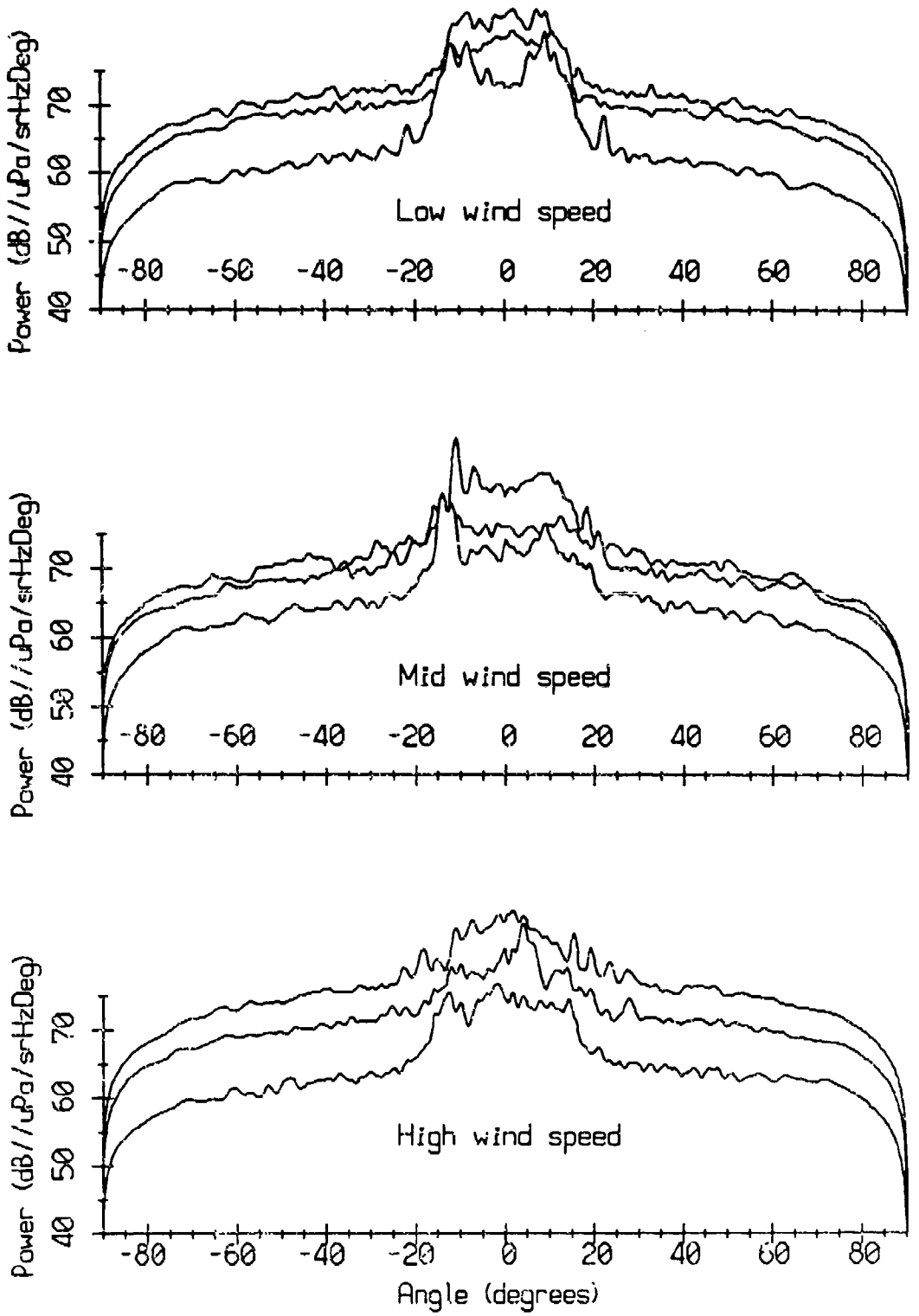

# Spatial Distribution vs. Depth at 105 Hz

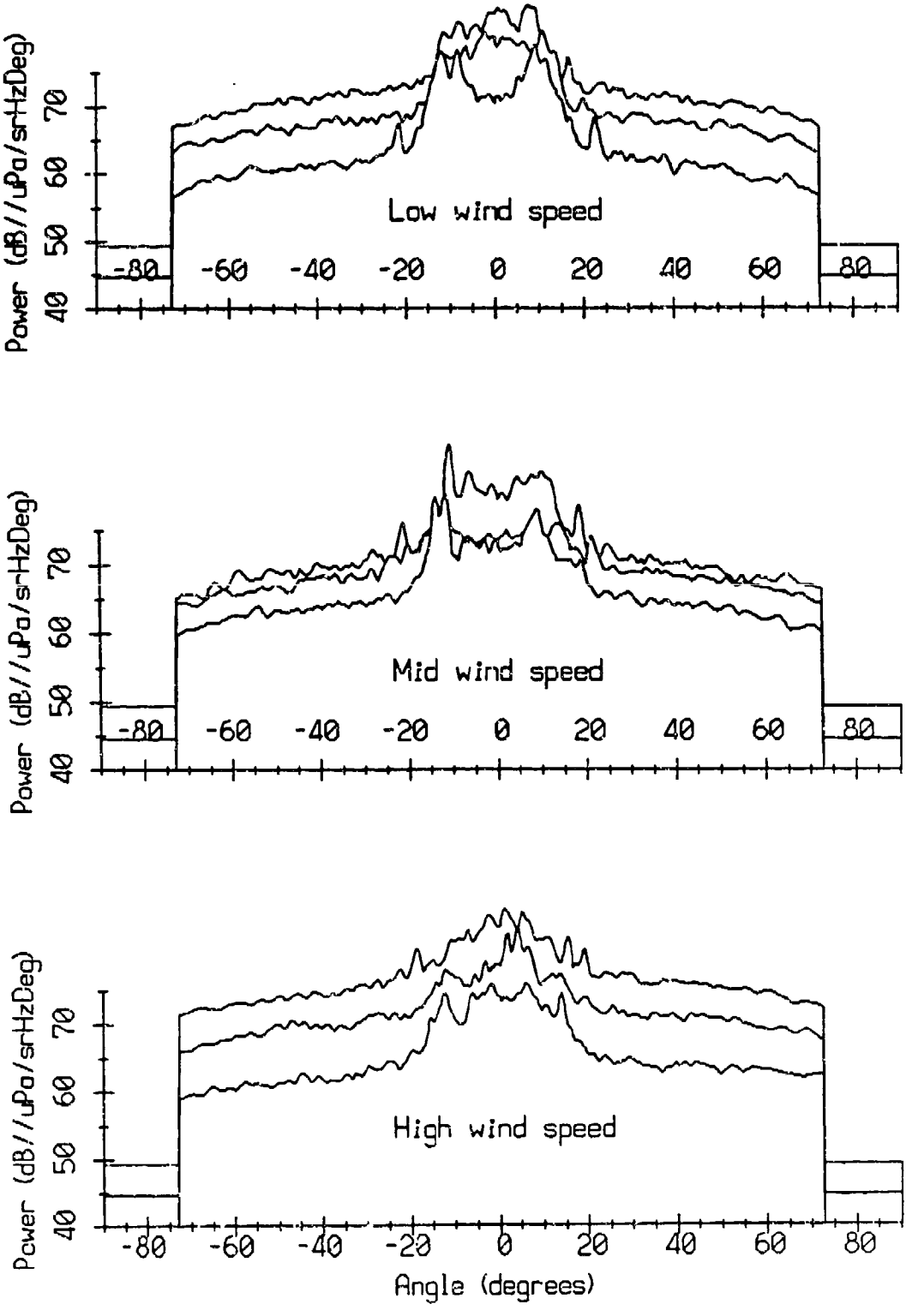

# Spatial Distribution vs. Depth at 110 Hz

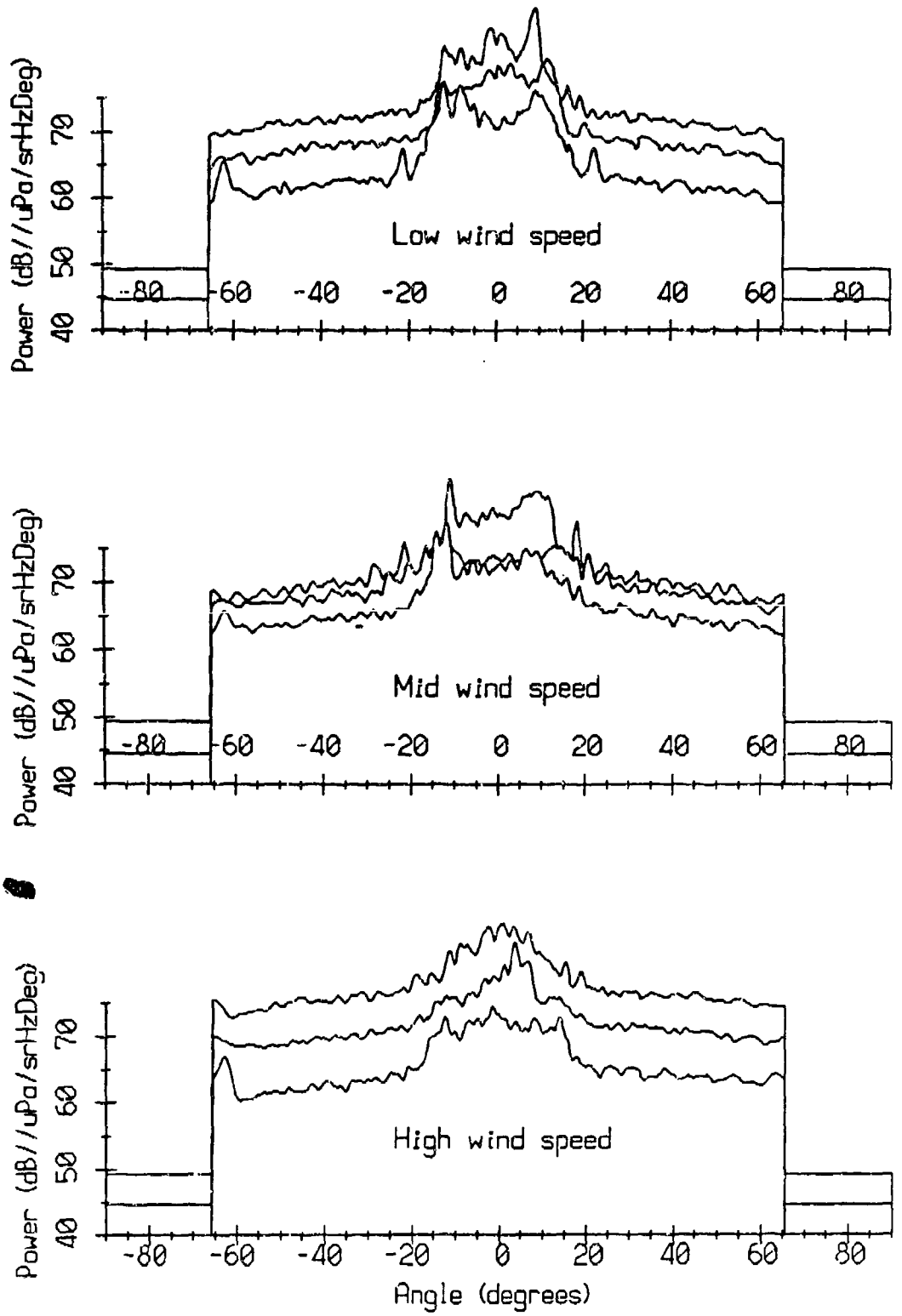

# Spatial Distribution vs. Depth at 115 Hz

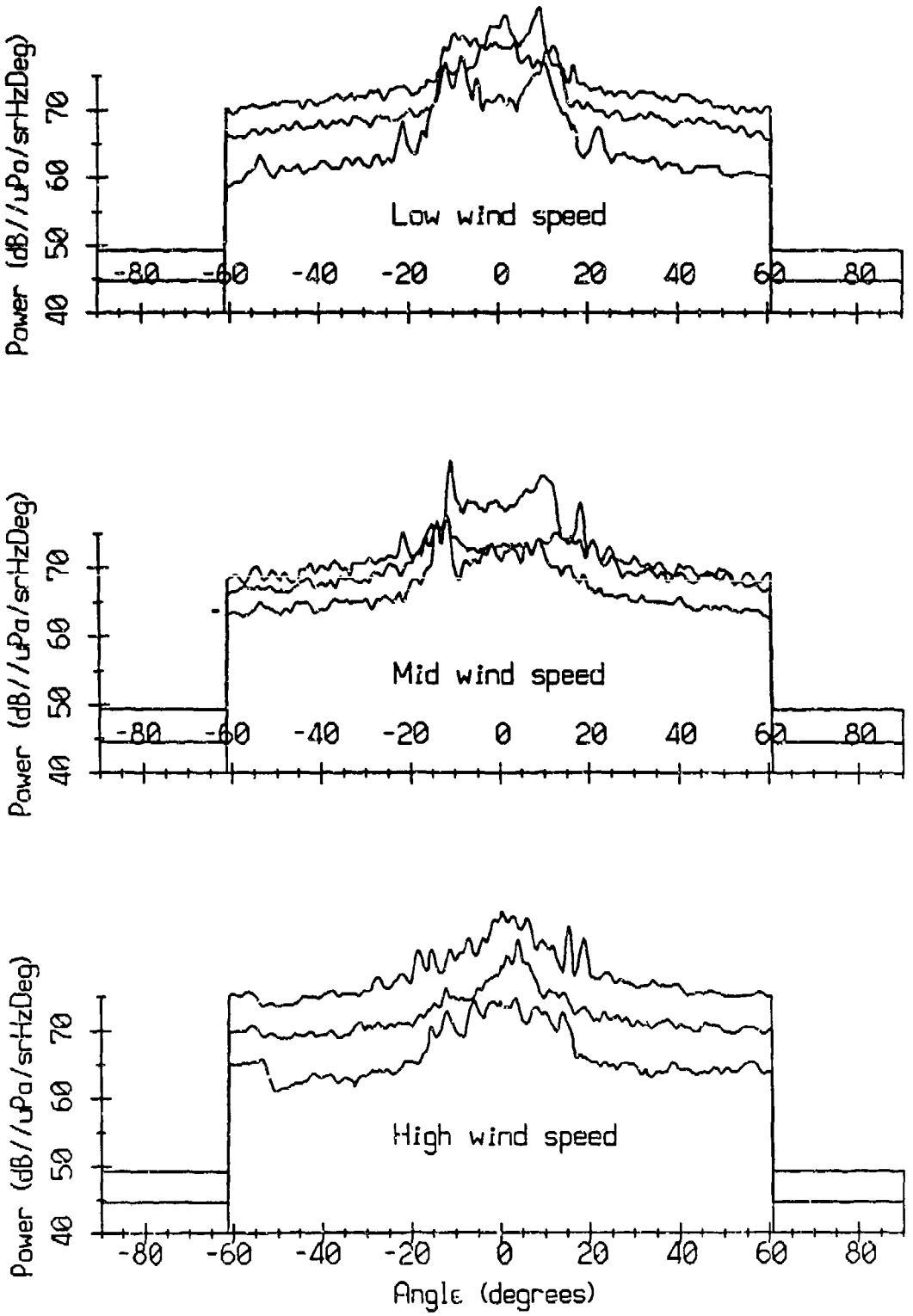

# Spatial Distribution vs. Depth at 120 Hz

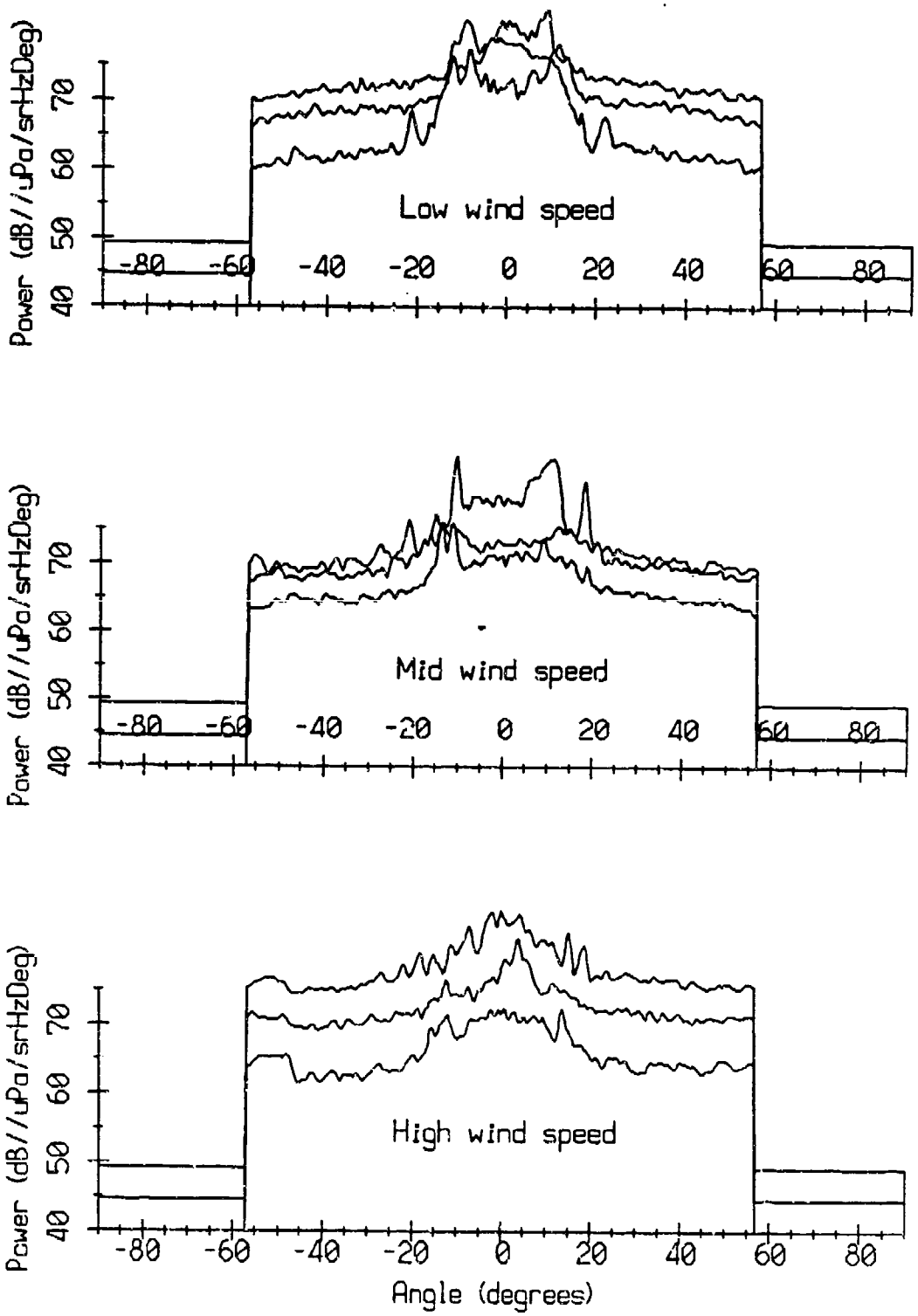

# Spatial Distribution vs. Depth at 125 Hz

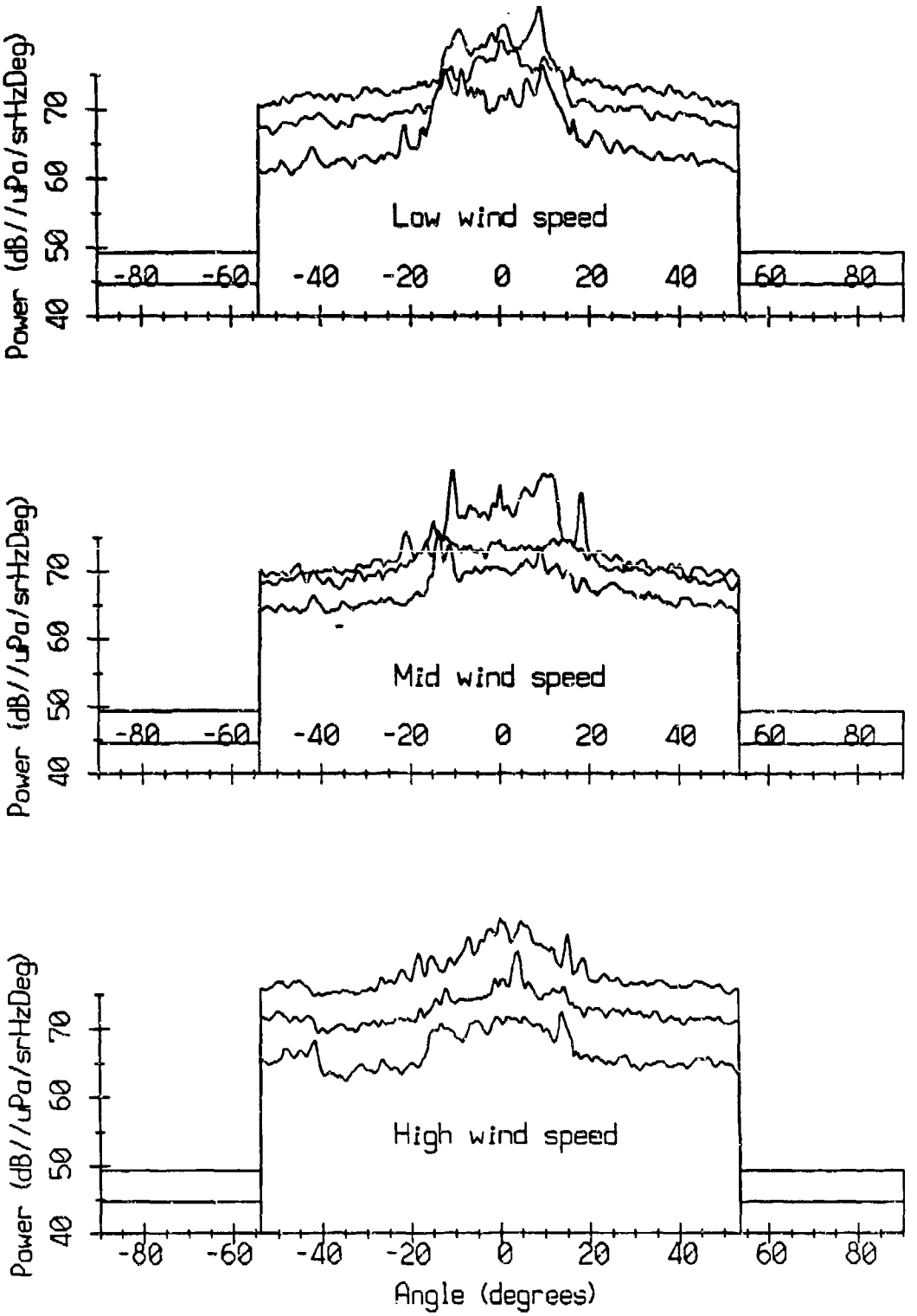

# Spatial Distribution vs. Depth at 130 Hz

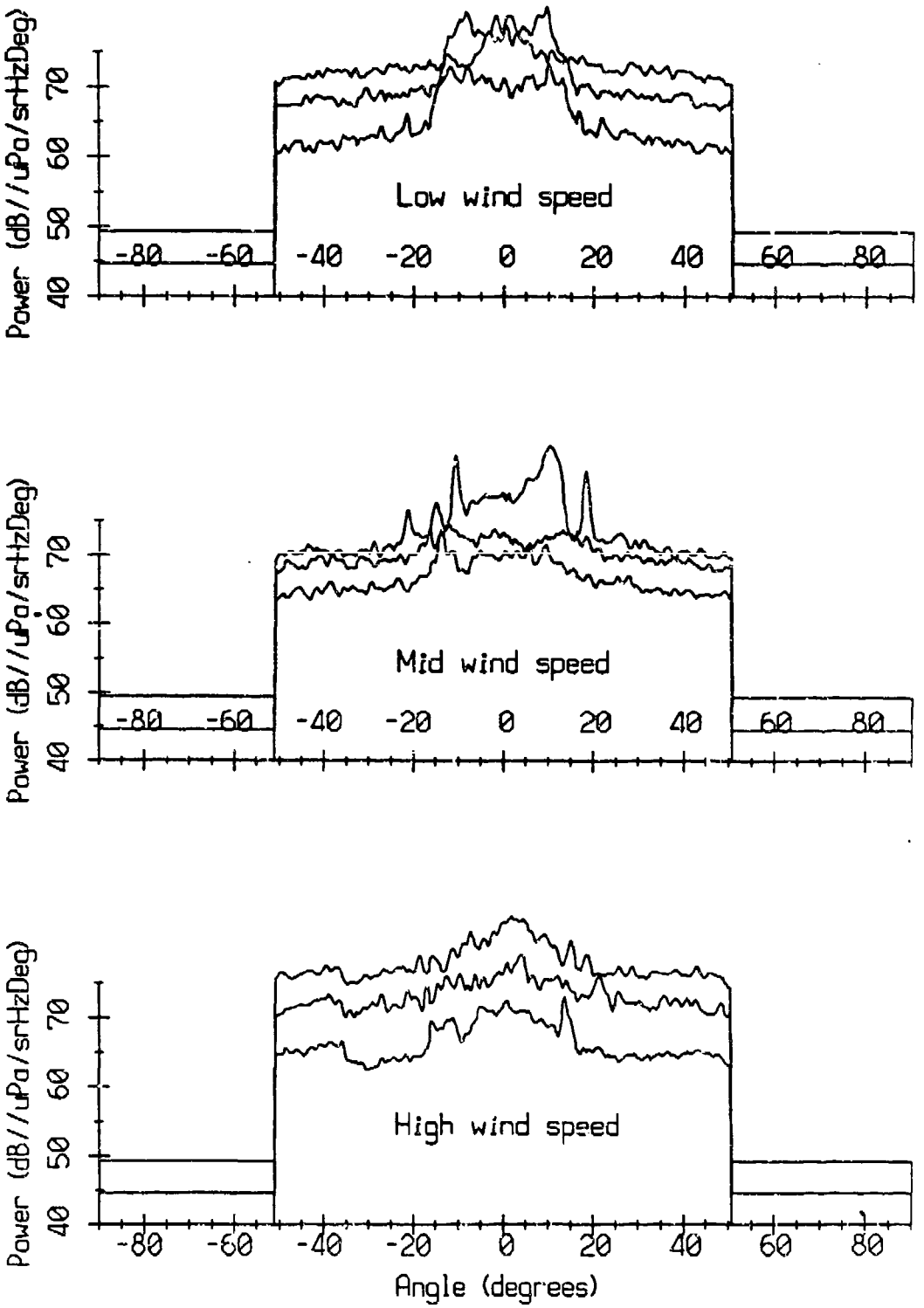

**Figure 8.**

**Spatial spectra versus wind speed at specified frequencies and array depths.**

# Spatial Distribution vs. Wind Speed at 15 Hz

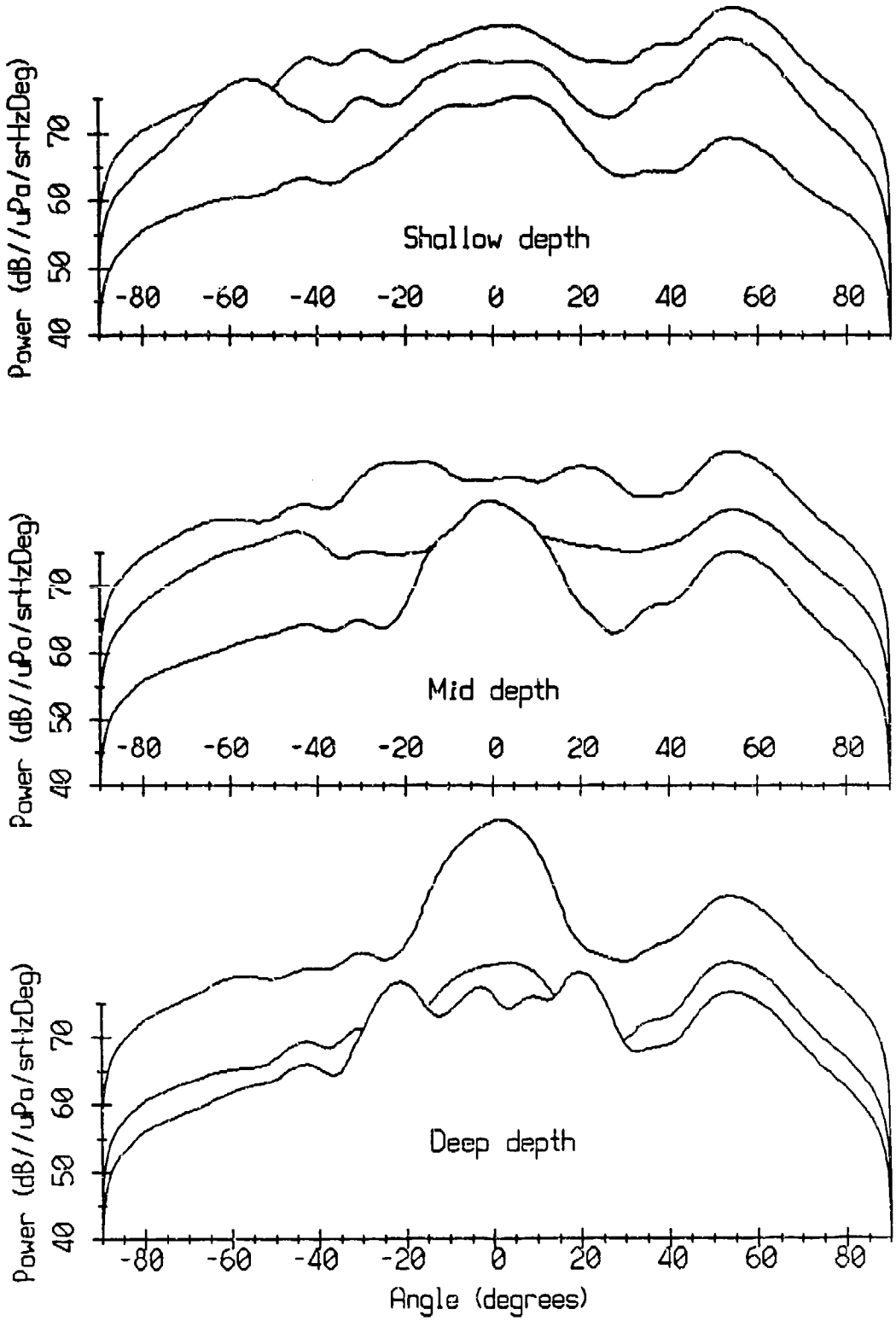

Spatial Distribution vs. Wind Speed at 20 Hz

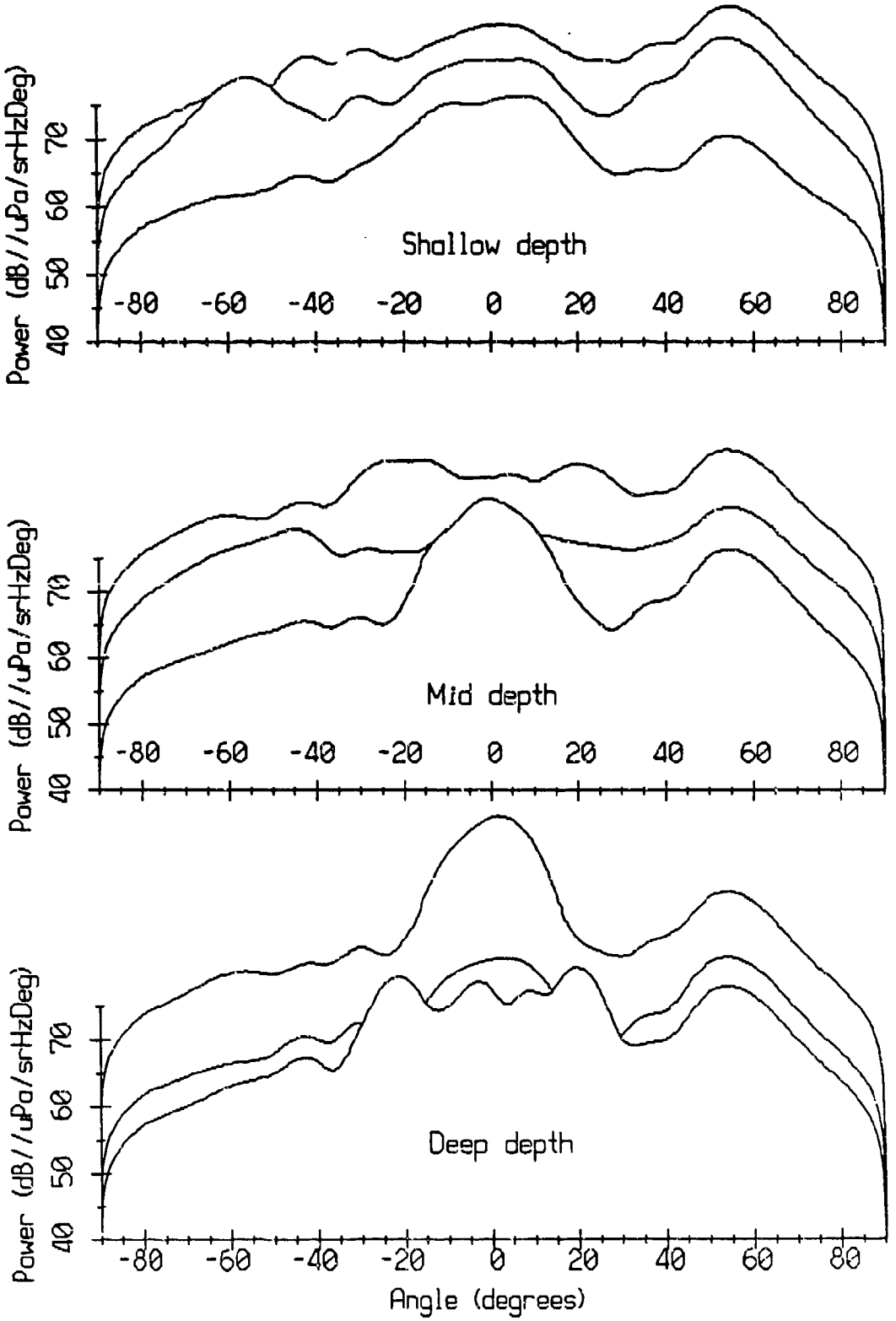

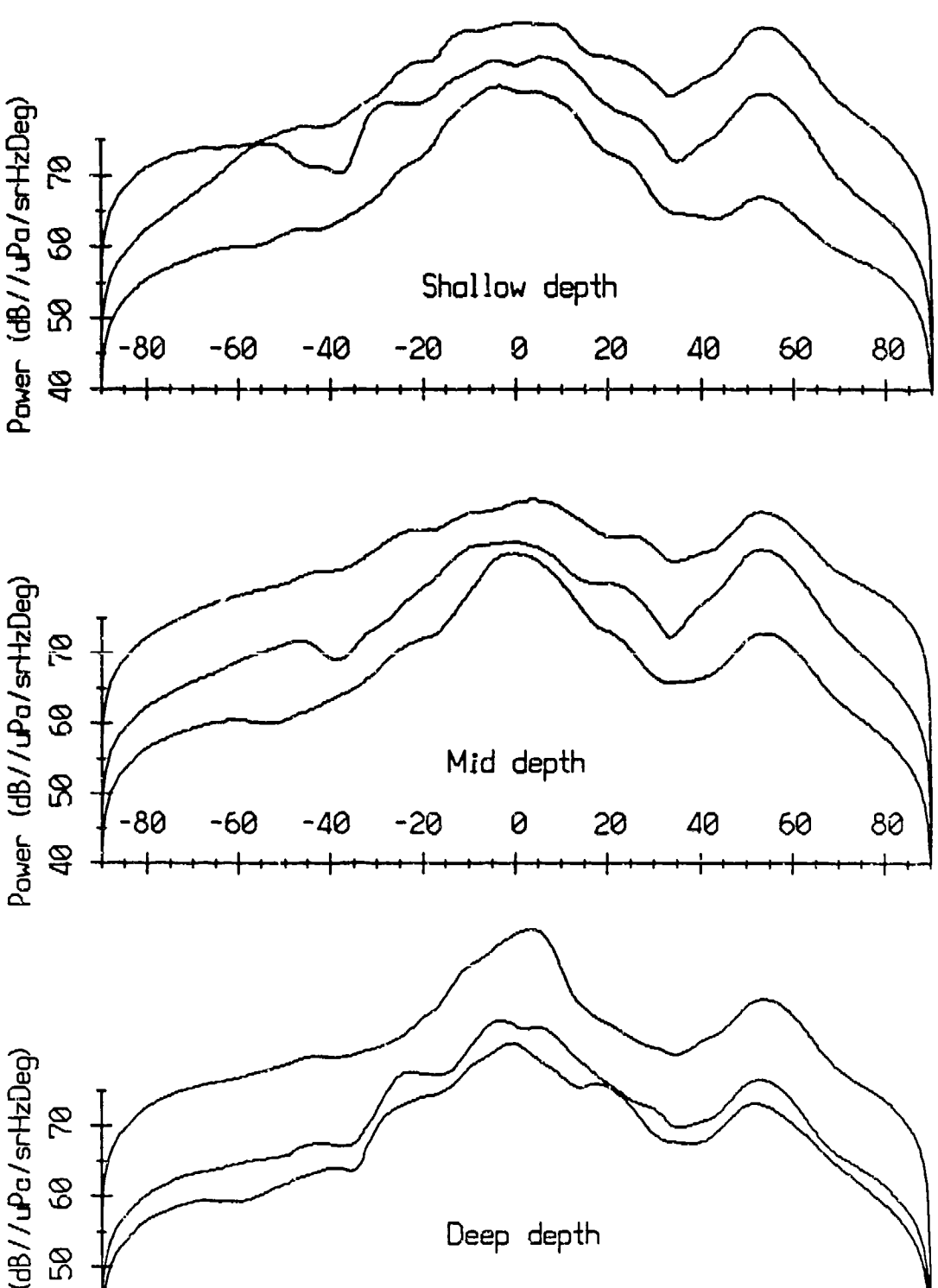
Spatial Distribution vs. Wind Speed at 25 Hz
Power (dB//uPa/srHzDeg)
40
50
60
70
Shallow depth
-80
-60
-40
-20
0
20
40
60
80
Mid depth
Deep depth
Angle (degrees)

# Spatial Distribution vs. Wind Speed at 30 Hz

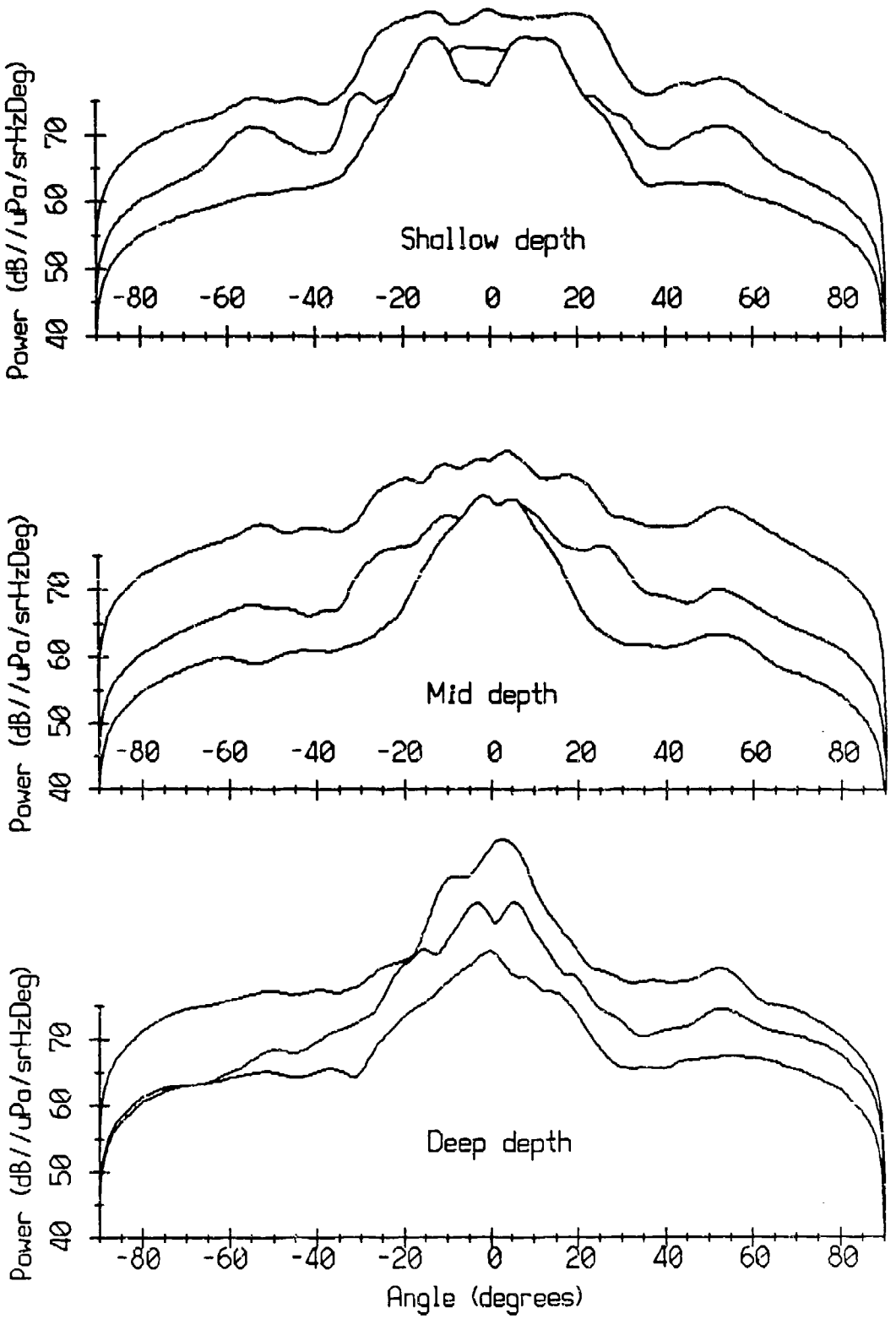

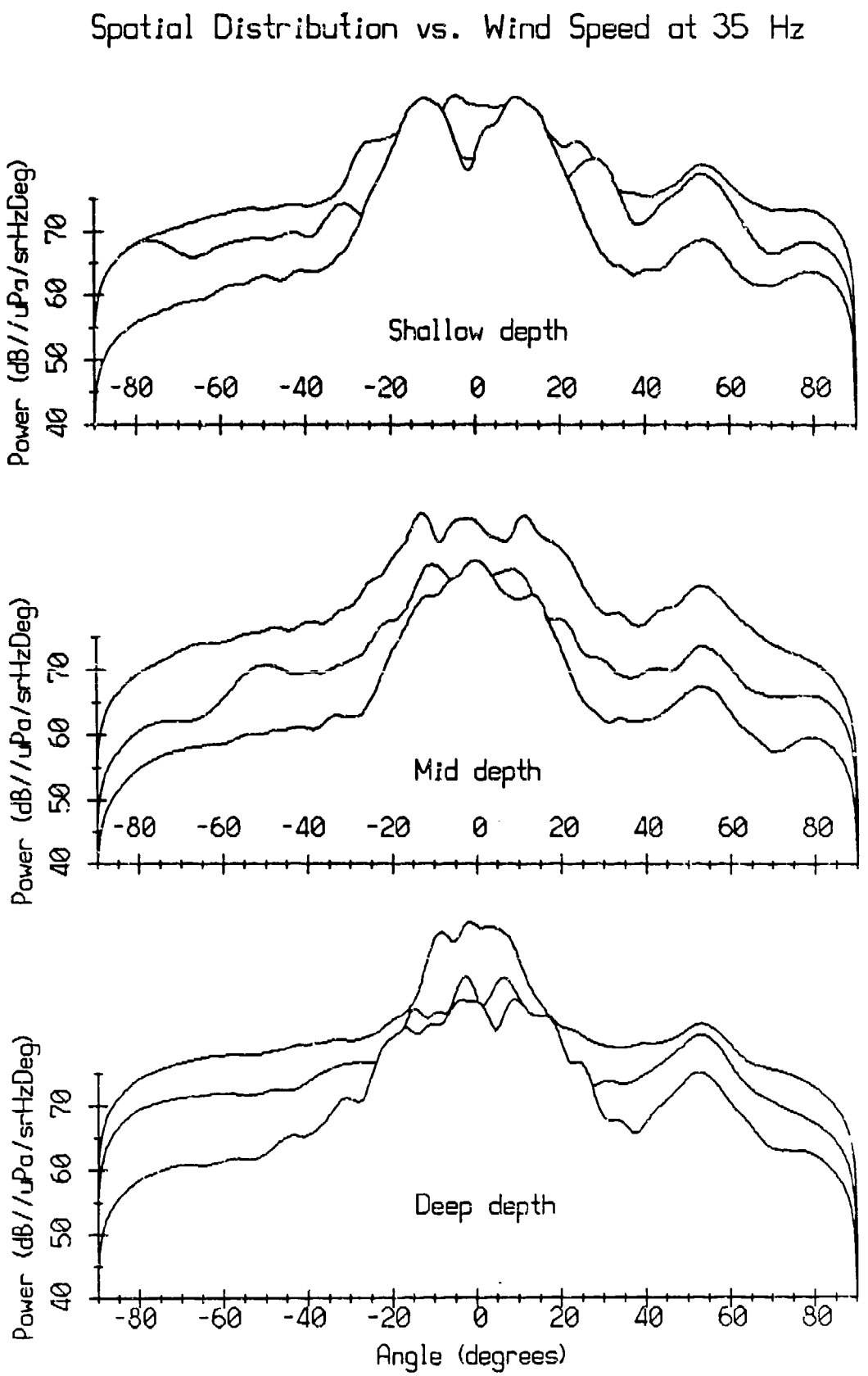
Spatial Distribution vs. Wind Speed at 35 Hz
Power (dB//uPa/srHzDeg)
40
50
60
70
Shallow depth
-80
-60
-40
-20
0
20
40
60
80
Mid depth
Deep depth
Angle (degrees)

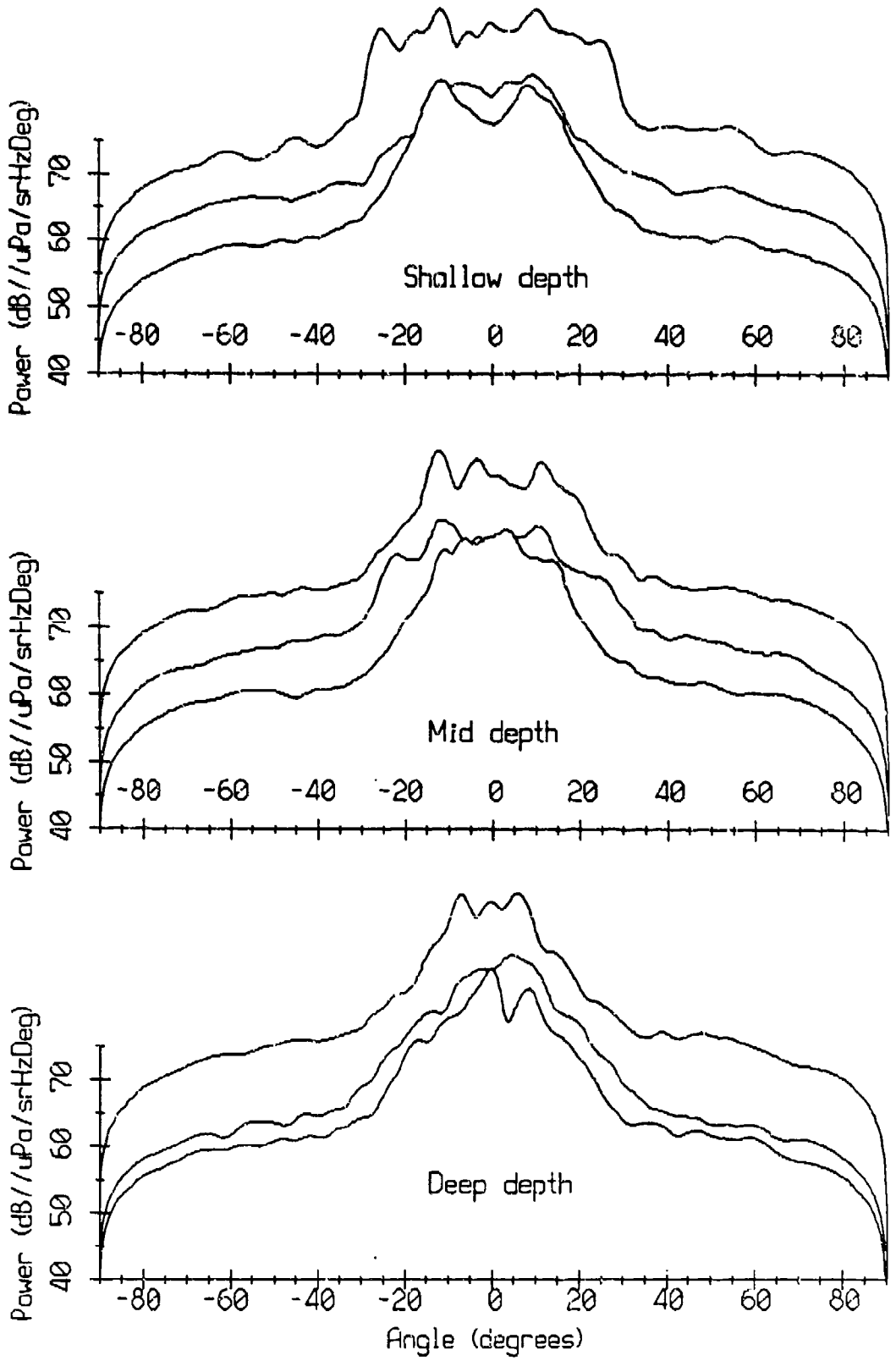
Spatial Distribution vs. Wind Speed at 40 Hz
Power (dB//uPa/srHzDeg)
40
50
60
70
Shallow depth
-80
-60
-40
-20
0
20
40
60
80
Mid depth
Deep depth
Angle (degrees)

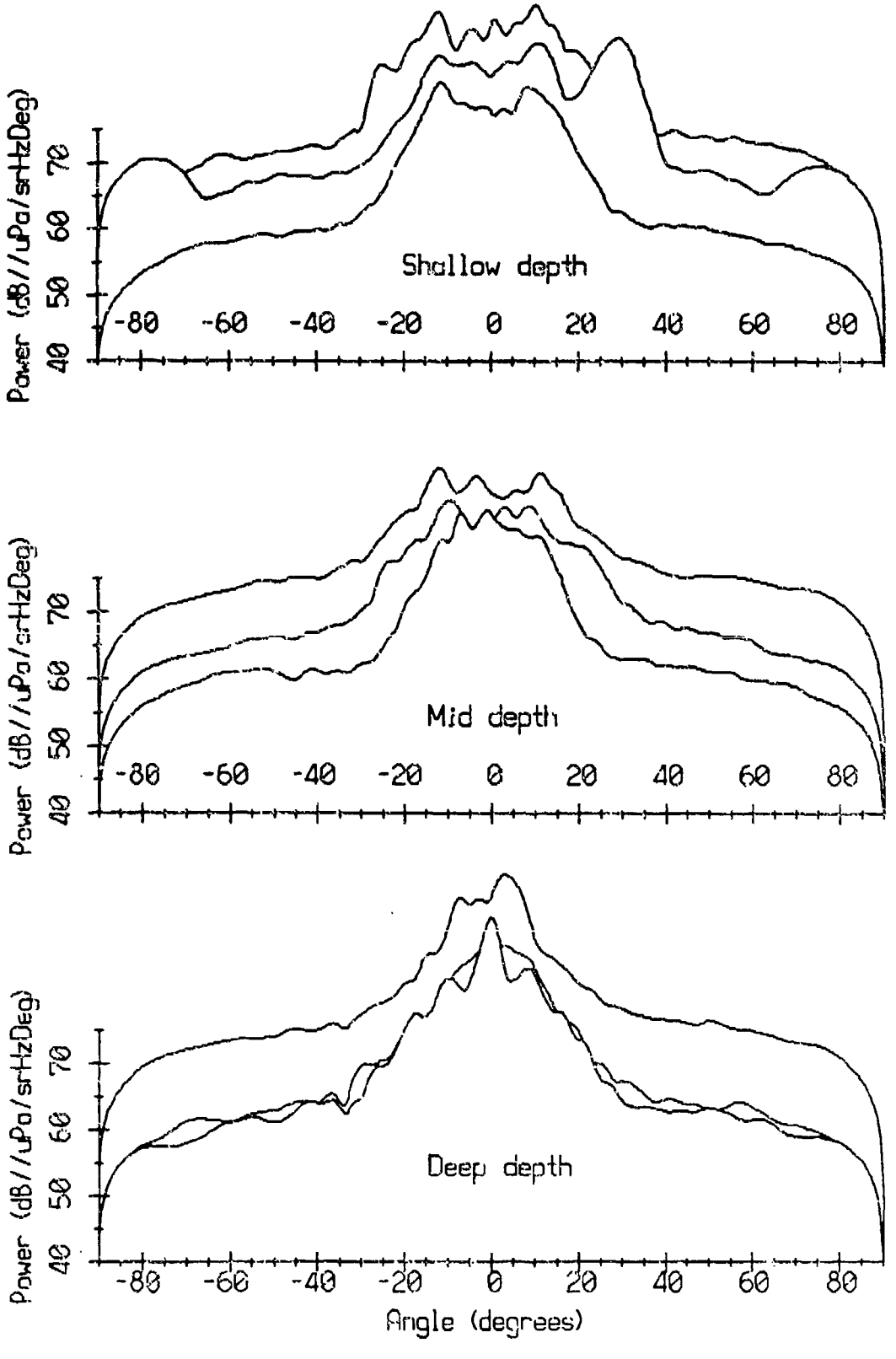
Spatial Distribution vs. Wind Speed at 45 Hz
Power (dB//uPa/srHzDeg)
40
50
60
70
Shallow depth
-80
-60
-40
-20
0
20
40
60
80
Mid depth
Deep depth
Angle (degrees)

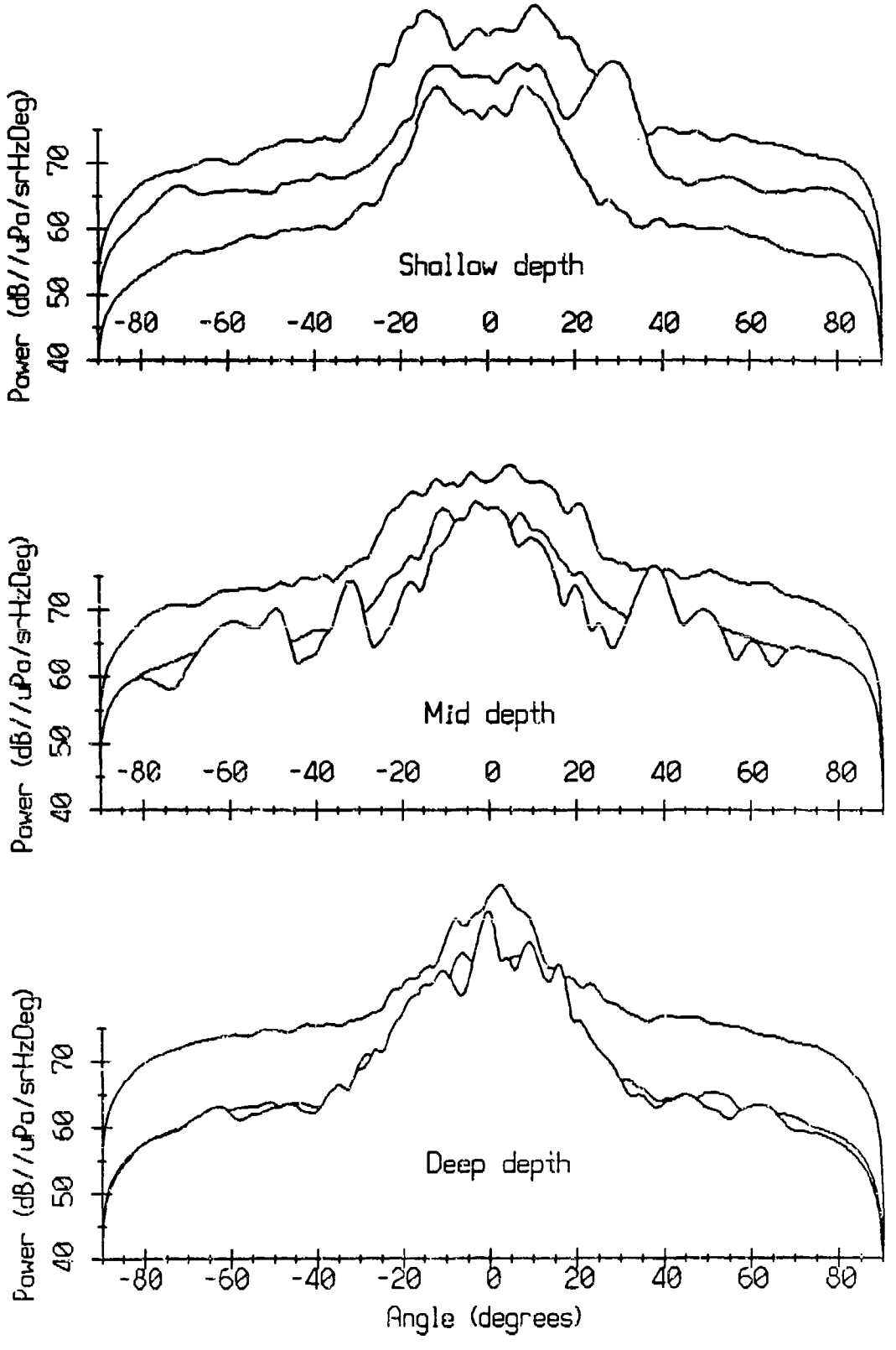
Spatial Distribution vs. Wind Speed at 50 Hz
Power (dB//uPa/srHzDeg)
40
50
60
70
Shallow depth
-80
-60
-40
-20
0
20
40
60
80
Mid depth
Deep depth
Angle (degrees)

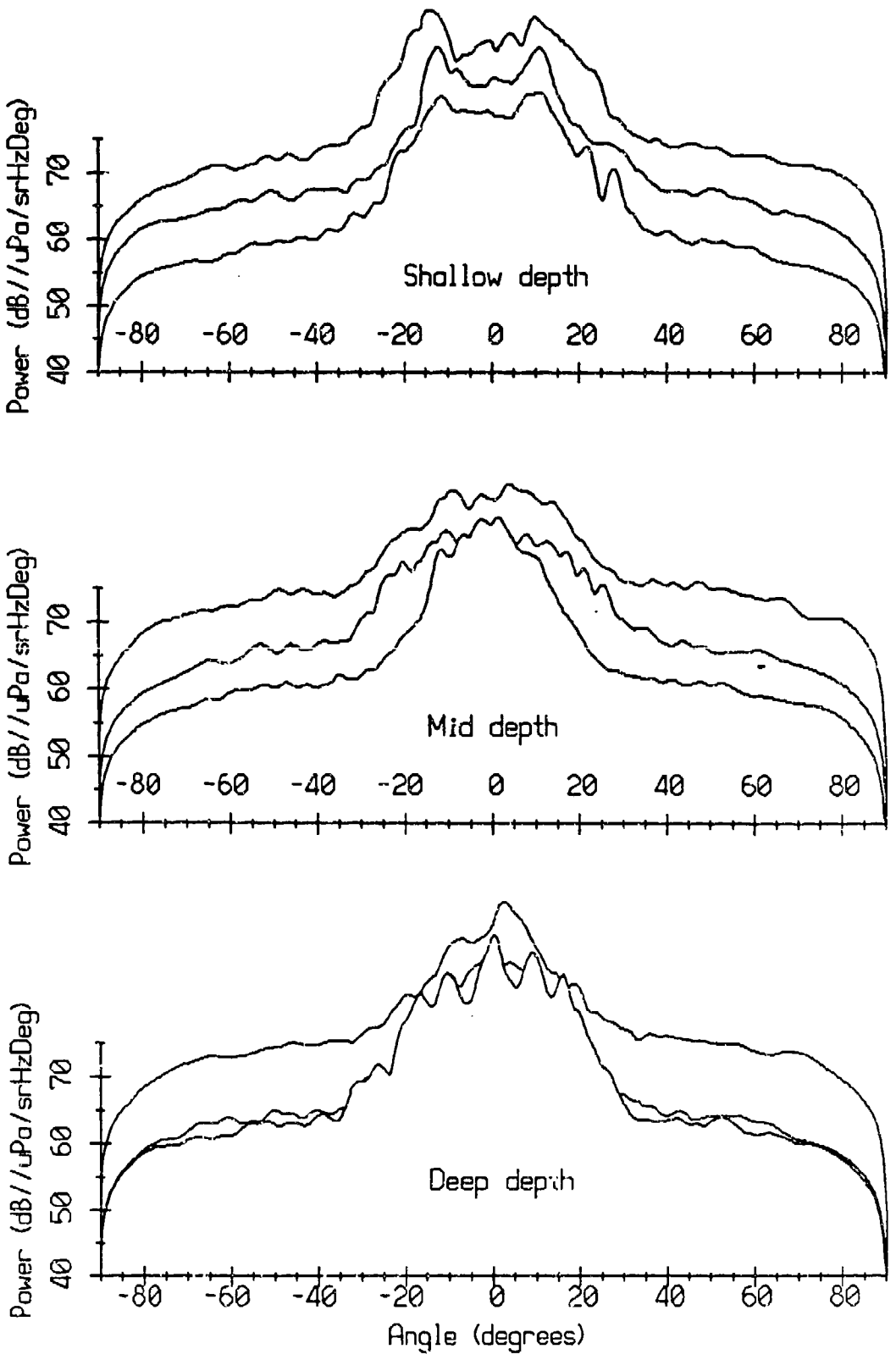
Spatial Distribution vs. Wind Speed at 55 Hz
Power (dB//uPa/srHzDeg)
40
50
60
70
Shallow depth
-80
-60
-40
-20
0
20
40
60
80
Mid depth
Deep depth
Angle (degrees)

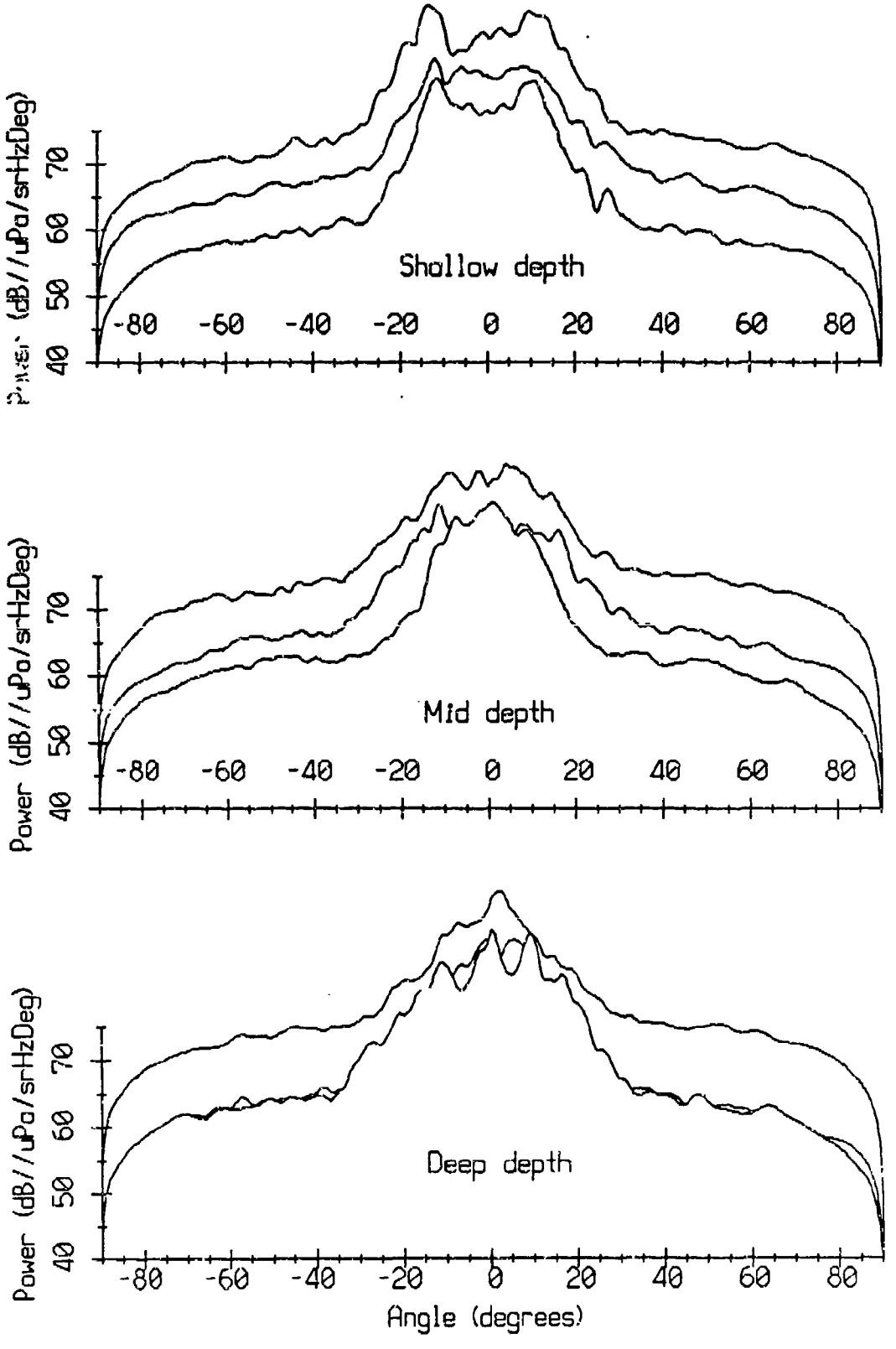
Spatial Distribution vs. Wind Speed at 60 Hz
Power (dB//uPa/srHzDeg)
40
50
60
70
-80
-60
-40
-20
0
20
40
60
80
Shallow depth
Mid depth
Deep depth
Angle (degrees)

# Spatial Distribution vs. Wind Speed at 65 Hz

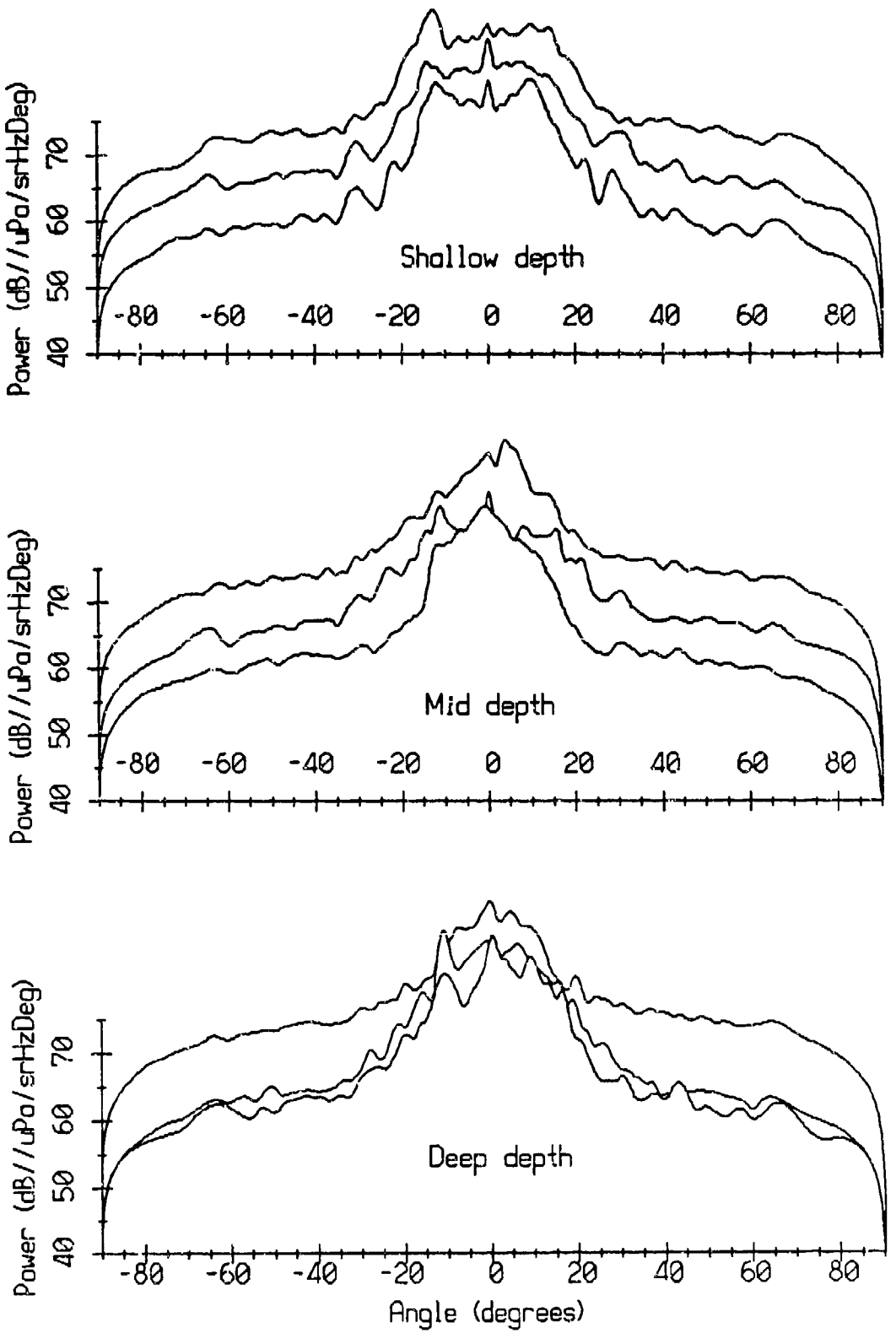

# Spatial Distribution vs. Wind Speed at 70 Hz

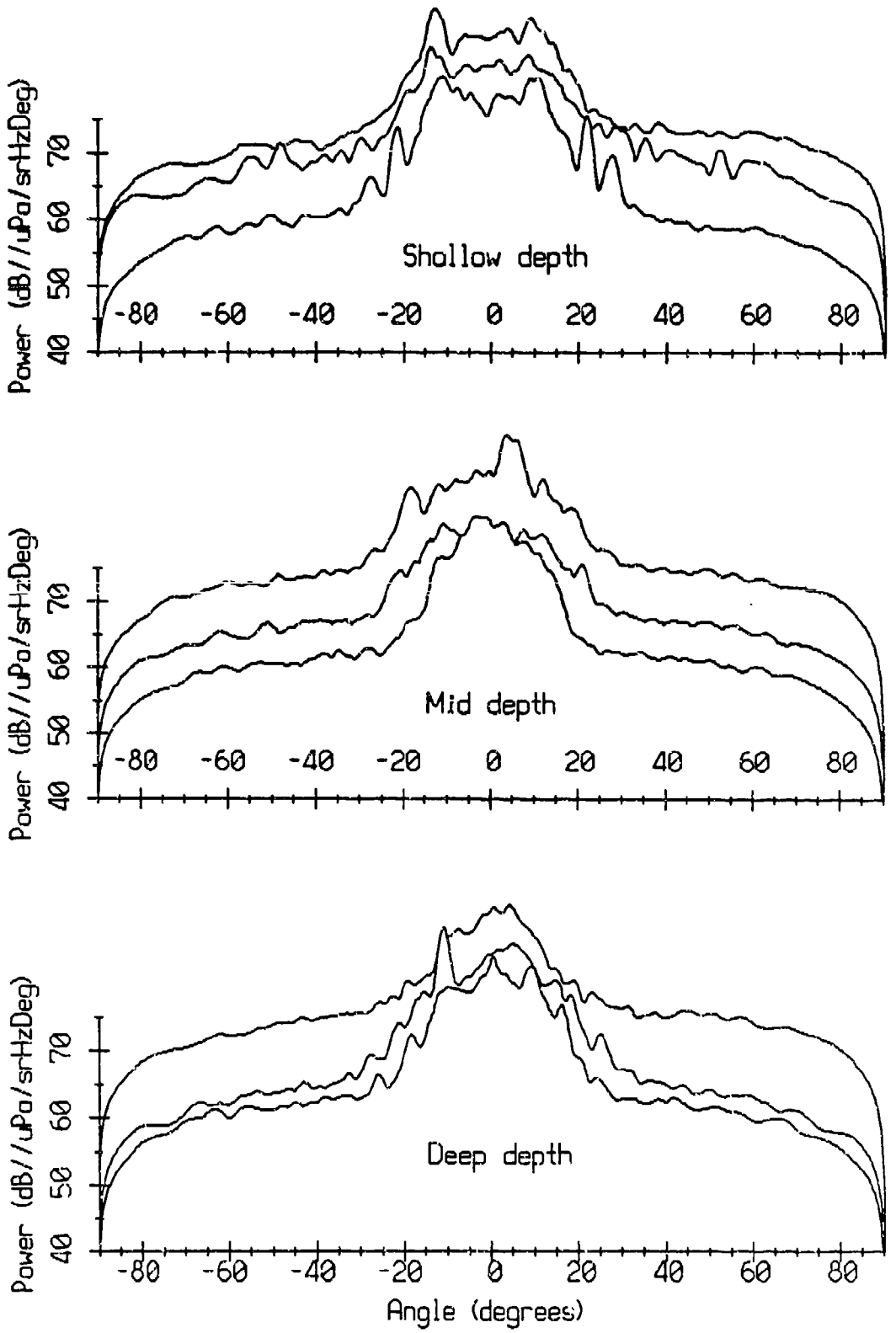

# Spatial Distribution vs. Wind Speed at 75 Hz

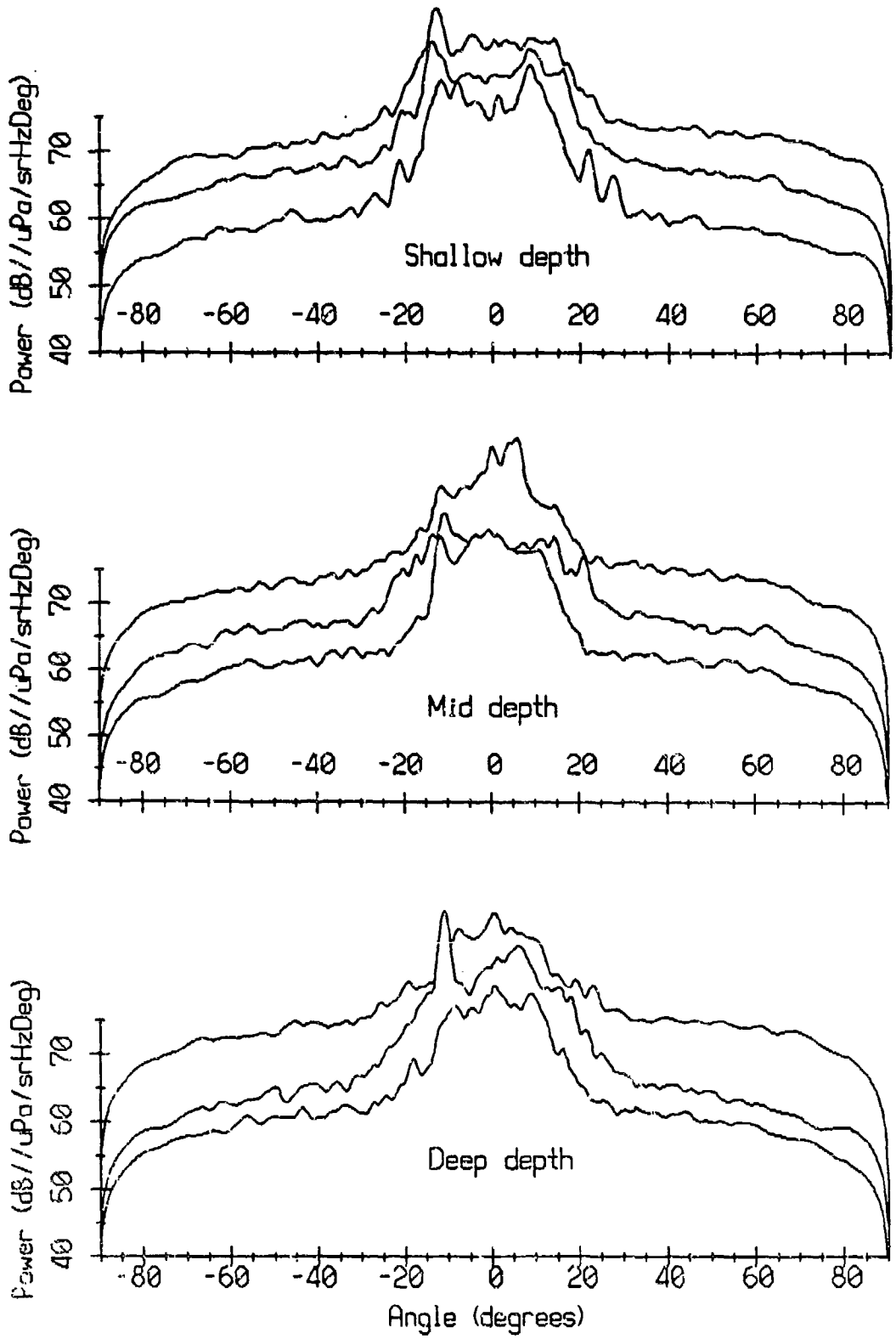

# Spatial Distribution vs. Wind Speed at 80 Hz

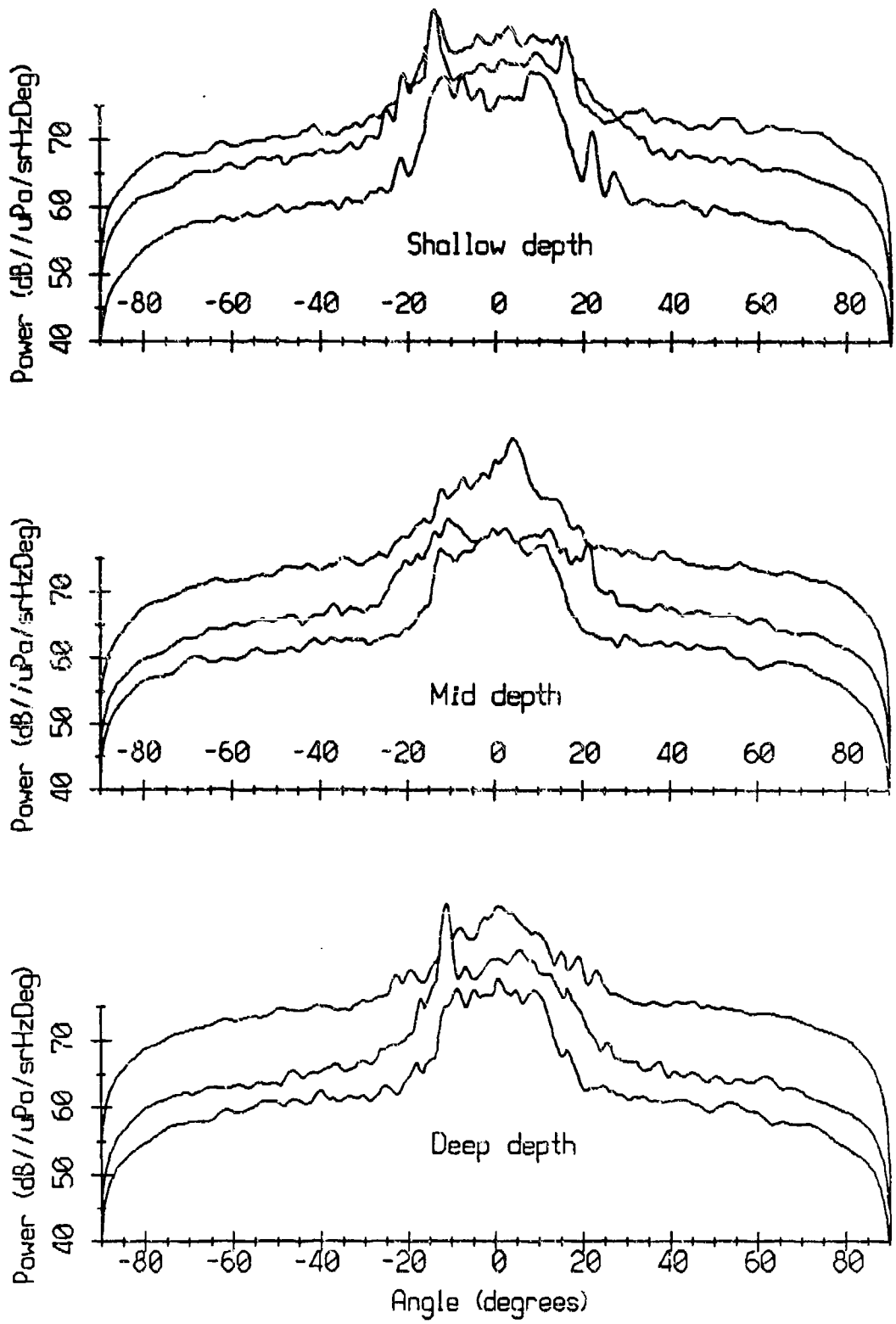

# Spatial Distribution vs. Wind Speed at 85 Hz

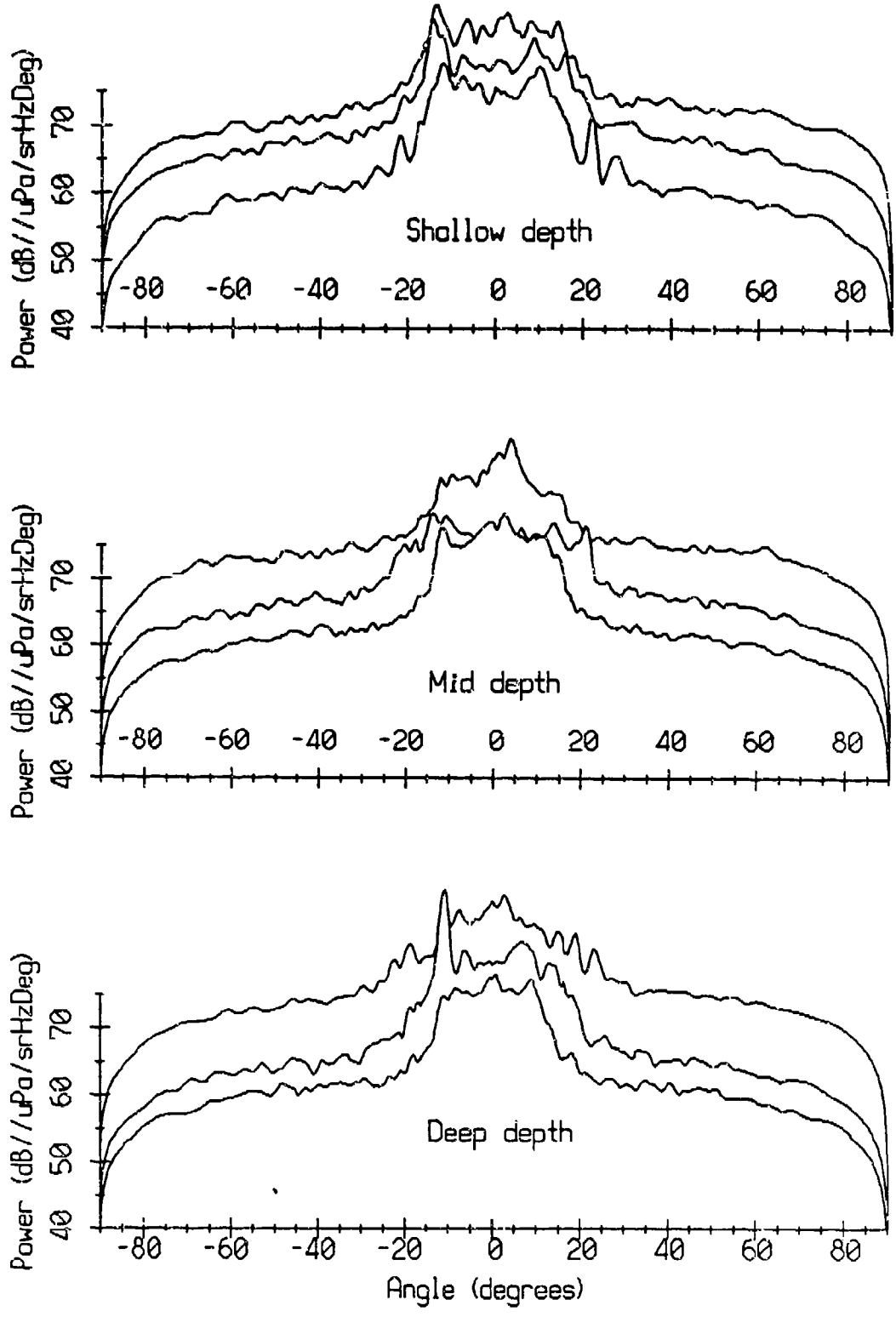

# Spatial Distribution vs. Wind Speed at 90 Hz

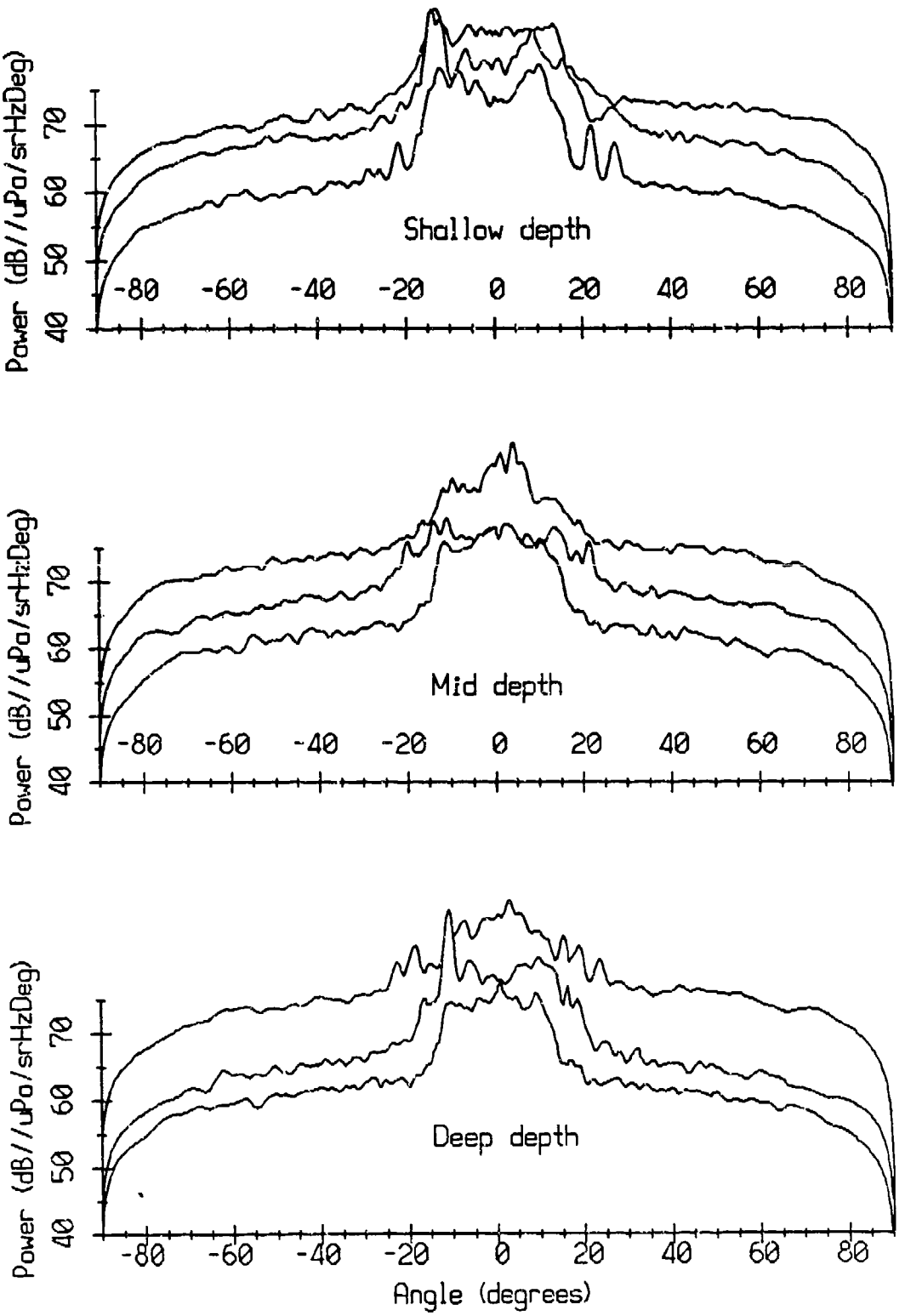

# Spatial Distribution vs. Wind Speed at 95 Hz

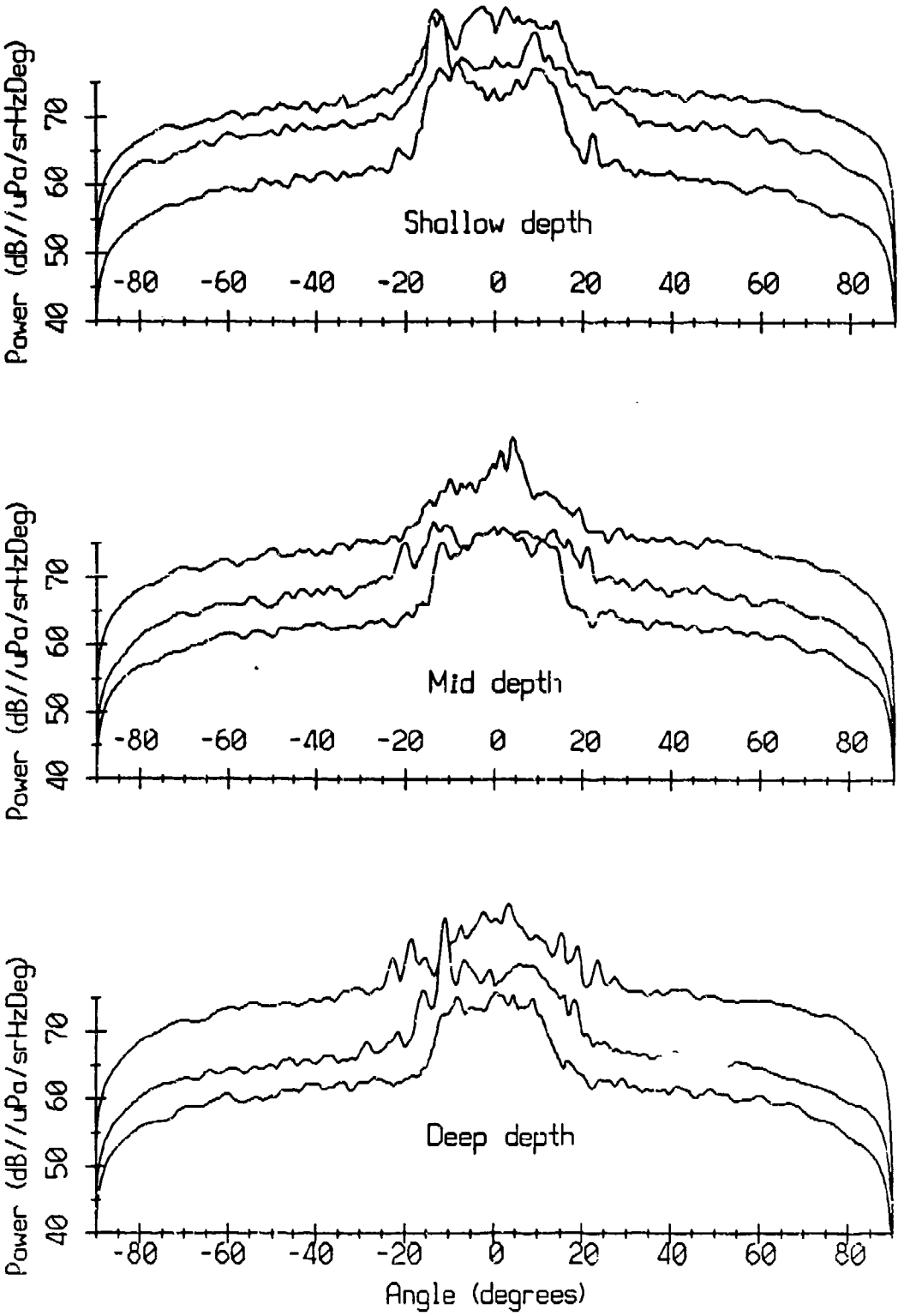

# Spatial Distribution vs. Wind Speed at 100Hz

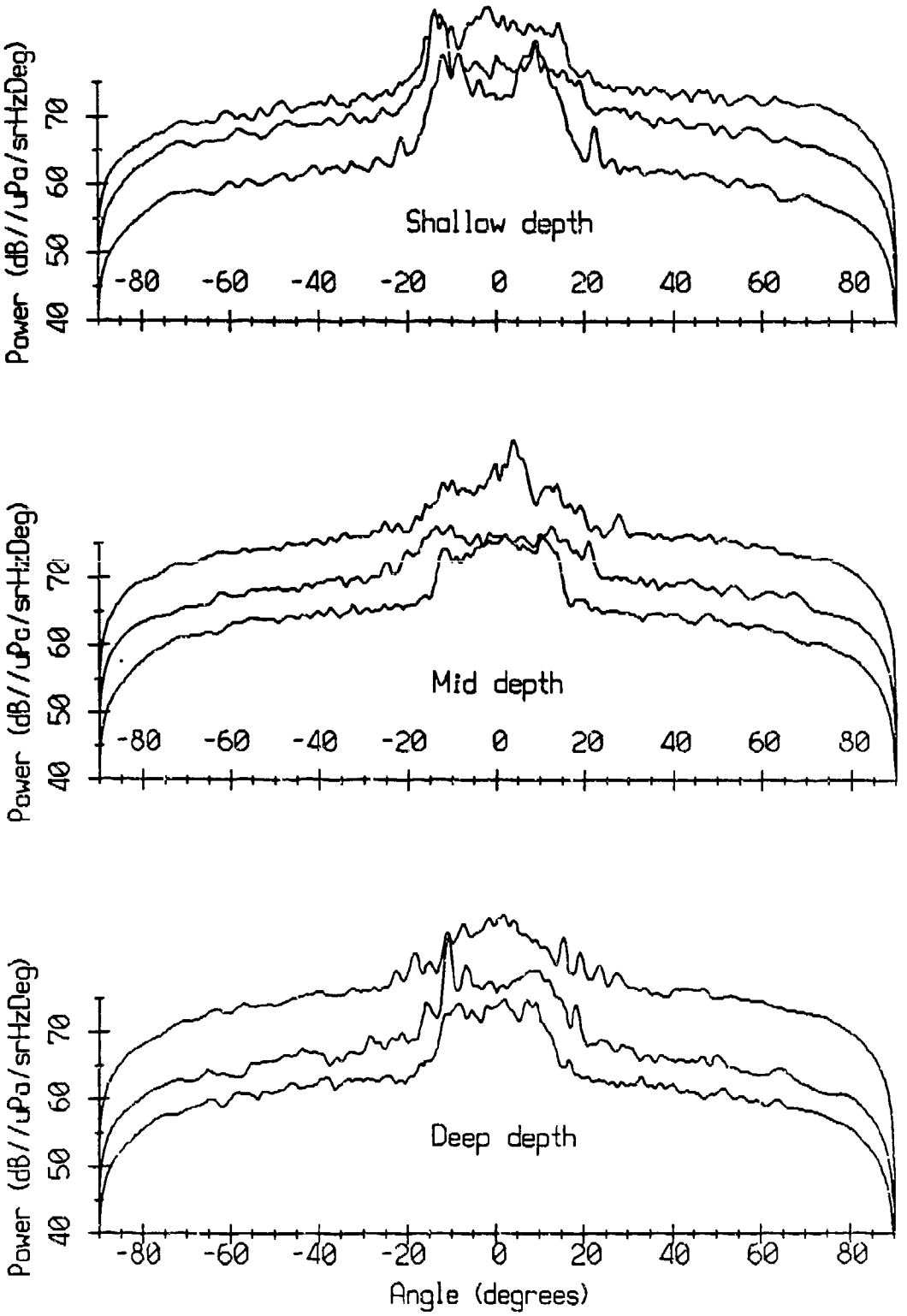

# Spatial Distribution vs. Wind Speed at 105Hz

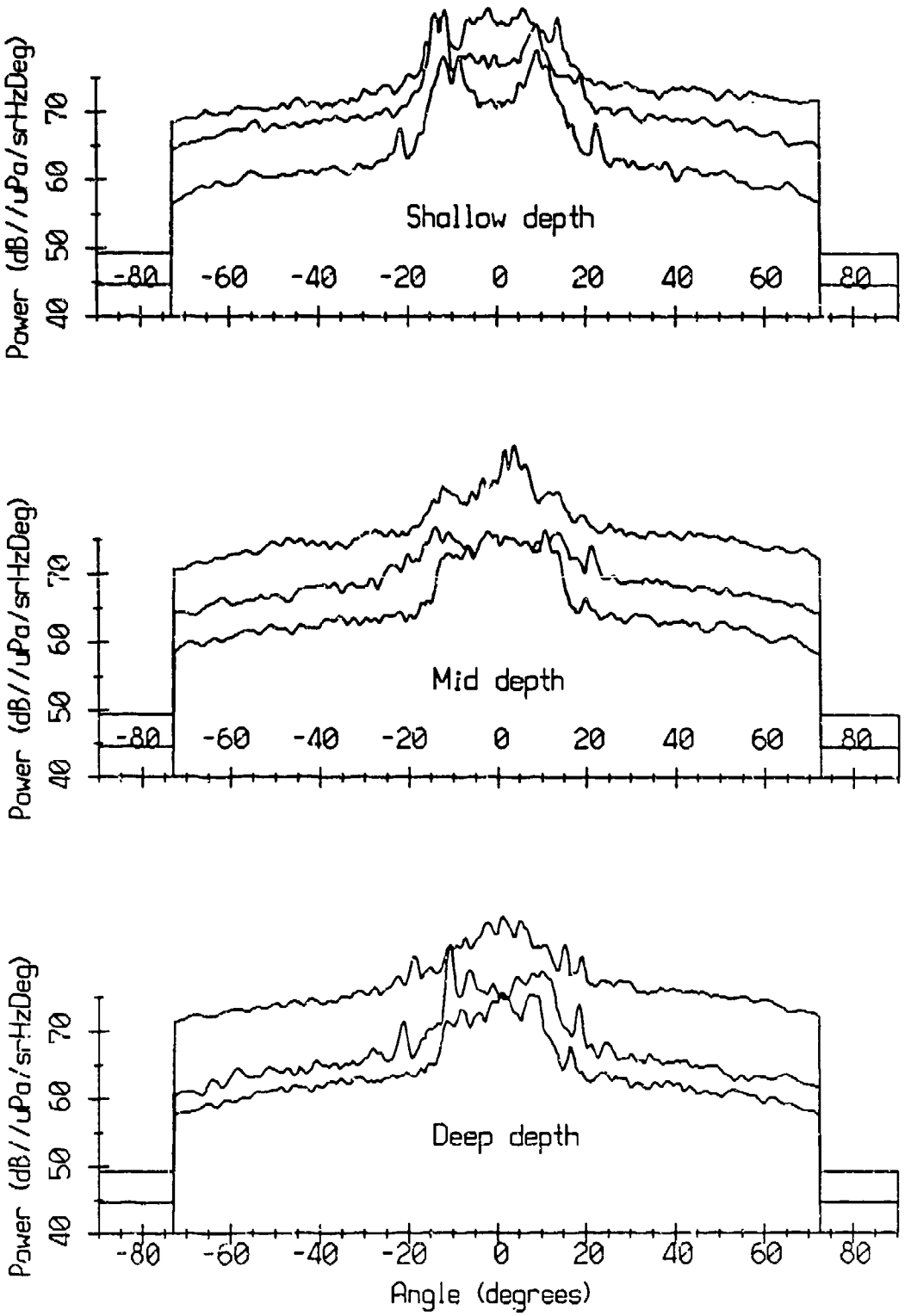

# Spatial Distribution vs. Wind Speed at 110Hz

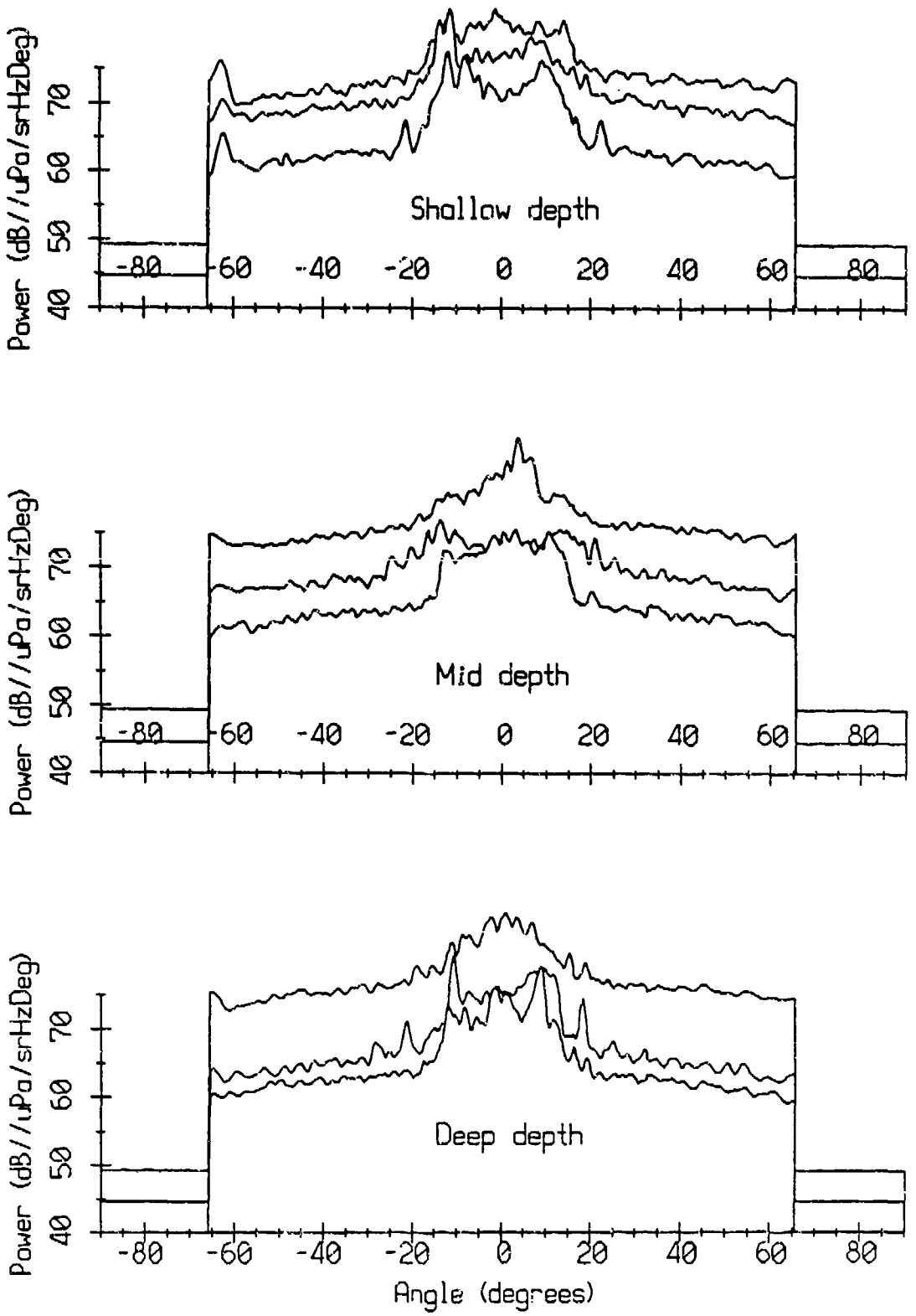

# Spatial Distribution vs. Wind Speed at 115Hz

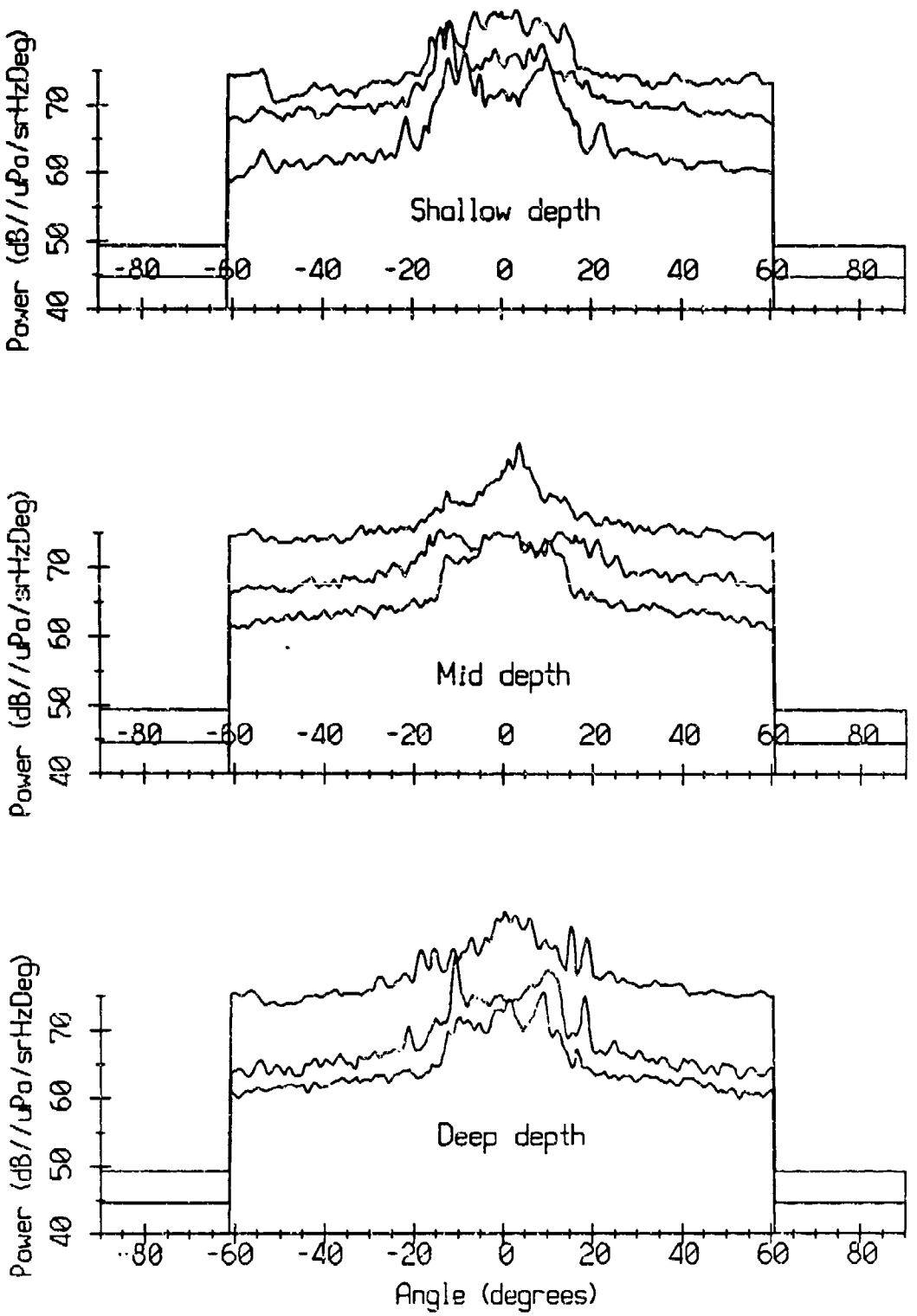

# Spatial Distribution vs. Wind Speed at 120Hz

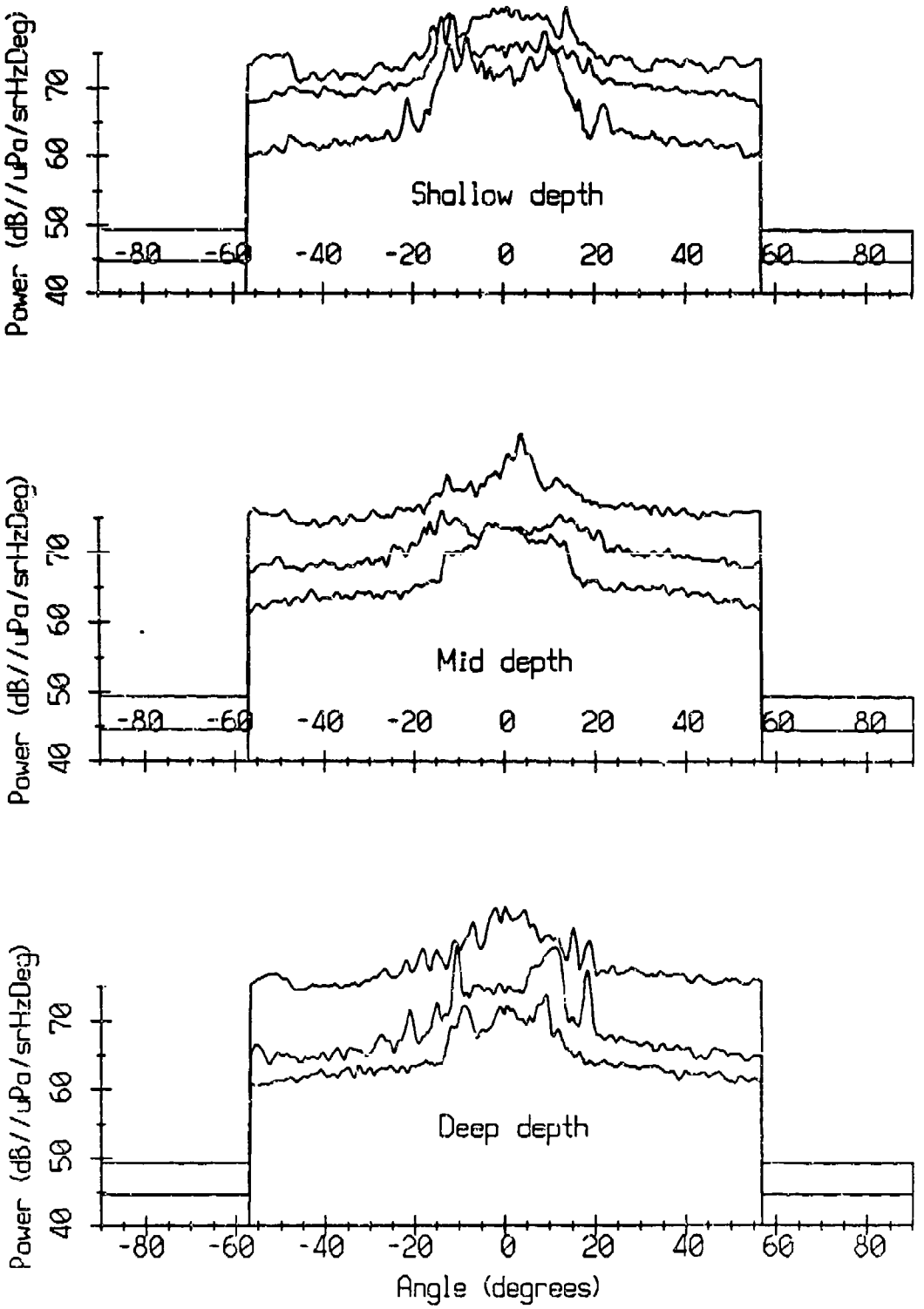

# Spatial Distribution vs. Wind Speed at 125Hz

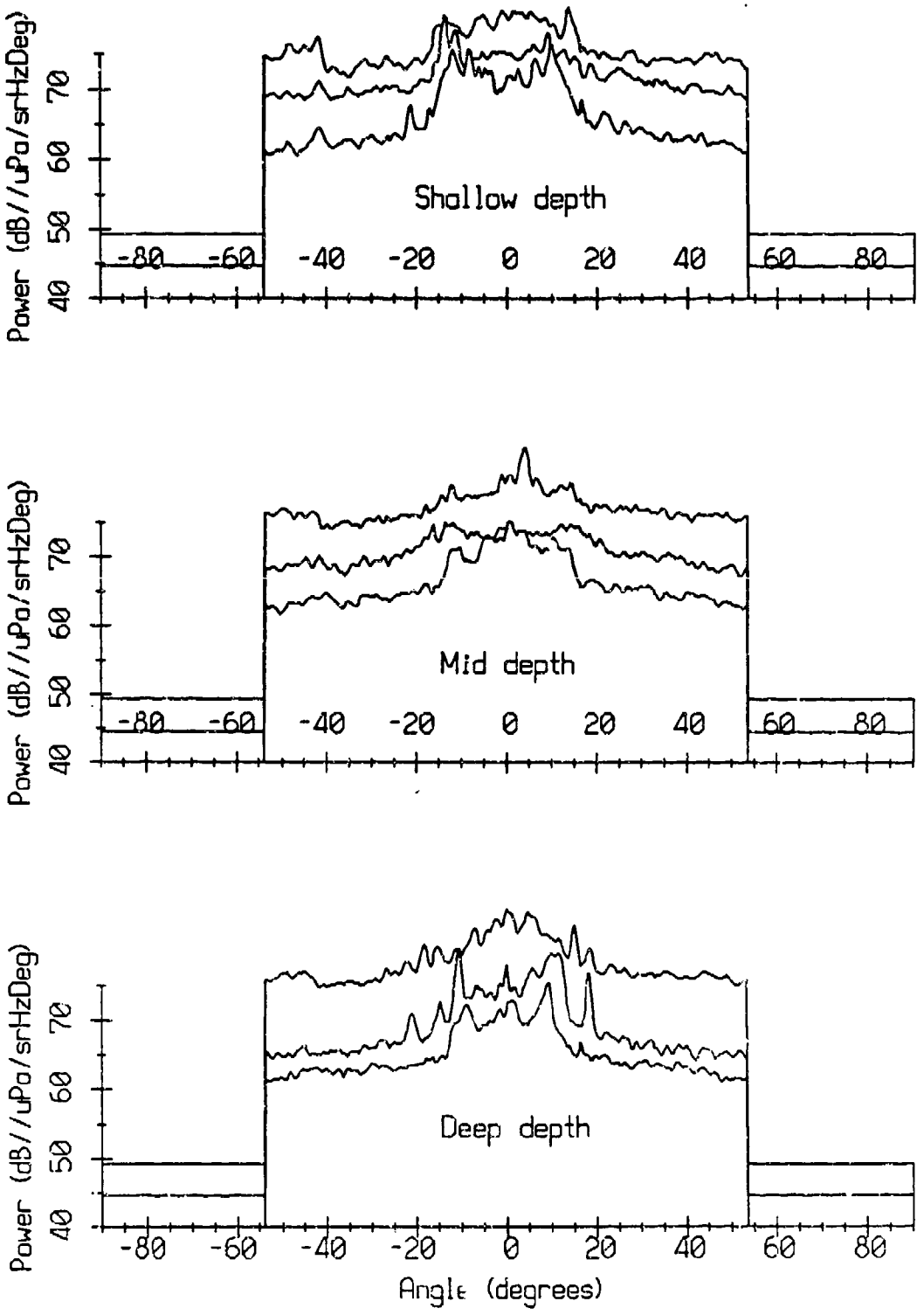

# Spatial Distribution vs. Wind Speed at 130Hz

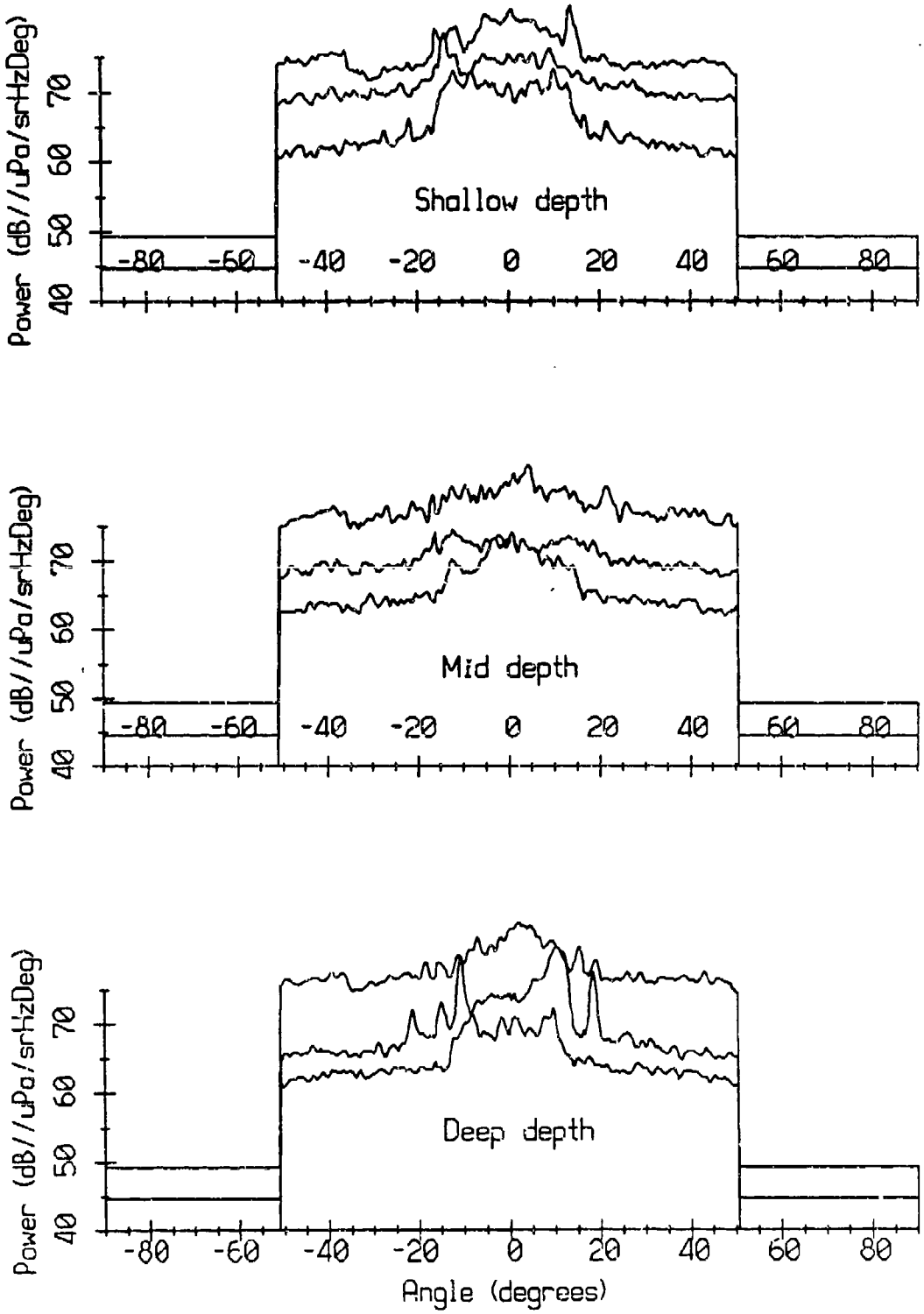

**Figure 9.**

**Spatial spectra versus frequency at specified array depths and wind speeds.**

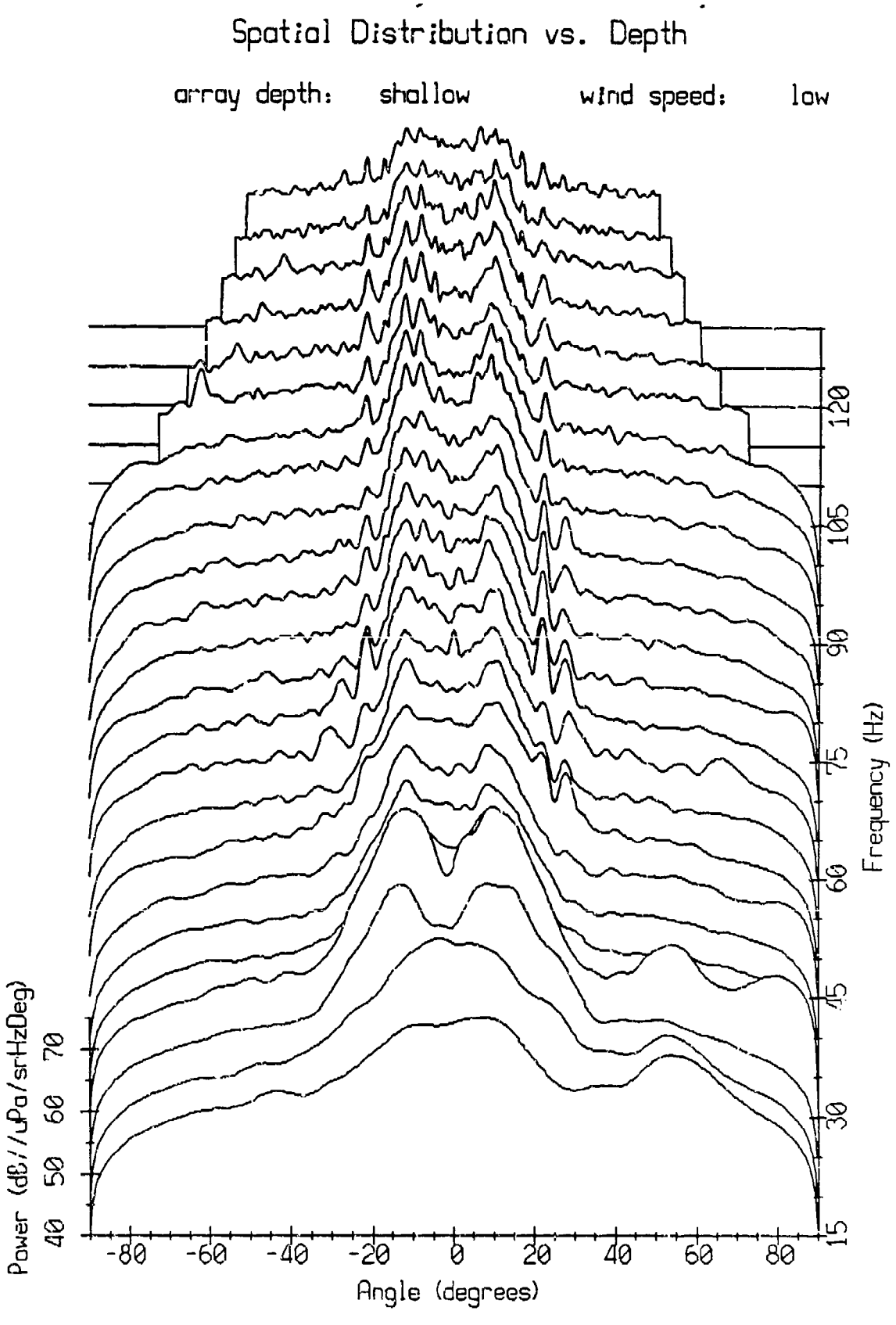
Spatial Distribution vs. Depth
array depth: shallow
wind speed: low
Power (dB//uPa/srHzDeg)
40
50
60
70
-80
-60
-40
-20
0
20
40
60
80
Angle (degrees)
15
30
45
60
75
90
105
120
Frequency (Hz)

**Figure 9.**

**Spatial spectra versus frequency at specified array depths and wind speeds.**

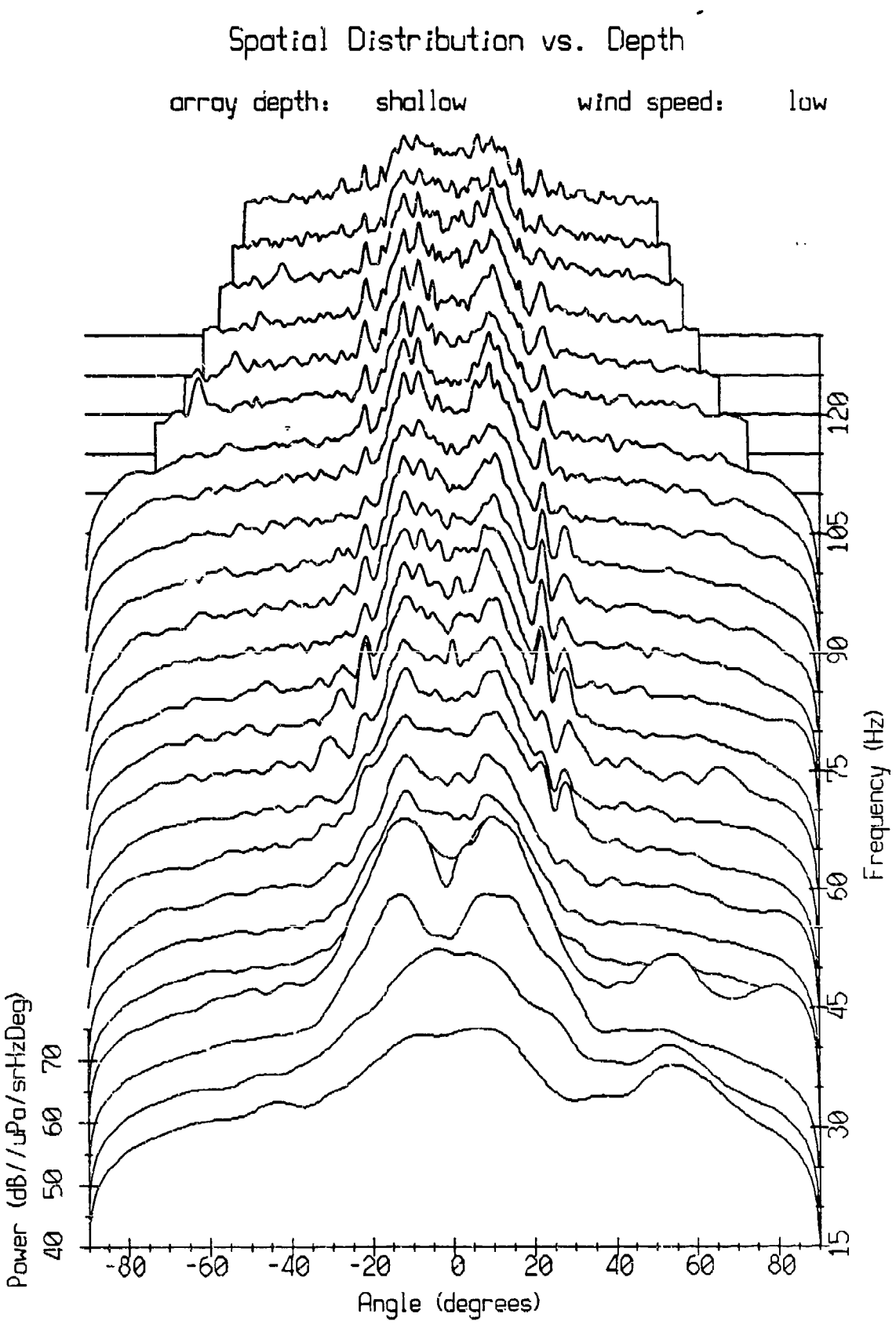
Spatial Distribution vs. Depth
array depth: shallow
wind speed: low
Power (dB//μPa/sr-HzDeg)
40
50
60
70
-80
-60
-40
-20
0
20
40
60
80
Angle (degrees)
15
30
45
60
75
90
105
120
Frequency (Hz)

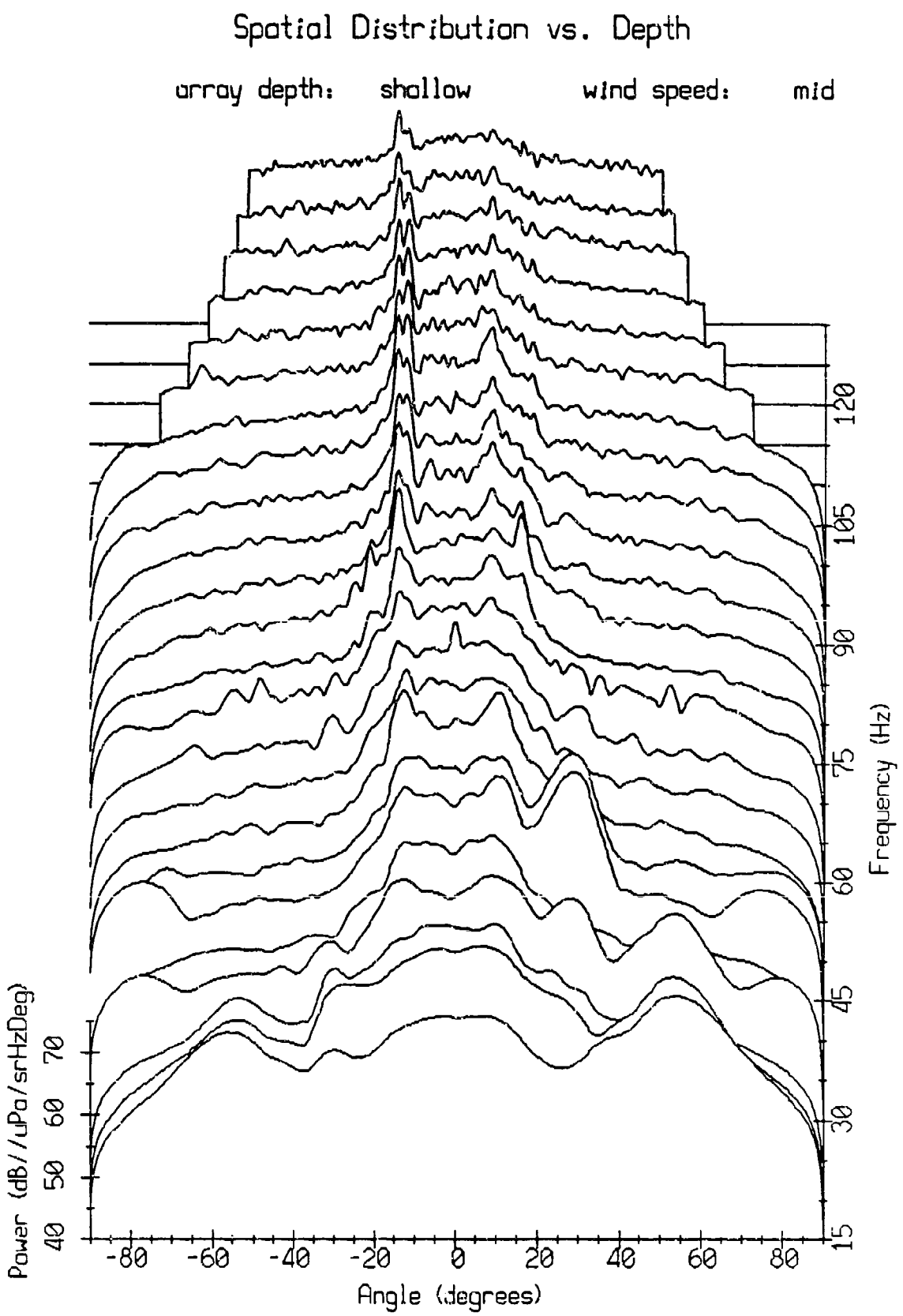
Spatial Distribution vs. Depth
array depth: shallow
wind speed: mid
Power (dB//uPa/srHzDeg)
40
50
60
70
-80
-60
-40
-20
0
20
40
60
80
Angle (degrees)
15
30
45
60
75
90
105
120
Frequency (Hz)

# Spatial Distribution vs. Depth

array depth: mid wind speed: mid

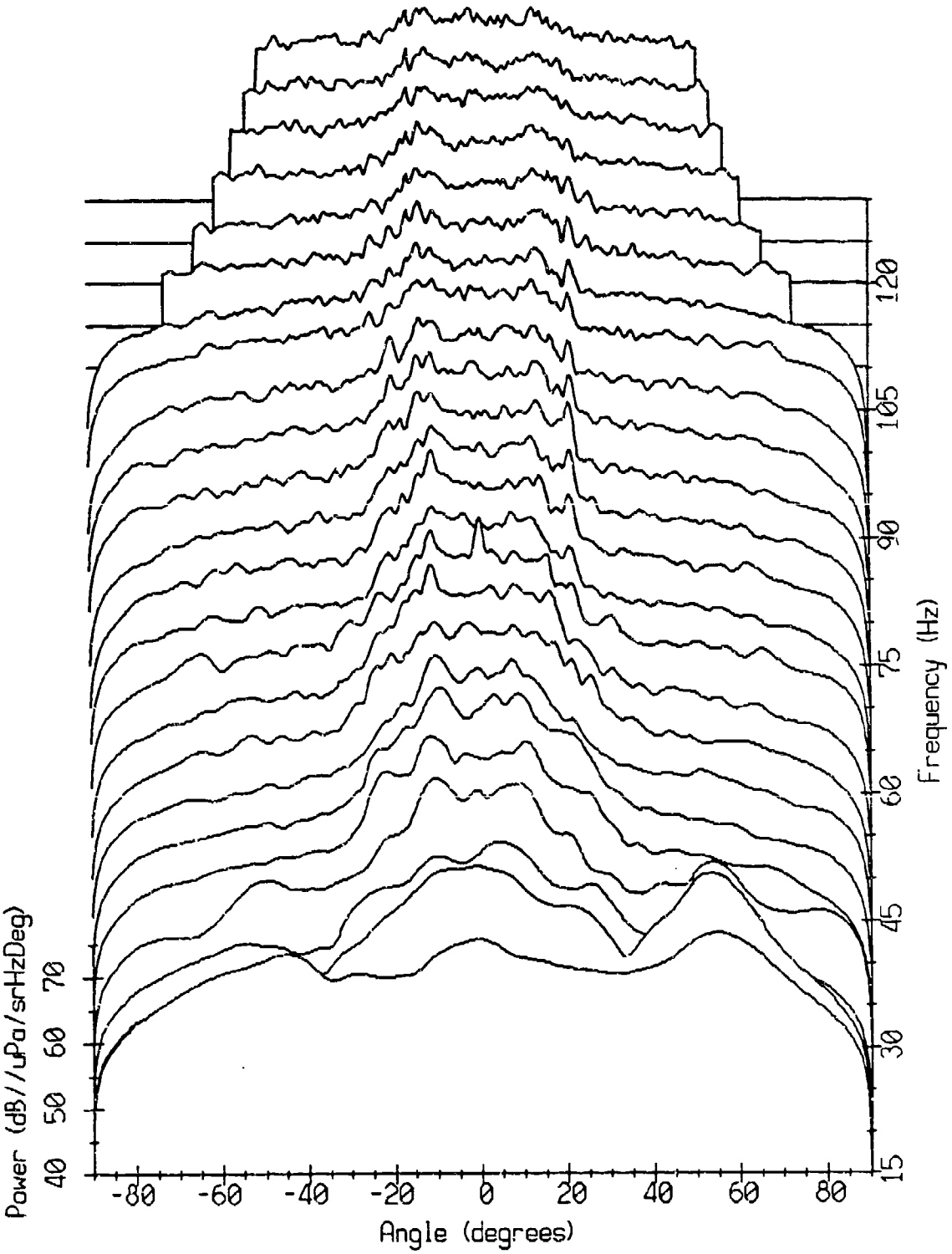

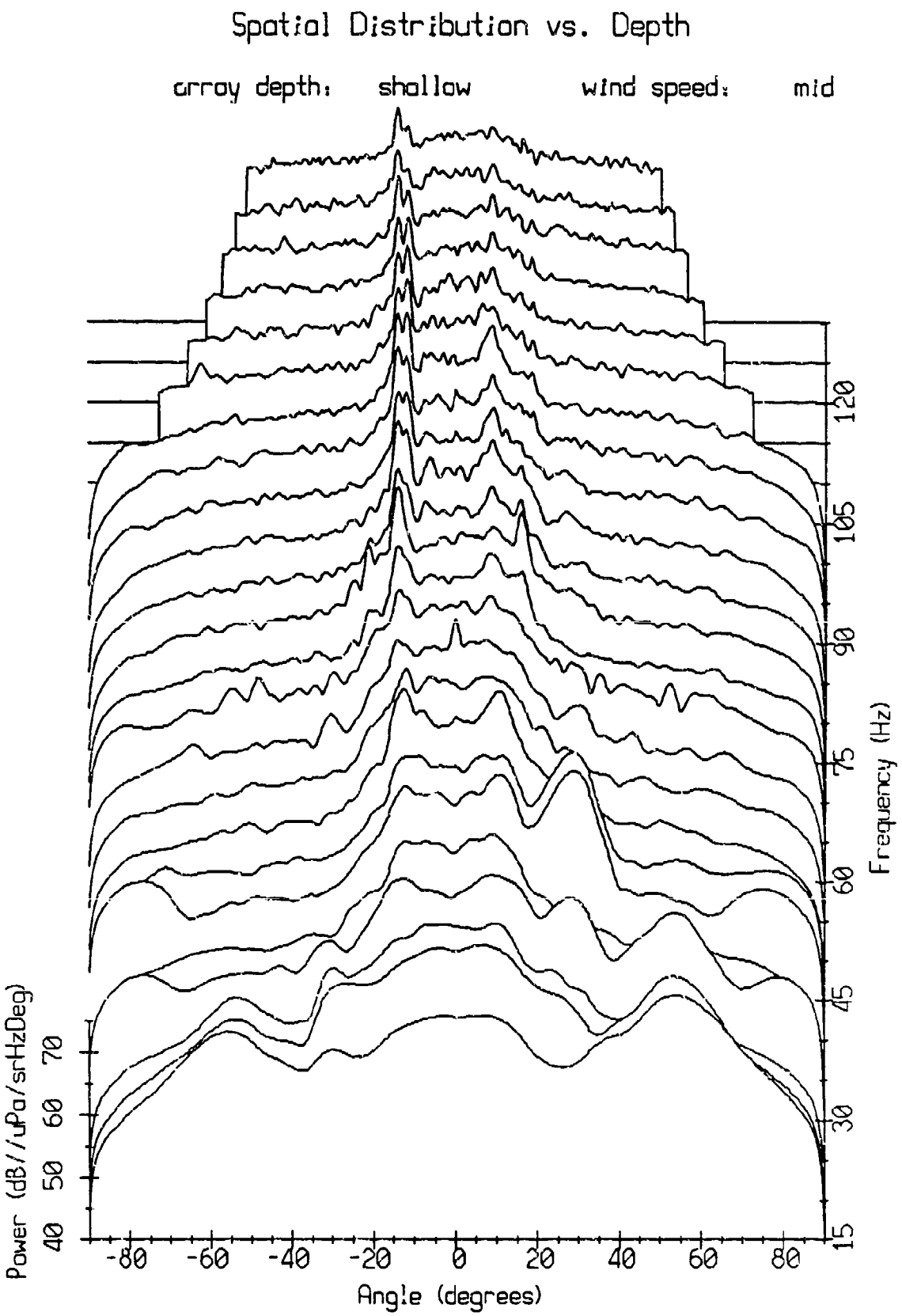
Spatial Distribution vs. Depth
array depth: shallow
wind speed: mid
Power (dB//uPa/srHzDeg)
40
50
60
70
-80
-60
-40
-20
0
20
40
60
80
Angle (degrees)
15
30
45
60
75
90
105
120
Frequency (Hz)

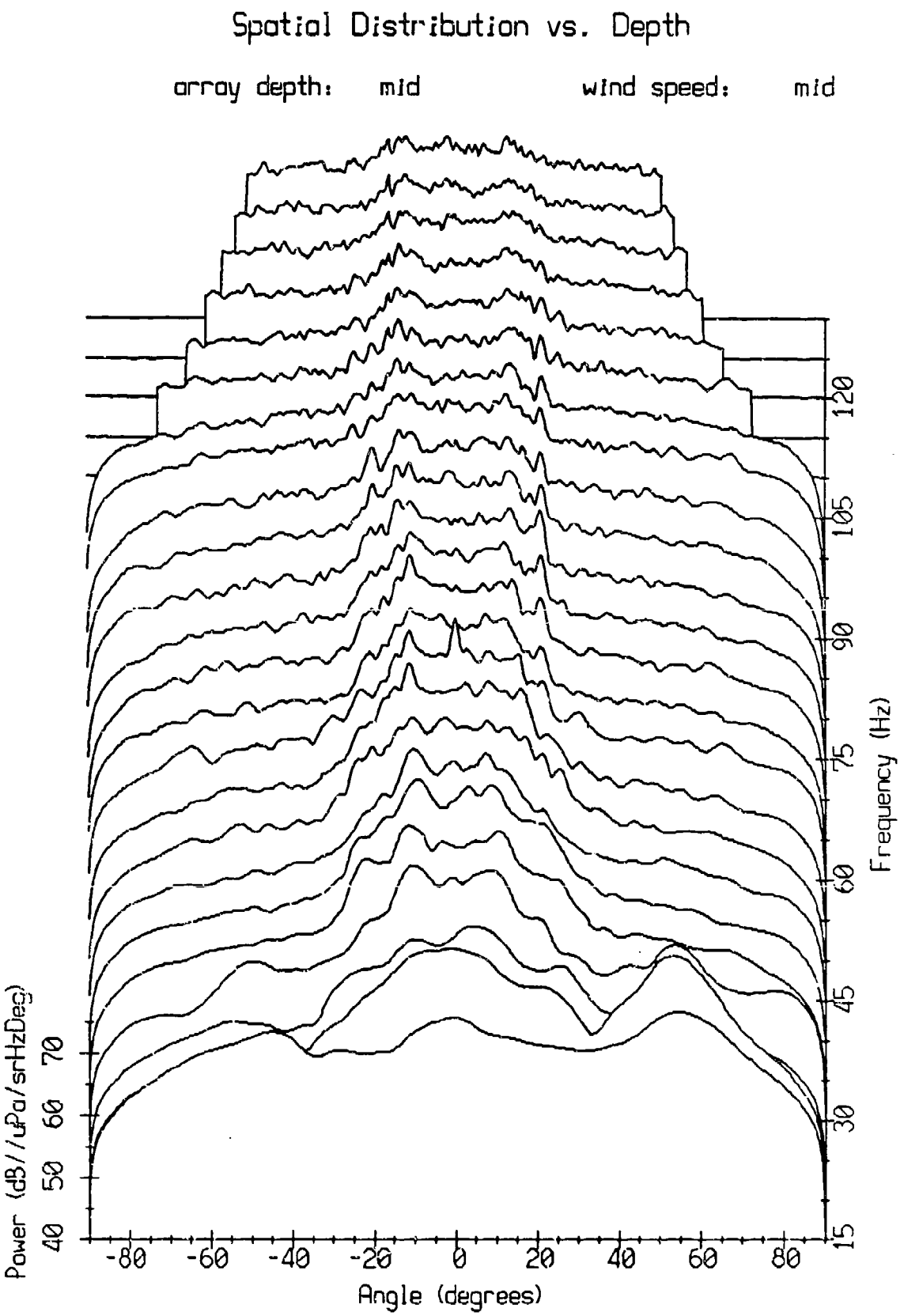
Spatial Distribution vs. Depth
array depth: mid
wind speed: mid
Power (dB//uPa/srHzDeg)
40
50
60
70
-80
-60
-40
-20
0
20
40
60
80
Angle (degrees)
15
30
45
60
75
90
105
120
Frequency (Hz)

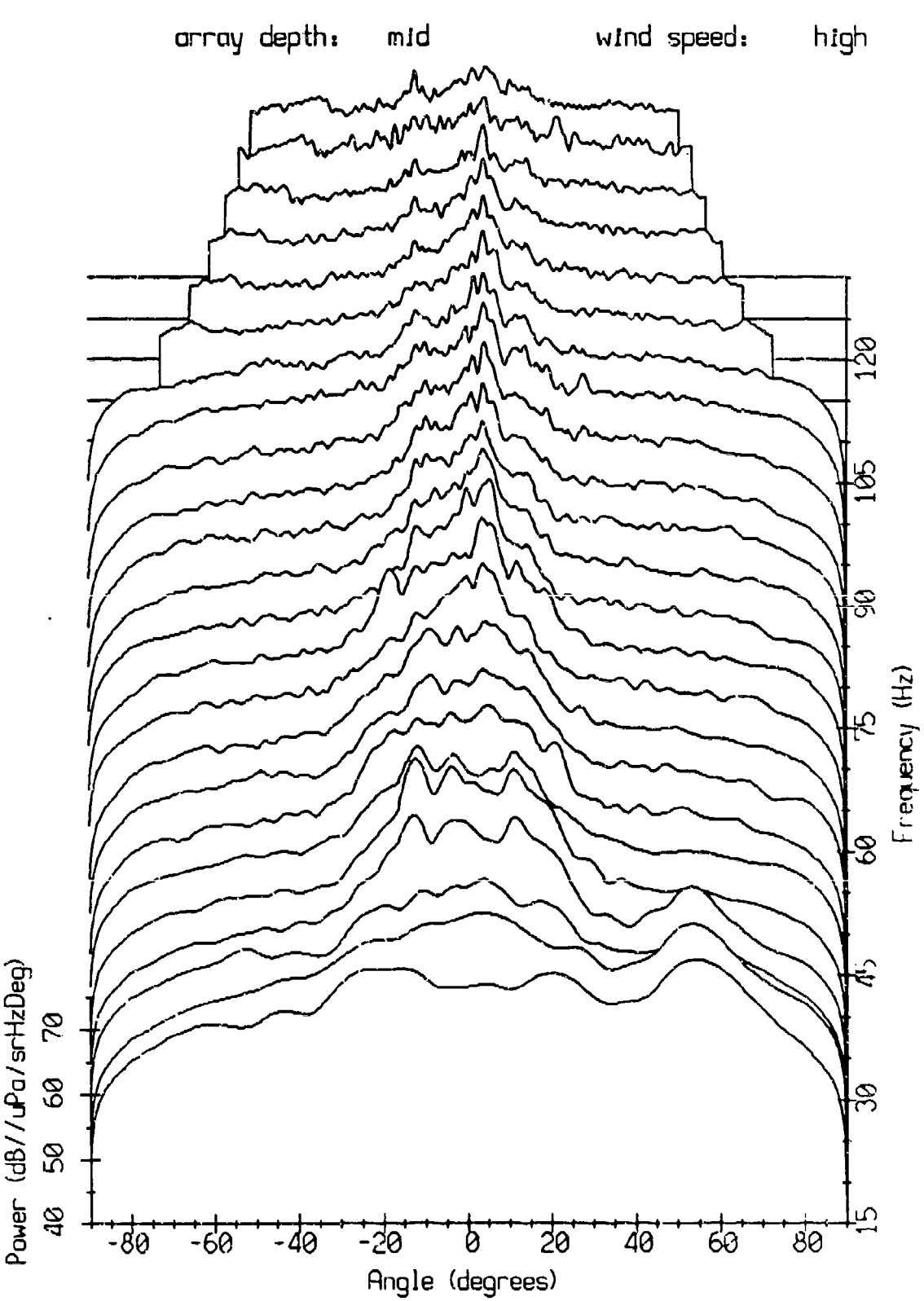
Spatial Distribution vs. Depth
array depth: mid
wind speed: high
Power (dB//uPa/srHzDeg)
40
50
60
70
-80
-60
-40
-20
0
20
40
60
80
Angle (degrees)
15
30
45
60
75
90
105
120
Frequency (Hz)

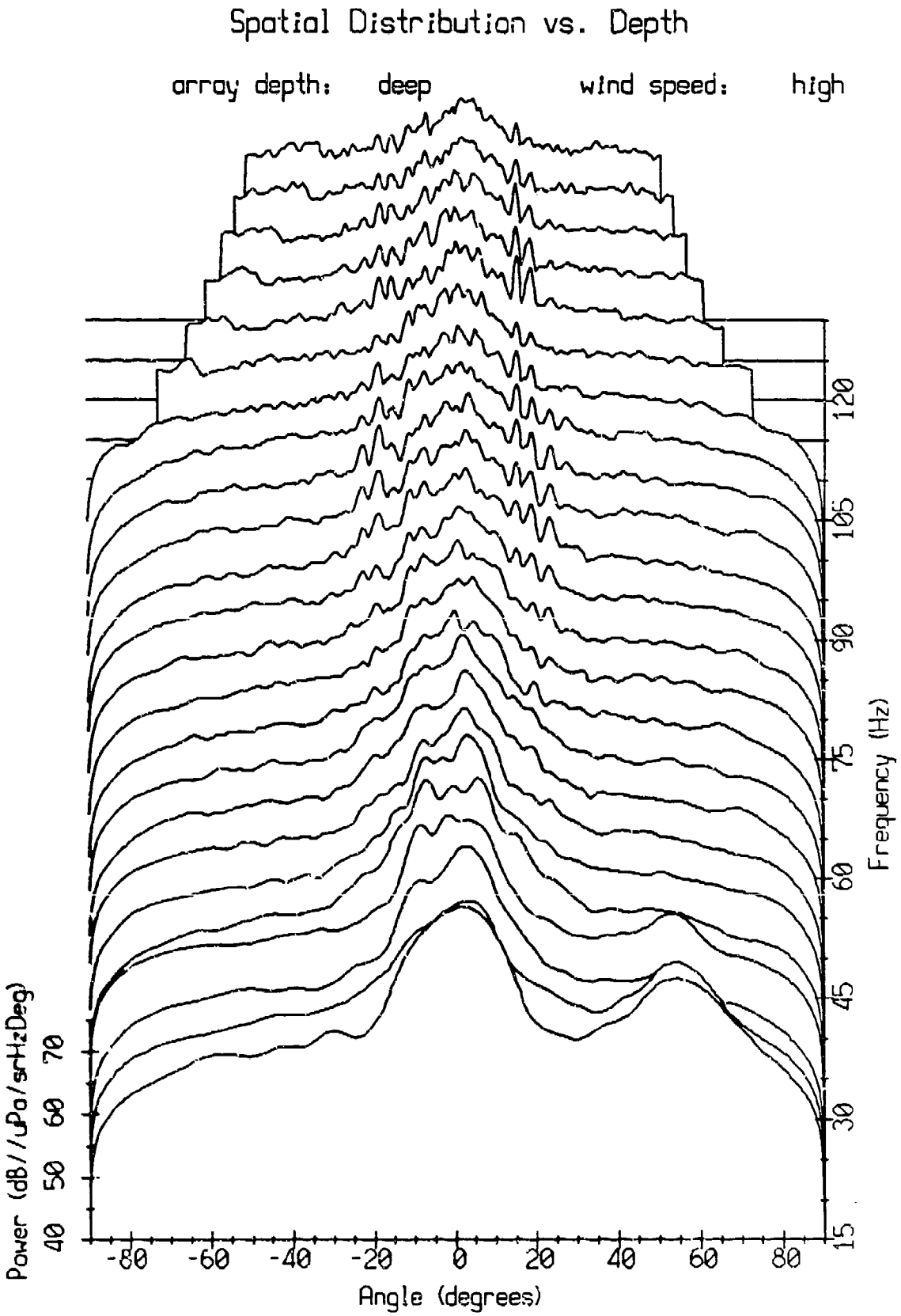
Spatial Distribution vs. Depth
array depth: deep
wind speed: high
Power (dB//μPa/srHzDeg)
40
50
60
70
-80
-60
-40
-20
0
20
40
60
80
Angle (degrees)
15
30
45
60
75
90
105
120
Frequency (Hz)

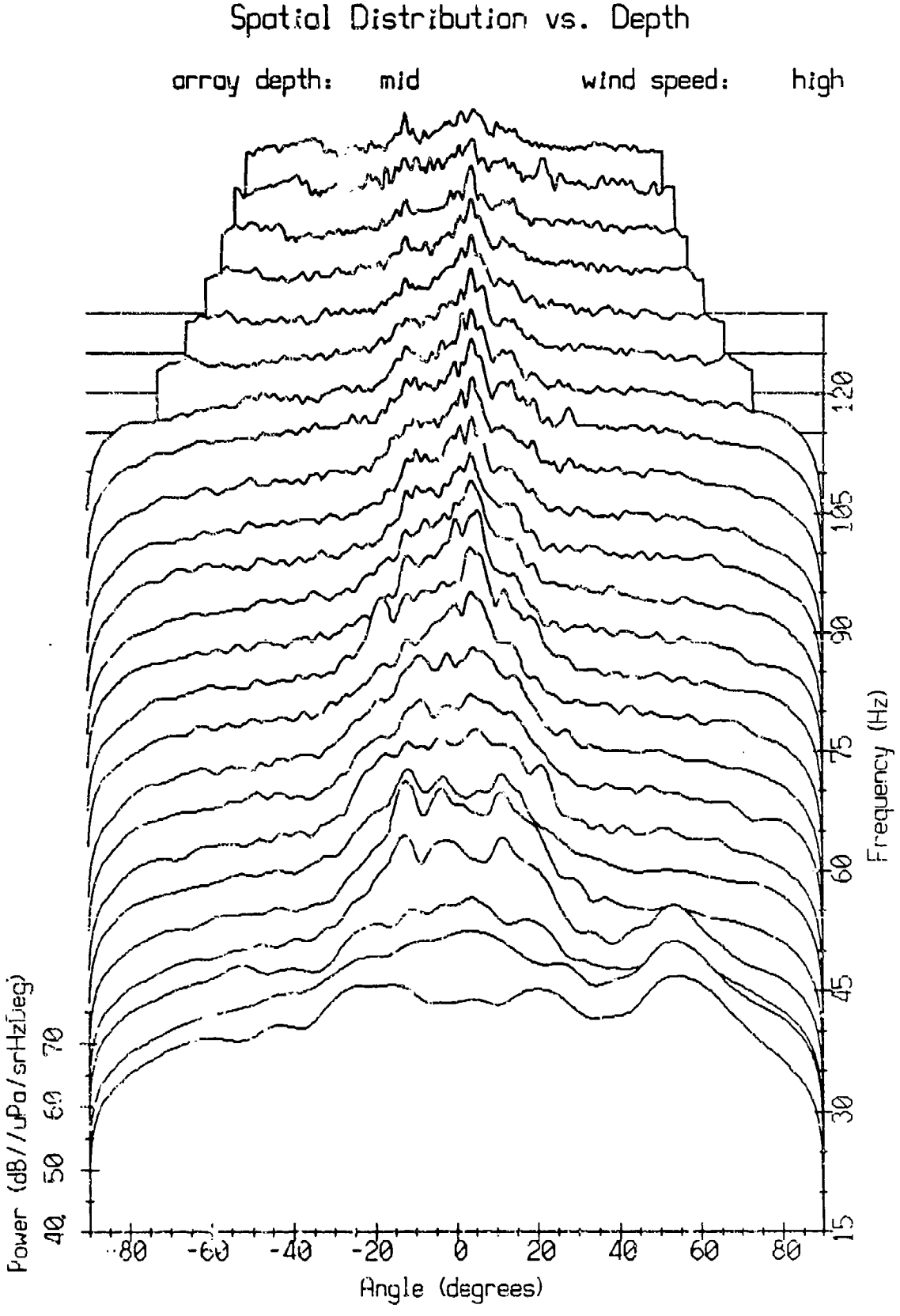
Spatial Distribution vs. Depth
array depth: mid
wind speed: high
Power (dB//uPa/srHz/deg)
40
50
60
70
-80
-60
-40
-20
0
20
40
60
80
Angle (degrees)
15
30
45
60
75
90
105
120
Frequency (Hz)

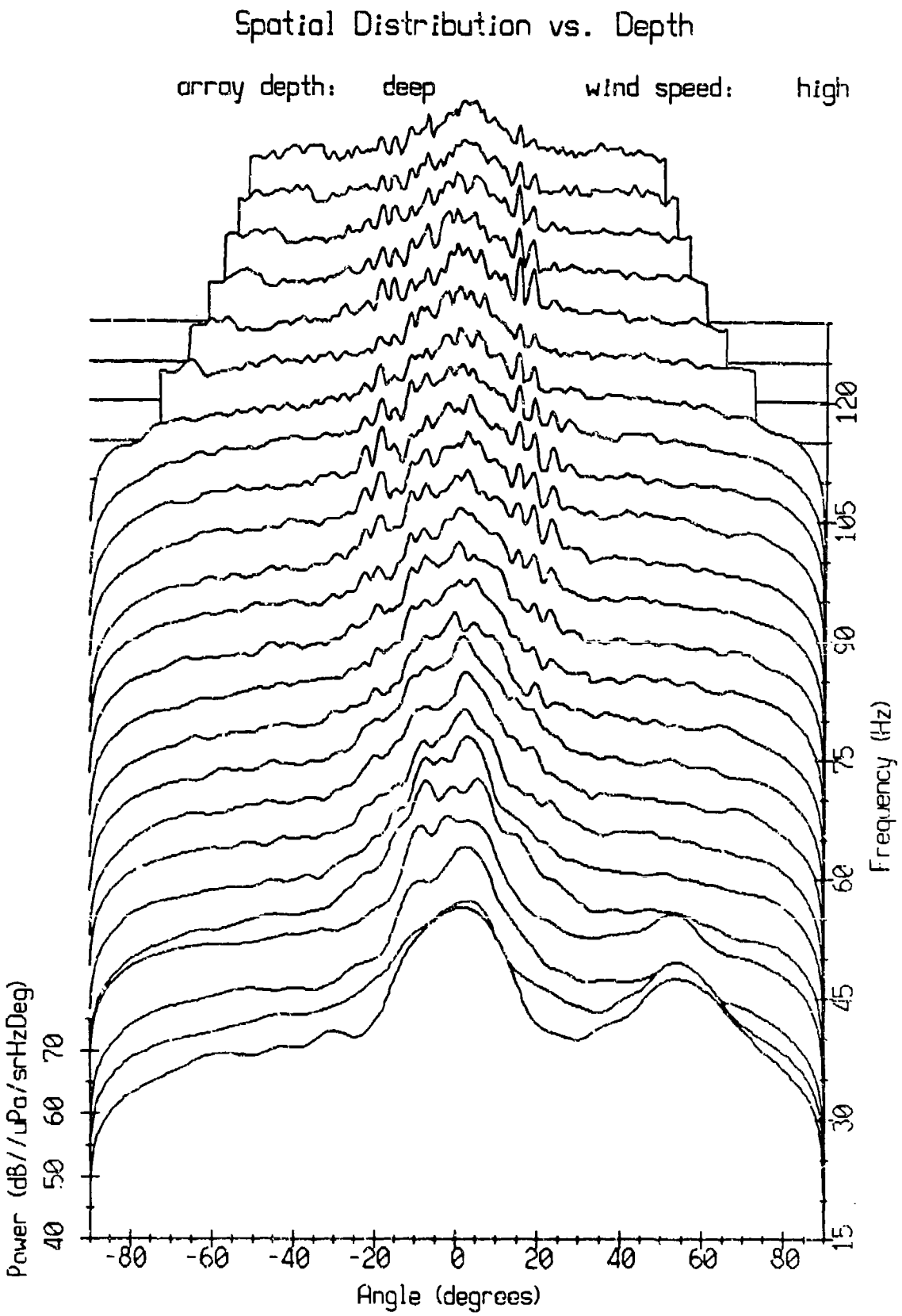
Spatial Distribution vs. Depth
array depth: deep
wind speed: high
Power (dB//uPa/srHzDeg)
40
50
60
70
-80
-60
-40
-20
0
20
40
60
80
Angle (degrees)
15
30
45
60
75
90
105
120
Frequency (Hz)